SERI/PR-234-2571
UC Category: 245

Fundamentals, Development and Scaleup of the Air-Oxygen Stratified Downdraft Gasifier

T. B. Reed[1]
B. Levie
M. S. Graboski[2]

August 1987

1. Now at Department of Chemical Engineering, Colorado School of Mines, Golden, CO 80401
2. Now at Syngas Inc., Golden, CO 80403

Prepared under Task No. WG54 3431

Solar Energy Research Institute
A Division of Midwest Research Institute

1617 Cole Boulevard
Golden, Colorado 80401-3393

Prepared for the
U.S. Department of Energy
Contract No. DE-AC02-83CH10093

SERI/PR-234-2571 August 1987

Fundamentals, Development and Scaleup of the Air-Oxygen Stratified Downdraft Gasifier

T. B. Reed
B. Levie
M. S. Graboski

Preface

This report covers work on the oxygen gasifier from January 1, 1980 through June 1, 1986. The research through September 21, 1984 was supported by the Office of Alcohol Fuels. Subsequent research was supported by the Office of Biomass Energy which has now become the Biofuels and Muncipal Waste Technology Division.

Thomas B. Reed, Principal Scientist
Thermochemical and Electrochemical Research Branch
(Currently, Research Professor in the Department of Chemical Engineering, The Colorado School of Mines, Golden, CO 80401)

Benjamin Levie, Staff Scientist
Chemical Conversion Research Branch

Michael S. Graboski
Vice President and Director of Research, Syngas, Inc., Golden, CO 80403

Approved for
Solar Energy Research Institute

Helena Li Chum
Manager, Chemical Conversion Research Branch

Stanley R. Bull
Director, Solar Fuels Research Division

NOTICE

This report was prepared as an account of work sponsored by the United States Government. Neither the United States nor the United States Department of Energy, nor any of their employees, nor any of their contractors, subcontractors, or their employees, makes any warranty, expressed or implied, or assumes any legal liability or responsibility for the accuracy, completeness or usefulness of any information, apparatus, product or process disclosed, or represents that its use would not infringe privately owned rights.

Printed in the United States of America
Available from:
National Technical Information Service
U.S. Department of Commerce
5285 Port Royal Road
Springfield, VA 22161

Price: Microfiche A01
Printed Copy A14

Codes are used for pricing all publications. The code is determined by the number of pages in the publication. Information pertaining to the pricing codes can be found in the current issue of the following publications, which are generally available in most libraries: *Energy Research Abstracts, (ERA); Government Reports Announcements* and Index (*GRA* and I); *Scientific and Technical Abstract Reports (STAR);* and publication, NTIS-PR-360 available from NTIS at the above address.

SUMMARY

PROGRAM OBJECTIVES

In 1979 the U. S. Department of Energy, Office of Alcohol Fuels, asked the Solar Energy Research Institute to develop a process for manufacturing methanol from biomass. This can be achieved by gasification of the biomass to a "synthesis gas" (syn-gas) (composed of primarily hydrogen and carbon monoxide) followed by catalytic conversion of the gas to methanol. The catalytic conversion of syn-gas is a well developed commercial process. There are a number of gasifiers for wood, but most of them make either a producer gas, high in nitrogen or a pyrolysis gas high in hydrocarbons. None were developed to make syn-gas. Thus the principal technical problem was to develop a gasifier to make synthesis gas from biomass. Work was performed at SERI from 1980-1985 which resulted in the development of a prototype 1 ton/day oxygen-biomass gasifier.

In 1985 a program was undertaken for Congress by the U. S. Department of Energy (DOE) to build a commercial scale (50-200 tons/day) medium energy gasifier, based on DOE or other research. A new company, Syn-Gas Inc. (SGI), had constructed a 24 tons/day air gasifier based on the SERI design and research. A contract was awarded to SGI to modify the air gasifier for oxygen operation for this project. This modification allowed extended tests of the gasifier with oxygen to determine the possibility of scaling up the SERI-SGI gasifier to 50-200 tons/day.

PROGRAM ACCOMPLISHMENTS

Early in 1980 Dr. Thomas B. Reed of SERI and Professor M. Graboski of the Colorado School of Mines designed the "stratified downdraft" gasifier, a simplified derivative of the downdraft gasifiers developed and widely used during World War II. The new design keeps the inherent ability of the downdraft gasifier to produce low-methane, low-tar product gas. This is due to the co-current flow of oxidant and feedstock in which the oxidant burns the pyrolysis products as they form. It departs from the earlier gasifiers with a streamlined geometry and fluid flow which simplifies modelling, scaling, construction, and operation. Modifications of the SERI design are now in use by a number of groups around the world. (It has also been called variously an "open top" or "topless" gasifier.)

A 1 ton/day, prototype, high-pressure, oxygen, stratified-downdraft gasifier was built and operated using the facilities of the Hazen Research Corporation in Golden, Colorado, between 1980 and 1985. The initial design of the gasifier in Phase I and improvements made in Phase II, starting in June 1982, are discussed in **Chapter 2.** The results obtained in Phase I and II for a number of the most successful runs are given in **Chapter 3** with mass and energy **balances.** In this gasifier we have demonstrated the following:

- Operation on oxygen to produce low-tar (typically 2000 ppm or 0.2%) syn-gas with an energy content of 10,000-12,800 kJ/Nm^3 (250-320 Btu/scf)

- Operation on air to produce low-tar (typically 1000 ppm or 0.1%) producer gas with an energy content of 5000-6000 kJ/Nm^3 (125-150 Btu/scf)

- o Operation at feed rates to 28 kg/h (62 lb/h) using feedstocks with up to 40% moisture)
- o Operation on wood chips, paper cubes, corn cobs, and peat
- o Operation at 1013 kPa (10 atm pressure), desirable for pipeline use, turbine operation or subsequent conversion to methanol, (although higher pressures are necessary for methanol synthesis)
- o Production of gas with minimal methane content (typically less than 4% by volume), desirable for methanol production
- o Production of low-sulfur syn-gas (62 ppm H_2S, 130 ppm SO_2, 20 ppm COS).
- o Production of a gas which was successfully converted to 2 L of methanol by Chem-Systems Inc.

A patent has been applied for on the SERI gasifier.

The gasifier received an IR-"Significant Development of the Year" award in 1982.

A three-day "Biomass to Methanol Specialists' Workshop" was sponsored by SERI in 1982 to evaluate the feasibility of methanol production from biomass. Experts were invited to discuss various aspects of methanol technology, including wood collection and comminution, pressure feeding of the feedstock, coal and biomass gasification, gas cleanup, and methanol synthesis. Proceedings of this conference have been published.

In 1981 the International Harvester Company (IHC) became interested in commercial development of the gasifier and acquired a license to develop a commercial model. Due to corporate financial difficulties this was not carried out by IHC but was carried out by a company, Syn-Gas, Inc. (SGI), formed with some of the assets of the IHC venture.

In 1985 SGI constructed a nominal 24 tons/day air gasifier. The design was based on the original patent and the results found during the research on the 1 ton/day gasifier. The initial intent was to operate a 1 MW diesel generator to produce electric power from wood chips.

The SGI gasifier was operated extensively on air during 1985 and made a 104-h "endurance" run. The gasifier was also operated on oxygen during 1985 and in 1986 a 65-h "endurance" run was completed on oxygen. The results of the oxygen gasification tests are reported in **Chapter 4**.

During the research on the practical engineering aspects of the gasifier a number of smaller gasifiers were constructed and operated with the purpose of determining the operating principles of the gasifier. These principles and several specific designs are discussed in **Chapter 5**. Some measurements of pressure drop and experience with various gas transport devices are also reported in this chapter.

Downdraft gasifiers produce the lowest tar levels of all the major gasifier types, but still require removal and disposal of the tars produced unless close-coupled to combustors. The production of tars is the Achilles Heel of

most biomass gasification systems. Measurements of tar composition and tar quantities are discussed in **Chapter 6.** Tests on the destruction of residual tars using both thermal and catalytic means are described. Tar levels were reduced to less than 400 ppm by passing the gas over any of several catalysts at temperatures as low as 600°C.

The chemistry and thermodynamics of biomass gasification are discussed in **Chapter 7.** Coal gasification involves primarily the reaction of the fixed carbon component which comprises 60%-90% of the coal, and coal gasification is generally described in terms of the reactions of carbon with CO_2 or H_2O (char gasification). However, fixed carbon comprises only 10%-25% of biomass, and so pyrolysis and partial oxidation of the volatile materials produced is the major process involved in biomass gasification, with char gasification playing a secondary role.

Although thermodynamics cannot by itself tell us what reaction conditions will prevail, it delineates large areas as impossible. It is the nature of downdraft gasification that the products pass through a hot bed of charcoal before leaving the gasifier and therefore approach thermodynamic equilibrium. Charts are presented in **Chapter 7** showing the gas composition predicted by thermodynamics. These values are compared to some actually measured.

It is very useful to have a model to use for scaling a gasifier that predicts the effect on the products and operation of changing the independent parameters and that determines optimal operating conditions. A two-stage model is developed in **Chapter 8** that predicts the behavior of the gasifier to a first approximation. In the first stage of "flaming pyrolysis," incoming oxygen burns the pyrolysis vapors as they are formed. During this stage charcoal is produced but is prevented from reacting with the combustion products by the presence of pyrolysis products and the low surface temperature of the char. An equation has been developed to predict the time required for flaming pyrolysis and this plus a knowledge of throughput permits designing the proper length zone required in the gasifier to accommodate the reaction.

When pyrolysis is complete, the high-temperature combustion gases are reduced by the charcoal to the final producer gas composition. This reaction is highly endothermic so the reaction is self-quenching. The gasification rate becomes impractically slow at a temperature of about 800°C. A model has been developed to predict the time required to reach this temperature, and this is combined with throughput to predict the length of the char reduction zone.

The prediction of flaming pyrolysis time is based on data obtained by Huff on wood combustion. A single particle reactor has been built to measure times of pyrolysis under well controlled conditions simulating the gasification conditions. It is expected that this reactor will supply useful data for gasifier modelling. Work is continuing in this field with other solid fuels such as Municipal Solid Waste (MSW) pellets.

The economics of biomass gasification with air and oxygen are discussed in **Chapter 9.** Two major studies have been made on using the SERI-SGI gasifier for methanol manufacture by Applied Engineering (APCO, a division of Fluor Corporation) and Stone and Webster (S&W). The results of these studies are presented in detail in **Chapter 9.** Other studies have been made on the manufacture of methanol from wood, MSW, coal, and natural gas, and these data are all scaled to 1987 costs using the consumer price index. A least square

fit results in a capital cost for a 100 tonss/day wood methanol plants of $27 million.

The cost of low- and medium-Btu gasification depends on many factors, but the principal factors are **feedstock cost** and **operating cost**, (including oxygen and power for medium-Btu gasification). A rule of thumb for estimating gas cost is presented. Examination of the collected studies permits construction of a simple economic model to predict the capital and operating cost of a methanol plant as a function of methanol output and feedstock costs. Table 9.5 shows the cost of a 100 and a 1000 tons/day plant using wood, MSW, coal, and natural gas. It also shows the cost of producing methanol from these plants using feedstock priced from $-20 to $+50/ton (the negative costs are appropriate to MSW type feedstocks). These give methanol costs ranging from $0.33 to $1.20/gal.

The authors give suggestions for future work in **Chapter 10** and conclusions in **Chapter 11**. Appendices give details on various aspects of this report.

PROGRAM STATUS

The SERI oxygen-air gasification program work was completed in 1985. The technology has been transferred to SGI, where the work reported in Chapter 4 was done in 1985-86. SGI is currently marketing gasifiers based on the technology developed here and is currently installing a 10 MW power plant on Long Island.

TABLE OF CONTENTS

CHAPTER 1 - OBJECTIVES AND HISTORY OF THE SERI/SGI OXYGEN-AIR BIOMASS GASIFIER
1.1 Program Objectives 1-1
1.2 Biomass Gasification 1-1
1.3 Origin and Conceptual Design of the SERI/SGI High-Pressure Oxygen Gasifier 1-2
1.4 Chronology of Air/Oxygen Gasification Development 1-3
References 1-7

CHAPTER 2 - DESIGN OF 1 TON/DAY EXPERIMENTAL GASIFIER
2.1 Phase I - Original Design 2-1
2.1.1 Gasifier Design 2-1
2.1.2 Piping and Instrumentation 2-3
2.2 Phase II - Modifications to Original Design 2-9
2.2.1 Reasons for Modification 2-9
2.2.2 Elimination of Oxygen Nozzles 2-9
2.2.3 Bed Stirring Assembly 2-12
2.2.4 Gas Clean Up Train 2-12
2.2.5 Feeder Modification 2-13
2.2.6 Gas Flow 2-13
2.2.7 Gas Sampling 2-16

2.3 Preferred Configuration 2-16
2.3.1 Open vs Closed top operation 2-16
2.3.2 Low Char-ash Removal and even Fuel distribution for low tar production
References 2-17

CHAPTER 3 - RESULTS ON 1 TON/DAY EXPERIMENTAL GASIFIER
3.1 Introduction 3-1
3.2 Phase I Results 3-1
3.2.1 Startup and Early Shakedown Tests 3-1
3.2.2 Atmospheric Pressure Oxygen Operation 3-1
3.2.3 High Pressure Oxygen Runs 3-4
3.2.4 Catalytic Grate Test 3-7
3.3 Phase II Results 3-7
3.3.1 Air Runs 3-7
3.3.2 Oxygen Runs 3-11
3.4 Co-Gasification of Methane and Biomass 3-14
3.5 Conclusions from Gasifier Runs 3-16
References 3-25

CHAPTER 4 - LARGE SCALE TESTING
4.1 Introduction 4-1
4.1.1 SERI/DOE Development work 4-1
4.1.2 Technology Transfer to Syn-Gas Inc. 4-1
4.2 Commercialization of Low and Medium Energy Gas 4-3
4.2.1 Syn-Gas Background 4-3
4.2.2 Application of Lowe and Medium Btu Gas 4-3

4.3 Gasifier Technology 4-4
4.3.1 Brief Description of Downdraft Gasifier Operation 4-4
4.3.2 Thermodynamic Model Predictions 4-4
4.4 SynGas Gasification Facility Description 4-8
4.4.1 Plant Description 4-8
4.4.2 Wood Handling and Feeding 4-8
4.4.3 Air and Oxygen Supply 4-10
4.4.4 SynGas Gasifier Description 4-10
4.4.5 Downstream Equipment 4-17
4.4.6 Demonstration Plant Instrumentation and Control 4-17
4.5 Experimental Procedure 4-18
4.5.1 Startup 4-18
4.5.2 Input Variables 4-18
4.5.3 Output Variables 4-18
4.5.4 Other Parameters 4-19
4.5.5 Heat and Material Balance Closure 4-19
4.6 Experimental Objectives 4-19
4.7 Feasibility Demonstration (Objective 1) 4-19
4.8 Identification and Solution of Operation Problems (Objective 2) 4-20
4.8.1 Oxygen Operation Problems 4-20
4.8.2 Observations on Oxygen 4-21
4.9 Results of Oxygen Parametric Test Runs (Objective 3) 4-23
4.9.1 Introduction 4-23
4.9.2 Summary of Oxygen Test 1 4-23
4.9.3 Summary of Oxygen Test 2 4-26
4.9.4 Summary of Oxygen Test 3 4-29
4.9.5 Summary of Oxygen Test 4 4-31
4.9.6 Summary of Oxygen Test 5 4-32
4.9.7 Effect of Fuel Moisture 4-33
4.9.8 Approach to Equilibrium 4-33
4.9.9 Oxygen Usage 4-33
4.9.10 Tar Production 4-33
4.9.11 Material & Energy Balance 4-35
4.9.12 Summary of Parametric Test Results 4-35
4.10 System Modifications After Test 5 4-35
4.10.1 Screw Feeder 4-35
4.10.2 Star Valve 4-36
4.10.3 Cooling 4-36
4.10.4 Ash Handling 4-36
4.10.5 Grate 4-36
4.10.6 Stirrer 4-36
4.11 Extended 100 Hour Air Run 4-36
4.11.1 Mechanical Proof of Concept 4-36
4.11.2 Feeding 4-37
4.11.3 Stirring 4-37
4.11.4 Grate 4-37
4.11.5 Gasifier Internals 4-37
4.11.6 Ash Removal System 4-37
4.11.7 System Control 4-37
4.11.8 Cyclone 4-37
4.11.9 Long Run Gasifier Operation 4-37
4.12 Extended Oxygen Run 4-39

4.12.1 Oxygen Test 6 4-39
4.12.2 Oxygen Test 7 4-39
4.12.3 Oxygen Test 8 4-39
4.12.4 Oxygen Test 9 4-39
4.12.5 Oxygen Test 10 4-40
4.13 Discussion 4-44
References 4-45

CHAPTER 5 - BASIC MECHANICAL STUDIES OF GASIFIER OPERATION
5.1 Principles of Biomass Gasifier Design 5-1
5.1.1 Fuel Considerations 5-1
5.1.2 Low Tar Production 5-1
5.1.3 Thermodynamic Temperature Stabilization 5-1
5.1.4 Kinetic Temperature Stabilization 5-2
5.1.5 Oxidant/Fuel Distribution 5-2
5.1.6 Reaction Front Stabilization 5-2
5.1.7 Planar Flame Front Stabilization 5-3
5.1.8 Insulation 5-3
5.2 Other Stratified Downdraft Gasifiers 5-3
5.2.1 A Simple Laboratory 5-20 kW Gasifier 5-3
5.2.2 Transparent Laboratory Gasifiers 5-7
5.2.3 The "Upside-Downdraft Gasifier" 5-13
5.3 A Single Particle Reactor 5-16
5.4 Gas Transport Through Packed Bed Gasifiers 5-19
5.4.1 Introduction 5-19
5.4.2 Practical Gas Transport Devices 5-19
5.4.3 Pressure Drop in Packed Beds 5-22
5.4.4 Influence of Gas Transport Device on Gasifier Behavior 5-23
References 5-25

CHAPTER 6 - TAR CONVERSION
6.1 Introduction 6-1
6.1.1 The Tar Problem in Gasification 6-1
6.1.2 The Nature of Gasifier tars 6-2
6.2 In Situ Mass Spectrometric Studies of Up- and Downdraft Gasifier Tars 6-3
6.2.1 Direct Measurement of Tar and Oil Spectra 6-3
6.2.2 Measurement of Downdraft Tar Composition 6-3
6.2.3 Measurement of Updraft Tar Composition 6-7
6.3 Factors Affecting Tar Production 6-7
6.4 Measurements of Producer Gas Tar Levels 6-9
6.4.1 Phase I Tar Production 6-9
6.4.2 Phase II Tar Production 6-9
6.5 Thermal Tar Destruction 6-11
6.5.1 Previous Studies on Thermal Tar Destruction 6-11
6.5.2 Tar Destruction Experiments in the 1 ton/day Gasifier 6-11
6.5.3 Thermal Tar Destruction in the Transparent gasifier 6-12
6.6 Catalytic Tar Conversion 6-13
6.6.1 Introduction 6-13
6.6.2 Apparatus for Catalytic Tar Cracking Tests 6-13
6.6.3 Results of Catalytic Tar Cracking Tests 6-16
6.6.4 Discussion of Results 6-18
6.7 Recommendations for Future Tests 6-23
6.8 Application of Catalytic Tar Conversion to Commercial Gasification 6-23
References 6-25

CHAPTER 7 - CHEMISTRY AND THERMODYNAMICS OF GASIFICATION
7.1 Chemistry of Biomass Combustion and Gasification 7-1
7.1.1 Composition of Biomass, Charcoal and Pyrolysis Oil 7-1
7.1.2 Biomass Thermal Conversion Reactions 7-4
7.1.3 Thermochemistry of Biomass Compounds 7-5
7.2 Thermodynamics of Biomass Gasification 7-5
7.2.1 Value of Thermodynamic Calculations 7-5
7.2.2 Thermodynamic Calculation of Gasification Temperature and Gas Composition 7-6
7.2.3 Calculation of "Adiabatic Reaction Temperature" 7-7
7.2.4 Gasifier Operating Point 7-14
7.2.5 Downdraft Gasifier Control Mechanisms 7-14
7.2.6 Kinetic Approach to the Operating Point 7-15
7.3 Carbon-Gas Equilibrium 7-16
7.3.1 The Role of Carbon Saturation in Gasification 7-16
7.3.2 Location of the Carbon Saturation Line 7-16
7.3.3 A Pseudo Gas-Char-Oil Phase Diagram for Biomass Pyrolysis/Gasification 7-20
7.4 Summary 7-20
References 7-22

CHAPTER 8 - MODELS OF DOWNDRAFT GASIFIERS
8.1 Introduction to Process and Gasifier Modelling 8-1
8.2 Qualitative Description of Downdraft Gasifier 8-2
8.2.1 Physical Basis of 2-Stage Model 8-2
8.2.2 Diagram of Stratafied Downdraft Gasifier Model 8-5
8.3 Pyrolysis, Flaming Combustion and Flaming Pyrolysis 8-9
8.3.1 Pyrolysis vs Flaming Pyrolysis 8-9
8.3.2 Pyrolysis Modelling 8-10
8.3.3 A Quantitative Formula for Flaming Combustion 8-10
8.3.4 Modification of Huff Equation to Estimate Time for Flaming Pyrolysis 8-11
8.3.5 The Heat of Pyrolysis 8-12
8.3.6 The Heat for Pyrolysis 8-12
8.3.7 Heat Transfer in Flaming Combustion 8-14
8.3.8 Heat Tranfer Mechanisms in Flaming Pyrolysis and Flaming Combustion 8-17
8.4 Adiabatic Char Gasification 8-18
8.4.1 Introduction 8-18
8.4.2 Char Reaction Chemistry 8-19
8.4.3 Charcoal Reaction Kinetics 8-20
8.4.4 Models of the Adiabatic Char Reduction Zone 8-21
8.5 A Predictive Model of the Stratified Downdraft Gasifier 8-28
8.5.1 Spreadsheet Model of the Stratified Downdraft Gasifier 8-28
8.5.2 Comparison of Model with Observed Gasification Conditions 8-35
8.6 Stablilization of the Flaming Pyrolysis Zone 8-35
Nomenclature 8-38
References 8-39

CHAPTER 9 - PROCESS COSTS AND ECONOMICS
9.1 Introduction 9-1
9.2 Costs of Low and Medium Energy Gasification for Process Energy and Synthetic Fuel Production 9-2
9.2.1 Basis of Gas Cost Calculations 9-2

	9.2.2 Low Energy Gas Production Cost	9-3
	9.2.3 Medium Energy Gas from Oxygen Gasification	9-3
9.3	Cost of Methanol Production from Biomass using the SERI-SGI Gasifier	9-4
9.4	Comparative Economics of Methanol Production from Various Feedstocks	9-6
	9.4.1 Capital and Operating Cost Estimates for Methanol from Production Biomass, MSW, Natural Gas, and Coal	9-6
	9.4.2 Scale Factor for Methanol Plants	9-10
	9.4.3 Feed Factor in Methanol Plant Cost	9-13
9.5	A Simplified Model of Cost of Methanol Plants and Production from Various Feedstocks	9-13
	9.5.1 Introduction	9-13
	9.5.2 Capital Cost of Various Size Methanol Plants	9-13
	9.5.3 Methanol Production Cost	9-13
	9.5.4 Simplified Methanol Cost Model	9-15
	9.5.5 Sample Costs of Methanol from Various Feedstocks	9-15
9.6	Conclusions	9-16
	Nomenclature	9-18
	References	9-18
10.	Future Directions for Fixed Bed Downdraft Gasifiers	10-1
11.	Summary and Conclusions	11-1

ACKNOWLEDGEMENTS
APPENDIX A Units and Conversion Factors
APPENDIX Chem Systems Letter
APPENDIX Economic Feasibility of A Small Scale Wood Gasification to Methanol Plant (H. Kostrin and D. A. Himmelblau, Stone and Webster) Summary of feasibility study

CHAPTER 1

OBJECTIVES AND HISTORY OF THE SERI/SGI OXYGEN-AIR BIOMASS GASIFIER

1.1 PROGRAM OBJECTIVES

In 1979 the U. S. Department of Energy (DOE), Office of Alcohol Fuels, asked the Solar Energy Research Institute (SERI) to develop a process for manufacturing methanol from biomass. This requires solution of technical problems and technology transfer for commercial success.

The most conventional route to methanol involves gasification of the wood to a "synthesis gas" (syn-gas) (composed of primarily hydrogen and carbon monoxide) followed by catalytic conversion of the gas to methanol. The catalytic conversion of syn-gas is a well developed commercial process. There are gasifiers for wood, but none were developed to make syn-gas, and most gas from wood contains large amounts of tar, nitrogen and methane, all detrimental in methanol manufacture.

Thus the principal technical objective was to develop a gasifier to make synthesis gas from wood. This report discusses a new type of gasifier developed for the gasification of biomass to produce a synthesis gas suitable for methanol production from oxygen.

Many of the early tests on the gasifier were performed on air, and we found that the gasifier produced a gas low in tar. Since low tar is particularly desirable for operation of engines and generation of power, the same gasifier has been developed with air to produce a low Btu gas for power generation.

A company, SynGas, Inc., was formed by one of the authors (Graboski) to scale up the new gasifier technology for commercial operation. They constructed and tested a 24 tons/day air gasifier based on the SERI design for generation of power or synthesis gas.

In 1985 a program was undertaken for Congress by DOE to build a commercial scale (50-200 tons/day) medium energy gasifier, based on DOE or other research. A contract was awarded to SGI by SERI to modify the air gasifier as a possible gasifier for this project. This modification allowed extended tests of the gasifier with oxygen to determine the possibility of scaling up the SERI-SGI oxygen gasifier to 50-200 tons/day.

1.2 BIOMASS GASIFICATION

Biomass has gained recognition as a fuel source with the potential to make a major contribution to our energy needs. Wood use in the United States has more than doubled since the 1973 Arab oil crisis. It is estimated that biomass alone has the potential to supply up to 16 quads of energy (about 20% of current consumption) (1). Furthermore, biomass utilization could be increased by appropriate waste utilization in agricultural, forest and urban environments. However, in order to incorporate the energy from biomass into the present energy infrastructure, wood and other forms of biomass must be transformed into more easily transportable and usable energy forms such as fuel gas, methanol or electric power. To this end, SERI and many other organizations are pursuing thermochemical and biochemical research and development to establish commercial biomass conversion technologies.

Gasification is a very old technology for converting coal and biomass solid fuels into a gas that can be used in various processes. It yields a gas that can be used to generate mechanical power and electricity, synthetic fuels and chemicals (2). In most gasifiers no external heat is required to maintain pyrolysis and gasification. **Coal gasification** was commonly used in the first half of this century to supply gas for cooking and lighting in the larger cities. **Biomass gasification** was used for smaller installations, particularly during World War II, supplying energy for transportation, electricity and heat.

Biomass gasification however, was not developed in the United States because of the easy access to natural gas and petroleum. For gasification to become a mature technology today, we will need to develop specific gasifiers for particular applications and specific fuels, develop fuel handling apparatus and automatic controls, and make gasifiers environmentally acceptable by eliminating tar disposal. In an effort to make information available on World War II experience with gasifiers, a translation of Gengas, the Swedish book detailing the science and technology learned during the war years was published by SERI (3).

In 1978-1980 SERI published a Survey of Biomass Gasification: Vol. I-III, which collected properties of biomass relevant for gasification and described existing gasifier processes (4). This collection of information was very useful when the DOE Office of Alcohol Fuels funded SERI to develop a process to make methanol from biomass starting in January 1980. Although many of the gasifiers described in the survey were designed to make gaseous fuels, none were suitable for making methanol synthesis gas.

In order to make a gas useful as a feedstock for liquid fuels and chemicals, an appropriate gasifier design is needed, and the parameters affecting gasification must be carefully controlled. For methanol production it is necessary to produce a gas high in CO and H_2 and to minimize the methane and higher hydrocarbons, nitrogen and char. To accomplish this, the SERI high pressure oxygen gasifier was designed, built and tested, starting in early 1980.

Although syn-gas for methanol can be made in principle in fixed-bed, fluidized-bed, or entrained-flow gasifiers, SERI staff chose to build a downdraft, fixed-bed gasifier because of its simplicity of operation, the ability to use larger particles such as wood chips or chunks, the low operating temperatures, high throughput, minimum production of tars and methane, and the suitability for moderate size methanol plants.

1.3 ORIGIN AND CONCEPTUAL DESIGN OF THE SERI HIGH-PRESSURE OXYGEN GASIFIER

Coal is often gasified in "**updraft gasifiers**" (Lurgi, Wellman Galusha etc.) in which char burning at the grate supplies hot gases to pyrolyze the incoming coal from above. This type of gasifier has proved unsuitable for biomass because the high volatile content of biomass results in the formation of 5% to 20% pyrolysis oil, which will clog delivery systems and burners if the gas is allowed to cool. In "**downdraft gasifiers**" the incoming air or oxygen burns the pyrolysis oils, resulting in typically less than 0.2% tar-oil.

The **oxygen gasifier** was initially designed based on the results of experiments on an Imbert type (sometimes called choke plate and nozzle and shown in Fig.

1-1) World War II gasifier operated successfully with oxygen for SERI in 1978 by Environmental Energy Engineering, Inc. (EEE) (5). In these tests it was found that the use of oxygen instead of air for gasification of wood chips increased the temperature less than 100°C, due to a "temperature buffering effect" not previously discovered. However, in Imbert gasifiers there are air injection nozzles at the side and a restriction (choke plate) to promote mixing of the char and gas. These features make it impossible to scale the gasifier to larger size.

The SERI gasification program has resulted in the development of a new class of gasifier which we call **"stratified downdraft gasifiers"** (see below). (Gasifiers of this geometry have since been used by other groups, sometimes under the name "open top" or "topless" gasifiers.) The stratified downdraft gasifier has evolved as a "de-invention" of the World War II downdraft gasifiers shown in Fig. 1-1. The oxygen gasifier of Fig. 1-2 has no restriction to the flow of solids. Air or oxygen comes through the top of the bed and is well mixed with the biomass throughout the reaction zone. By creating a negative pressure (vacuum) on the downstream side of the gasifier, the top can be open for feeding or measurements in air operation. With oxygen gasification, the oxygen can be injected at the top of the gasifier. We have named this geometry "stratified downdraft," since the biomass feed zone, the flaming pyrolysis zone, the active char gasification zone and inactive char zone are distinct, stratified zones through which the biomass particle moves in succession.

1.4 CHRONOLOGY OF AIR-OXYGEN GASIFIER DEVELOPMENT

The project reported here extended from late 1979 through May 1986. The dates of the major stages are given below:

Phase I operation

- o Oct. 1979-Jan. 1980: Conceptual design of gasifier, Graboski and Reed
- o Jan. 1980-Mar. 1980: Detailed design of gasifier, Graboski and Reed assisted by personnel of Hazen Research
- o Apr. 1980-Aug. 1980: Construction of Phase I gasifier under contract to Hazen Research
- o Aug. 1980-Dec. 1980: Shakedown of gasifier operation on air
- o Jan. 1981-June 1981: Operation of gasifier on oxygen
- o July 1981 - Chem Systems converts SERI syn-gas to methanol in the test plant
- o June 1981-Sept. 1981: Design and installation of lock hopper system for pressure operation
- o Sept. 23, 1981: Patent on stratified downdraft gasifier filed
- o Oct. 1981-Mar. 1982: Operation of gasifier at 10 atm pressure

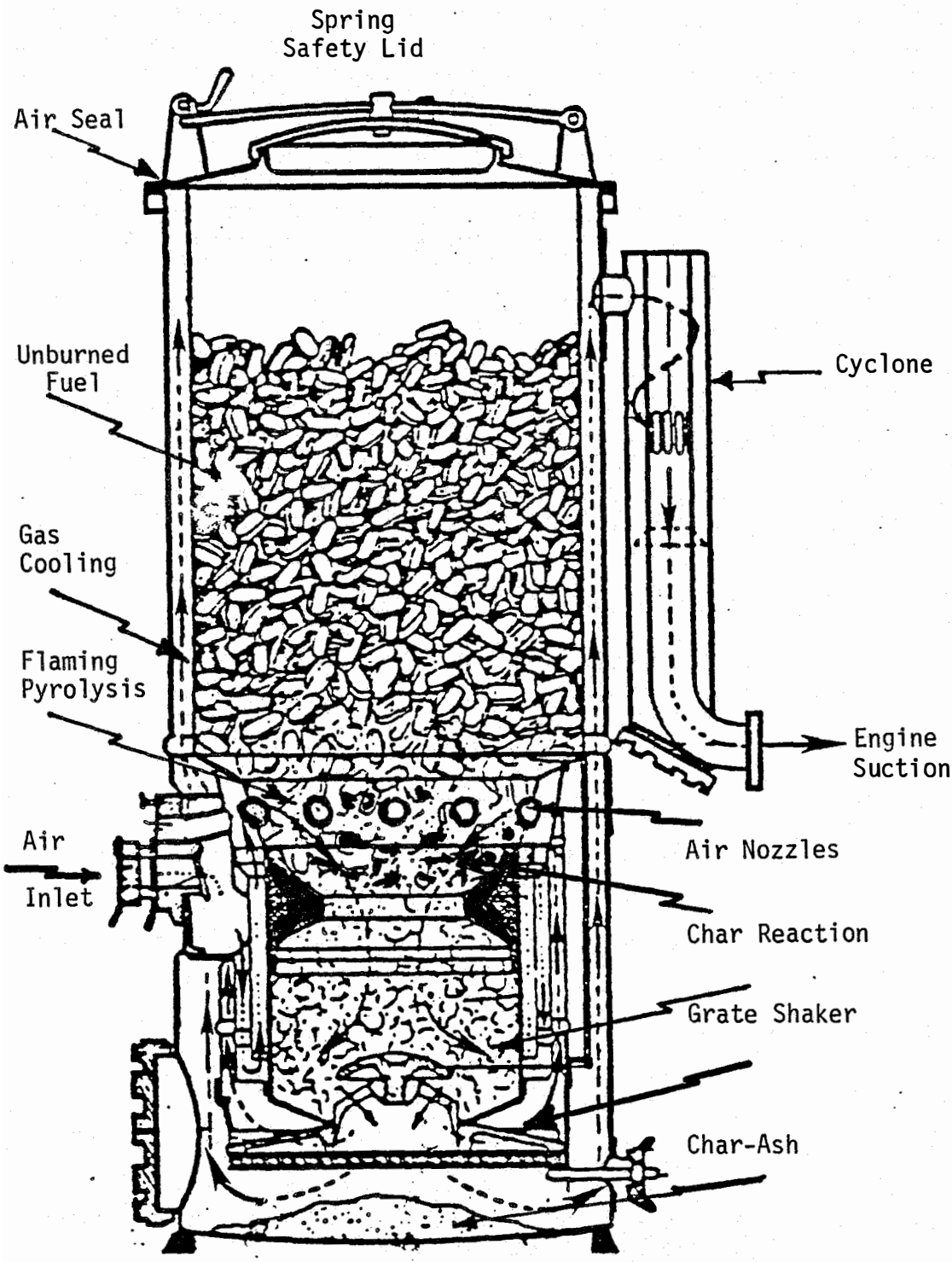

Figure 1-1. Imbert (World War II) Downdraft Gasifier

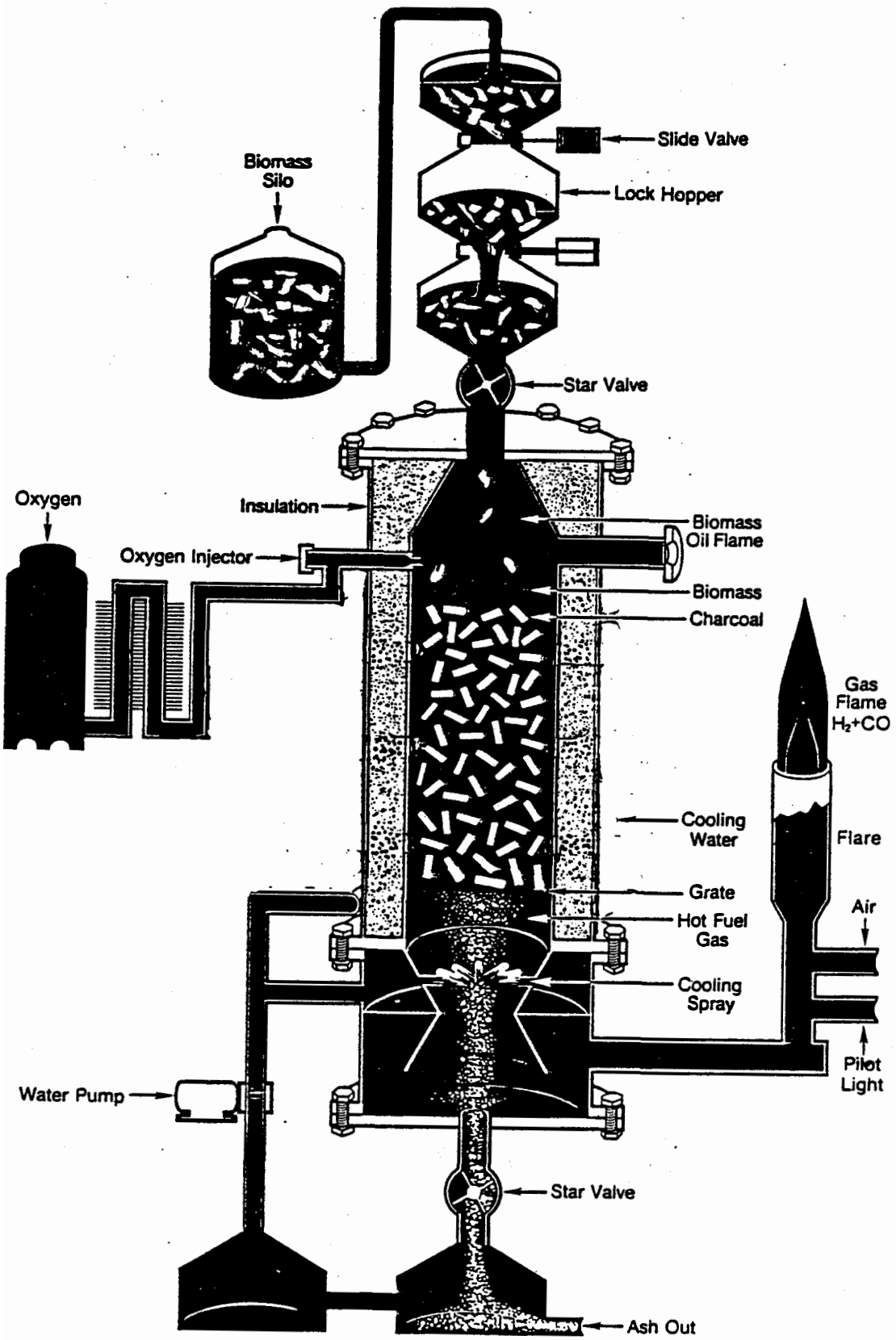

Figure 1-2. SERI/Syn-Gas High Pressure Oxygen/Air Gasifier

o Mar. 3-5 1982:	Biomass-to-Methanol Specialists' Workshop in Tamarron, CO. (Proceedings published in late 1982.) Phase I results described and published (6)
o Mar. 1982-Dec. 1982:	Construction and operation of simplified stratified downdraft gasifiers ("5 gallon" and first transparent gasifier) for scientific testing of gasifier parameters
o Oct. 18, 1982:	Presentation of first modelling paper and poster session "Biomass Gasification Reaction Velocities" at conference"Fundamentals of Thermochemical Biomass Conversion," Estes Park, CO. (7)
o Jan. 1983-July 1983:	Modelling of stratified gasifier based on gasifier studies, papers presented and published 1983-85 (8)

Phase II Operation

o June 1982-Mar. 1983:	Design and modification of gasifier for Phase II testing
o Mar. 1983-June 1983:	Shakedown of Phase II modifications
o July 1983-Jan. 1984:	Parametric testing of Phase II gasifier on wood, corn cobs and peat
o Jan. 1984-Dec. 1984:	Construction and operation of gold insulated transparent gasifier for thermal tar cracking studies
o July 1984:	Formation of SynGas, Inc., to scale up gasifier
o Jan. 1985:	1 ton/day gasifier moved from Hazen to new SERI Field Test Laboratory Building (FTLB) storage
o Jan. 1985-Dec. 1985:	Catalytic tar cracking studies with transparent gasifier
o Aug. 1985-May 1986:	Parameteric and "endurance tests" of 24 tons/day SynGas, Inc., gasifier with air and oxygen

REFERENCES

1. "Energy from Biological Processes," Office of Technology Assessment, OTA-E-124 (1980).

2. C. J. Singer,"History of Technology," (Oxford, 1958), Vol. IV, p. 252.

3. Generator Gas: The Swedish Experience from 1939-1945, SERI/TP-49-183, edited by T. B. Reed (Solar Energy Research Institute, Golden, Republished with index by TIPI Workshop, Allenspark, Colorado, Nov. 1982.

4. T. Reed, editor "A Survey of Biomass Gasification, Vol. I-III," SERI/TR-33-239, (Solar Energy Research Institute, Golden, CO, 1979). Published in hard cover as , Biomass Gasification: Principles and Technology, Energy Technology Review No. 67 (Park Ridge, NJ: Noyes Data Corp, 1981.)

5. Bailey, R. "Hesselman Gas Generator Testing", The Environmental Energy Engineering, Inc., SERI P. O. # AH-8-1077-1, 1979.

6. T. B. Reed and M. Graboski, editors "Biomass-to-Methanol Specialists Workshop," Solar Energy Research Institute, Tamarron, CO, 3-5 March 1982, SERI/CP-234-1590 (Solar Energy Research Institute, Golden, CO, 1982).

7. Reed, T. B. and Markson, M. "Reaction Velocities in a Downdraft Gasifier." in Fundamentals of Thermochemical Biomass Conversion, Edited by R. P. Overend, T. A. Milne, and L. Mudge, Elsevier Applied Science Publications Ltd., 1985.

8. Reed, T. and Markson, M. "A Predictive Model of Downdraft Gasification," in Progress in Biomass Conversion 4, ed. D. Tillman and E. Jahn, Academic Press, 1983 pp 217-255.

CHAPTER 2

DESIGN OF 1 TON/DAY EXPERIMENTAL GASIFIER

2.1 PHASE I - ORIGINAL DESIGN

2.1.1 Gasifier design

A number of biomass gasifiers were commercially available when the design phase of this program started [1]. However most of them produce a gas high in tars and methane, and many were only suitable for small particles or for very large scale. The downdraft type of gasifier used during World War II and shown in Fig. 1-1 produces a very clean, low methane gas. However none of these gasifiers had been built at a large scale or operated on oxygen.

The general design of the oxygen gasifier is shown conceptually in Fig. 1-2 and in more detail in Fig. 2-1, the initial Phase I configuration. A photograph of the installation is shown in Fig. 2-2. The gasifier was located at Hazen, Research, Inc. in Golden, Colorado.

The gasifier is designed to:

- o provide cleaner gas by more uniform mixing of fuel and oxidant at the top of the bed
- o avoid high temperatures and slagging with oxygen operation by reacting the oxygen with the pyrolysing biomass, rather than the charcoal as in updraft gasifiers
- o maintain more even temperatures in the pyrolysis zone by premixing fuel and oxidant
- o operate in a continuous mode using a star type feeder and lock hopper rather than the batch mode in which all previous downdraft gasifiers operated
- o operate at a pressure greater than atmospheric
- o permit combustion of pyrolysis vapors in an insulated chamber above the solid bed, (in the oxygen or closed top mode) reducing heat loss and increasing efficiency
- o permit improved material flow by eliminating the choke plate
- o permit geometric scaling to larger size by eliminating oxidant injection at the side

The original Phase I configuration is shown in detail in Fig. 2-1. The gasifier vessel was constructed from nominal 12-in. diameter, schedule 80 pipe lined with a three in. layer of cast high alumina refractory [2]. The burner and oxygen lances entered through welded ports, and the ends were closed with flanges as shown in Fig. 2-1. The vessel was constructed with a high length/diameter ratio so that the pyrolysis/combustion gas would have adequate contact with the char. It was hoped that this would also give additional cracking of the tar vapors.

A bucket elevator raises the feed to a star valve for atmospheric pressure

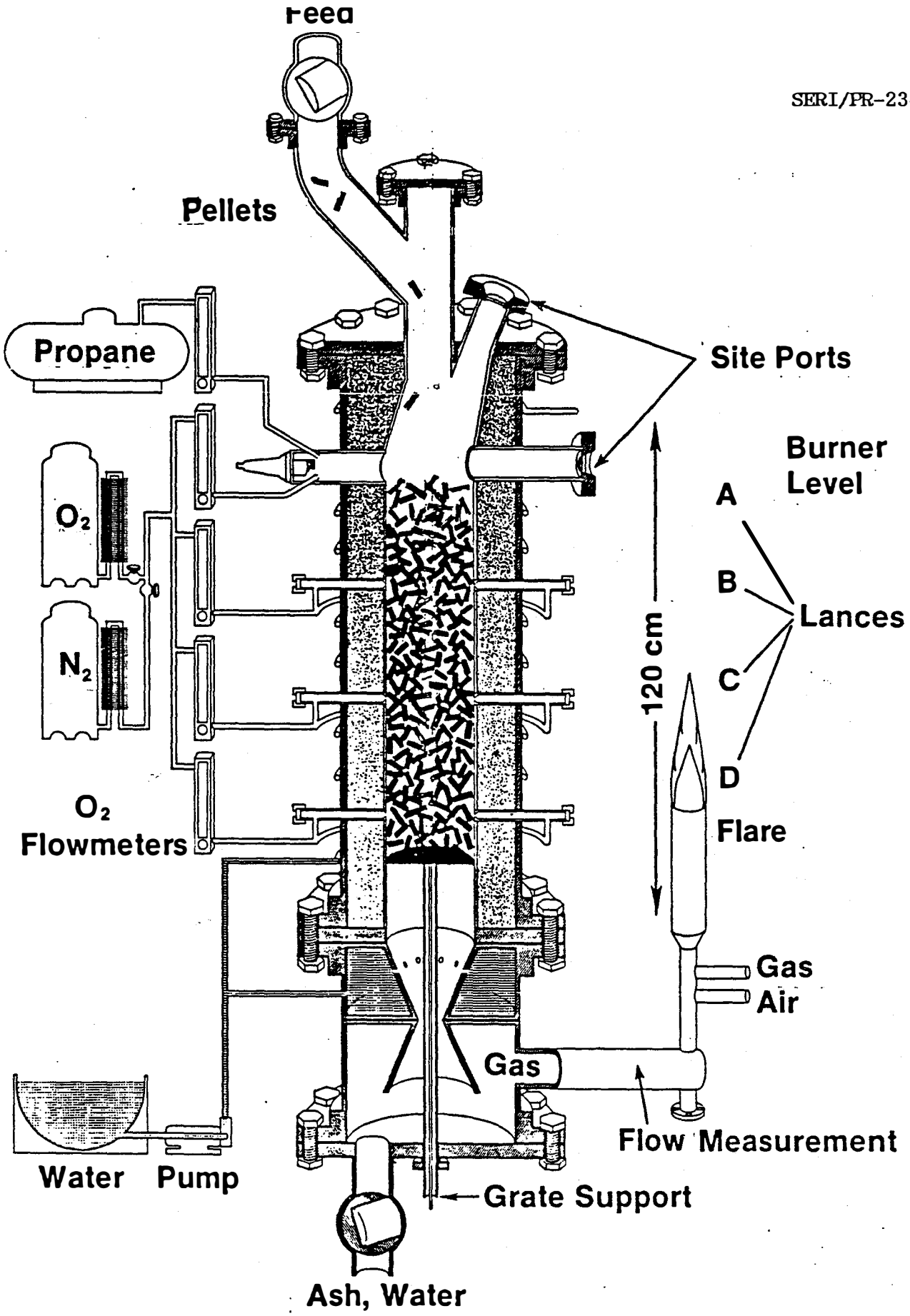

Figure 2-1. Phase I oxygen gasifier configuration

operation or a lock hopper system for high pressure operation. The off-gas enters a Venturi scrubber after leaving the grate and is finally flared. A photograph of the complete installation including the lock hopper is shown in Fig. 2-2. A flowsheet of the system is shown schematically in Fig 2-3; details of the lock hopper system are shown in Fig. 2-4, and the complete piping and information diagram is shown in Fig. 2-5.

The gasifier bed comprises four zones that are reasonably well delineated from each other. These are described in more detail in Chapter 8 (Modelling). A tangential propane burner is incorporated in the top section (which is free from feedstock particles) to preheat the refractory and ignite the fuel on startup. Feedstock falls through this topmost burner zone onto the bed. It was found that during oxygen operation, the flaming pyrolysis zone (see chapter 8) was established above the surface of the bed, and much of the volatile material of the feedstock was convected upward into this section where it burns in the gas phase with a hot flame in oxygen. However, with air operation, the flaming pyrolysis zone occurs generally below the surface of the feed, and no flame is visible on top. In this case the pyrolysis oil flame above the bed is replaced by the unburned feed particles, forming a feedstock reservoir.

Pyrolysis is completed in the second stage as hot gases and fuel pass down the vessel. This second zone may be many centimeters thick for large feed particle size and high rates of throughput, or very thin for small particles with low throughput.

In the third stage very hot combustion products from the pyrolysis-air/oxygen flame contact the charcoal remaining after pyrolysis to reduce the CO_2 and H_2O to CO and H_2. This reaction is very endothermic and cools the gases to about 800°C where the reaction is very slow.

Finally, the bottom zone ,which is supported on the grate, is composed of char/ash that is too cold to react significantly with the gases. It is very important that the smaller particles be continuously removed from this zone to

prevent pressure buildup. As the gas comes off the wire-mesh grate, it is quenched in a venturi scrubber. The water is removed in a settling tank, and the gas is flared.

2.1.2 Piping and instrumentation

The piping and instrumentation diagram of the original high-pressure oxygen gasifier is shown in Fig. 2-5. Tanks holding approximately 100 gallons of liquid oxygen and liquid nitrogen were installed behind our laboratory and filled by truck as required. A 250-gallon propane tank was also installed and used for startup of the gasifier. A flare was used to incinerate the gas produced during runs. A boiler was available to provide steam for the gasifier and later for the ejector. A high-pressure water pump supplied water for cooling to various assemblies. A compressor was used to fill cylinders to 1000 psi for methanol synthesis.
The details of the feed and lock hopper system are shown in Fig. 2-4. Wood or other biomass is lifted to the entrance to the star valve or lock hopper system by a bucket elevator. The rate of feed is controlled by the rotation rate of the star valve.

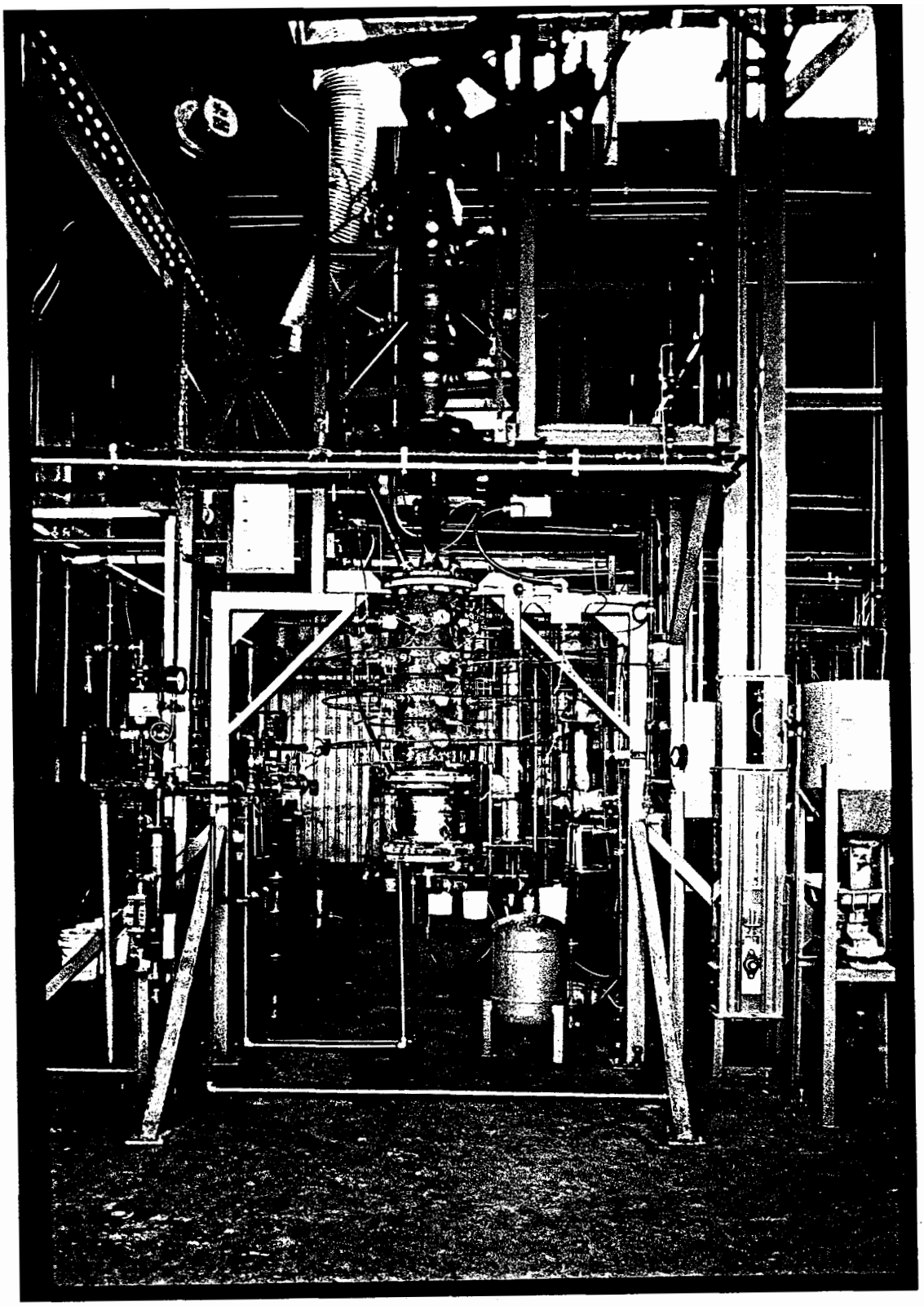

Figure 2-2. Photograph of high pressure gasifier installation: The Fuel hopper and elevator can be seen at right carrying fuel to the lock hopper system at top. Rotary valve and gasifier are directly below lock hopper. Oxygen supply line to nozzles at each of four levels is visible on vessel. Venturi scrubber located at bottom of vessel. Pressure letdown and gas piping to flare located at left.

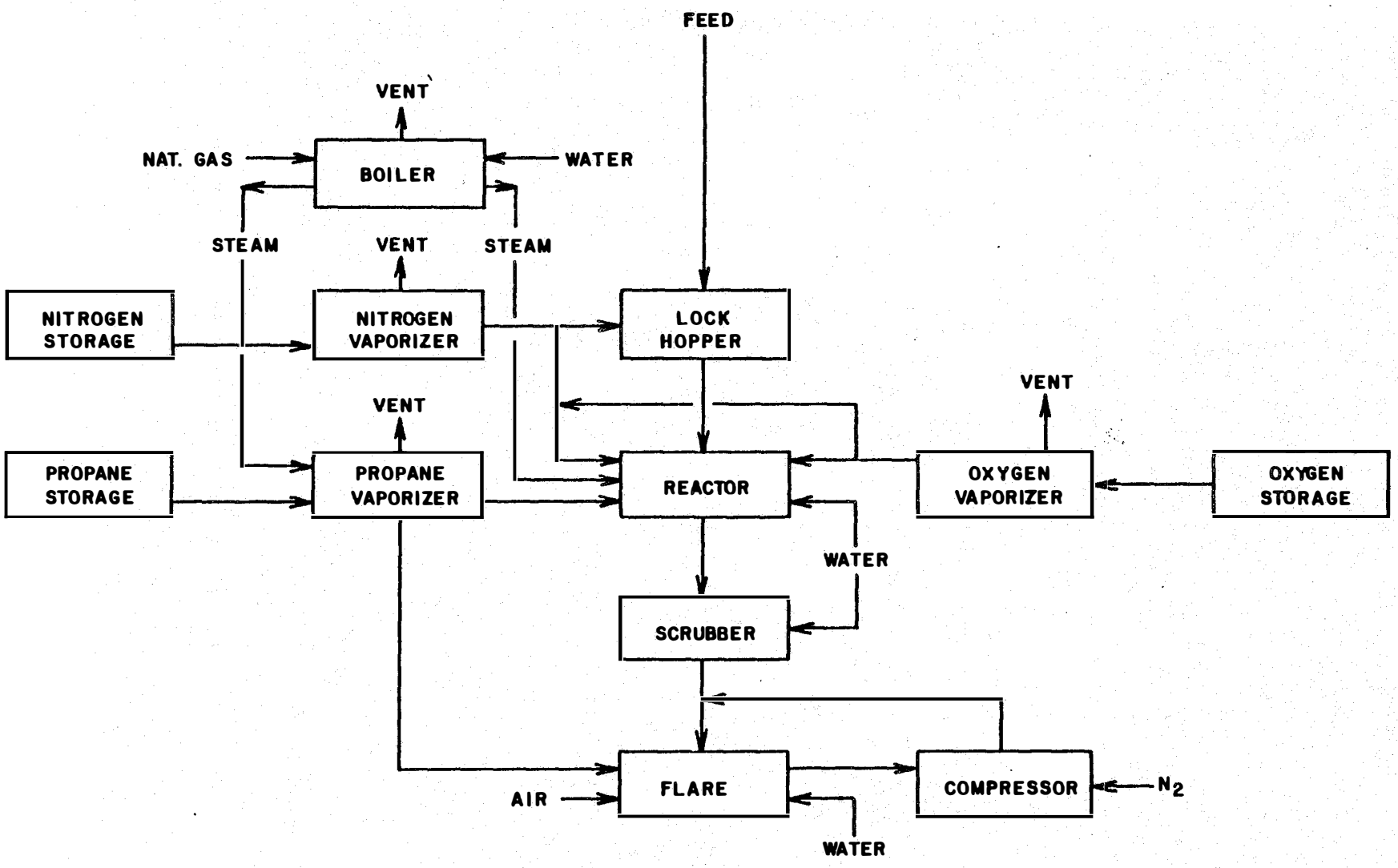

Figure 2-3. Schematic of SERI high Pressure oxygen downdraft biomass gasifier system flowsheet

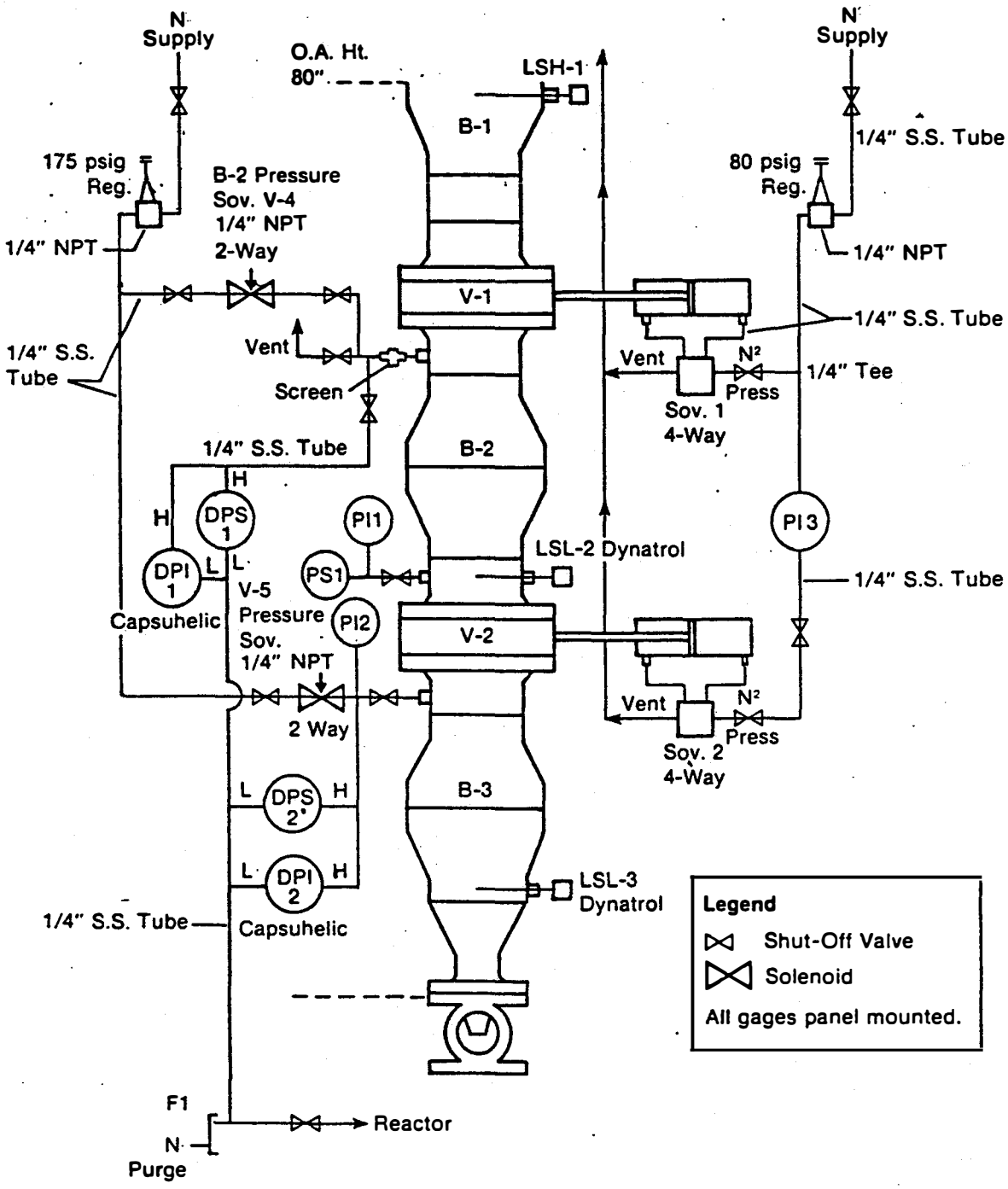

Figure 2-4. Details of SERI Lock hopper feeder system

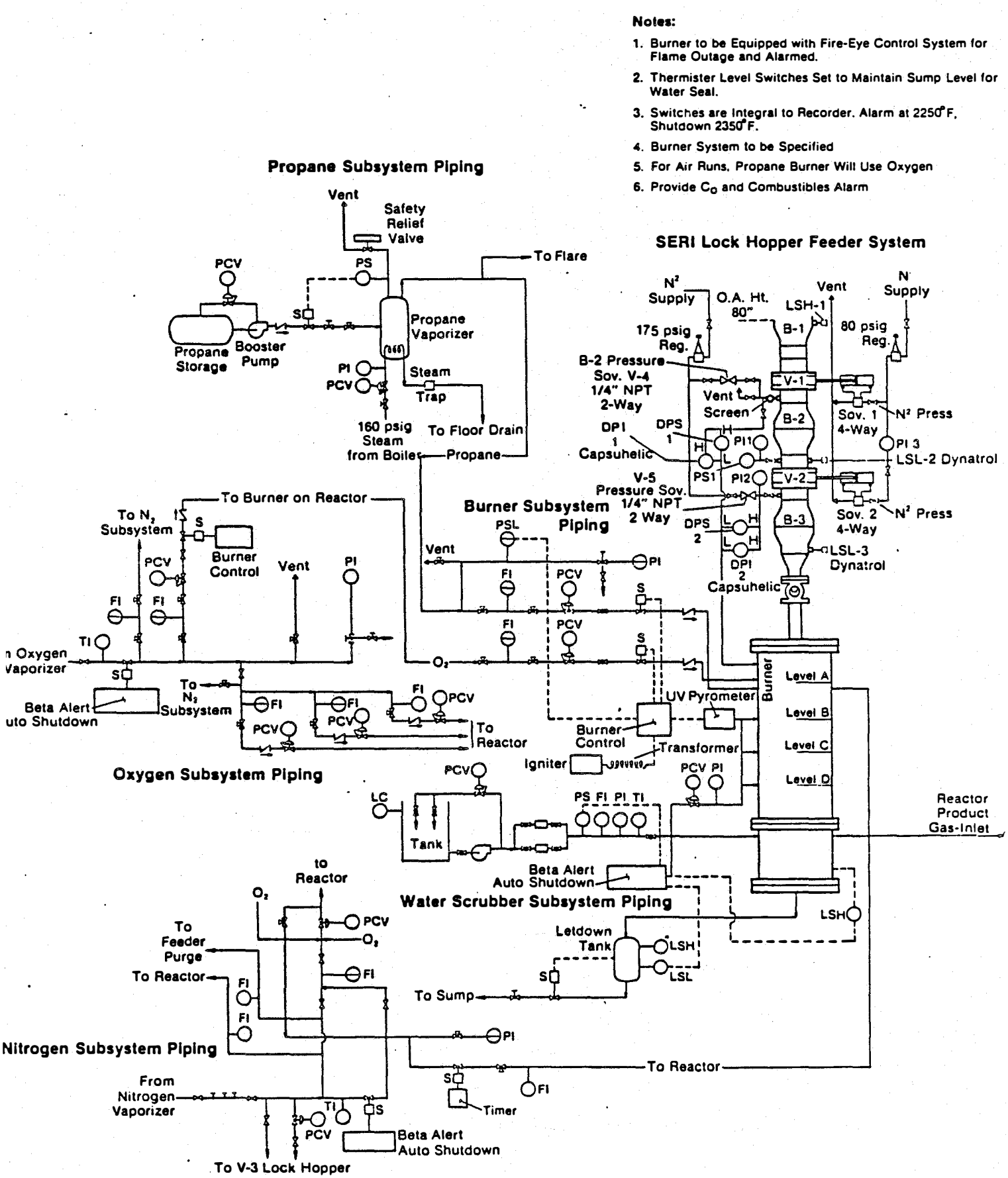

Figure 2-5. Piping and Instrumentation Diagram

Electrical Requirements

1. Propane Booster Pump 1 HP, 110 V, 1 Ø
2. Propane Vaporizer (5 GPH @ 150 Btu/lb — Steam Heated or 1.5 kW Heater — Highrate for Start-Up—)
3. Propane — Line Heat Tracing Required
4. SCR — Control for Feeder — 1 HP DC Drive
5. Steam Boiler — 100V, 1 Ø — Natural Gas
6. Water Supply Pump — 5 HP, 230V, 3 Ø
7. Ash Letdown Lock — 1 HP, DC Drivep
7. Ash Letdown Lock — 1 HP, DC Drive
8. Oxidizer Blower — 1 HP — 230V, 3 Ø

Instruments

1. Burner Igniter/Flame Switch
2. Solenoid Valves — 2 Each
3. Water Flow Switch
4. Vaporizer Controls
5. Temp. Recorder
6. Feed Bin Level
7. Scrubber Level
8. Thermocouple Bundle
9. Flow Transmitter — MV Signal

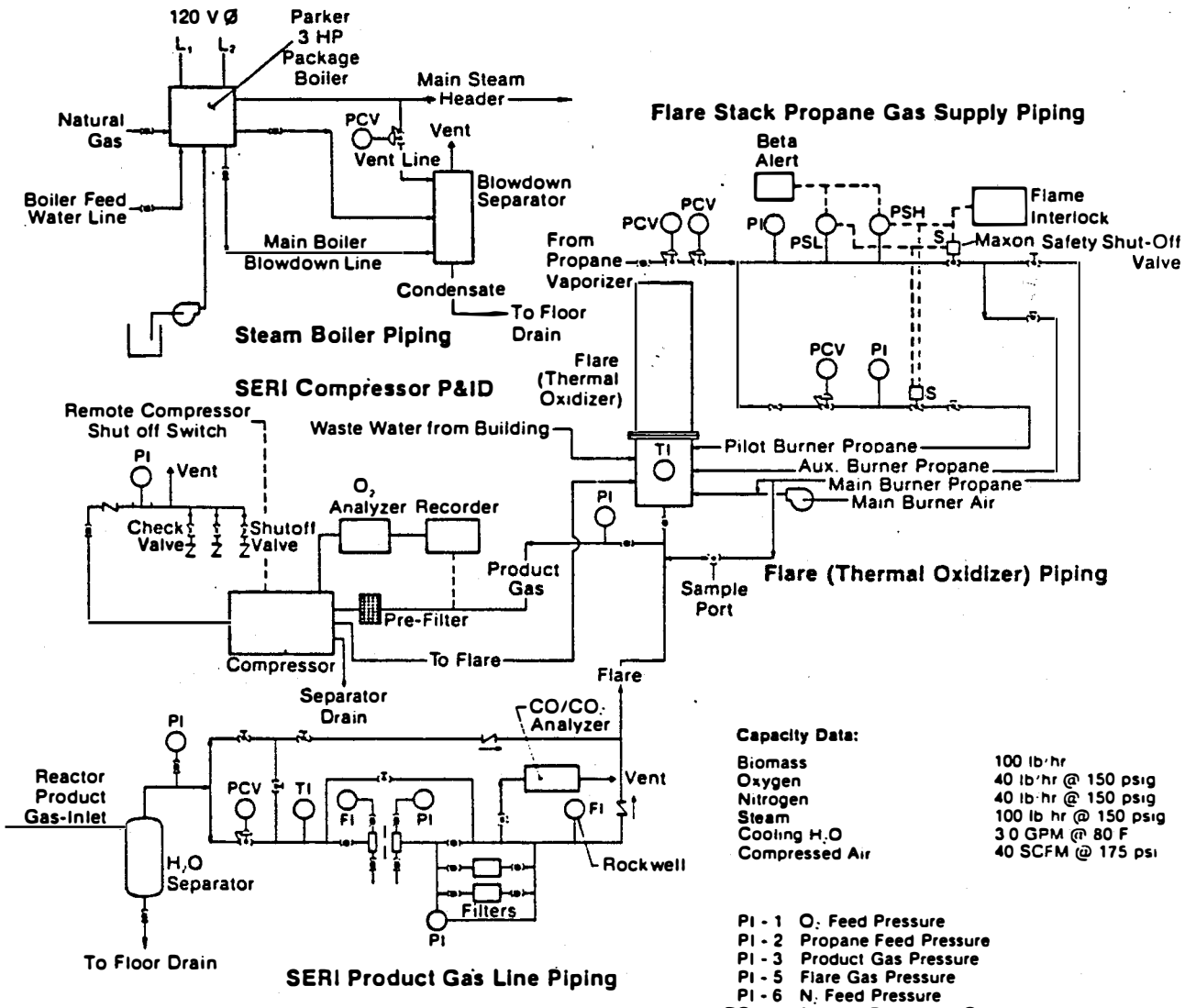

Capacity Data:

Biomass	100 lb/hr
Oxygen	40 lb/hr @ 150 psig
Nitrogen	40 lb/hr @ 150 psig
Steam	100 lb/hr @ 150 psig
Cooling H_2O	3 0 GPM @ 80 F
Compressed Air	40 SCFM @ 175 psi

PI - 1	O_2 Feed Pressure
PI - 2	Propane Feed Pressure
PI - 3	Product Gas Pressure
PI - 5	Flare Gas Pressure
PI - 6	N_2 Feed Pressure
DPI - 1	Reactor Differential Pressure
FI - 1	Main O_2 Flow → Gasifier
FI - 10	Main N_2 Flow → Gasifier
FI - 2	O_2 to Propane Burner
FI - 3	Propane to Propane Burner
FI - 4	Secondary O_2 to Gasifier — Top
FI - 5	Secondary O_2 to Gasifier — Mid
FI - 6	Secondary O_2 to Gasifier — Bottom
FI - 7	Quench H_2O Flow
FI - 9	Jacket Cooling Water

Figure 2-5. Piping and Instrumentation Diagram (Cont.)

The lock hopper is composed of three vessels of equal capacity separated by 8 in. slide valves. The top vessel is always at atmospheric pressure; the middle vessel cycles between atmospheric pressure and system pressure, and the bottom vessel is always at system pressure. Level controllers are used to cause an automatic sequencing of two slide valves to fill the top vessel from the elevator when the top vessel is empty, to drop the feed from the top vessel into the middle vessel when the middle vessel is empty, to close the upper valve and bring the middle vessel to operating pressure, and to open the lower valve when the lower vessel is empty.

A star valve made by modifying a 2-in. plug valve is located at the bottom of the bottom vessel and delivers feed to the gasifier. Feeding was the principal source of trouble in all our work and we recommend that much more attention be paid to feeding problems in any new gasifier projects. Since the time of our work, Thomas R. Miles Consulting Design Engineers has built and improved a number of high-pressure feeders that have performed in a satisfactory manner [3].

The initial piping and instrumentation diagram is shown in Fig. 2-5. Various changes were made as time progressed. Thermocouples are inserted at 10 cm intervals along the wall of the gasifier. They provide important information on the operation and flaming pyrolysis zone position in the gasifier. The temperatures and the pressure drop across the bed are monitored continuously on a 24-point chart recorder. A sample record is shown in Fig. 2-6.

When operating at pressure, the high pressure gas is scrubbed in the Venturi, passed to a regulator which drops the pressure to atmospheric pressure and piped to the flare.

2.2 PHASE II - MODIFICATIONS TO ORIGINAL DESIGN

2.2.1 Reasons for modification

While the original reactor produced high-quality, low-tar gas for periods up to 8 h, the pressure drop across the bed slowly increased from about 0.005 atm at start-up to as high as 1 atm after 4-8 h. This was due to the accumulation of char-ash fines in the bed. Eventually the pressure drop would be so high that a channel would form through the dense bed, allowing oxygen to reach the char at the grate and cause melting of the grate.

In Phase II, changes were made to alleviate this pressure drop increase in the gasifier, allow for larger particles to be fed in the closed top mode, and permit easy, accurate measurement of the char, tar, ash and gas constituents of the product gas. These modifications, shown diagramatically in Fig. 2-7 were made in Spring 1982, and have been instrumental in giving us the capability of making more complete mass and energy balances.

2.2.2 Elimination of oxygen nozzles

It was initially feared that if all the oxygen were added at the top of the bed with the incoming feed, the temperature would be too high for normal metals and refractory materials used in construction. Therefore, a number of nozzles were inserted through the wall at intervals down the vessel to permit addition of part of the oxygen below the oxygen inlet in the top section to moderate temperatures in the top section.

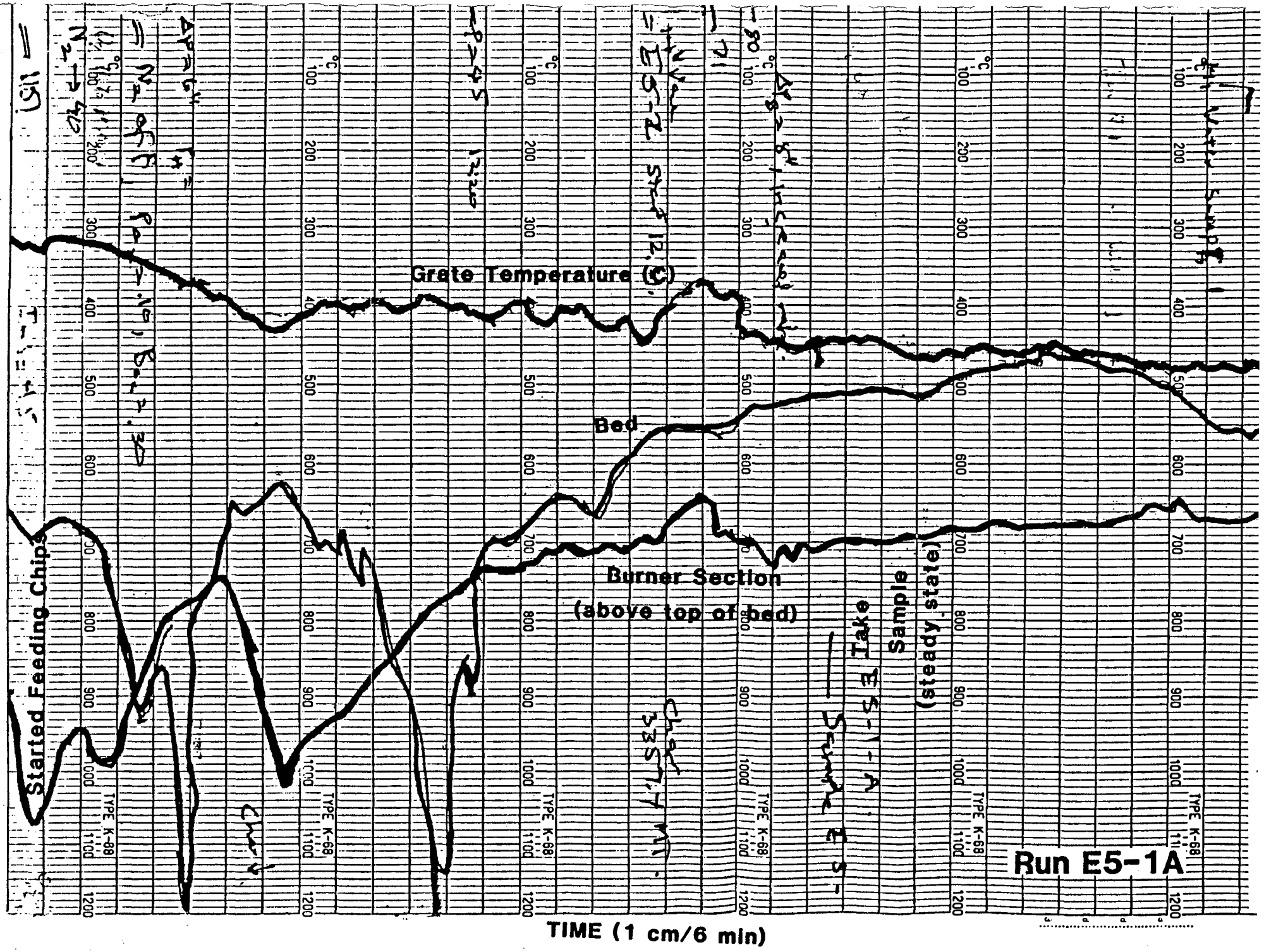

Figure 2-6. Typical temperature trace during run

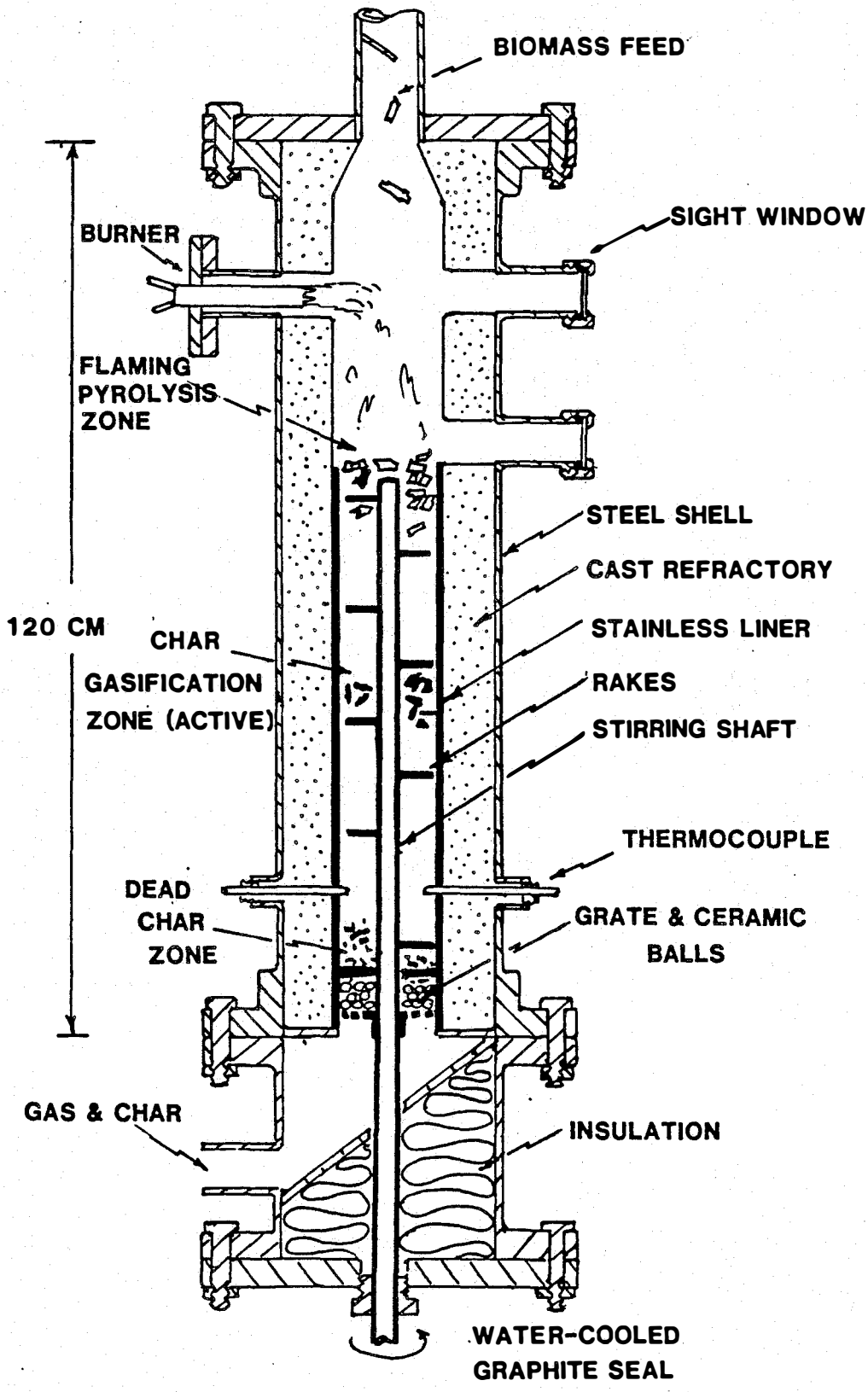

Figure 2-7. Phase II modifications

It was later discovered that the nature of the diffusion flame around each particle and the endothermic nature of pyrolysis moderates the rate of heat release (as long as fresh material is continually available for pyrolyzing) and prevents excessive temperature in the top zones. This modification is an important one in terms of scaling up the reactor, since the penetration of an oxygen jet into a bed of solids would not be possible in large diameter vessels.

2.2.3 Bed stirring assembly

To maintain a low pressure drop in the reactor and permit feeding a wider variety of biomass feeds, a stirring assembly was built as shown in Fig. 2-7. This consists of a 1.32 m (52 in.) stainless steel rod with eight rakes attached and an inconel grate with large slots cut out. Sometimes a few layers of 9.5-25 mm (3/8 to 1-in.) alumina balls were used on the grate to pass spent char at a rate depending on the size of the balls, the hole size in the grate and the rotation rate.

The rakes or plows are constructed from a 0.3-mm stainless steel sheet and installed at a 20 degree angle to gently lift the bed at each rotation. Four 6 mm (1/4-in.) stainless steel bars were inserted 25 mm (1-in.) into the bed through the reactor wall and 5 cm (2 in.) above the grate to insure that the bed would not rotate as a solid unit. Beneath the grate is a dry chamber, consisting of a refractory bottom at a 45 degree angle to facilitate char removal by gravity to the pipe leading into the cyclone. There is a water-cooled mechanical seal of graphite, which keeps the stirrer assembly gas tight. A 2 kW (3 hp) motor operating through gear reducers rotates the assembly at rates from 0 to 2 rpm.

In retrospect we believe that it would have been more desirable to have independent rotation speeds on grate and bed. Sometimes it is desirable to provide rapid bed rotation to minimize bridging, but it may not be desirable to rotate the grate at this speed, since this will cause removal of char that is still reacting, and the gas will become more tarry.

2.2.4 Gas cleanup train

The gas cleanup train, consisting previously of only the Venturi scrubber, located below the grate in Fig. 2-1, was completely redesigned, as shown in Fig. 2-8. The old scrubber was designed to remove char, ash and tar simultaneously, by entrainment in large quantities of water. The Venturi scrubber gave clean and cool gas but produced large quantities of slightly contaminated water. This precluded separation of char, ash and tar and thus making an accurate mass balance impossible. We eliminated the Venturi scrubber and allowed the gas to run directly to the cyclone and from there to the flare.

The char outlet of the cyclone was valved and attached to a quick release 18.9 L (5 gallon) container fabricated to store char from the cyclone. This permits continuous operation. The char production rate is measured by weighing this vessel periodically, generally when emptying it.

A water scrubber for tar knock out is located downstream of the cyclone. This scrubber is a 57 L (15 gallon) vessel with three high pressure nozzles. The scrubber uses 10-23 lph (4-6 gph) of water instead of the 450 lph (120 gph) in the original design. The contaminated water is vaporized and burned in the

flare. This scrubber reduces buildup of tar in the piping up to the flare as well as the orifice plate.

2.2.5 Feeder modification

A 76mm (3-in.) plug valve with almost four times the capacity of the original plug valve was installed to permit feeding of larger particles. This valve passes 450 cm^3 per dump and has two dumps per revolution. This change required increasing the diameter of the pipe connecting the reactor and the lock hoppers.

The new feed valve has been the source of unexpected trouble. The increased capacity typically gives surges of feed of 10-30 s duration. This alternately produces an excess of biomass, greatly increasing pyrolysis gases and tar, followed by an excess of oxygen which drives the temperature up and permits rapid pyrolysis when the next feed arrives. This has been moderated using foam insulation to decrease the size of the valve pocket . A more suitable solution would be continuous feed with a screw feeder or a higher throughput with a faster cycle such that the dump cycle time is much shorter than the reactor response time.

2.2.6 Gas Flow

In Phase I, high-pressure oxygen and nitrogen were used to move the gas through the system. In Phase II, a large capacity blower was installed to operate the system at a slightly negative gauge pressure. With air operation, this permits running with an open top so that probes can be inserted in the bed for measurements, and larger feeds can be charged in the reactor. It also permits operating in oxygen with approximately zero pressure drop across the plug valve to minimize leakage. The blower moves 500 m^3/h (2400 cfm) of gas and maintains a pressure drop of 3.4 kPa (14 in. of water) in the open top mode of the system.

During the first low-pressure oxygen run, a flashback (explosion) occurred, probably due to an air leak through the shaft bearing of the blower. The expanding gases damaged the sheet metal casing of the fan. In order to avoid the possibility of this occurring again it was decided to replace the fan with the gas ejector (sometimes called an eductor) shown in Fig. 2-9 An eductor uses a high-pressure gas, called the motive gas, to entrain the suction gas, in this case producer gas. High-pressure nitrogen was used as the motive gas for early runs and steam in the later runs. The ejector we have designed entrains about twice the volume of gas as the nitrogen or steam which is injected.

The present design uses a Fox Venturi with a 17-mm (0.676-in.) diameter throat. The nozzle for the high-pressure nitrogen has a 1.1-mm (0.045-in.) throat reamed to a 1.4-mm (0.055-in.) exit diameter to permit supersonic flow. The nozzle is mounted in a 9.5-mm (3/8-in.) diameter stainless steel tube which is permitted to swivel and move in and out on a ball joint attached to the piping in front of the Venturi as shown in Fig. 2-9. Figure 2-10 shows the pressure (negative) vs. flow for this ejectcor, with a motive flow of 3.4 m^3/h (120 scf/h) of nitrogen. More recently we have operated the ejector on steam. Both gases are very satisfactory. Since it is completely enclosed in a arun of pipe, the ejector operates quietly, an important safety feature for personnel exposed 6-12 h during a run.

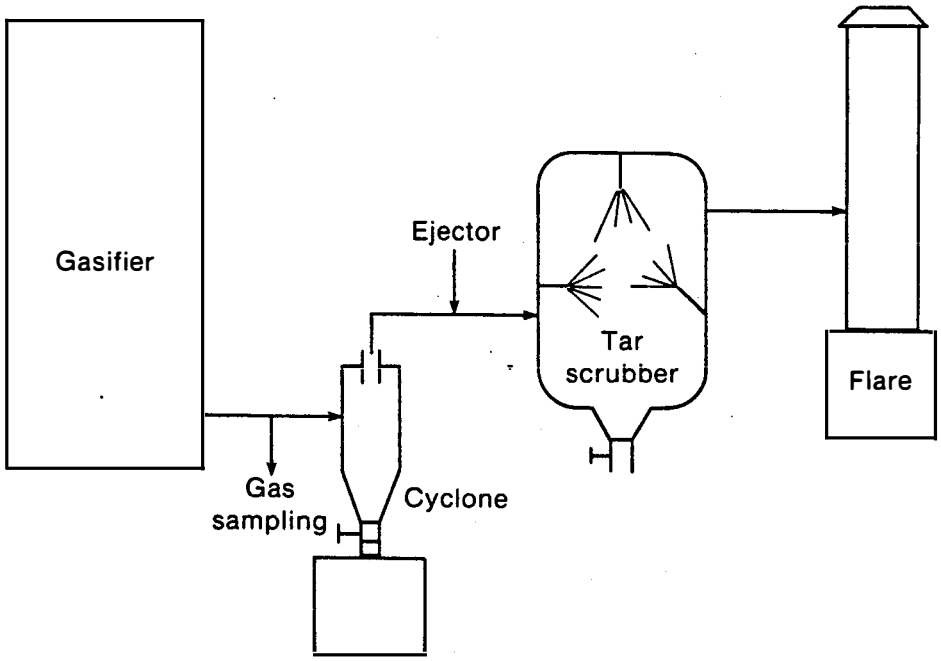

Figure 2-8. Gas cleanup train

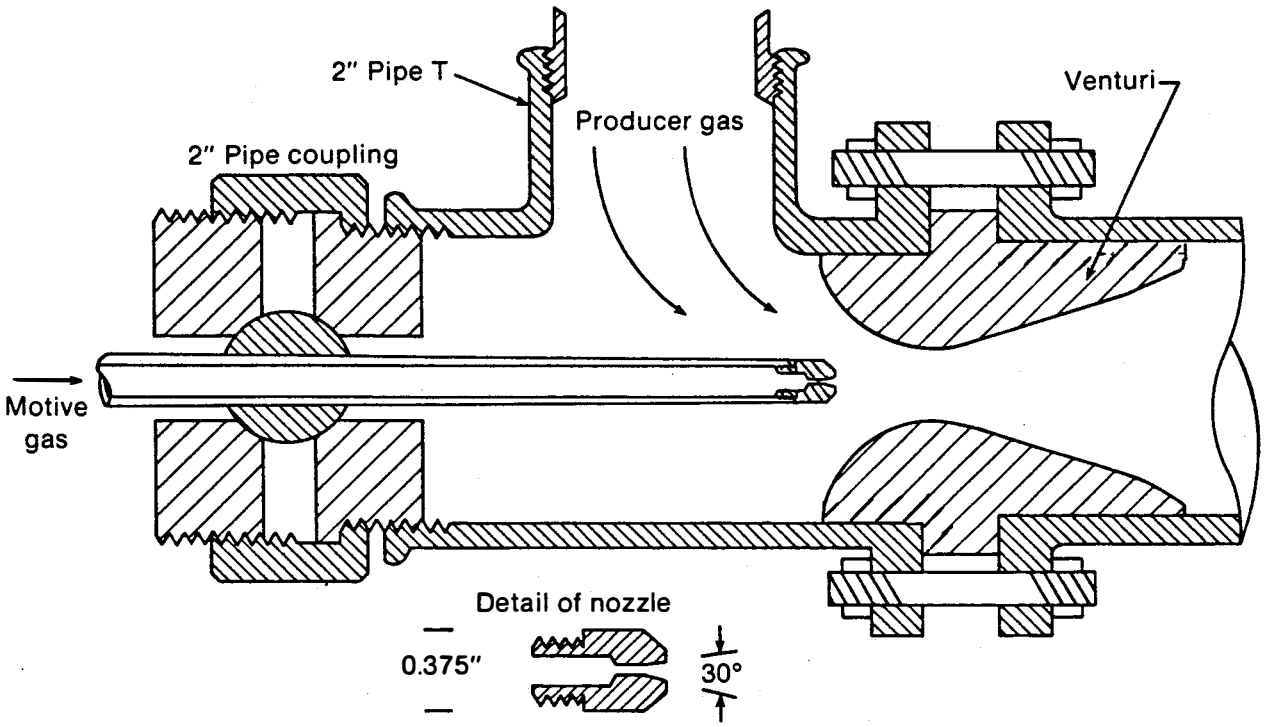

Figure 2-9. Steam ejector for moving hot gas

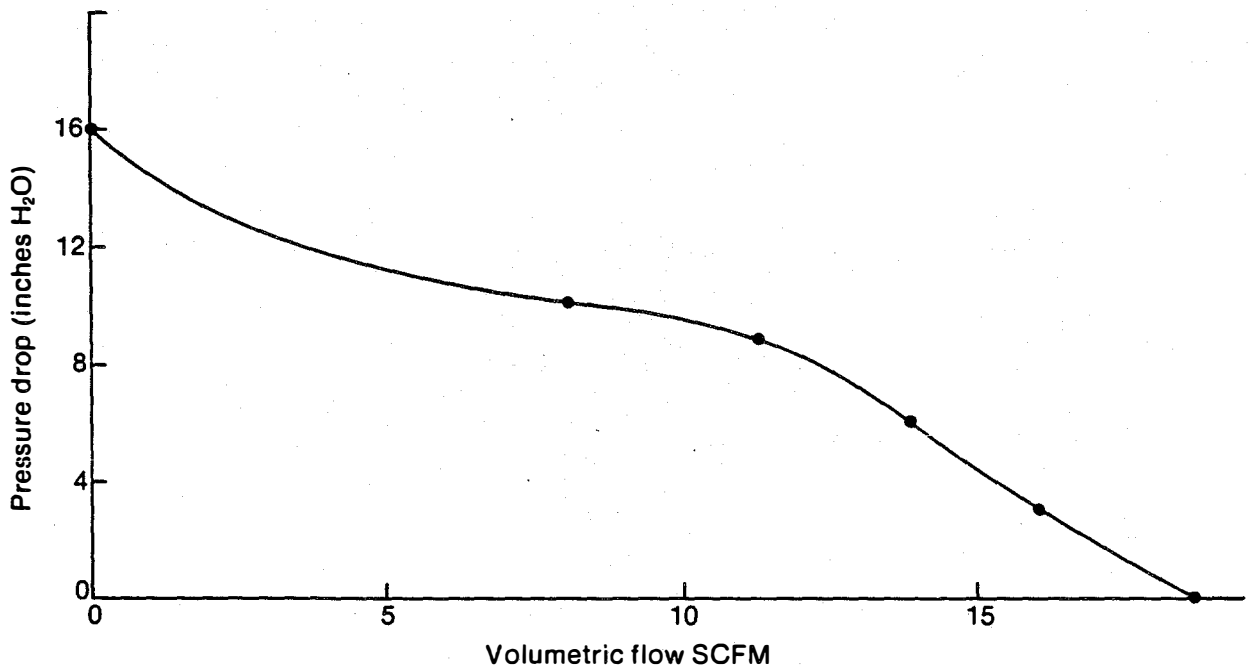

Figure 2-10. Relation of pressure to gas flow in ejector

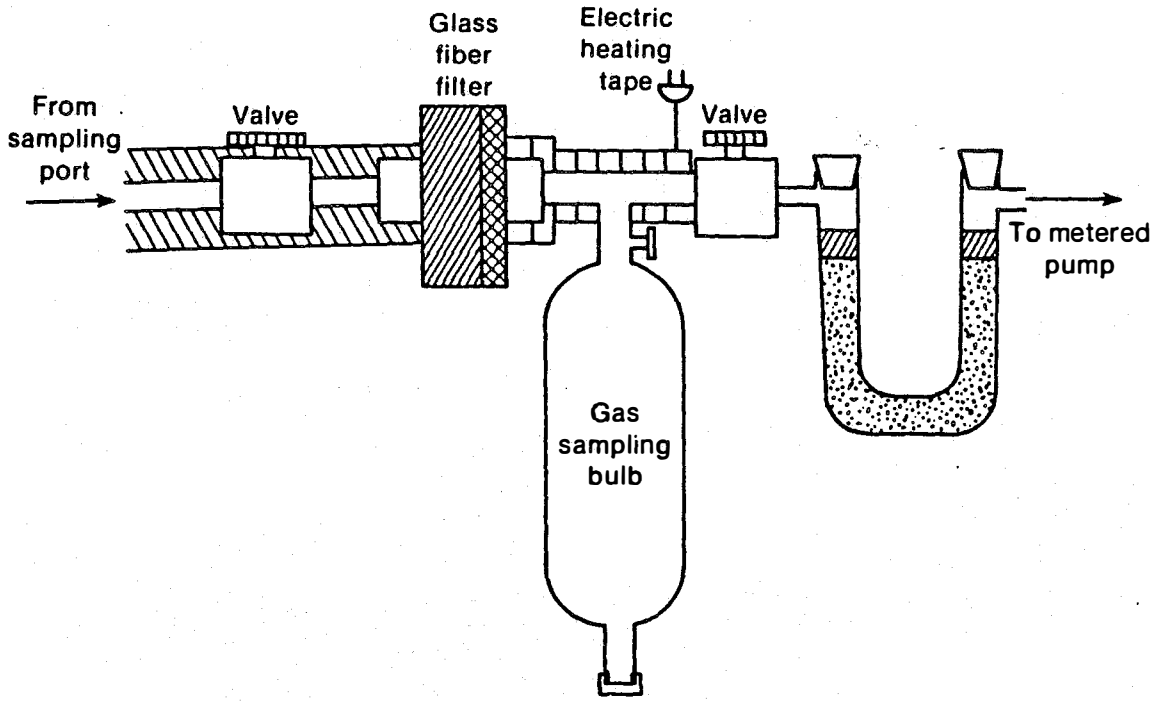

Figure 2-11. Gas Sampling Train

2.2.7 Gas sampling

In order to make a mass and energy balance on the gasifier it is necessary to analyze the gas and measure the amount of tar produced. The gas sampling train in our system has evolved considerably to the configuration shown in Fig. 2-11. A sampling port downstream of the cyclone is used to take a slip-stream of gas through a heated filter, a preweighed drierite trap, and a handpump with which we typically extract 3 liters (0.1 ft^3) of gas from the system. A chilled, evacuated steel sample bulb is also filled downstream of the filter and subsequently analyzed on a Carle gas chromatograph. This has proved the most satisfactory method of gas sampling, but an accurate continuous method also would be desirable to show trends and instantaneous results.

2.3 PREFERRED CONFIGURATION

2.3.1 Open vs closed top operation

In the period since the stratified downdraft gasifier was invented at SERI a number of other gasifiers have appeared with similar geometry and operation, sometimes after discussions with SERI personnel during visits [4-6]. Feedback from these similar units has been an aid to us in development of the gasifier.

We have found, and others have observed, that it is possible to operate the gasifier in air with no upper seal, provided the moisture content of the wood is less than 20% and more than 8%, wet basis. or other stabilization is provided. In this case there is then a layer of unburned biomass which distributes the incoming air and provides insulation above the flaming pyrolysis zone. This has a number of advantages. It eliminates the need for a star valve or other sealing device at the feedstock input. It also makes possible easy insertion of sensors from above without requiring seals.

On the other hand, the open top design has several disadvantages. Obviously, the gasifier cannot be operated at positive pressure nor with pure oxygen. Not so obvious is the fact that the flaming pyrolysis zone is quite different in nature. With the open top, the reaction must move up against the incoming cold air, while the heat produced by the pyrolysis moves primarily downward with the gas. With a closed insulated top, the gasifier can be operated with the combustion of some of the pyrolysis products occurring in the gas phase on top of the bed. The resulting luminous flame heats the refractories to a high temperature, and they in turn radiate to the bed, providing ignition, tar combustion and some fraction of the pyrolysis above the bed. The highest throughput observed with the open top gasifier is 10 GJ/h-m^2 (1 MM Btu/h-ft^2) while for the closed top the highest rate has been 30 GJ/h-m^2 (3 MM Btu/h-ft^2). This may also be due to the ability to force more air/gas through the bed in a pressurized gasifier.

2.3.2 Low char-ash removal and uniform feed distribution for low tar production

The gasifiers described in this report typically produce less than 1% tar and often less than 0.1% tar, but more attention needs to be paid to the factors that minimize tar.

In Phase II we learned that a grate with variable rotation can modulate the amount of char-ash produced, from a minimum of 3% at no rotation to over 10%

with 1 rpm rotation. At higher rates of char-ash removal, less oxygen/air is required for gasification so less is available for flaming pyrolysis, and the pyrolysis zone is colder. We have produced 5% tar by operating with vigorous char-ash removal. A similar effect has been observed by Chern and Walawender [7,8].

We also observed that the biomass and air/oxygen must be uniformly distributed both in space and time. We observed higher tar levels with the larger feed valve that added feed every 20-30 s. Also we observed an increase in tar production when the biomass was not uniformly distributed across the bed.

REFERENCES

1. "A Survey of Biomass Gasification, Vol. I-III", *SERI/TR-33-239*, ed. by T. Reed, Solar Energy Research Institute, Golden, CO, 1979. Published in hard cover as "Biomass Gasification: Principles and Technology", T. Reed, editor, Energy Technology Review No. 67 (Noyes Data Corp, Park Ridge, NJ, 1981).

2. Castolite 30 from A. P. Green Co.

3. Thomas R. Miles, Consulting Design Engineers, 5475 S. W. Arrowwood Lane, Portland, Or 97225.

4. Rogers, C., Personal Communication, The Buck Rogers, Co., 150 Industrial Parkway, Industrial Airport, KS 66031, 1985.

5. Kaupp, A., "Gasification of Rice Hulls: Theory and Praxis", published by *Deutsches Zentrum fur Entwicklungstechnologien - GATE.* Vieweg, Wiesbaden, 1984.

6. LaFontaine, H., Personal Communication, H. LaFontaine, The Biomass Energy Institute, 1995 Keystone Blvd., Miami, FL 33181, 1984.

7. Chern, Shyh-Ming, "The Gasification of Biomass in Commercial Downdraft Gasifiers", *Masters Thesis,* Kansas State University, 1985.

8. Wallawender, W. P., Chee, C. S. and Fan, L. T., "Operating Parameters Influencing Downdraft Gasifier Performance", in *Energy from Biomass and Wastes Symposium XI,* Orlando Fla., March 1987 to be published.

CHAPTER 3

RESULTS ON 1 TON/DAY EXPERIMENTAL GASIFIER

3.1 INTRODUCTION

This chapter includes data on the most important runs made on the 1 ton/day gasifier. Since this was a new type of gasifier it was necessary to learn its principles of operation and its advantages and limitations. The gasifier was continually modified in an effort to improve its performance, and only enough data was taken at each stage to determine the results of the latest change.

It is important to realize while evaluating the data that this project developed into an equipment development program, rather than an attempt to establish performance of an established apparatus. The authors did not initially intend that the new design would be radically new, but the design changes turned out to be very significant, resulting in a new gasifier type widely used now around the world. Viewed in this light, the data tells a great deal about the behavior of stratified downdraft gasification, but one will find gaps and inconsistencies.

3.2 PHASE I RESULTS

3.2.1 Startup and Early Shakedown Tests

The system was started by filling the gasifier with charcoal a distance of 20 cm above the grate. The charcoal and gasifier were heated to 600°C with the propane burner at level A of Fig. 2-1. Wood chips were then fed slowly until they reached the viewport at level A, forming a deep bed of chip charcoal. Finally, the burner was extinguished and the oxygen flow established, typically with 70% of the oxygen injected into the top section and 10% in each of the injectors bands at levels B-D.

In order to achieve a steady state, it is important to maintain a constant level in the bed. In operation, the level of chips was maintained constant by observation and adjustment of the feed rate. Although this was relatively satisfactory, it required constant attention. A K-Ray Gamma Radiation bed level controller was installed for runs 26 and following runs, and was used to control the bed level by varying the feed rate through the plug valve. The controller maintained the bed level within 3.8 cm (1 1/2 in.) and was relatively satisfactory.

3.2.2 Atmospheric Pressure Oxygen Operation

The results of 15 early runs were reported at the Tamarron meeting in March 1982 [1]. Some of these results are included here. Runs 1-10 were a learning experience for the operating crew. They were qualitative in nature and indicated needed changes in apparatus or method of operation. The notebooks are filled with data and observations, but they do not give any consistent picture.

Although a variety of sizes of feedstock were tested, most of the work in Phase I was done with 5 mm (3/16 in.) wood pellets, 6 mm (1/4 in.) pellets and small "mini" chips approximately 1 cm x 1 cm x .3 cm (3/8 in. x 3/8 in. x 1/8in.), which we prepared from pine lumber. These sizes were dictated by the

tendency of the 5 cm (2 in.) plug valve (used as a star type feeder) to become jammed when larger material was fed. Analyses of these fuels are given in Table 3-1.

Table 3-1. Feedstock Analyses (Air Dried Samples)[a]

Feedstock	4 mm Pellets[b]	6 mm Pellets[c]	6 mm Pine Chips[d]
Proximate Analysis (Wt %)[e]			
Moisture	3.58	8.36	7.02
Volatile matter	79.91	67.19	78.48
Fixed Carbon	15.65	11.94	14.07
Ash	0.86	12.51	0.43
Ultimate Analysis (Wt %)[e]			
Moisture	3.58	8.36	7.02
Carbon	47.45	41.73	43.79
Hydrogen	5.83	5.03	5.31
Nitrogen	0.23	0.18	0.06
Sulfur	0.03	0.48	0.02
Oxygen	42.02	31.71	43.37
Ash	0.86	12.51	0.43
Total	100	100	100
Gross heating value (kJ/g)	18.1	16.0	18.1
(Btu/lb)	7944	7031	7938

a) Analyses performed by fuel laboratory at Hazen Research, Inc., Golden, CO.
b) 4 mm diameter sawdust pellets from Guarantee Fuels, Inc. Independence, Kansas
c) 6 mm diameter bark pellets from Tennessee Woodex, Inc.
d) 6 mm x 6 mm x 3 mm average lodgepole pine wood chips from Prof. H. Schroeder, Colorado State Univ.
e) Measured as received by Hazen Research Inc. Golden, CO.

3.2.2.1 Atmospheric Pressure Oxygen Results

Pertinent data on oxygen gasification and fuel consumption using 6 mm (1/4 in.) pellets for several of these tests are given in Table 3-2. Gasification tests using pure oxygen were conducted at steady feed rates of 12 to 28 kg/h (25-62 lb/h) of the biomass pellets. Runs lasted typically 4-8 hours.

Table 3-2. Atmospheric Pressure Oxygen Runs

INPUTS					
Test Number	13A	13B	14A	14B	15A
Fuel	<-------4 mm pine sawdust pellets----->				
Wood feed (kg/h, dry)	15.3	12.0	17.2	28.0	16.5
Oxygen Gas (kg/h)	6.8	5.1	7.4	11.7	7.0
O_2/Feed (kg/kg)	0.44	0.43	0.43	0.42	0.43
OUTPUTS					
Dry Gas Analysis (Vol %)					
CO	48.2	-	40.6	48.4	45.2
CO_2	14.7	-	18.8	14.2	18.2
H_2	31.6	-	31.6	32.0	25.1
CH_4	2.2	-	3.9	2.8	4.1
N_2	3.3	-	5.2	2.8	7.3

3.2.2.2 Methanol Synthesis

In order to test the suitability of the product gas for methanol synthesis, a contract was given to Chem Systems to make a small amount of methanol on their test apparatus in Fairfield, N. J.

A high-pressure fuel gas compressor was used to fill 10 ten K size cylinders with product gas, and the cylinders were shipped to Fairfield. The tests are described in Appendix B where Dr. D. B. Blum gives his opinion "that the results are quite comparable to those we have obtained with the similar Koppers-Totzek gas."

3.2.2.3 Discussion of Results

These results were very encouraging and demonstrated that the new gasifier could make a low-methane, low-tar synthesis gas at atmospheric pressure with reasonable oxygen consumption.

The feed rates of Table 3-2 correspond to **specific feed rates** of 620 to 1530 kg/m^2-h (127-314 lb/ft^2-h) at atmospheric pressure. (For comparison, a typical throughput of coal for the updraft pressurized Lurgi gasifier is 680 kg/m^2-h (140 lb/ft^2-h) and the throughput of the pressurized slagging Lurgi gasifier operating at 1800°C (3300°F) is 3252 kg/m^2-h (666 lb/h-ft^2). The highest rate shown in Table 3-2 may not represent the upper limit for the gasifier, since it was limited by the ability to purge the bed of char.

It was a general problem in all runs of Phase I that the pressure drop in the reactor increased gradually with time during each run. When the pressure became high enough, a channel penetrated through the bed through which high pressure oxygen flowed, leading to combustion of the char and possible burnout of the grate, and a sudden drop in pressure.

The problem was finally diagnosed as a buildup of fine char-ash particles at the bottom of the gasification zone. As the char breaks up, small particles build up at a distance of 10-20 cm below the top of the bed and well above the grate. There is no agitation or mechanism for their continued motion so they build up at this point. Several times we noted that the original startup charcoal was still present below this packed zone after 8 h of operation.

The solution to char buildup was operation of the gasifier with shorter beds and installation of an agitator to keep the pressure drop at a minimum, as described in Chapter 2, Phase II.

The **oxygen/fuel ratio** averaged 0.43 for these runs. This ratio is an important dependent parameter, since it affects the economics of gas production. High ratios are associated with high heat loss or high off-gas temperatures; they increase gasification cost, and they burn up more product than necessary. Low ratios do not completely convert the volatiles and char to gas and indicate incomplete gasification.

The **dry gas analyses** for oxygen runs 13-15 are shown in Table 3-2. The nitrogen concentrations in these runs result from purges of the feeder and sight ports. The **methane production** is relatively low (2.3% to 4.4% on a nitrogen-free basis). It is important to have low methane for chemical synthesis since it acts as a diluent that must be purged from the synthesis loop for methanol or ammonia production.

It was not possible to make a mass balance in these runs because the char and tar were washed away by the Venturi scrubber. A different system was installed in Phase II.

3.2.3 High-Pressure Oxygen Runs

3.2.3.1 Description of Runs

The high-pressure runs were typically much more difficult than atmospheric runs. This was due in part to the feeding and sealing problems of our "home-made" lock hopper system. Commercial lock hopper systems for biomass (such as the Tom Miles feeder [2]) have become available since those runs; however, they also continue to have operational problems. A second problem was that the insulation, which was satisfactory at atmospheric pressure, permitted some oxygen and gas to bypass sections of the bed so that not all gas passed through the whole bed.

The data available for high-pressure operation is less extensive and less reliable than that for atmospheric pressure operation. We present what is available here with all its problems in hopes it can be useful to future workers in this field.

We recommend that future gasification programs put much more stress on reliable feeding, level control systems, and high-presure feed systems. Also, in retrospect, the 15 cm inside diameter may be too small a scale at which to test high-pressure gasification.

The gasifier was started at atmospheric pressure and brought to a steady state, a process requiring about 90 m. The pressure in the system was gradually increased using the back-pressure regulator shown in Fig. 2-5, generally in several stages. A steady state was maintained while gas samples were taken.

3.2.3.2 High-pressure Oxygen Results

Table 3-3 gives the inputs and outputs to the gasifier for runs 19, (a-d) at pressures of 700 and 1100 kPa (90 and 150 psi) using wood pellets and chips as feedstocks.

Another set of runs was made after the bed level controller was added and these are shown in Table 3-4. Gas analyses from these runs are shown.

3.2.3.3 Discussion of Results

A number of derived results are also shown in the tables. The extended tables in this chapter were produced with a Lotus 123 spreadsheet. The format of this table is followed for most of the remaining data in this chapter.

Gas analyses measured on a gas chromatograph are presented in Tables 3-3 and 3-4. Nitrogen levels are undesirably high because of leakage through the lock hopper and feeder plug valve. Though the gas energy content is high relative to air gasification, it falls off at the highest pressure (Run 19d) with a corresponding increase in oxygen consumption.

In retrospect the increase in oxygen consumption and the decrease in gas

quality are probably due to a relatively high heat loss caused by the small gasifier size and poor insulation. The heat loss would be expected to increase along with oxygen consumption at high-pressure as was observed. These losses would be greatly reduced on larger systems.

Table 3-3. High-pressure Oxygen Gasification Results

INPUTS				
Test Number	19-B	19-C	19-D	19-A
Fuel	<--6mmX6mmX3mm pine chips->			<-6 mm Wood->
Fuel Analysis (Vol %)				Pellets
Moisture (%)	7.0	7.0	7.0	8.4
Carbon	47.1	47.1	47.1	45.5
Oxygen	46.6	46.6	46.6	34.6
Hydrogen	5.7	5.7	5.7	5.5
Nitrogen	0.1	0.1	0.1	0.2
Ash	0.6	0.6	0.6	14.2
HHV (MJ/kg,dry,ash free)	18.1	18.1	18.1	18.5
Gasifier conditions				
Pressure (kPa)	700	700	1120	700
Wood feed (kg/h,dry)	14.58	14.58	11.41	17.50
Oxygen Gas (kg/h)	7.67	7.67	5.97	7.90
Nitrogen gas(kg/h)	4.14	3.85	9.22	7.14
OUTPUTS				
Dry Gas (kg/h)	21.3	25.0	28.6	27.5
Water (g/NM3)	266	152	38	152
Char-ash (est.) kg/h	0.6	0.6	0.5	3.0
Dry Gas Analysis (Vol %)				
CO	44.7	44.2	24.1	39.7
CO_2	20.9	19.6	22.4	14.3
H_2	13.7	18.9	15.8	20.9
CH_4	1.7	3.2	7.2	2.5
N_2	19.1	14.2	30.6	22.6
Gas Properties				
Mole Weight (g)	27.6	25.8	26.6	24.6
Dry Gas HHV (MJ/NM3)	8.7	10	8.5	9.3
Gas Density (kg/NM3)	1.33	1.25	1.28	1.18
OPERATING RATIOS				
O_2/Dry Feed	0.57	0.57	0.57	0.49
CO/CO_2	2.14	2.26	1.08	2.78
H_2/CO	0.31	0.43	0.66	0.53
MASS BALANCE AND ENERGY EFFICIENCY				
Mass in/Mass out	0.98	0.93	0.91	0.98
Dry Gas efficiency	0.68	0.87	0.95	0.67

Table 3-4. Enriched Air Gasification and Oxygen Gasification [a]

Run	31-A	31-B	31-C	31-D
Oxidant	Enriched air (60% O_2)		Oxygen	
Pressure	101 kPa	101 kPa	101 kPa	772 kPa
Dry Gas Analysis (Vol %)				
CO	23.98	38.27	43.00	25.17
CO_2	9.06	14.35	20.09	27.53
H_2	15.47	23.92	30.40	20.22
CH_4	1.77	3.76	3.04	4.27
N_2	49.72	19.70	3.47	22.81
MJ/nm3	5.6	8.8	9.8	6.2
MJ/nm3 (N_2 free)	10.5	10.9	10.1	8.1
T°C (below grate)	852	760	760	624
CO/CO_2	2.65	2.67	2.14	0.91
H_2/CO	0.65	0.62	0.71	0.80

a) 3/16 in. diameter sawdust pellets from Guarantee Fuels, Inc. Independence, Kansas

Table 3-3 presents a calculated mass and energy balance. The mass balance accounts for 0.91 to 0.98 of the input in output gas and char. Char-ash was not measured on these runs, so for this mass and energy balance the amount of char was estimated as 4% of the biomass feed plus whatever ash was in the feed. This estimate was taken from later runs of a similar nature where char was measured.

The dry gas efficiency is taken as the energy value in the dry gas produced divided by the energy in the feed. The efficiency of the gasifier varied between 68% and 95% for these high-pressure runs. One weakness of the energy balance is that the gas is typically sampled over 30-60 s, while the feed is measured over a 30-60 min period. Thus short term variations in the gas quality can give a gas analysis that doesn't correspond to the feed composition.

It was observed in the early runs that the amount of oxygen injected at levels B-D did not seem to make much difference in the operation of the gasifier. The off-gas composition was not seen to vary significantly with the change in oxygen distribution. It was determined to test operation with all the oxygen injected with the fuel, since this would be a much simpler method of operation, if successful.

In Run 29, the 12 oxygen lances, which supplied oxygen at levels B-D along the bed, were removed. The oxygen entered only tangentially through the propane start-up burner at the top of the reactor or axially from the main oxygen line, also above the bed. No change in off-gas temperature from previous runs occurred when the oxygen was introduced only above the bed. Also the tar, CO_2, H_2 and CH_4 were similar to previous runs. Therefore the lances were removed for all subsequent runs and in Phase II.

Gas analyses are shown in Table 3-4 for run 31 on wood chips made with air, enriched air, and O_2 at atmospheric pressure and O_2 at high-pressure. On a nitrogen-free basis, the gas produced from air gasification has the equivalent energy content to that produced with oxygen. The dry gas analyses for these runs are shown in Table 3-4. Again, as in Run 19, the high-pressure run gives a low CO/CO_2 ratio and high N_2 concentration. As before, .high-pressure decreases gas quality, probably due to high heat loss in the small reactor.

3.2.4 Catalytic Grate Test

The methane content of the gases in Tables 3-2 to 3-4 is low compared to that produced by other gasifiers. Nevertheless, the requirement of low methane for methanol synthesis would make further reduction desirable. A sample of honeycomb catalyst made by Corning was placed on the grate to test whether it would catalytically reduce the methane concentration. The dry gas analysis is seen in Table 3-5. Gases were sampled just above and below the catalytic grate. The data shows a reduction in methane, but this may not be statistically significant and other tests would be required to make a quantitative evaluation of catalytic methane reduction within the gasifier. The catalyst would probably work better if it could be kept at a higher temperature.

3.3 PHASE II RESULTS

3.3.1 Air Runs

3.3.1.1 Air Gasification Startup and Operation

After the modifications described in Chapter 2 were completed the gasifier was operated initially with the top open in the "suction mode" to permit air gasification of biomass for preliminary testing. The gasifier was operated by pulling air through the gasifier using the fan described in Chapter 2 and later the ejector operated on nitrogen or steam. With the new 3 in. plug valve it was possible to feed materials with larger characteristic dimensions than before.

The system was started by filling the gasifier with charcoal a distance of 15 cm above the grate. The fan or ejector was started at a low flow rate, and the charcoal was ignited with burning paper brands. The charcoal was burned for 10-20 min to establish the char bed and heat the cyclone. When the thermocouple below the grate reached a temperature of 600°C, the first charge of the biomass was added above the charcoal.

Table 3-5. Catalytic Grate Test[a]

Run	26-A		26-B	
	Above Grate	Below Grate	Above Grate	Below Grate
CO	46.6	50.8	50.7	49.7
CO_2	11.3	13.2	12.5	16.0
H_2	26.8	22.0	23.0	25.8
CH_4	3.7	2.4	1.8	1.6
C_2H_4	0.2	0.0	0.2	0.4
N_2	11.3	12.2	11.7	5.6
CO/CO_2	4.1	3.8	4.1	3.1
H_2/CO	0.58	0.43	0.45	0.52
MJ/nm^3	9.4	8.6	8.8	9.3

a) Run 26 on 6 mm Wood Chips at 1 atmosphere pressure

In operation on air the flaming reaction zone was buried below the top of the fuel, and the gasifier operated in the "grate stabilized mode" in which the flaming pyrolysis and char zones remained a fixed distance from the grate. In operation with oxygen, however, the flaming pyrolysis zone always moved to the top of the bed so that it was necessary to have a closed top.

The shakedown air runs were made on pine chips with dimensions of about 2.5 cm x 2.5 cm x 1 cm (1 in. x 1 in. x 3/8 in.). The wood chips produced a 0.5 kPa (2 in ga water height) pressure drop through a 20 cm bed with stirring at about one RPM. The temperature of the off gas ranged from 617°-678°C.

The feed was charged into the reactor batchwise every 15-30 min.. The feed rate was calculated by weighing the feed, then adding a batch to the gasifier whenever the flaming pyrolysis front was just becoming visible from above. The time until the front was visible again was recorded and divided into the weight to give feed rate. This assumes a constant level of the flaming pyrolysis zone.

Char production rates were measured every 30 min by weighing the cyclone char collection vessel before and after a period of running. Pressure drops in the reactor, the cyclone and the orifice downstream of the cyclone were monitored. Also, the temperature of the gas at the grate and cyclone were recorded. The stirring assembly was kept rotating at a constant rate during the runs.

Gas flow was measured using an orifice plate. It was not practical to meter the air input with the open top so the air input was calculated from a species balance on N_2 in the GC analysis of the producer gas.

3.3.1.2 Air Air Gasification results

Typical results for air gasification are shown in Table 3-6 for wood chips, wood pellets and peat pellets. Results for air gasification of hammer-milled corn cobs, about 25 mm (1 in.) in diameter and no longer than 38 mm (1 1/2 in.) are shown in Table 3-7. These runs lasted six h with at least 30 min of steady state operation per analysis.

Table 3-6. Air Gasification of Wood Chips, Wood Pellets and Peat Pellets

INPUTS				
Test Number	4-A	10-A	2-B	3-B
Fuel Analysis	2.5 cm	6 mm Wood	5mm	
Fuel	Chips	Pellets	<--Peat Pellets->	
Moisture (%)	2.8	3.6	32	32
Carbon	50.2	49.2	59.1	59.1
Nitrogen	0.1	0.2	1.2	1.2
Oxygen	42.5	43.6	29.1	29.1
Hydrogen	6.2	6.0	5.0	5.0
Ash	0.9	0.9	5.7	5.7
HHV (MJ/kg, dry)	19.6	20.1	22.7	22.7
Gasifier conditions				
Feed (kg/h,dry)	5.7	11.8	6.2	5.7
Gasifier air (kg/h	17.2	15.9	14.7	19.5
OUTPUTS				
Dry gas (kg/h)	22.8	23.6	19.7	26.2
Water (g/NM3)	66	90	89	28
Char-ash (kg/h)	0.15	0.08	2.30	2.35
Tar ppm	585	1290	9744	3696
Dry Gas Analysis (Vol %)				
CO	19.0	21.0	18.8	25.0
CO_2	14.0	17.0	19.9	16.2
H_2	17.0	13.0	3.4	2.2
CH_4	2.0	4.0	2.1	1.3
N_2	48.0	45.0	55.8	55.4
Mole Weight (g)	25.6	26.9	30.1	29.9
Dry Gas HHV (MJ/nm3	5.8	6.3	3.9	4.2
Gas Density (kg/NM3)	1.23	1.30	1.45	1.44
OPERATING RATIOS				
O_2/Dry Feed	0.64	0.28	0.50	0.72
CO/CO_2	1.36	1.24	0.94	1.54
H_2/CO	0.89	0.62	0.18	0.09
MASS BALANCE AND ENERGY EFFICIENCY				
Mass in/mass out	0.95	1.10	1.02	0.96
Cold Gas Efficiency	0.96	0.49	0.38	0.60

Table 3-7. Air Gasification of Corn Cobs

INPUTS			
Test Number	2(a)	3(a)	1(b)
Fuel Analysis		4 cm Corn	
Fuel	<--------	Cobs	-------->
Moisture (%)	7.1	7.1	7.1
Carbon	47.7	47.7	47.7
Nitrogen	0.3	0.3	0.3
Oxygen	44.4	44.4	44.4
Hydrogen	5.8	5.8	5.8
Ash	1.8	1.8	1.8
HHV (MJ/kg, dry)	18.6	18.6	18.6
Gasifier conditions			
Feed (kg/h,dry)	6.2	5.1	8.8
Gasifier air (kg/h	17.6	11.3	23.2
OUTPUTS			
Dry gas (kg/h)	23.5	16.2	35.6
Water (g/NM3)	92	119	55
Char-ash (kg/h)	0.02	0.19	1.13
Tar ppm	1727	1411	6216
Dry Gas Analysis (Vol %)			
CO	20.0	18.0	20.1
CO_2	15.0	19.0	23.2
H_2	14.0	14.0	8.5
CH_4	2.0	2.0	0.5
N_2	50.0	47.0	47.7
Mole Weight (g)	27.7	27.2	29.4
Dry Gas HHV (MJ/nm3	5.5	5.2	4.1
Gas Density(kg/NM3)	1.30	1.31	1.42
OPERATING RATIOS			
O_2/Dry Feed	0.60	0.47	0.55
CO/CO_2	1.33	0.95	0.87
H_2/CO	0.70	0.78	0.42
MASS BALANCE AND ENERGY EFFICIENCY			
Mass in/mass out	0.96	0.93	0.86
Cold Gas Efficiency	0.87	0.68	0.60

(a) Runs 7/13/83

3.3.1.3 Discussion of Air Gasification Results

The gasifier operated quite well on air with the new modifications partly because the reserve feed covered the reaction zones and insulated them from the batch feeding. The problems of Phase II did not show up until we began oxygen operation.

Peat, supplied from the Old Colony Peat Farm, with a moisture content of 50% by weight was compressed into 5-mm (3/16-in.) diameter pellets in a development size California Pellet Mill. Preliminary gasification tests on the pellets were made in the laboratory quartz tube gasifier at moisture contents up to 40%. We measured 71% conversion of the peat to gas (wet basis, 42% on a dry basis).

The peat was high in ash and fixed carbon, so that a great deal of carbon was left in the char-ash, and the cold gas efficiency was low. This was aggravated by the small size of the pellets relative to the grate openings, which allowed particles to pass through before complete reduction.

The corn cobs behaved very well in the gasifier. Although it is reported that they tend to form slag in updraft gasifiers, no problems were encountered in these runs.

3.3.1.4 Operation on Large Wood Cubes

"Energy cubes" (from Papakube Corp., San Diego, Calif.) measuring 3.2 cm x 3.2 cm x 5-10 cm (1 1/4 in. x 1 1/4 in. x 2-4 in.) made of compressed waste wood were fed in the open top of the gasifier. This run did not last long enough to obtain mass and energy data. Operating with this feed resulted in overheating and melting of the grate. From this experiment and our modeling we believe that these cubes need a much longer pyrolysis and char reduction zone than we maintained because of our inexperience. Too short a bed does not allow enough residence time for the cubes to completely pyrolyze, and no time at all for char gasification. Thus the sensible heat from flaming pyrolysis is not converted to chemical energy. In retrospect, if we had added the cubes at a low rate until a much deeper bed of cube-char had been established, the grate would not have overheated.

3.3.2 Oxygen Runs

3.3.2.1 Phase II Oxygen Operation

After running a variety of fuels on air in the open top mode, we tested the gasifier improvements by operating on oxygen. Because of the difficulty of pressure operation and since it had been determined that the high-pressure gasifier yielded qualitatively similar gas at low or high-pressure operation, it was decided to test the modifications at atmospheric pressure.

The oxygen gasifier was started with a 15 cm charge of charcoal above the grate. The propane burner was started and allowed to operate until a temperature of 600°C was recorded below the grate. At this time the burner was turned off, a flow of oxygen was set and biomass feeding was started.

3.3.2.2 Oxygen Operation at High Stirring Rates

A series of runs was made at high grate speed and is shown in Table 3-8. The tests were made before the relationship between stirring rate, oxygen/fuel ratio, high char-ash and high oil production was appreciated. Note the low oxygen/fuel ratio (0.21-0.26), the high methane and hydrocarbon content (6%-9%), the high char production (8%-15%) and the high tar production (0.8%-2.2%).

These results are closer to the operating conditions of an updraft gasifier or a pyrolyzer than a downdraft gasifier and were very surprising when first evaluated.

3.3.2.3 Discussion of High Stirring Rate Runs

Several unexpected results in Phase II operation fundamentally changed our thinking about the gasification process after we began to understand them. They are discussed more fully in Chapter 8. They are consistent with our model and their understanding will permit future investigators to design and operate stratified downdraft gasifiers more satisfactorily.

Mechanically the stirring rod and rotating grate operated quite satisfactorily. However, the ability to control the rate of removal of char by a combination of grate rotation and grate hole size introduced a new variable that was only gradually understood.

High rotation rates greatly increase the char-ash produced. If char leaves the gasifier as elemental carbon, the cold gas energy efficiency drops dramatically. (The char may have potential for sale in some areas though this has not yet been demonstrated commercially.)

More important, when carbon rather than CO leaves the gasifier, the oxygen/fuel ratio will be greatly reduced. The reduced oxygen then does not provide sufficient oxygen to burn all the pyrolysis oils, and we have observed oil production rates as high as 5% of the feed. We also have observed very low grate temperatures, approximately 400°-500°C. In later runs we reduced rotation to 5-10 rph which decreased oil levels, increased char conversion and raised temperatures.

We recommend in future designs using independent controls to stir the bed (if needed) and to agitate the grate to remove the char-ash dust. The bed stirrer should rotate at a speed sufficient to break up bridges, channels and hot spots and ensure uniform bed porosity. The grate stirring rate should be the minimum required to prevent pressure buildup at the grate.

Table 3-8. Oxygen Gasification of Wood Chips at High Stirring Rates

INPUTS					
Test Number	E4-1A[a]	E4-1B	E5-1A[b]	E5-1B	E6-1[b]
Fuel Analysis					
Moisture (%)	7.0	7.0	7.0	7.0	7.0
Carbon	47.1	47.1	47.1	47.1	47.1
Oxygen	46.6	46.6	46.6	46.6	46.6
Hydrogen	5.7	5.7	5.7	5.7	5.7
Nitrogen	0.1	0.1	0.1	0.1	0.1
Ash	0.6	0.6	0.6	0.6	0.6
HHV (MJ/kg, dry)	19.9	19.9	19.9	19.9	19.9
Gasifier Conditions					
Feed (kg/h,dry)	13.1	11.6	13.5	13.5	10.9
Gasifier O_2 (kg/h)	2.6	2.6	2.6	2.6	2.6
Nitrogen (kg/h)	0.7	0.1	2.2	0.7	0.8
Temperature (°C)	450	450	450	480	450
Grate Speed (rph)	30-60	30-60	100	100	60
OUTPUTS					
Dry gas (kg/h)	16.5	14.7	18.3	17.0	14.3
Char-ash (kg/h)	1.44	1.39	1.62	1.08	0.65
Water (g/NM3)	27.4	27.4	27.4	27.4	49.4
Tar (ppm)	not measured		7694	22761	7493
Dry Gas Analysis (Vol %)					
CO	49.1	49.1	47.1	47.1	47.8
CO_2	18.9	19.0	16.8	20.3	19.2
H_2	22.6	22.2	17.5	18.6	19.7
CH_4	4.6	5.7	3.7	6.4	4.9
N_2	3.6	0.7	10.7	3.7	4.9
C^{2+}	2.3	3.4	2.2	3.9	3.6
Mole Weight (g)	25.1	24.8	25.3	25.9	25.6
Dry Gas HHV (MJ/NM3)	13.41	14.59	11.97	14.52	13.86
Gas Density (kg/NM3)	1.21	1.19	1.22	1.25	1.23
OPERATING RATIOS					
O_2/Dry Feed	0.21	0.24	0.21	0.21	0.26
CO/CO_2	2.60	2.59	2.81	2.32	2.49
H_2/CO	0.46	0.45	0.37	0.40	0.41
MASS BALANCE AND ENERGY EFFICIENCY					
Mass in/Mass out	0.95	0.92	0.95	0.96	0.97
Cold Gas efficiency (%)	0.72	0.80	0.69	0.76	0.78

(a) runs performed 7/26/83; (b) runs performed 8/15/83

3.3.2.4 Effect of Intermittant Feeding

The new 7.5 cm (3 in.) rotary plug valve feeder was installed to permit operation with larger feedstocks, such as corn cobs. However, a second unanticipated effect was "pulsed operation" resulting from the dumping of feed every 10-40 s rather than the 2-8 s associated with the 5 cm (2 in.) plug valve feeder. The effect was immediately apparent in the increase of gas flow when material was fed. The pressure drop across the bed increased

by as much as 5 kPa (20 in. water gauge). It was also observable in the bed temperature, which dropped precipitously when material was fed and then rose rapidly when pyrolysis was complete and char began to burn.

The effect of discontinuous feed is to permit the downdraft gasifier to operate alternately, first in an endothermic pyrolysis mode, generating oil and high hydrocarbon gas with dropping temperatures; then in a char combustion mode producing largely carbon monoxide and high temperatures. This effect did not occur with open top operation with air because there was always a buffer of unburned feed material. Therefore, in general, there was less tar generated with air.

A further consequence of this pulsation is that the gas flow increases dramatically in quantity and changes in composition during the pyrolysis pulse. This makes measurement of producer gas flow and composition difficult. We have therefore used the oxygen balance to calculate gas flow rather than relying on direct measurement. In taking gas samples we use low sampling slip-stream flow rates to try to average over several pulses.

The problem was reduced (but not eliminated) by partially filling the pockets of the plug feeder with plastic to reduce the volume per dump and increase the dumps per min. However, this was only a partial solution.

We recommend in the future that top-stabilized gasifiers use a continuous feed device (such as an auger) to achieve truly steady feed conditions. In addition, it is important to have uniform spatial distribution of fresh feed on the top of the bed to permit maximum oil burnout.

3.3.2.5 Oxygen Gasification of Peat

Peat was run at varying grate speed and oxygen-to-nitrogen ratios. The operating conditions and results are given in Table 3-9. First a mixture of oxygen and nitrogen which simulates air, was used to gasify the peat. With a grate speed of 9 rph, the concentration of tar in the producer gas, as measured with a Gelman filter, was only 1100 mg/nm^3, roughly 1100 ppm. The char/feed ratio was quite high with the simulated air, indicating a small percentage of char being gasified by the endothermic Boudouard reaction and water gas reactions and/or high char carryover. Switching to oxygen led to more tar for the same grate speed, although perhaps not significantly more.

When we increased the grate speed to 22.5 rph, the increase in tar from 2000 ppm to 22,000 ppm was dramatic and would be unacceptable for methanol synthesis. The O_2/dry feed ratio was extremely low for peat, an oxygen lean fuel. Thus, although the throughput of feed was high, not enough oxygen was available for reaction because of the high rate of char removal.

3.4 CO-GASIFICATION OF METHANE AND BIOMASS

We were asked to study the possibility of utilizing methane, in areas where it may be in abundance, to upgrade the synthesis gas from gasification of biomass and especially to increase the H_2/CO ratio. We set out to determine experimentally if biomass and methane could be co-gasified in the same gasifier to yield a better quality synthesis gas.

Table 3-9. Air and Oxygen Gasification of Peat Pellets

INPUTS			
Test Number 10-12-83	M2-1(a)	M2-2	M2-3
Oxidant	Syn-Air	Oxygen	Oxygen
Fuel Analysis			
Moisture (%)	13.9	13.9	13.9
Carbon	59.1	59.1	59.1
Oxygen	29.1	29.1	29.1
Hydrogen	5.0	5.0	5.0
Nitrogen	1.2	1.2	1.2
Ash	5.7	5.7	5.7
HHV (MJ/kg, dry)	22.7	22.7	22.7
Gasifier Conditions			
Feed (kg/h,dry)	3.14	4.70	8.04
Gasifier O_2 (kg/h)	1.58	2.80	2.80
Nitrogen (kg/h)	6.50	1.06	1.67
Temperature (C)	300	330	300
Grate Speed (rph)	9	9	22.5
OUTPUTS			
Dry Gas Analysis (Vol %)			
CO	15.5	26.5	27.5
CO_2	12.5	31.8	32.8
H_2	17.1	24.5	20.2
CH_4	1.1	3.9	3.2
N_2	53.7	11.2	14.3
C^{2+}	0.0	2.2	2.1
Mole Weight (g)	25.4	26.4	27.7
Gas Quality (MJ/NM3)	4.9	10.2	9.4
Gas Density (kg/NM3)	1.22	1.27	1.34
Water (g/NM3)	25.7	28.5	51.3
Tar (ppm)	1090	1970	23500
Char-Ash (kg/h)	0.91	0.61	1.77
Dry Gas (Kg/h)	10.93	8.46	10.93
OPERATING RATIOS			
O_2/Dry Feed	0.50	0.59	0.35
CO/CO_2	1.24	0.83	0.84
H_2/CO	1.10	0.93	0.73
MASS BALANCE AND ENERGY EFFICIENCY			
Mass in/Mass out	0.98	1.01	1.06
Gas efficiency (%)	0.62	0.63	0.42

Notes: (a) high nitrogen simulates air operation

In a preliminary experiment we fed methane and oxygen through the preheat burner of the gasifier into the empty gasifier with various ratios of oxygen to establish the product distribution resulting from methane/oxygen combustion. The results of this experiment are shown in Table 3-10.

Table 3-10. Gas Composition from Methane Combustion

Run	Burner Temp C	O_2/CH_4	< Volume Concentration in Gas > CH_4	CO	CO_2	H_2	H_2O	O_2	H_2/CO
1[a]	1050	2.6	0.0	1.4	27.0	0.0	55.4	16.2	-
2[b]	1050	1.6	2.5	11.5	21.3	9.8	54.1	0.0	0.99
3[b]	1000	0.9	7.2	22.2	9.5	31.5	29.6	0.0	1.44

(a) lean flame (b) rich flame

Stoichiometric combustion of methane with oxygen requires a mixture with an O_2/CH_4 ratio of 2. In order not to exceed the temperature capability of the refractory (about 1050°C) it was necessary to use either a leaner or a richer mixture. It is seen in Table 3-10 that the methane was cracked into CO and H_2 in the rich flames at the expense of burning some of the methane to CO_2 and H_2O. (Methane is a very stable molecule and it requires a lot of energy to crack it.)

Methane and oxygen were then fed together into the gasifier after it had been started in the normal fashion with wood chips. Run conditions are shown in Table 3-11 for co-gasification of wood and methane with oxygen. Gasifying wood chips with lean and rich mixtures of methane and oxygen resulted only in marginal improvements in the H_2/CO ratio of the resulting gas. In addition, the rich methane/O_2 feed yielded higher tar levels, as would be expected, because of the resulting decreased O_2/dry feed ratio.

It appears that methane robs oxygen from the feed, precluding adequate tar combustion in the gasifier. A more practical approach to using methane with biomass would be to crack the methane separately in a methane burner as was demonstrated in Table 3-11 and add this hydrogen-rich synthesis gas to that from the gasifier.

3.5 CONCLUSIONS FROM GASIFIER RUNS

In Phase I it was demonstrated that biomass could be gasified with oxygen in a downdraft gasifier to produce a very low tar synthesis gas suitable for manufacture of fuels such as methanol and gasoline. We discovered that it is possible to feed all the oxygen and biomass together at the top of the gasifier without overheating at any point. We showed that the stratified downdraft gasifier can produce a typical producer gas with air and a synthesis gas comparable to that of the Koppers Totzek coal gasifier with oxygen. The synthesis gas was easily converted into methanol using standard methods.

Table 3-11. Co-Gasification of Wood and Methane[a]

INPUTS			
Test Number	M3S6A	M3S7	M3S8
INPUTS			
Fuel Analysis (Vol %)			
Fuel	---------5 mm Pine Chips---------		
Moisture (%)	7.02	7.02	7.02
Carbon	47.08	47.08	47.08
Oxygen	46.6	46.6	46.6
Hydrogen	5.71	5.71	5.71
Nitrogen	0.06	0.06	0.06
Ash	0.55	0.55	0.55
HHV (kJ/kg, dry)	19857	19857	19857
Gasifier Conditions			
Wood feed (kg/h)	6.51	6.51	6.51
Oxygen feed (kg/h)	1.87	1.87	1.74
Nitrogen Feed (kg/h)	1.59	1.85	1.70
Methane feed (kg/h)	0.21	0.21	0.21
Grate Speed (rph)	30	15	15
OUTPUTS			
Dry gas (kg/h)	9.41	9.76	9.63
Water (g/NM3)	148	205	200
Char-ash	0.44	0.43	0.36
Tar (ppm)	33600	33600	62370
Temperature (C)	350	310	330
Dry Gas Analysis (Vol %)			
CO	41.21	40.11	36.37
CO_2	16.38	14.95	10.83
H_2	20.40	20.60	25.82
CH_4	6.55	6.13	9.73
N_2	15.32	20.02	16.88
C^{2+}	2.75	1.05	3.01
Mole Weight (g)	25.43	25.17	22.78
Gas Quality (kJ/NM3)	13.2	11.7	14.8
Gas Density (kg/NM3)	1.22	1.21	1.10
OPERATING RATIOS			
O_2/Dry feed	0.31	0.37	0.34
CO/CO_2	2.52	2.68	3.36
H_2/CO	0.49	0.51	0.71
MASS BALANCE AND ENERGY EFFICIENCY			
Mass in/mass out	1.01	1.00	0.95
Cold gas efficiency (%)	0.72	0.66	0.68

a) Date of Run: 12/22/83

We demonstrated that operation at high-pressure is basically similar to atmospheric pressure but is difficult to test in a small gasifier without a considerable improvement in feed techniques and improved insulation. It was not possible to make runs over 8 h long because of pressure buildup caused by inadequate char removal and plugging of the bed.

In Phase II we made major design changes to solve problems found in Phase I. We solved the plugging problem by installing stirring and grate rotation and we installed a larger rotary feed valve to accommodate larger fuel particles. These changes corrected the original problems, but they brought other problems that gave us a greater appreciation of the stratified downdraft gasifier.

It was found that stirring permits steady state operation without pressure buildup, precluding grate meltdowns caused by channeling. However, excessive stirring also causes increased char-ash removal, lower oxygen fuel ratios, lower pyrolysis temperatures and higher tar-oil production. We believe that adjusting bed height to the feedstock, operating conditions, proper grate opening size and moderate stirring will give continuous production of low-tar synthesis gas. We have since operated smaller gasifiers to establish these relationships.

We also discovered that the pulsed operation resulting from the greater amount of feed per dump cycle in the larger feeder gave alternating pyrolysis-charcoal gasification operation which increased tar-oils and made gas measurements difficult. We recommend that any gasifiers built to operate in the downdraft, top-stabilized mode have a continuous feeder mechanism such as an auger.

Although the gasifier was designed to be a "1 ton/day" gasifier, the highest rate observed was 0.74 ton/day, (corresponding to a heat rate of 2.5 MM Btu/h-ft^2). Most runs were at considerably lower rates. We do not know what the maximum rate could be with optimized char removal and feeding, so we have continued to call it a "1 ton/day" gasifier. In fact the above rate is close to that measured on the 25 tons/day scaled up version, so maybe it should be called a "1/2 ton/day" gasifier.

REFERENCES

1. Reed, T. B., Markson, M. and Graboski, M., "The SERI High Pressure Oxygen Gasifier", *Biomass-To Methanol Specialists' Workshop, Tamarron, Colorado, 3-5 March 1982,* Edited by T. B. Reed and M. Graboski, SERI/CP-234-1590, Golden, CO: Solar Energy Research Institute, 1982.

2. Thomas R. Miles, Consulting Design Engineers, 5475 S. W. Arrowwood Lane, Portland, Or 97225.

CHAPTER 4 - LARGE SCALE TESTING

4.1 INTRODUCTION

4.1.1 SERI/DOE Development work

Since its establishment in 1977, SERI has conducted extensive research in the field of thermal biomass conversion. A one ton/day prototype oxygen-blown downdraft gasifier was designed, built and operated to make fuel and synthesis gas from wood and other forms of biomass. Several key conclusions were established during this program:

- A gas of 140-165 Btu/scf was consistently produced with air; a gas of 250-300 Btu/scf was produced with oxygen
- The gas produced was low in tars and oils, a major problem in all other gasification systems
- Carbon conversion efficiencies at or above 95% were achieved, resulting in a very low volume of ash residue
- The process was demonstrated to be 92% efficient. (92% of the Btus contained in the solid wood chips were present in the hot product gas as chemical and sensible heat)
- The gasifier proved to operate well at throughputs as low as 25% of rated capacity, with a number of fuels and at a variety of fuel moisture levels. No slagging was detected.

The SERI gasifier was the recipient of an IR-100 award presented by Industrial Research and Development magazine as one of the best 100 inventions of 1982.

4.1.2 Technology Transfer to Syn-Gas Inc.

Dr. Michael S. Graboski, co-inventor (with Dr. Thomas B. Reed), acquired the patent rights to the SERI gasifier through the DOE's government technology transfer program and subsequently assigned those rights to SynGas, Inc., for the purpose of commercializing the gasification technology. SynGas is currently developing its technology for air-blown operation at a scale up to 25 MMBtu/h gas output. The comp[any has built and operated the gasifier on air at its Golden, Colorado, test facility.

The air-blown version of the gasifier is designed for boiler retrofits and other thermal application and to produce gas for use in internal combustion-based cogeneration systems. The prototype gasifier operated in Golden is suitable for retrofitting a 250 hp boiler or fueling a 750 kW engine-generator set.

In 1985, SynGas, Inc., entered into a contract with SERI to provide test data for the oxygen blown gasification of wood at a scale significantly larger than the 1 ton/day SERI prototype downdraft gasification test unit. No changes were made in the gasifier itself for oxygen operation. SynGas has now demonstrated that the SynGas gasifier is suitable for producing medium Btu gas from wood and oxygen in its test facility using up to 25% moisture content (wet basis) wood chips. This chapter describes the SynGas, Inc., system and

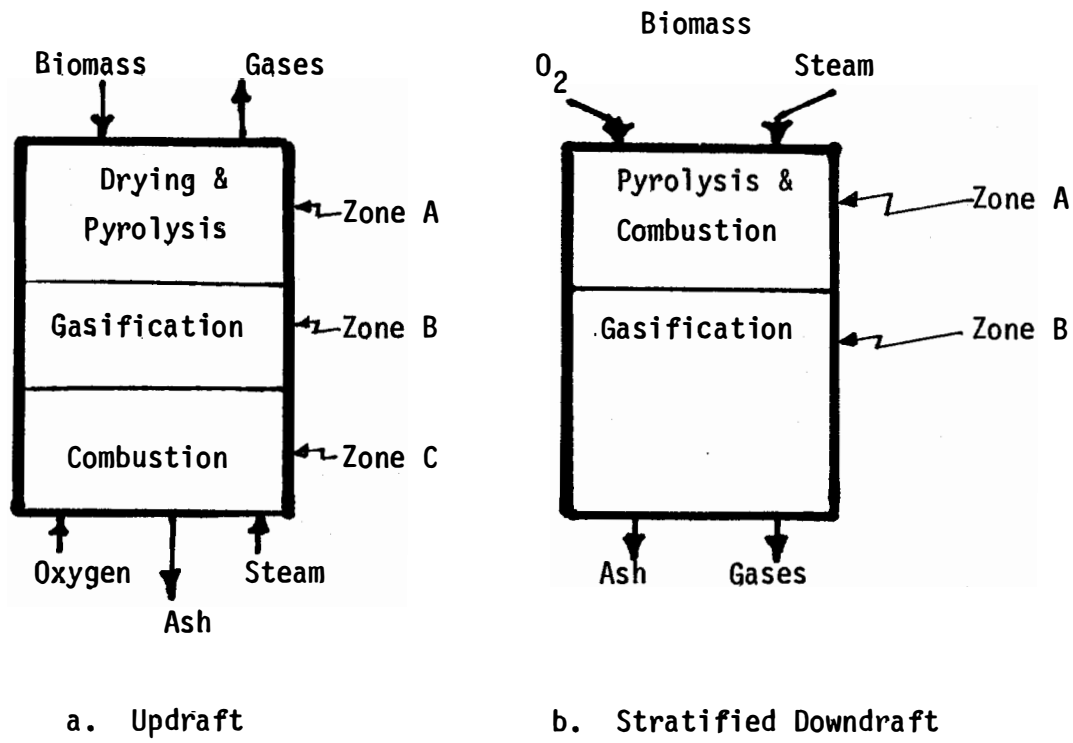

Figure 4-1. Modes of Fixed Bed Gasifier Operation

presents the results of a brief test matrix of oxygen runs that produced a medium-Btu gas. The data is useful for providing a basis for further gasifier design and scaleup using oxygen to produce medium-Btu gas.

4.2 COMMERCIALIZATION OF LOW- AND MEDIUM-ENERGY GAS

4.2.1 Syn-Gas Background

SynGas, Inc., was formed in 1983 by former members of the management of the International Harvester Biomass Energy Program and the Charter Financial Group of Houston, Texas. The company owns a proprietary wood gasification technology and since that time has been engaged in the development of two new products: a nominal 25 MMBtu/h, air-blown fuel gas generator and a 2.5 MW power generation system. At the present time, the company has completed final product development on the air gasifier and has begun marketing its fully engineered products, the fuel gas and generator system, for both gas replacement and power generation. A 10 MW power system is being planned for installation in Long Island, N. Y.

4.2.2 Applications of Low- and Medium-Btu Gas

Low Btu gas driven internal combustion engines can produce power with an efficiency of about 40% and without the complexity of pressure operation and without the use of oxygen. Low Btu gas is the short-term focus of SynGas Inc.

The production of medium-Btu gas by either pyrolysis or oxygen blowing is substantially more expensive than the production of low Btu gas achieved by air blowing, because of the high capital cost of the complex pyrolysis reaction system or the operating cost associated with oxygen supply. Therefore, medium Btu gas must command a higher use value than low Btu gas in the marketplace to justify its production and use.

Medium-Btu gas cannot compete with low Btu gas or conventional fossil fuels as a boiler fuel. In the pipeline distribution of fuel gas, the higher energy content of medium Btu gas can justify the added cost. Power generation using advanced combustion gas turbines can achieve an efficiency of just over 40% It may require a higher energy gas and can possibly justify the added cost of making medium Btu gas.

The most important high value use of medium Btu gas is as a chemical synthesis gas. "Synthesis gas" or syn-gas is the name used to describe a gas mixture containing predominantly carbon monoxide and hydrogen with relatively small amounts of hydrocarbons as the combustible components. Such a gas can be produced from biomass directly only by oxygen blowing.

Synthesis gas can be converted to fuels and chemicals using standard, well developed technology. Methanol has been found to be a suitable fuel substitute for gasoline and an excellent, low polluting fuel for gas turbine and automotive applications. Syn-gas is also used to make synthetic natural gas, gasoline, diesel fuel and ammonia for fertilizers. The value of the SynGas approach is that the gas produced by oxygen blowing is of synthesis gas quality, as reported in Appendix B. This sets the SynGas approach apart from the other competing technologies.

A recent study commissioned by the Southern California Edison Co. and conducted by Fluor Technology, Inc,. recommends the use of the SERI/SynGas

gasifier for the production of methanol synthesis gas (1). The Fluor Corporation cited the following advantages of the SERI type gasifier over other available technologies (1):

- o Minimal feedstock preparation because field-chipped wood does not require additional grinding to reduce size
- o Low methane production which results in a design that does not require the added cost and complexity of steam methane reforming
- o Low tar and oil production which minimizes synthesis gas clean-up and reduces the quantity of wastewater which requires treatment
- o Development level, for biomass applications, is equal to or greater than the development level of the other systems. The gasifier was developed specifically for wood and for smaller scale applications
- o The gasifier appears to be less complex, with a lower profile (elevation) which fits into the modular concept better
- o The gasifier does not require steam for gasification which results in a potentially easier plant start-up and permits a design without a steam system.

4.3 GASIFICATION TECHNOLOGY

4.3.1 Brief Description of Downdraft Gasifier Operation

The design and operation of the SERI 1 ton/day gasifier are described in Chapters 2 and 3. The scientific basis of gasification design is described in detail in Chapter 5, and the chemical and thermodynamic principles are described in Chapter 7. A model consistent with the operation of the SERI/SynGas gasifier is discussed in Chapter 8. Only those points necessary to understand the work reported in this chapter will be summarized here.

The modes of fixed bed gasifier operation are shown in Fig. 4-1 (a and b). In the updraft gasifier shown in Fig. 4-1(a) air passes up through the bed, burning charcoal in zone C, gasifying the combustion products with more charcoal in Zone B and finally drying and pyrolyzing the incoming fuel in Zone A. Because the gas is cooled by the pyrolysis reaction, this type of gasifier results in high production of tars and oils.

In the downdraft design, the air (or oxygen) enters the gasifier at the top of the fixed (moving) bed with the feed. The volatile material burns as the bed moves down in the upper "flaming pyrolysis" stage, A. The products of this combustion react with the charcoal in the second "char reduction" stage, B.

4.3.2 Thermodynamic Model Predictions

A few gasifiers, such as the downdraft gasifier or fluidized bed gasifier with recycle, will approach chemical equilibrium between the char and the gas. For these systems, equilibrium predictions are useful in modelling gasifier performance.

The gas from the downdraft gasifier approaches the composition of an "equilibrium gas." It consists of CO, H_2 ,CO_2 and H_2O with a small amount of

methane and other light hydrocarbons. The gas typically contains less than 1% tar. Steam for gasification of the char is obtained from fuel moisture, pyrolysis, and combustion, unlike the updraft case where steam must usually be added to effect char gasification. Thus additional steam is not equired for the downdraft configuration.

The oxygen/fuel ratio is the most important factor determining the operation of oxygen and air gasification, but the ratio suitable for gasificaiton varies with feedstock composition and moisture. To permit a general description of wood pyrolysis, gasification and combustion, the concept of equivalence ratio is used. The equivalence ratio (ER), Φ is defined as the oxidant to fuel weight ratio actually used divided by the ratio required for stoichiometric combustion, that is:

$$ER = \Phi = \frac{\text{weight oxidant/weight dry wood}}{\text{stoichiometric oxidant/weight dry wood}} \qquad (1)$$

The equivalence ratio is the most important measure of gasifier performance and is discussed at length in Chapter 7. If the oxygen/fuel required for stoichiometric combustion, R_s, is known, Φ can be calculated from R_s and vice versa. Wood with a typical composition of $CH_{1.4}O_{0.6}$ requires 1.48 kg of oxygen (lb oxygen) per kg (lb) of wood for complete combustion, so R_s is 1.48.

Equilibrium calculations have been made by Desrosiers for a wide variety of gasification conditions (2). The calculations were based on a typical analysis for dry, sulfur free and ash free wood. Carbon as graphite is the only solid product considered. Sample results of equilibrium calculations for dry wood gasified in oxygen are shown in Figs. 7-3 to 7-6.

The equilibrium products at an equivalence ratio of zero in Fig. 7-4 correspond to pure pyrolysis at $\Phi = 0$. They are solid carbon H_2, H_2O, CO_2, CO and CH_4. Tar is not thermodynamically stable at the temperatures found in a downdraft gasifier. As the equivalence ratio is raised to the end of the carbon stability region, ($\Phi \approx 0.25$), gasification is taking place, and solid carbon is consumed. The principal products for gasification are H_2 and CO.

The energy content of the gas reaches a maximum at the gasification equivalence ratio, $\Phi = 0.25$, as shown in Fig. 7-5. Addition of oxygen beyond $\Phi = 0.25$ results in consumption of H_2 and CO until combustion is complete at $\Phi = 1.0$. Note that in these figures there is an inflection point in the curves at $\Phi = 0.25$, which corresponds to total carbon conversion. This is the point at which an oxygen blown gasifier would operate if all char were consumed to give minimum product oxidation. At this point the mass ratio R_s is 0.25 x 1.48 = 0.37.

In practice the operating point may be at a higher Φ (because of heat losses), or lower, due to removal of unconverted carbon or tars. In fact carbon removal at the grate is the second most important control factor in downdraft gasification.

A Fortran model of expected gasifier performance has been made at SynGas Inc. It is based on the assumption of equilibrium between CO, CO_2, H_2 and H_2O, but not with methane. Inputs to the model are % carbon conversion, fraction carbon occurring as methane, exit gas temperature, and fuel analysis. The model computes the heating value of the gas, the exit composition of the gas and the amount of oxygen required to balance the reaction.

Gasifier performance predictions were made using this model. "Runs" were computed at atmospheric pressure to show the effect of moisture and incomplete hydrocarbon conversion on overall gasifier performance. Table 4-1 shows the base operating case for the gasifier. The gas heating value, calculated by method ASTM D 3588-81, is estimated to be 306 Btu/scf for 20% moisture content wood feed, and 95% carbon conversion. No steam is required for gasification. The oxygen/wet wood requirement is 0.284 lb/lb. The O_2/dry wood requirement is 0.378 lb/lb. This corresponds to an equivalence ratio Φ of 0.255 as shown in Table 4-1.

Fig. 4-2 and 4-3 show the effect of free moisture and degree of hydrocarbon cracking on oxygen usage and gas Btu. An exit temperature of 1350F is assumed in all cases. The hydrocarbon production is treated as a parameter. The model prediction shows that 300 Btu/scf gas or greater will be achieved with 20% MC fuel or drier with a gas hydrocarbon content as methane of 3.3% (correspondence to 5% of the carbon converted to CH_4). Gasifier performance data show methane concentrations of 3%-6%. Thus, wetter fuels can be used if richer gas is generated.

Table 4-1. Oxygen Gasifier Performance Computed from Equilibrium Model

PREDICTION OF GASIFIER PERFORMANCE	
Wood Rate, Lb./h	2520.00
Oxidizer Rate, scf/min	141.89
Product Gas Rate, scf/min	985.81
Wood to O_2, Lb./h/scf/min	17.76
Product Gas to O_2, scf/min/scf/min	6.95

FUEL ANALYSIS, DAF BASIS	
Carbon	51.00
Hydrogen	6.00
Oxygen	43.00
Moisture	25.00
Volatile Matter	85.00
Ash	1.00
Gross Heating Value, Btu/lb.	8673.88

PRODUCT RESULTS

Temperature, °F	1350.6		
	Moles/h	Vol % Wet	Vol % Dry
Water	31.72	.204	.000
Hydrogen	43.31	.278	.349
Carbon Dioxide	20.28	.130	.163
Carbon Monoxide	54.10	.347	.436
Nitrogen	.00	.000	.000
Methane	6.37	.041	.051

Assumed Carbon conversion, %	95.00
Carbon Loss, lb/h,	51.00
Heat Loss, Btu/lb dry	.00
Oxygen/Dry Fuel ratio	0.38
Oxygen equivalence ratio	0.255

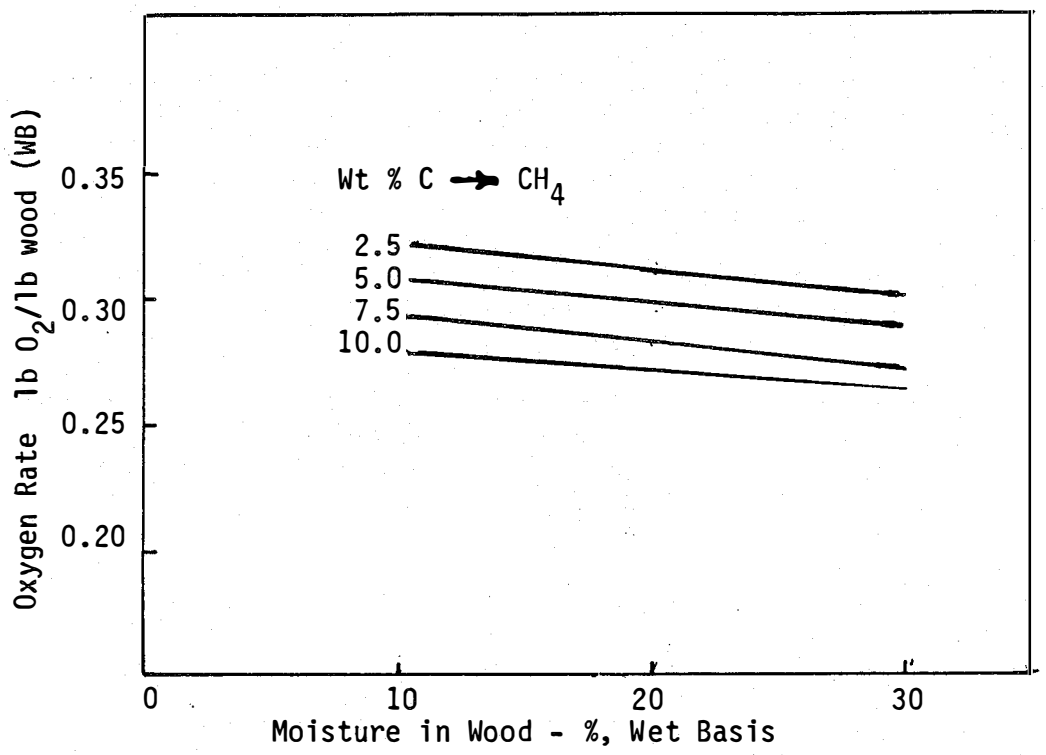

Figure 4-2. Effect of Wood moisture Content on Oxygen/Wood ratio

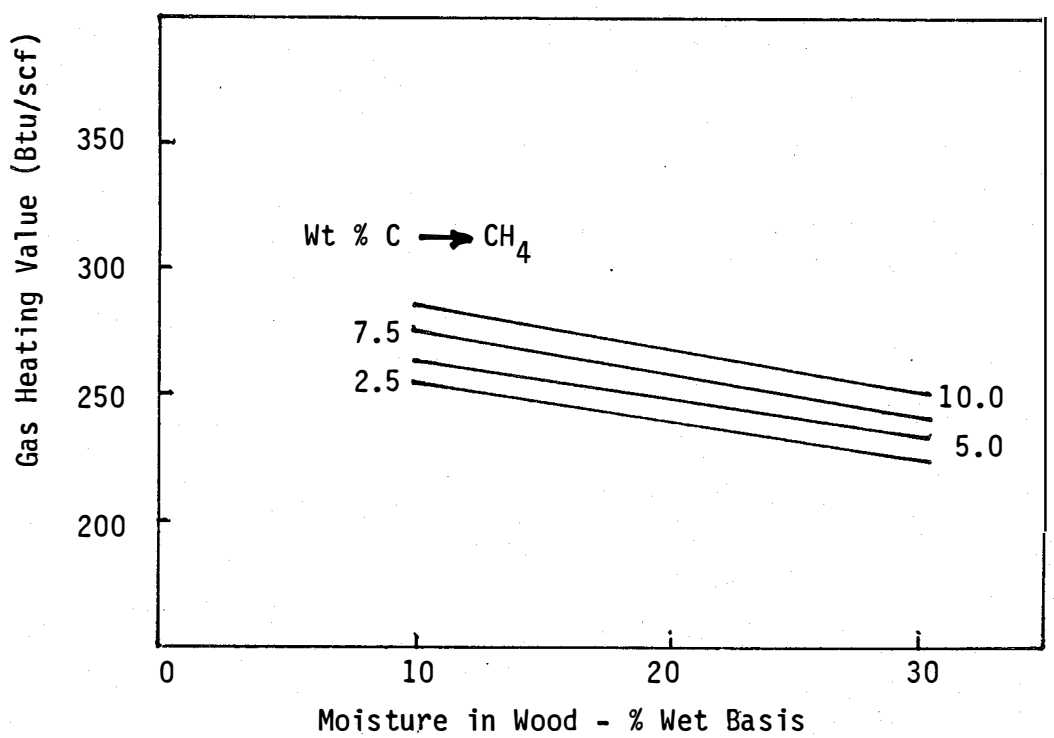

Figure 4-3. Effect of Wood Moisture Content on Gas Higher Heating Value

4.4. SYNGAS GASIFICATION FACILITY DESCRIPTION

4.4.1 Plant Description

The SynGas Golden, Colorado, pilot plant gasification system is sized to produce 10 MMBtu/hour hot lower heating value (lhv) basis fuel gas. This requires 1650 lb/h of 15% moisture content wood feed to the downdraft gasifier. The gasifier configuration being tested is for boiler retrofits and other thermal applications using air or oxygen. In this situation, the major system components are the following:

- o Wood feeder
- o Forced draft fan
- o Gasifier
- o Ash handling system
- o Cyclone
- o Fuel gas burner.

For boilers, the gasification system is operated at a slight positive pressure to permit gas to be delivered hot to the user. In this mode of operation, both the chemical heat (LHV basis) and a significant portion of the sensible heat can be utilized.

The SynGas demonstration facility process flow diagram is shown in Fig. 4-4. The full facility includes the gasifier train, wood handling and storage equipment, combustion user and small gas cleaning system. For the purpose of oxygen testing, a liquid oxygen storage system and flow regulating system were added to the plant. This system permits the plant to be readily switched over to oxygen from air during operation.

4.4.2 Wood Handling and Feeding

SynGas' initial experience was with wood chip fuels. More recently urban wood waste and densified refuse derived fuels (DRDF) have been gasified. The wood handling and feeding system operates satisfactorily with chip fuels in the size range of pulp and whole tree chips. Coarse fuels are more suitable than fine materials.

In the present application, fuels received are essentially greater than 1-inch in major dimension with varying quantities of fines, and with a moisture content of up to 25% on an as-received basis. SynGas does not now have on site fuel drying capability. Since dried fuels are required, commercial field applications must include a fuel dryer or use predried fuel.

The demonstration plant includes sufficient covered storage for one day of plant operation. Fuel is moved from covered storage using a bucket loader to a storage bin equipped with a live bottom feeder. The bin holds approximately 5 tons of dried wood fuel. The storage bin provides surge capacity for the plant and is used to maintain inventory in the feed bin. Wood fuel which is transferred from the storage bin to the feed bin, can be screened to remove a portion of the sawdust in the feedstock using an auger screen.

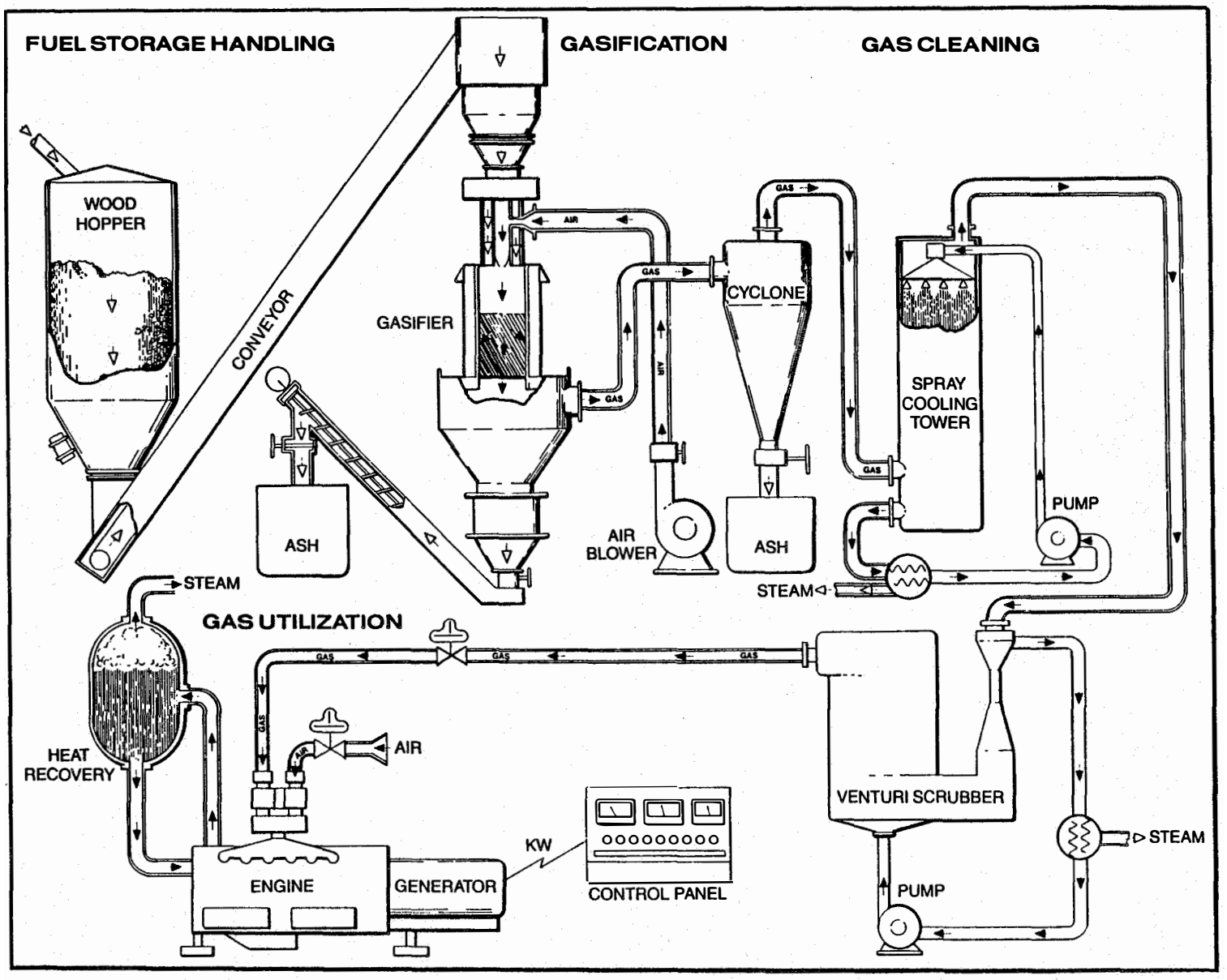

Figure 4-4. SynGas Demonstration Facility Process Flow Diagram

The wood feed bin has approximately a 1500 lb capacity of dried chips and is equipped with a live bottom feeder. The bin feeder is used to keep the reactor feeder inlet flooded with wood chips. The reactor feeder serves two important functions. It is used to determine the rate and total quantity of wood fed to the gasifier. It is also used to maintain a fixed inventory in the reactor by varying the feeder throughput.

Initial air and oxygen tests used a weigh belt feeder. Later tests used a variable speed screw feeder. Wood feed is transferred to the gasifier through a rotary lock valve. The valve provides a nearly gas tight seal between the reactor and the environment. Back leakage through the valve is made up by supplying sufficient purge gas to the reactor side of the valve. The lock operates at a constant speed such that the valve pockets are only partially filled at the design wood flow rate to minimize the shearing and cutting requirements placed on the valve. The wood that exits the valves passes through the wood feed chutes to the top of the gasifier bed.

4.4.3 Air and Oxygen Supply

Air is supplied to the reactor using a pressure blower capable of supplying the necessary air at sufficient head. The air input to the reactor is damper controlled. The system is designed so that the gasifier can be started up on air and readily switched over to oxygen when a stable air operation is achieved.

Oxygen is supplied to the reactor from liquid storage. The oxygen is vaporized at a typical line pressure of 150 psig. The oxygen flow is metered, controlled and supplied to the reactor through a letdown regulator. All gas lines to the head of the reactor in contact with the oxygen feed system are isolated using swing check valves to ensure that oxygen cannot accumulate in the system infeed piping. The oxygen flow can be immediately terminated from a remote location by closing a solenoid block valve.

4.4.4 Syngas Gasifier Description

The SynGas gasifier was developed to embody the findings of the SERI downdraft gasifier in a configuration that can be scaled to large size. A schematic of the SynGas commercial gasifier is shown in Fig. 4-5. The major features of the gasifier are the following:

- o continuous fuel feed system
- o pyrolysis gas/combustion zone
- o long char bed
- o radial gas takeoff
- o ash grate/ash removal system.

The general arrangement and overall gasifier dimensions are shown in Fig.4-6. Figures 4-7 to 4-9 show respectively an overall view, the gasifier top gear with the weigh belt feeder and the gas plenum with ash grate at the bottom of the gasifier.

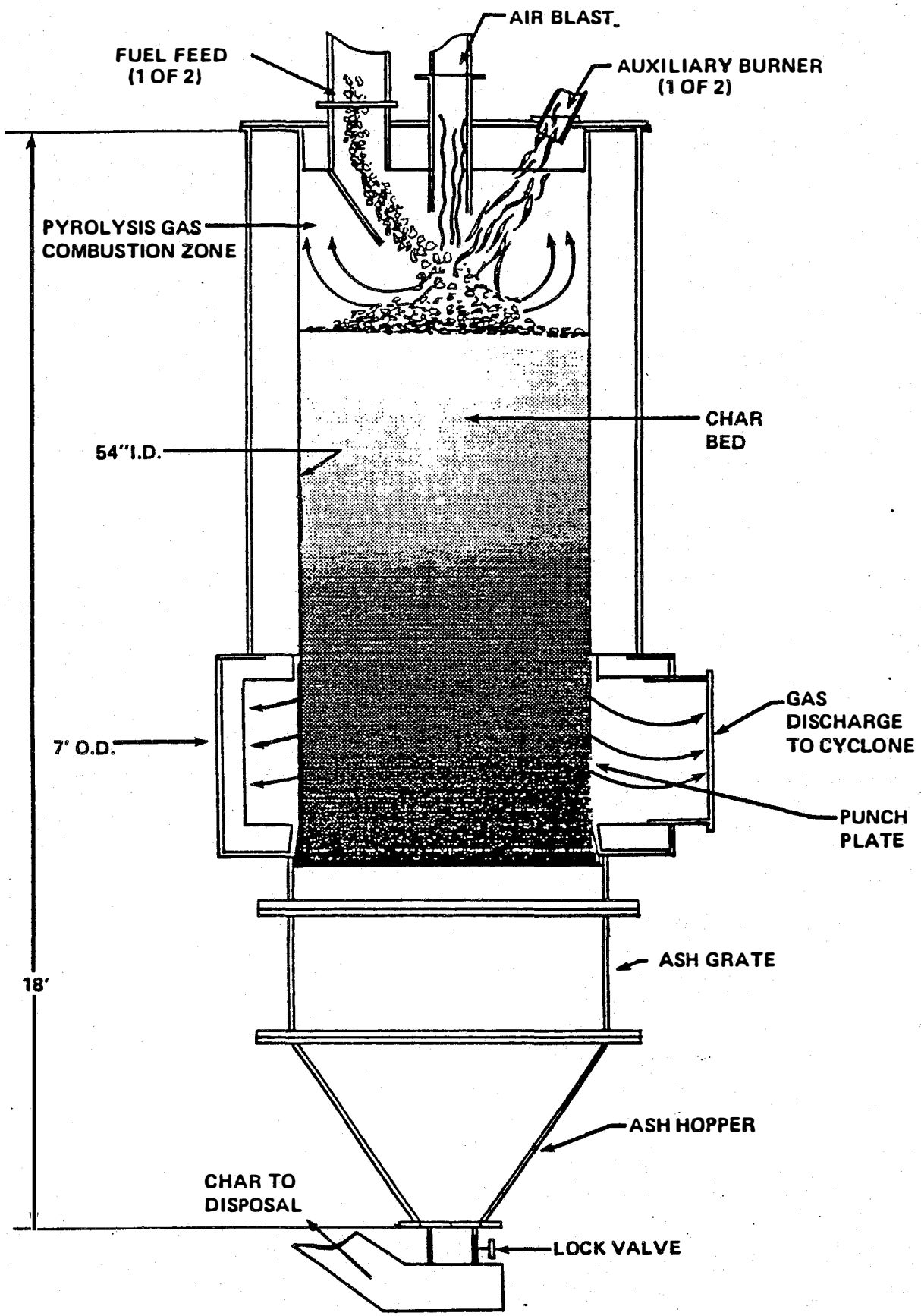

Figure 4-5. Schematic of the SynGas commercial Gasifier

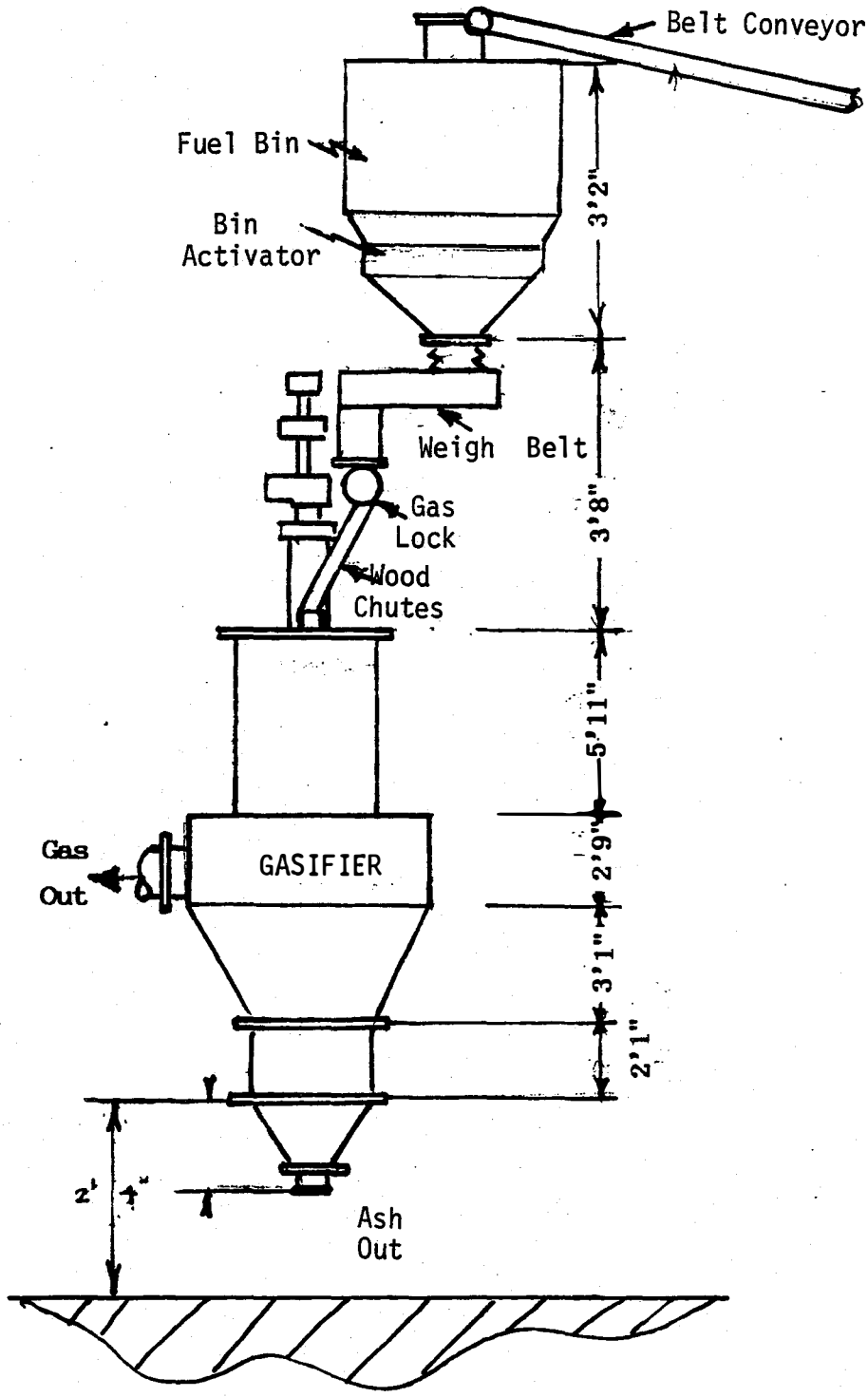

Figure 4-6. SynGas Demonstration Plant-General Arrangement

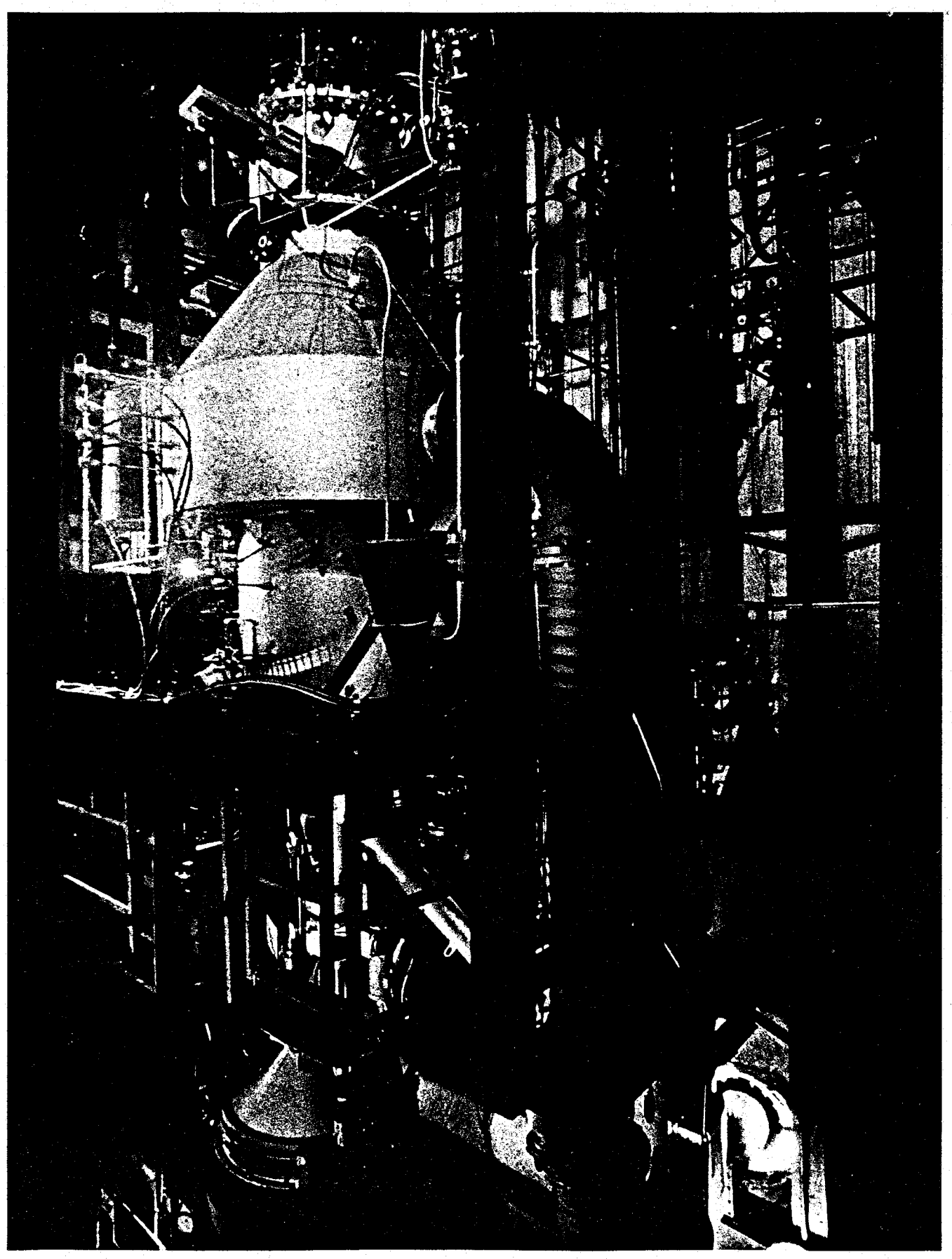

Figure 4-7. Gasifier Full View

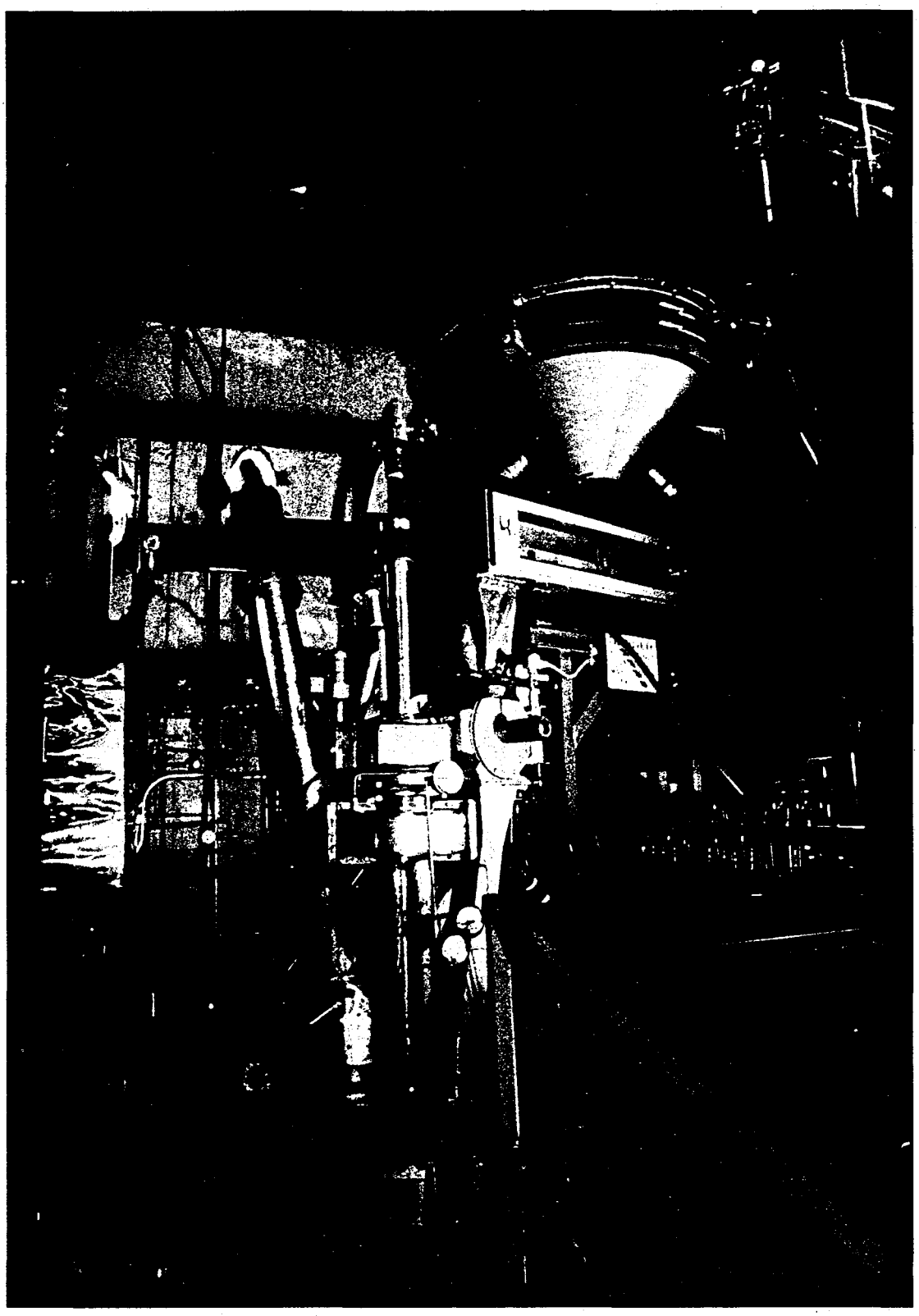

Figure 4-8. Gasifier Top Gear

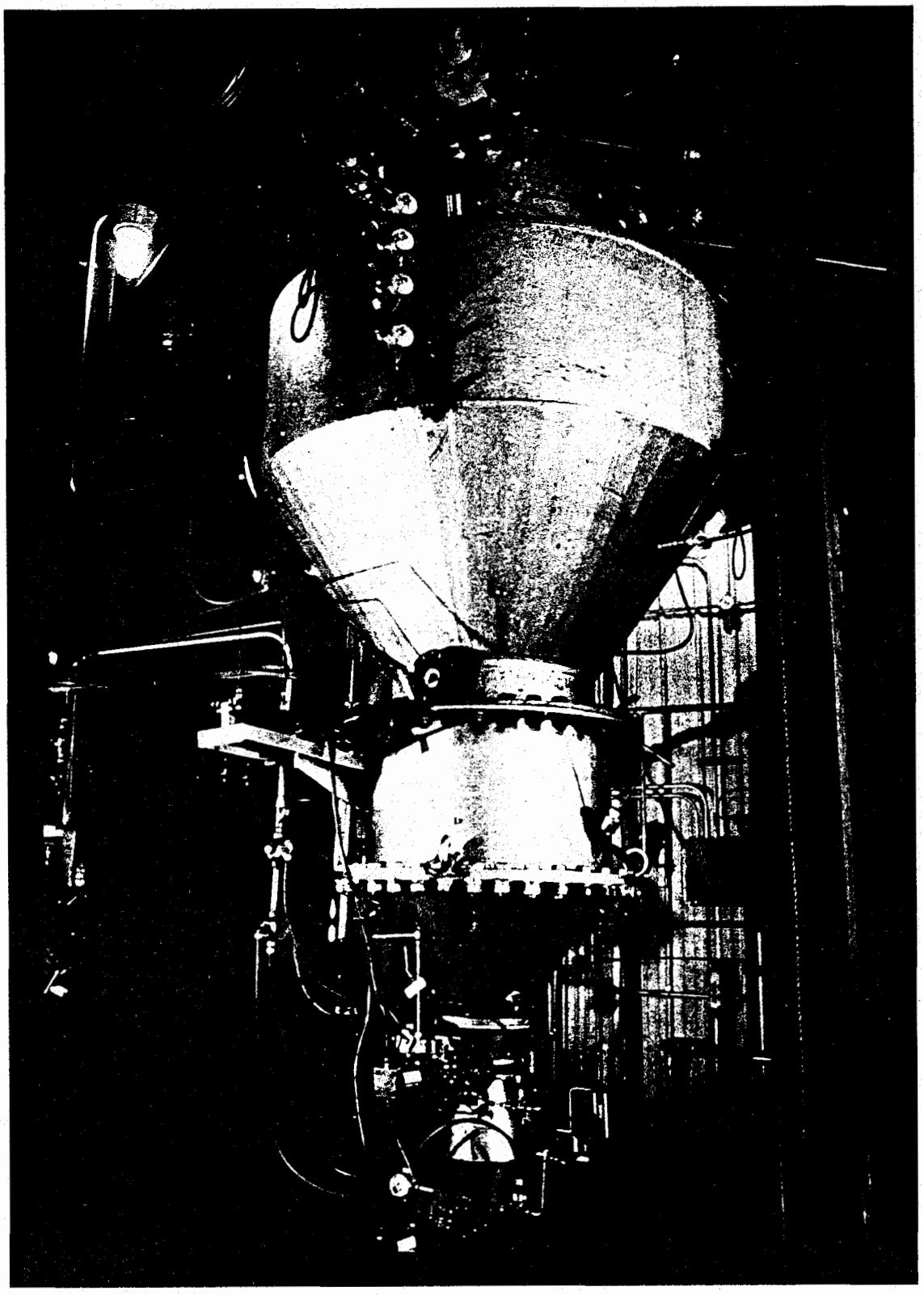

Figure 4-9. Gas Plenum and Ash Grate

The gasifier is a cylindrical refractory lined vessel with a 30 inch inside diameter. Unlike other downdraft gasifiers, it does not contain a choke plate or throat. With small gasifiers having throats of 6 inches or less, it is possible to distribute the oxidizer across the whole throat and thus uniformly react the pyrolysis vapors. Large, choke plate gasifiers have not been successful. The prime difficulty is the slippage of tars through the choke becasue of the inability to distribute the oxidizer so as to maintain a uniformly high temperature in the choke region.

The SynGas gasifier eliminates the need for a choke by maintaining the fire zone on the top of the fuel bed. With oxygen, the upward flame propagation velocity is sufficient to cause the fire to burn on top. Fuel and oxygen are directed to a point on the top of the bed. The solid is distributed on the surface by the oxidizer blast. Good wood distribution minimizes tar slippage. The oxygen blast on the surface causes a recirculating flow in the freeboard above the bed surface. Pyrolysis gases are burned in this region. The burning on the bed surface and in the freeboard result in a headspace temperature above 1600°F on air and above about 2200°F on oxygen. This temperature aids the pyrolysis reaction to occur rapidly and results in a high specific throughput of 2-3 MMBtu/ft^2-h. With chip fuels, pyrolysis is complete within several inches of the bed surface. The majority of tar and hydrocarbon gases is destroyed in this region of the gasifier.

Conventional downdraft gasifiers contain a large inactive biomass fuel inventory. Because of the rapid pyrolysis, the SynGas gasifier contains no inactive fresh fuel. This feature is important in permitting rapid startup and shutdown. The thin fuel layer also minimizes tar slipping through the pyrolysis zone, as all of the pyrolysis vapors will "see" some oxygen.

Below the pyrolysis gas combustion zone, the charred wood forms the char gasification zone. In conventional downdraft gasifiers, the depth of the char zone is only several inches. The Syngas gasifier is operated to maintain a total char bed of 1-3 ft. The greater depth of char is important for minimizing upsets in gasifier performance due to bridging and channel flow. It also provides inventory in case of loss of fuel feed which minimizes the chance of oxygen breakthrough into the offgas line.

The gasifier contains no stirring mechanism. Conventional downdraft gasifiers have employed shaker grates and stirrers to assist in gas flow distribution. SynGas uses a proprietary grate action to liven the bed and totally eliminate fuel flow problems in the reactor.

The gas at the top of the char gasification zone is at the pyrolysis zone temperature of 1600°-2200°F. Char gasification occurs rapidly just under the bed surface and the char and gas temperature fall to the 1300°F-1400°F exit temperature near the bed surface. Little reaction actually occurs in most of the char bed.

Gas is extracted through a vertical perforated plate grate. The plate holds char back while allowing gas to diffuse to the plenum where it is collected and passed to the cyclone for particulate cleaning.

The char-ash is removed from below the gas takeoff by a proprietary grate system. No hot gases flow through the grate. Char ash is locked from the system as required. On air, the SynGas gasifier normally operates at

2-3 MMBtu/ft^2-h of gas production rate. Similar fuel rates have been observed with oxygen.

Fuels with up to 30% moisture have been fed to the air blown gasifier. Wetter fuel can be used with oxygen. Carbon conversion in the gasifier ranges from 90 to 95%. Richer gas is obtained at lower carbon conversion, but CO and H_2 are favored at high carbon conversions. The carbon conversion is controlled by the grate extraction rate. With air blown gasification, 75%-80% of the wood heating value will be present in the cold gas. Oxygen cold gas efficiency is 80%-85%, due to the absence of nitrogen in the product.

The wood feed rate is controlled using the reactor bed level as the control parameter. The overall stoichiometry is based on wood and oxidizer input, carbon extraction using the grate and carbon blowover to the cyclone.

The reactor itself is constructed of carbon steel. Since the operating pressure is under 15 psig, the vessel does not require an ASME code stamp. For oxygen application, the oxidizer piping in the gasifier head is made from 304 stainless steel. Additional reactor internals are fabricated from light gauge stainless steel.

4.4.5 Downstream Equipment

The gasifier off-gas piping to the cyclone is fabricated from carbon steel and is wrapped with a copper cooling coil. Cooling water is supplied to the pipe coil using the stirrer pump. A commercial system will employ refractory lined piping.

The gas is cleaned of particulates using a 304 SS medium efficiency hot cyclone. The device has approximately a 25 micron cut point. The remaining fine solid residues pass hot directly to the combustor (John Zink incinerator with modified low-Btu gas burner) where they are incinerated along with the gas.

4.4.6 Demonstration Plant Instrumentation and Control

The system is highly instrumented to monitor flows, compositions, temperatures and pressures. The principal measured flows are

Stream	Device
Wood	Gravimetric or volumetric feeder
Air	Orifice meter
Product gas	Orifice meter or nitrogen tracer
Purges	Orifice and rotameter
Startup fuel	Orifice meter
Cooling water	Averaging pitot tube
Oxygen	Turbine meter
Char extraction	Batch weighing

With compositional data, mass and energy balances can be made. The gas composition is determined using a Perkin Elmer MGA-1200 dedicated mass spectrometer and a Carle analytical refinery gas chromatograph.

The reactor and system are instrumented for temperature and pressure profiles. A Kaye data logger and IBM PC are used to extract and analyze important flow,

composition, temperature and pressure process data.

Gasifier control is managed with two feedback control loops:

- o Wood feed from gasifier inventory level
- o Oxidizer rate as set by system demand.

The grate speed is used to control pressure drop. Emergency shutdown is an important consideration. Upon an emergency, the oxidizer and wood are stopped and gas is directed to the flare. The gasifier banks itself within minutes of the shutdown.

4.5 EXPERIMENTAL GASIFIER PROCEDURE

4.5.1 Startup

The gasifier is started up on air using the procedure developed for SynGas's air test program. The details of the startup procedure are proprietary. The gasifier is brought to a steady state as is evidenced by constant feed and product rates, compositions, and a steady temperature profile. When the steady condition is achieved on air, the majority of the purge air used to sweep the startup burner, wood feed pipes and gasifier rupture disc vent line is eliminated, and a small amount of carbon dioxide purge is introduced. This is necessary so as to not substantially dilute the oxidizer in the head of the vessel.

The gasifier is rapidly switched over to oxygen by backing down on the air infeed damper and introducing oxygen into the gasifier through the oxygen flow control system. After a short transient period, the gasifier stabilizes on oxygen. An important part of the startup procedure is to ensure that the piping is hot enough to prevent condensation and deposition of materials in the piping. On oxygen operation, the gas temperature is about 300°F at the incinerator as a result of piping thermal line losses since the gas piping is uninsulated.

4.5.2 Input Variables

During testing, the major inflows and outflows are determined as follows:

o **Wood Feed** - The wood feed rate to the gasifier is continuously monitored using a weigh-belt or volumetric screw feeder (in later runs) capable of yielding instantaneous feed rate and total wood fed to the system. The wood moisture is obtained by drawing batch samples off the weigh belt and drying in a microwave oven.

o **Oxygen** - The instantaneous oxygen rate is continuously measured by a turbine meter and controlled.

o **Purge Gas** - Purge gases may enter the system at various points. All purge gas flows are measured with flow meters and are accounted for in data reduction.

4.5.3 Output Variables

o **Product Gas Flow Rate** - The product gas rate is continuously monitored by an orifice meter. The instantaneous flow rate is integrated over steady state

periods to determine the average gas production rate.

o **Product Gas Composition** - The product gas is filtered free of tar and dust. The gas composition is determined using an on-line Perkin Elmer MGA-1200 mass spectrometer capable of determining the major components: carbon dioxide, carbon monoxide, hydrogen, water, methane, nitrogen, ethylene and propylene. Additionally, a Carle analytical refinery gas chromatograph is used to determine the following components from batch samples: carbon monoxide, carbon dioxide, hydrogen, methane, nitrogen, oxygen, ethane, ethylene, acetylene, and total C_n hydrocarbons.

The mass spectrometer analysis is available on a one minute basis with a sample lag time of one minute. The gas chromatograph is used to process batch samples.

o **Unburned Carbon (Char), Tar and Condensates** - Carbon can leave the system in three places: the plenum, the cyclone and the incinerator. During steady state periods, the quantity and rate of solid withdrawn at the plenum and cyclone are determined by weighing. Tar and dust that exit the cyclone are determined by withdrawing a known quantity of gas through a 0.3 micron filter element. The filter elements are dried to remove moisture. Tar is differentiated from dust by an acetone wash of the filter element. Condensates are not recovered from the system.

4.5.4 Other Parameters

Pressures, temperatures and flows (particularly cooling loops) are measured to permit additional process characterization and control as required.

4.5.5 Heat and Material Balance Closure

The degree of heat and material balance closure is obtained by utilizing the direct mass flow and compositional data collected during testing. In this manner, closure is not forced by difference.

4.6 EXPERIMENTAL OBJECTIVES

The test program on oxygen has four major objectives:

1. Demonstrate that oxygen operation is possible with the downdraft gasifier

2. Determine what configurational changes and procedure modifications are necessary to improve operation on oxygen

3. Generate basic parametric test data on oxygen

4. Demonstrate an extended operating period on oxygen

All of these objectives have been met, and details of the results are described in the following sections.

4.7 FEASIBILITY DEMONSTRATION (OBJECTIVE 1)

The gasifier has been operated on wood chip feedstock with air and pure oxygen. The overall conclusion from the testing to date is that low and

medium Btu gas can be successfully produced in a large downdraft gasifier of this design. The succeeding sections detail the results.

4.8 IDENTIFICATION AND SOLUTION OF OPERATIONAL PROBLEMS (OBJECTIVE 2)

The SynGas gasifier was initially designed to run on air. In switching over to oxygen operation, no special safety or "fatal flaw" operational problems have been encountered. However, some minor problems have existed, and some limitations of the present system have been identified.

4.8.1 Oxygen Operation Problems

Overheating in Feed System
In the SynGas Gasifier, wood and oxidizer are introduced into the head space of the gasifier where a fire is maintained on the surface of the bed. Under air operation, the wood introduction ports are purged with a significant quantity of reaction air. This serves two purposes: to make up feeder leakage and to cool the feed pipes

On air operation, SynGas has had no problem with utilizing teflon gaskets for making seals between the gasifier head and the air and wood infeed piping.

On switching to oxygen, the operating procedure requires that purges be reduced to a minimum so as to not dilute the oxygen. Only enough carbon dioxide purge is added under the rotary feed valve on the wood feed pipes to make up for valve leakage plus provide a small sweep of gas down the pipes. Because of the low gas flow using oxygen, significant dilution of the product gas results from the purge. The fire on the surface of the bed is much hotter on oxygen than on air. With the lower purge velocity, heat has tended to travel back through the feed pipes and cause failure of the Teflon gasket material, forcing gasifier shutdown. An attempt to water cool the feed pipes with a surface cooling trace provided only modest improvement. The seals were protected in the extended run by dripping water directly on the flanges and reactor cover to provide the necessary cooling. Any future design must correct this problem.

Headspace Temperature Excursions
The intensity of the fire in the headspace is dependent on the momentum of the oxygen jet issuing from the oxidizer feed nozzle onto the wood surface. A low momentum jet produces a relatively quiescent fire on the bed surface, while a high momentum jet greatly enhances the pyrolysis in the headspace and causes burning of the volatiles to occur in the entire headspace void volume. This latter mode of operation is most desirable from the aspect of decreasing tar production and results in a headspace appearance similar to that achieved in the SERI 1 ton/day gasifier.

However, with the high momentum nozzle, the temperature experienced in the headspace exceeded 2500°-2600°F as was evidenced by damage to the 316SS oxygen nozzle and the refractory in the headspace in comparison to the 2000°F-2200°F temperature experienced with the low momentum nozzle. Gasifier tests were run with the latter nozzle so as to not damage SynGas equipment. However, it is clear that in a design specific to oxygen, the intimate headspace mixing should be an important design consideration.

Refractory Failure
During one of the last oxygen runs, a refractory failure occurred as was

evidenced by a hot spot on the shell. An investigation of the problem revealed that some of the oxygen had bypassed the bed by traveling through voids in the refractory which were accessed through thermocouple well penetrations in the headspace. Fuel gas accessed the same voids through penetrations below the bed level. The potential problem may have existed on air but did not materialize due to the inability to ignite the mixture.

The original refractory consisted of two layers of low iron castable. The insulating material was 6-in. thick and had a bulk density of 60 lb/ft^3. It was applied to the vessel by a gunning process. The outer castable was 3-in. thick and had a bulk density of 120 lb/ft^3. The inner layer had a 2400°F rating while the outer layer was rated at 2600°F. The inner, low density layer failed.

The refractory was replaced with a single 9-inch layer of 90 lb/cf 3000°F low iron castable with comparable insulating qualities. No further problems were encountered with the refractory.

Slagging

During the 50 h extended duration test, it was observed that a thin layer of granular slag formed on the gasifier wall at the wood oxygen interface. The slag appears to be composed of fine granular material and is a result of either the deposition of sand and dirt on the wall or the product of the complete combustion of deposited wood char. No slag had been observed in any previous air or oxygen test. A further consideration of this phenomenon is important in gasifier scaleup/design.

Tar Deposition in Piping

SynGas has experienced more tar production on oxygen operation than on air. The mass flow rate of product gas is less on oxygen than on air for the same wood feed rate. This results in a greater cooling of the product gas because of heat loss in the downstream piping (About 100 feet uninsulated piping from cyclone to incinerator). Less gas also results in a higher dewpoint temperature for the gas/tar stream because of the higher partial pressure of tar species. The net effect is that a greater potential for tar deposition in the piping exists with oxygen than for air operation.

Tar was found to deposit and collect on the incinerator gas check valves and the gas distribution plenum in the incinerator. Although the actual amount of tar deposited was very small (several pounds), those surfaces were cold enough to reduce the flowability of the tar to the point where blockage occurred causing an increase in pressure drop at the incinerator which had an impact on the ability to maintain the throughput in the gasifier. A drop leg was installed on the incinerator plenum, and the piping around the incinerator was insulated. This has reduced the problem. In any medium Btu scaleup, the hot piping runs should be insulated to prevent deposition of tar prior to gas cleanup.

4.8.2 Observations on Oxygen

Nature of the Fire

The oxygen fire at the top of the bed is shown in Fig. 4-10. The fire appears to be much hotter than the fire with air. The intensity of the heat transfer in the headspace is directly related to the inlet momentum of the oxygen jet which is directed at the surface of the bed.

For oxygen operation, the "freeboard" region of the gasifier was maintained at approximately 30 in. below the cover. The oxygen was directed against the midpoint of the bed surface. Two nozzle diameters were tested. These were 1.625-in. ID and 3-in. ID, respectively. The smaller diameter nozzle produced an oxygen jet with a velocity of approximately 80 to 160 fps and the larger nozzle yielded velocities between 24 and 48 fps.

With the larger (low momentum) nozzle, the headspace of the gasifier was quiescent. The fire was stable on the top of the bed, and the observed temperature in the proximity of the bed surface was about 2100°F. When the small nozzle was used, the headspace was observed to be turbulent. The fire in the freeboard was so intense that the bed surface could not be observed. The temperature in the headspace exceeded 2500°F, which was the maximum measurable with the Type K thermocouples employed. In fact, the nozzle was overheated and a hole was burned through the 316L stainless steel. After the test, the refractory near the bed surface was observed and found to have been overheated as was evidenced by a glazing of the refractory surface. As the temperature limitation of the refractory was 2600°F, the temperature of the impinging gas on the surface reached at least that value.

An observation of the gas composition with the high momentum nozzle showed a methane content of 3% compared to 6% with the low momentum nozzle. The results indicate that the appropriate way to operate the gasifier to produce synthesis gas is with a high momentum jet while medium-Btu gas with a richer heating value is favored with the low momentum jet. Although no quantitative measurements of tar content in the gas were made with the high momentum nozzle, the lower hydrocarbon content of that gas would suggest a lower tar content gas.

Because the gasifier was not designed to tolerate the heat release in the gasifier headspace encountered with the high momentum nozzle, it was necessary to operate with the larger diameter oxygen inlet. Thus, the test program had to be limited to the production of the richer gas.

Wood Feed Distribution

The wood is introduced to the top of the gasifier through two feed points arranged along the diameter of the cover and placed at the mean square radius of the gasifier. On air, the distribution appears satisfactory. On oxygen, it has been observed that the reduced turbulence in the head results in the wood being poorly distributed. The net effect is that two regions of gasifier bed exist, one with little wood and hence little tar production and the other with the bulk of the wood feed and excessive tar production. The overall impact of the poor wood distribution appears to be greater hydrocarbon gas and tar slippage through the gasifier. Two regions on the top of the bed where raw wood is observed to be adjacent to white hot charcoal are shown in Fig. 4-10. After Test 4, the wood infeed was modified to promote better distribution. This appears to have had a very positive impact on reducing tar production in the gasifier.

These two observations with oxygen have a significant impact on the quality of the gas produced in the gasifier and should be addressed in any subsequent gasifier design for oxygen.

Pressure Drop

A major purpose of the grate is to remove spent fuel and ash while maintaining gas throughput. The latter is directly related to the permeability of the

bed. A char bed with low permeability will exhibit a high pressure drop. On air, pressure drop is readily controlled at 30 to 50 in. water column with grate action. Because of the lower volumetric flow rate through the bed due to the absence of nitrogen in the oxidizer gas, it was anticipated that the pressure drop for a given Btu production rate would be lower than on air.

The oxygen supply pressure at the gasifier head was limited to approximately 135 in. wc (5 psi) by letdown regulators. Since the oxygen flow is mass controlled, for a given flow set point, the oxygen delivery pressure will assume that required by the system resistance. As long as the resistance is less than the maximum delivery pressure, the system pressure drop can vary while gas throughput is maintained.

During the early, short-term oxygen runs, high throughputs were obtained for short test periods. However, during the long duration runs, it was observed that the steady pressure drop was actually much higher (typically 130 in. or more) on oxygen than on air when maintaining a steady throughput in excess of 8 MMBtu/hr. The grate had to be operated at the maximum withdrawal rate in order to control the bed resistance and thus not lose gas flow.

The long-term test was made on Colorado pine feedstock. It was observed that the spent char from the grate was much finer using oxygen in place of air on the same feedstock. Apparently, the action of oxygen on the wood caused the charcoal to fragment to a much greater degree. Since the pyrolysis in the headspace is driven by a much hotter fire, it is possible that a portion of the wood is exploded under the oxygen fire. The pressure drop issue must be addressed in any future design work for oxygen gasification.

4.9 RESULTS OF OXYGEN PARAMETRIC TEST RUNS (OBJECTIVE 3)

4.9.1 Introduction

The following section presents a summary of the oxygen test work. Table 4-2 summarizes the test runs and objectives.

Runs 1 through 7 were conducted to obtain information about the proper operating configuration for the gasifier. Runs 8 and 9 were made for checkout for the extended run. Run 10 was the extended test on oxygen.

4.9.2 Summary of Oxygen Test 1

Oxygen Test 1 was carried out for the purpose of shakedown on oxygen. The wood fuel used was cedar chips, which were produced by onsite chipping of dried stock. The cedar feedstock was relatively fine in size distribution, being similar to 3/4 in. pulp chips, but with considerably more sawdust. The analytical data for the cedar is given in Table 4-3.

The gasifier was started up on air in the usual manner. The product gas piping was heated to 400°F at the incinerator. Wood feed was initiated at 1000 lb/h to the gasifier and the grate was stoked slowly (Period 1). After the unit reached steady state, it was switched to oxygen by reducing the air supply and introducing oxygen to the head space. In the process, carbon dioxide purge was introduced to the wood feed pipes to purge the feed system and make up for the leakage out of the star valve which is estimated to be 20 scfm. An intermediate state of operation was experienced in the transition (Period 2) because of excessive air purge through the startup burner and other

ports. When these purges were eliminated, operation on oxygen was effected (Period 3) and a stable condition achieved.

The run had to be terminated when a gasket failed on the reactor feed pipes resulting from overheating because of the low purge employed in oxygen operation. Table 4-4 presents an operating summary for the shakedown run. During the operation on pure oxygen, Period 3, a product gas with a dry higher heating value of 319 Btu/scf was obtained at a wood feed rate of 12 MMBtu/h, LHV basis. The tar production was not determined but was qualitatively observed to be higher than in air runs. (The cedar wood also appeared to generate significantly more tar on air than other feedstocks did.)

The gas produced was relatively rich in hydrocarbons. During Period 3, approximately 13% of the wood feed carbon was converted to C_1, C_2 and C_3 hydrocarbons. Additionally, based on Oxygen Run 3 where 20,000 ppm of tar was observed, approximately 4% of the carbon could have been present as tar. The relative richness of hydrocarbons in the gas yields a good combustion fuel gas but does not result in a gas which is suitable for chemical synthesis without additional processing. It is probable that some gasifier modifications would be effective in further cracking the gas.

After switching over to oxygen, no significant difference in reactor temperature profile was apparent. The reactor head space temperature and gas exit temperature were basically the same on air and oxygen.

Table 4-5 presents a raw material balance for the Oxygen Test Period 3. The carbon balance closure is good. The oxygen balance is poor and appears to suggest that the oxygen feed rate is incorrect as the indicated wood mass ratio is only 0.16 while a computer simulation suggests a ratio of approximately 0.25 for the quantity of hydrocarbon found in the gas. Such a difference would help oxygen closure. Table 4-5 shows the raw energy balance. Closure is within 13%. Test 1 demonstrated that oxygen operation is feasible.

Table 4-2. Summary of Oxygen Test Runs

Run #	Date	Objective
1	11/11/85	Shakedown
2	11/14/85	Vary feed rate on cedar
3	11/22/85	Compare cedar & pine operation
4	12/12/85	Add pilot fuel to improve fire on bed surface
5	12/20/85	Vary feed rate on pine
6	4/16/86	High momentum nozzle checkout
7	4/24/86	Low momentum nozzle checkout
8	4/28/86	Extended run attempt
9	5/27/86	Checkout for extended run
10	5/29/86	Extended run

TABLE 4-3. Cedar Feed Analytical Data

Ultimate Analysis,* Dry%		Proximate Analysis, Dry%	
C	52.6	VM	74.0
H	5.8	FC	25.4
O	41.0	ASH	0.6
ASH	0.6		

Moisture Content, Wet Basis	10%
Heating Value - Gross, Dry Basis	9,238 Btu/lb
Net, as fed	7,600 Btu/lb

*Fuel Oxygen by direct determination

Table 4-4. Results for O2 Test 1

Variable	Period 1	Period 2	Period 3
Wood lb/hour	990	1480	1630
Air, scfm	310	107	0
Oxygen, scfm	0	37	53
Propane, scfm	5.2	0	0
Product Gas, scfm	570	560	580
Purge Gas (CO_2) scfm	-	-	≈30
Char, lb/hour			85
Tar, ppm by weight			≈20,000
Product Gas			
Gas Analysis, GC/(MS)			
CO	21.51(16.2)	33.30(23.80)	40.54(29.60)
CO_2	13.44(7.60)	28.29(14.30)	28.59(17.30)
H_2	13.29(11.90)	16.65(28.70)	18.76(16.30)
H_2O	--- (14.67)	--- (16.52)	--- (13.93)
N_2	46.18(46.40)	13.49(13.00)	3.98(16.00)*
CH_4	3.68 (2.19)	5.73(03.48)	5.70(04.45)
C_2H_2	0.15	0.37	0.41
C_2H_4	1.05(0.96)	1.61(01.66)	1.49(02.16)
C_2H_6	0.19	0.36	0.34
C_3	0.51 (0.08)	0.20(00.16)	0.20(00.26)
Pressure Drop in WC	7	90	75
Reactor Temperatures °F			
Head Space	1740	1500	1600
Product Gas	1320	1380	1210
Gas Lower Heating Value, Btu/scf Wet Basis	148	208	232
			255**
Gas Higher Heating Value, Dry Basis			319**
Carbon Conversion %			91

Note: * Sample system air leak; ** Corrected for CO_2 and air purge,

4.9.3 Summary of Oxygen Test 2

Oxygen Test 2 was carried out on 10% mc cedar wood. The objective of the test was to determine the effect of wood feed rate on gasifier operation, and particularly, what the upper limit feed rate was to the gasifier (within the 2000 lb./hr. limitation of the weigh belt feeder).

The wood feed pipes were modified prior to the run to have a water trace for cooling. The purpose was to protect the gasket that failed during the first test. Instruments and controls were checked and recalibrated as necessary.

Table 4-5. Material & Energy Balance, Run 1 - Period 3

	INPUTS (lb/hr)				OUTPUTS (lb/hr)			
	Wood	CO_2	O_2	Total	Gas	Char	Tar	Total
C	772	57	--	829	756	69	35	860
H	103	--	--	103	81	--	3	84
O	746	152	268	1166	1438	6	8	1452
Total	1621	209	268	2098	2275	75	46	2396

Energy In:	
Wood, LHV	12,388,000
Gas, LHV	8,073,600
Char, LHV	1,106,615
Tar, LHV	700,000
Gas, Sensible	888,100
Energy Out	10,768,316

As in Run 1, the gasifier was started up on air. When the piping at the incinerator reached 450°F, wood feed was initiated and the gasifier was stabilized. The system was switched over to oxygen and wood rates of 1000, 1500 and 2000 lb/h were set to the gasifier. During the test, it was observed that there was an increase in pressure drop across the incinerator that became substantial enough to force a system shutdown. Subsequently, it was found that tar deposited on the cold surfaces of the incinerator check valves and the incinerator burner gas distribution plenum plugging the valves and gas injectors. Test Period 1, 1000 lb/h, consisted of a 4-h duration. Since it was apparent that the pressure drop was going to cause a shutdown, the test periods at 1500 lb/h. (Period 2) and 2000 lb/h (Period 3) were limited to 1 h to obtain the maximum information possible from the test.

Table 4-6 presents the test results for Run 2. For the three time periods, the O_2 wood ratio was independent of wood flow rate. Further, the product gas flow rate was directly proportional to the wood rate. The gas composition was essentially independent of the wood rate. The carbon dioxide content of the product gas decreased with increasing wood rate because of the impact of increased gas production on the constant CO_2 purge rate. The reported gas compositions are representative of the test periods and did not vary by more than about 10% for any component over any period duration. The indicated carbon conversion from the recovered char ranged from 88% to 91%. Table 4-7 presents char analytical data from the grate and cyclone for Run 2.

During the three test periods, reactor temperatures were essentially independent of wood flow rate. Further, the pressure drop across the reactor was independent of wood rate. In the reactor, there is a pyrolysis zone and a char gasification zone. The majority of the pressure drop is always experienced in the gasification zone. This is apparently because of the generation of fines in the pyrolysis section that accumulate below and choke the bed. Increasing the wood rate tends to increase the depth of the pyrolysis zone at the expense of the char gasification zone resulting in a shorter char bed. The observed result is a pressure drop that is not strongly dependent on wood rate.

The major observation to be made is that the reactor ratio is held constant by the method of operation resulting in a constant gas composition exiting the gasifier. Therefore, the production of chemical Btu from the gas depends on the wood rate only for a given feedstock.

Table 4-6. Results for Oxygen Test 2

Variable	<----Period----> 1	2	3
Wood lb/hour	900	1500	1980
Oxygen, scfm	46	70	103
Product Gas scfm	330	540	730
Purge Gas (CO_2)scfm	20	20	20
Char lb/hour	66	93	106
Tar ppm by weight**	--	--	--
Gas Analysis GC/(MS)			
CO	39.18(35.1)	44.37(39.2)	45.21(40.50)
CO_2	30.18(20.8)	26.74(17.6)	24.57(15.60)
H_2	21.23(18.4)	21.52(18.5)	22.09(19.40)
H_2O*	-- (18.93)	---(17.05)	--- (16.85)
N2	0.20	0.00	0.00
CH_4	6.22(4.69)	5.18(4.90)	5.69(04.90)
C_2H_2	0.26	0.40	0.46
C_2H_4	1.51(1.88)	1.36(2.52)	1.54(02.50)
C_2H_6	0.42	0.28	0.30
C_3	0.24(0.20)	0.15(0.26)	0.15(00.25)
Pressure Drop in WC	75	75	60
Reactor Temperatures °F			
Head Space	1600	1600	1700
Product Gas	1260	1282	1270
Gas Lower Heating Value, Wet Basis	212	269	250
Carbon Conversion %	87.5	89.4	90.8
Oxygen/Wood ratio	0.258	0.235	0.262
Equivalence Ratio Φ	0.172	0.158	0.176

* Estimated by Diff. since max H_2O span on mass spectrometer is 15%.
**Tar yield not determined.

During Test 2, the indicated wood rate ranged from 1.4 MMBtu/ft²-h to 3.0 MMBtu/ft²-h LHV feed. The higher rate may not be the maximum that can be fed to the gasifier; however, it represents the maximum feed rate possible with the test stand configuration.

Table 4-7. Char Analytical Data from Oxygen Run 2

	Weight Percent in	
	Cyclone	Grate
C		94.49
H		0.75
O		0.89
N		0.19
S		0.05
Ash	7.30	3.72
VM	4.15	3.26
FC	88.55	93.02
% C Conversion from ash balance	91.80	85.20

Table 4-8. Material & Energy Balance Results on Oxygen Run 2 - Period 2

	INPUTS (lb/hr)				OUTPUTS (lb/hr)			
	Wood	CO_2	O2	Total	Gas	Char	Tar	Total
C	710	38	--	748	686	86	35	807
H	95	--	--	95	81	0.7	3	85
O	687	101	354	1142	1341	0.8	8	1345
	1492	1393	54	1985	2108	88	46	2337

Energy In (MMBtu/hr)	
Wood, LHV	11,400,000
Gas, LHV	8,715,600
Char, LHV	1,079,000
Tar, LHV	700,000
Gas, Sensible	840,000
Energy Out	11,334,600

Table 4-9. Lodgepole Pine Feed Analytical Data

Ultimate Analysis* Dry %		Proximate Analysis, Dry %	
C	51.23	VM	84.35
H	6.04	FC	15.45
O	42.78	Ash	0.20

Moisture Content, Wet Basis	12.8%
Heating Value, Gross, Dry Basis, Btu/lb	8,742

* Fuel Oxygen by direct determination

The O_2/wood ratio ranged from 0.235 to 0.262 on a weight basis. The equivalence ratio was from 0.159 to 0.176. This is in good agreement with computer simulations based on the amount of hydrocarbon present in the gas. The major hydrocarbons present are methane, ethylene, acetylene, methane and propylene. While a C^{4+} analysis is not available, C^{4+}s have never been

observed in air test data and should not be present in oxygen gas. The quantity and nature of the hydrocarbons in gas are the same as observed in oxygen Test 1.

Qualitatively, the tar production was greater than for air testing. The dried tar was found to be 77.2% C, 5.8% H, and 17% O by weight. This is essentially the same analysis as obtained on air runs.

Table 4-8 presents material and energy balance data for Test Period 2, Run 2. The closure on the elementary balances is very good, being within 15% for all species. The energy balance closure is also excellent. The balance shows that more than 90% of the wood energy was converted to chemical and sensible heat exclusive of the char.

4.9.4 Summary of Oxygen Test 3

Oxygen Test 3 was conducted using 10% moisture content cedar chips and dried lodgepole pine pulp quality chips. Prior to Test 3, a number of minor system changes were made, including the installation of a drip leg on the incinerator in order to drain accumulated tar.

The gasifier was started up as usual on air. After wood feeding was initiated, it was observed that a pinhole water leak existed on the rake causing liquid water to enter the gasifier. It was decided to continue the run and repair the leak after the test.

The gasifier was continued on dried cedar and the wood rate set at 1500 lb/h of cedar. A 4-h test period was completed. The gasifier was then switched over to 12.8% mc pine pulp chips and operated at 1000 and 1500 lb/h for 2-h periods. Table 4-9 gives the pine fuel analysis.

The action of the fire on the pulp quality pine was different than on cedar. This appeared to be a result of lack of fines that are removed from pulp feedstock and that normally pyrolyze in the head space of the gasifier. On pine, the fire on the reactor surface appeared to be non-homogeneous. When the gasifier operates on air, the oxidizer velocity into the reactor is sufficient to assist in distributing the wood and associated fire. On oxygen, the velocity is low enough that the oxygen does not assist in generating turbulence or backmixing. The wood tends to pile under the distribution points and is spread by the stirrer, that does an inadequate job of moving fresh wood over the entire surface of the bed. The net effect is a region of bed rich in wood and a region more akin to a charcoal gasifier. In this mode, tar is able to slip through the portion of the bed overloaded with wood, resulting in a hydrocarbon rich gas. Since an important objective for oxygen operation is to make synthesis gas, distribution of wood and creation of a uniform fire are important considerations.

Table 4-10 compares the gases produced from cedar and pine. Even though the feedstocks are different, the gas produced is very similar. The same observation has been made on air operation with a variety of softwoods.

Table 4-10. Oxygen Test 3 Dry Gas Composition Comparison For Two Wood Feedstocks

	CEDAR (10% mc)	PINE (5% mc)
CO	41.26	41.93
CO_2	25.16	25.14
H_2	20.38	21.71
H_2O	---	
N2	5.23	3.00
CH_4	5.73	5.83
C_2H_2	0.41	0.35
C_2H_4	1.36	1.41
C_2H_6	0.31	0.38
C3	0.16	0.24

Table 4-11. Results for Oxygen Test 3

	Period		
	1	2	3
Variable	Cedar	Pine	Pine
Wood lb/hour	1450	1440	920
Oxygen, scfm	62	56	36
Product Gas, scfm	530	570	450
Purge Gas (CO_2) scfm	20	20	20
Char, lb/hour	102	91	74
Product Gas Analysis GC/(MS)			
CO	41.26(36.5)	41.93(39.6)	39.66(41.2)
CO_2	25.16(24.5)	25.14(23.8)	30.72(21.5)
H_2	20.38(20.9)	21.71(22.5)	20.41(25.8)
H_2O	(4.54)	--- (3.32)	0.00(3.37)
N2	5.23(5.84)	3.00(1.90)	0.15(00.0)
CH_4	5.73(5.72)	5.83(5.16)	6.52(6.23)
C_2H_2	0.41	0.35	0.25
C_2H_4	1.36(2.19)	1.41(2.63)	1.54(2.13)
C_2H_6	0.31	0.38	0.46
C3	0.16(0.28)	0.24(0.44)	0.28(0.36)
Pressure Drop in WC	90	80	70
Reactor Temp. °F			
Head Space	1700	1700	1600
Product Gas	1275	1260	1220
Oxygen/Fuel	0.210	0.186	0.192
Equivalence Ratio Φ	0.141	0.125	0.130

Table 4-11 presents raw data for cedar and pine operation. The results for the first period on cedar essentially duplicate those for Period 2, Run 2. The product gas moisture content as reported by the mass spectrometer appears to be very low, probably suggesting that some condensation was occurring in the sampling system.

The results for pine show a similar trend to those obtained for cedar. The required oxygen per unit of fuel is slightly lower. This is probably because of the lower moisture content of the fuel and probably the carbon content of the fuel. The gas composition is essentially independent of rate as was found for cedar. The temperature and pressure drop behavior are similar to that found for cedar.

Test 3 shows that the gasifier performance is similar on different softwoods in terms of throughput, pressure drop and gas composition.

A gas sample taken on pine operation showed an indicated tar and dust loading of 770 mg/scf amounting to 24,000 ppm by weight in the gas. The tar was estimated to represent 20,000 ppm of the gas by weight or 3.5% of the wood feed by weight. The effort for the fourth test was therefore directed at reducing the hydrocarbon and tar content of the gas.

4.9.5 Summary of Oxygen Test 4

Oxygen Test 4 was conducted using 5% mc lodgepole pine pulp chips. In preparation for Test 4, the incinerator plenum, check valves and associated piping were insulated, and the drip leg on the incinerator plenum was heat traced to further assist in eliminating fouling of the burner. The leakage problem in the reactor stirrer was repaired. The purpose of the test was to bench mark the system on air with the pine chips and duplicate an oxygen point obtained in the previous run. An attempt was made to distribute the fire better with the addition of a small amount of pilot fuel to the gasifier and to reduce the carbon extraction rate. The purpose of the latter effort was to try to increase the O_2/wood ratio, that should reduce the hydrocarbons.

The gasifier was started up on air at a steady state rate of 1000 lb/h was established. The gasifier was switched over to oxygen and a short steady period at 1000 lb/h of wood was established. The test had to be terminated when a gasket on the support bearing for the rake failed. This resulted when pilot fuel as propane was added to the oxygen to improve the distribution of heat across the top of wood feed, that in turn could have improved pyrolysis and reduced the tar. In the previous runs, it had been observed that wood tended to form piles under the feed chutes such that tar could potentially slip through cold areas in the reactor. Because of the low velocity in the oxygen feed pipe, the oxygen propane fire backed up into the pipe and caused the gasket to fail.

The test was run long enough to establish that the insulation on the incinerator was effective in eliminating tar buildup in the burner, that had been an ongoing problem with oxygen.

Table 4-12. Oxygen Test 4 Results Gas Composition Data

	Air	Nitrogen Free	Oxygen
CO	20.97	39.09	41.47
CO_2	13.79	25.71	29.88
H_2	13.94	25.99	20.19
H_2O	--	--	--
N_2	46.36	--	0.00
CH_4	3.21	5.98	5.69
C_2H_2	0.19	0.35	0.40
C_2H_4	1.09	2.03	1.69
C_2H_6	0.16	0.30	0.39
C_3	0.29	0.55	0.29

Table 4-13. Whole Tree Chip Analysis - Dry Basis

C	52.20
H	5.94
O	40.75
Ash	1.11
	100.00
HHV, Btu/lb	9051
mc%, as fed	22.8

Table 4-12 presents steady air and oxygen composition data on pine chips as obtained from the gas chromatograph. The air composition is also shown on an oxygen-free basis for comparison purposes. It is apparent that the major difference between air and oxygen operation is nitrogen dilution and that the hydrocarbon production rate is very similar.

4.9.6 Summary of Oxygen Test 5

Oxygen Test 5 was conducted on 12.8% mc lodgepole pine pulp chips and 22.8% mc lodgepole pine whole tree chips. Prior to Test 5, the wood feed chutes were modified to improve the wood distribution and the speed of the stirrer was increased to also enhance the distribution.

The test was initiated on the pulp chips defined in Table 4-9, with a moisture content of 12.8% on a wet basis. Midway through the test, the gasifier feed was changed to 22.8% moisture content pine chips described in Table 4-13.

Startup was made on air. The wood feed distribution was considerably improved based on the visual inspection of the bed surface. A tar sample was collected and analyzed. The indicated tar production rate was 286 ppm by weight in the product gas.

The gasifier was switched to oxygen and the wood rate was maintained at 1900 to 2000 lb/hr for a six hour test period. An estimated 15,300 lb of wood chips were fed during the test. Steady test periods were obtained on the dry and wet feedstocks.

4.9.7 Effect of Fuel Moisture

The effect of wood moisture on gasifier performance at similar wood feed rates is shown in Table 4-14. As the moisture increases, the required oxygen per pound of wood feed increases. On a wet feed basis, 10% more oxygen was required for the 22.8% fuel than for the 12.8% fuel.

The H_2/CO_2 ratio increases with increasing feed stock moisture as shown in Table 4-14. For 12.8% mc fuel, the measured ratio is 0.48, for the 22.8% fuel, the ratio is 0.65.

The higher heating value of the product gas as determined by ASTM Method D 3588-81 indicates that the heating value of the gas falls as the moisture content of the fuel is increased (3). An indicated heating value of 329 Btu/scf was obtained on the 12.8% mc feedstock while a gas produced with 22.8% mc fuel had a heating value of 307 Btu/scf. Because the char extraction rate was higher for the dry wood, richer gas would be expected during Period 1. Therefore, a quantitative statement regarding the decline in heating value cannot be made.

4.9.8 Approach to Equilibrium:

For Period 2 in Run 5, the temperatures corresponding to the equilibrium constant for the water gas shift and steam-carbon equilibrium were computed from the gas composition data (based on an ambient atmospheric pressure of 0.8 atm and the wet gas analysis). The temperatures corresponding to the experimental equilibrium ratios are 1340° and 1196°F, as shown in Table 4-14. These temperatures are in excellent agreement with the observed product gas temperature of 1204°F. Thus, the gas appears to be equilibrated at the reactor exit temperature.

4.9.9 Oxygen Usage

The oxygen consumption in Test 5 during Period 1 was higher than experienced in Test 3 using the same fuel. On a CO_2-free basis (that eliminates purge gas dilution), the hydrocarbon content of the gas produced in Test 3 is higher than that produced in Test 5. These two results are an indication of better fuel distribution in the gasifier.

4.9.10 Tar Production

Tar in the exit gas was measured by filtering a slipstream from the gasifier with a 0.3 micron DOP filter. This filter collects all particles > 0.3 microns with an efficiency of 99%. It also collects a significant quantity of smaller particles.

Tar production data for the operating periods of Run 5 is presented in Table 4-15. The tar production rates for all periods are higher than normally experienced on air, ranging from 0.7% to 2.5% by weight of the gas. There is no apparent correlation between wood moisture content and tar production. There is a relationship between gasifier exit temperature and tar production. The higher the exit temperature, the lower the tar in the effluent. As Table 4-15 indicates, the exit temperature is also related to the char extraction rate. Generally, the greater the extraction rate, the lower the exit temperature. Basically, the results indicate that by extracting greater

amounts of char, the reactor operates more in a pyrolyzer mode yielding richer gas.

Table 4-14. Effect of Moisture on Gasifier Performance

	Period 1	Period 2
Wet wood, lb/hr	2008	1990
Wood mc, %	12.8	22.8
Oxygen, SCFM	90	99
Product gas flow, SCFM	650	680
Purge gas, SCFM (est)	20	20
Char rate, lb/hr	145	100
O2/wood, lb/lb	0.23	0.25
Product Gas Analysis	GC	GC/MS
CO	44.07	38.41/36.32
CO_2	25.39	28.36/22.99
H_2	21.08	24.96/23.93
H_2O	0.0	0/10.99
CH_4	6.1	5.56/5.20
C_2H_2	0.71	0.58/0.00
C_2H_4	1.79	1.42/2.77
C_2H_6	0.40	0.32/0.00
C_3	0.44	0.39/10.29
N_2	0	0.00/0.00
Pressure drop in WC	100	110
Product gas temperature, °F	1125	1204
Gross Heating Value, Btu/SCF (dry)	329	307

T_{shift} = 1340°F for K_{shift} = 1.378
$T_{steam\ carbon}$ = 1196°F for $K_{steam\ carbon}$ = 0.633

Table 4-15. Tar Production

PERIOD	WOOD RATE lb/hr	WOOD mc, %	O2 lb. / WOOD lb.	EXIT TEMP, °F	CHAR EXTRACTION lb/hr	TAR ppm BY WT.
1	1045	12.8	0.22	1283	113	8970
2	1809	12.8	0.22	1070	110	22954
3	2008	12.8	0.23	1125	145	25214
4	1990	22.8	0.25	1204	100	12678
5	1016	22.8	0.27	1236	74	7381

During this test, the grate speed was necessarily high to maintain an acceptable pressure drop of 100 to 125 in. during the test period. Table 4-15 suggests that cleaner gas can be made by accepting a higher pressure drop and consequently reducing the char extraction rate.

4.9.11 Material & Energy Balance

Table 4-16 presents a material and energy balance for Run 5, Period 2. The carbon balance closure is within 11%, and the energy balance closure is within 16%. The test was conducted at 2.4 MMBtu/ft^2-hr of wood feed. The indicated tar free cold gas efficiency (lhv) is 80%, and the carbon conversion was estimated to be 91.2%.

4.9.12 Summary of Parametric Test Results

The results of Test 5 demonstrate that the gasifier can be operated at high throughputs in the atmospheric oxygen mode. The gas produced is relatively rich in hydrocarbons; additional cracking of hydrocarbons is necessary to produce synthesis quality gas. The test indicates that better fuel distribution and lesser char withdrawal will lessen the hydrocarbon content.

4.10 SYSTEM MODIFICATIONS AFTER TEST 5

Between oxygen tests 5 and 6, a number of significant systems improvements were made to enhance the continuous operability of the system. The majority of these were made as part of the SynGas test program. These are summarized as follows:

Table 4-16. Material & Energy Balance Results on Oxygen Run 5 - Period 2

	Inputs				Outputs			
	Wood	CO_2	O_2	TOTAL	Gas	Char	Tar*	TOTAL
C	802	38		840	833	78	24	935
H	141			141	107		2	109
O	1029	101	500	1630	1533	5	6	1544
ASH	17			17	0	17		17
TOTAL	1989	139	500	2628	2473	100	32	2605

Energy In	
Wood LHV	12,049,394
Energy Out	
Gas LHV	11,462,927
Char LHV	1,118,480
Tar LHV	700,000
Gas, Sensible heat	1,005,762
	14,287,169
	Δ = 15.7%

% LHV in gas 80.2%
% Carbon Conversion <90.7% (CO_2 purge free)
* 12,678 PPM by wt. in gas.

4.10.1 Screw Feeder

The weigh belt feeder was replaced with a variable speed twin screw feeder. The weigh belt was useful for closing mass balances. However, the chips

exhibited a tendency to break the belts. The screw feeder proved to be reliable and accurate to within approximately 10% after calibration.

4.10.2 Star Valve

The original star valve was not rugged. During testing, the valve was found be subject to severe wear. This was traced principally to the lack of shearing capability and improper filling of the pockets. The rotor was not designed for heavy duty service. Several blades were bent during operation causing excessive gas leakage to the surroundings. The valve was replaced with a Rader model 14x18 valve. This valve has been satisfactory.

4.10.3 Cooling

Heat trace piping was installed on the head cover and feed chutes for oxygen operation to protect the Teflon seals. On critical seals, the heat trace was perforated to allow water to cool the seal areas by direct contact. This eliminated the seal degradation problems encountered in early runs.

4.10.4 Ash Handling

An automated ash handling system was installed. It consisted of a gasifier slide gate lock valve, a 6-in. inclined ash screw and a screw discharge slide gate valve. The programmable logic controller code was modified to operate the system in unison with the grate and to manage the lock valves. The system operated satisfactorily and permitted continuous operation with reduced manpower.

4.10.5 Grate

A number of proprietary modifications were made to the grate to enhance its operability.

4.10.6 Stirrer

The stirrer was removed from the system. Testing had indicated minimal value to stirring the bed.

4.11 EXTENDED 100-H AIR RUN

During early March, 1986 a 100-h run was conducted on air by SynGas. This demonstrated that the modifications yielded a system that could be operated continuously on air. The operation was conducted using Colorado soft wood feedstock composed primarily of whole tree ponderosa pine and lodgepole pine chips. The feedstock was dried off site to approximately 15% moisture on a wet basis. The objectives of the test were as follows:

- o Prove the final mechanical configuration of the gasifier
- o Operate the gasifier at its rated capacity for an extended period.

4.11.1 Mechanical Proof of Concept

The overall test program demonstrated a number of important aspects of the gasifier, that were factored into the commercial design. These are summarized in this section.

4.11.2 Feeding

The wood feed system composed of the Rader rotary lock valve and custom designed twin-screw variable speed feeder worked satifactorily.

4.11.3 Stirring

The SynGas gasifier was originally designed with a water cooled agitator that was used to stir the bed to level the fuel on top and eliminate large voids in the bed. During the test, the influence of the stirrer was evaluated in conjunction with several improvements made in the grate action and wood distribution parts before the test. It was concluded that the agitator is not necessary for gasifier operation. Thus, the agitator and associated components required for cooling were deleted.

4.11.4 Grate

The importance of the grate operation to gasifier operation was firmly established. The test demonstrated that the single most important piece of the gasifier is the grate. The grate is used to control reactor pressure drop and hence maintain the gas production rate. During the test, there were several brief gasifier outages that were all a result of grate drive malfunction.

4.11.5 Gasifier Internals

All hot metal parts operated satisfactorily during the test.

4.11.6 Ash Removal System

Performance of the ash lock hopper and ash screw system for removing char/ash from the gasifier was generally acceptable. Because of the small surge capacity available in the lock hoppers, several screw shutdowns were experienced during the test, that did not result in gasifier outage. Adjustments were made to the design to minimize ash handling problems.

4.11.7 System Control

The plant is run by a PLC logic controller that is responsible for monitoring alarms, managing safety shutdown, monitoring and moving wood fuel from storage to the surge hopper, and monitoring the grate and ash load out systems. The PLC system operated the plant without any major problems, proving that (nearly) unattended operation of the commercial equipment is a realistic goal.

4.11.8 Cyclone

The hot gas cyclone/ash lock out system performed adequately during the test. No mechanical problems were encountered with the cyclone or lock out valves.

4.11.9 Long Run Gasifier Operation

Material Flows

During the test, an estimated 70 tons of 10% to 15% mc wood fuel was fed to the gasifier. An estimated 5750lb of char was extracted from the gasifier. The input Btu rate to the gasifier averaged approximately 10 MM/h LHV basis.

Based on these macroscopic data, the overall carbon conversion is estimated to be the following:

Carbon in char	
Char weight	5,736 lb
Ash (calculated from wood analysis)	<1,275>
Char (ash free)	4,461 lb
Carbon in char (95%)	4,238 lb
Carbon in wood	
140,000 x 0.835 x 0.5L =	60,060
Carbon Conversion, %	93

Effect of Wood Rate/Air Rate

During the majority of the test, the gasifier was operated at the considered rated capacity of the pilot plant, namely 530 scfm of air with approximately 1350 lb/h of wood fuel. At an average 12.5% MC, the wood fuel lhv is 7181 Btu/lb.

In the later stages of the test, the wood rate was increased. Table 4-17 presents important trend results for the feed rate variation. The trends indicate that the gas heating value and reactor pressure drop are almost independent of throughput.

The highest indicated wood rate represents a 14,000,000 Btu/h input. The test period at this rate was unfortunately brief as the air fan and wood feeder were being operated at and above rated capacity, resulting in operating difficulties. With properly designed components, this rate probably could have been maintained or exceeded.

As the wood rate was increased, the required char extraction rate remained essentially constant. The grate speed is used to control pressure drop. Pressure drop has been observed to be not strongly dependent on flow. This suggests that carbon conversion will be higher for higher throughputs.

Table 4-17. Effect of Wood Rate on Gross Gasifier Performance

Indicated Wood Rate lb/h	Indicated Air Rate SCFM.	Gasifier Pressure Drop, in WC	Gas Heating Value Btu/SCF LHV	Grate Speed Rev/hr	Reactor Off-gas Temp.°F
1270	520	34	146	7.5	1340
1550	640	40	150	7.5	1363
1828*	720	40	145	10.0	1380

* Not steady state condition.

The exit temperature rose slightly with increased throughput. It has been observed that a low exit temperature is indicative of greater tar production. The increased off gas temperatures suggest that cleaner gas was being produced, although no experimental data is available to substantiate the assumption. The constant gas heating value shows that air breakthrough did not occur at the higher rates.

4.12 EXTENDED OXYGEN RUN

4.12.1 Oxygen Test 6

The purpose of Test 6 was to check out the system on oxygen in preparation for the extended run. In order to minimize hydrocarbon production, an oxygen nozzle was used that would produce a high velocity jet on the surface of the bed. This would cause significant backmixing and therefore, burning in the headspace. A 1.5-in. ID nozzle was employed that would produce a 170 fps jet at 100 scfm of oxygen input to the gasifier.

The gasifier was started up in the usual fashion on air and switched to oxygen. The fire in the headspace, on oxygen, was turbulent and bright and it was not possible to observe the bed surface. With previous tests, a low momentum nozzle was employed. Typically 5%-6% methane is present with the low momentum nozzle that has a 3 in. diameter. With the high momentum nozzle, the methane concentration in the gas was 3% and less.

The oxygen nozzle was not cooled except by the oxygen flow. The hot recirculating gases impinged on the outside of the 316 stainless steel nozzle. The hot metal failed, causing the oxygen jet to be directed at the refractory wall. The test was terminated.

After the test, the reactor was inspected. The nozzle was burned through, and the adjacent refractory was glazed severely on the surface. It was decided that the present gasifier could not be run in this mode even though it would be the appropriate way to operate the unit to produce synthesis gas. The headspace internals would have to be redesigned and provided with internal water cooling. Additionally, a better refractory would be required. Because of limited funds remaining in the contract, SynGas elected to make the extended test with the low momentum nozzle. The nozzle was replaced and the unit readied for the next checkout test.

4.12.2 Oxygen Test 7

The purpose of Test 7 was to check the system out on oxygen in preparation for the extended run. A "low momentum" oxygen nozzle was employed. No quantitative test data was collected. The gasifier operated satisfactorily. However, several failures in the ash removal system affected the steadiness of operation. The system was deemed acceptable for the extended run.

4.12.3 Oxygen Test 8

Oxygen Test 8 was intended to be the extended oxygen run. The gasifier was configured with the low momentum oxygen nozzle.

The gasifier was started up on air and switched to oxygen. After several hours of operation, a hot spot was observed on the reactor shell. This was an indication of a refractory failure problem. The test was aborted to protect the equipment.

The reactor was disassembled for inspection. The refractory at the location of the shell hot spot was chiseled out. At that point, located several feet below the bed surface, tunnels existed in the refractory, that provided for a gas path from the headspace to the plenum. Oxygen and fuel gas apparently

ignited next to the shell, causing the observed hot spot on the refractory. The damage was so severe that a refractory patch would probably not have been adequate to permit a successful extended test. It was decided that the refractory would have to be replaced.

The original refractory was installed in two layers. Six inches of 2400°F low iron lightweight backing was gunned onto the shell. A low iron hardface with 2600F rating was cast in place 3 in. thick over the backing. When the backing refractory was removed, it was observed that large uncured pockets of refractory existed. These were probably due to the insufficient use of water in the gunning process. The uncured material would be extremely porous to gas. Also, tunnels existed in the refractory where gas passage occurred. The surface of the hardface had been damaged in Oxygen Run 6. The refractory shrank and cracked in this area.

The shell area refractory was replaced with 3000F A. P. Green Co. Castolite 30 medium weight insulation. The entire 9-in. thickness was cast in place. To minimize any chance of gas passage, all thermocouples and pressure taps were installed before the pour. Therefore, the instruments became an integral part of the casting.

4.12.4 Oxygen Test 9

Oxygen Test 9 was the checkout run for the extended oxygen test. The gasifier was configured with the low momentum nozzle.

During Test 9, the refractory performed well. A minor problem occurred with the gas disengager in the reactor during the checkout. This was repaired after the checkout, and the gasifier was deemed ready for the extended run.

4.12.5 Oxygen Test 10

Test 10 was the extended oxygen run. A total of 56.5 h of operation was conducted with 53.5 h on oxygen. During the test, steady wood feed rates up to 1500 lb/h were maintained, amounting to 10,000,000 Btu/h LHV wood feed.

Mechanical Proof of Concept
The test overall demonstrated a number of important aspects of the gasifier that should be factored into a commercial reactor design for oxygen. These are summarized in this section.

Feeding
The wood feed system consisting of the Rader rotary lock valve and custom designed twin screw variable speed feeder worked satisfactorily. However, leakage through the Radar valve results in the need for a significant quantity of inert purge gas to the feeder. In the air-blown system, air is used for purge, while in the oxygen tests, carbon dioxide was used. Ways to reduce the leakage should be explored.

Grate
The importance of the grate operation to the gasifier operation was again firmly established. The test demonstrated that the single most important piece of the gasifier is the grate. The grate is used to control reactor pressure drop and hence maintain the gas production rate. During the test, there were several gasifier outages due to the grate drive malfunction. Additionally, the char/ash extraction rate was higher on oxygen than on air,

resulting in a temperature under the grate high enough to damage a viton seal. The loss of this seal resulted in the loss of an important proprietary grate action. The combined failures ultimately caused the test to be terminated. SynGas has done considerable redesign of the grate since the test.

Gasifier Internals
All hot metal parts operated satisfactorily during the test. The refractory was satisfactory for oxygen operation. The shell temperature profile as determined by infrared pyrometers is shown in Fig. 4-11. During the test, a layer of agglomerated ash built up on the refractory at the bed surface. This appears to be due to the deposition of flaming embers on the wall and their subsequent combustion in oxygen. For a commercial application, this deposition must be controlled. This can be accomplished by limiting the concentration of oxygen in the headspace either by promoting backmixing or introducing auxiliary fuel.

Ash Removal System
Performance of the ashlock/ash screw system for removing char/ash from the gasifier was generally acceptable. Because of the small surge capacity available in the lockout hoppers, several screw shutdowns were experienced during the test, that did not result in gasifier outage.

External Seals
All external seals remained intact during the test. Headspace seals had to be protected by the objectionable method of dripping liquid water onto sensitive flanges. In a commercial unit, integral headspace cooling will be a necessity.

Test Data
Operating data and gas compositions for the test are summarized in Tables 18 and 19. The reporting times in Table 18 are correlated with gas chromatographic sampling times. During the test, the mass spectrometer was generally unreliable. Table 18 presents relevant flow, temperature and pressure data and important dependent variables. During the test, the wood feed rate was maintained at approximately 1200 lb/h (to the greatest extent possible). The available operating pressure drop was 140 in. water column of oxygen gas. When grate outages occurred, the gasifier discharge would rapidly choke with fine charcoal, limiting gas passage. At such times, the feed rates had to be reduced until maintenance was completed.

The data in Table 18 shows that the oxygen-to-wood ratio ranged from 0.164 to 0.329 during the test. The oxygen-to-wood ratio is fixed by the rate of charcoal extraction, that in turn affects bed pressure drop. The effect of O_2/wood ratio on gas heating value is shown in Fig. 4-12. At the lowest O_2/wood ratios, the gas heating values achieve the highest values. Therefore, to maximize heating value, char extraction should be maximized; to produce synthesis gas, it should be minimized.

Table 19 presents gas analysis results for the test. The analyses show that the gas is rich in hydrocarbons and that the gases are similar to those obtained in previous testing. Limited mass spectrometer data indicate that the moisture content of the gas is approximately 20%. Using the gas moisture content along with Table 19, equilibrium ratios for the water-gas shift and carbon carbon dioxide reactions were estimated. Apparent equilibrium temperatures were derived from this data and are compared with experimental exit temperatures in Fig. 4-13. The figure shows that the water-gas shift

Figure 4-10. Oxygen Fire on the Top of the Gasifier

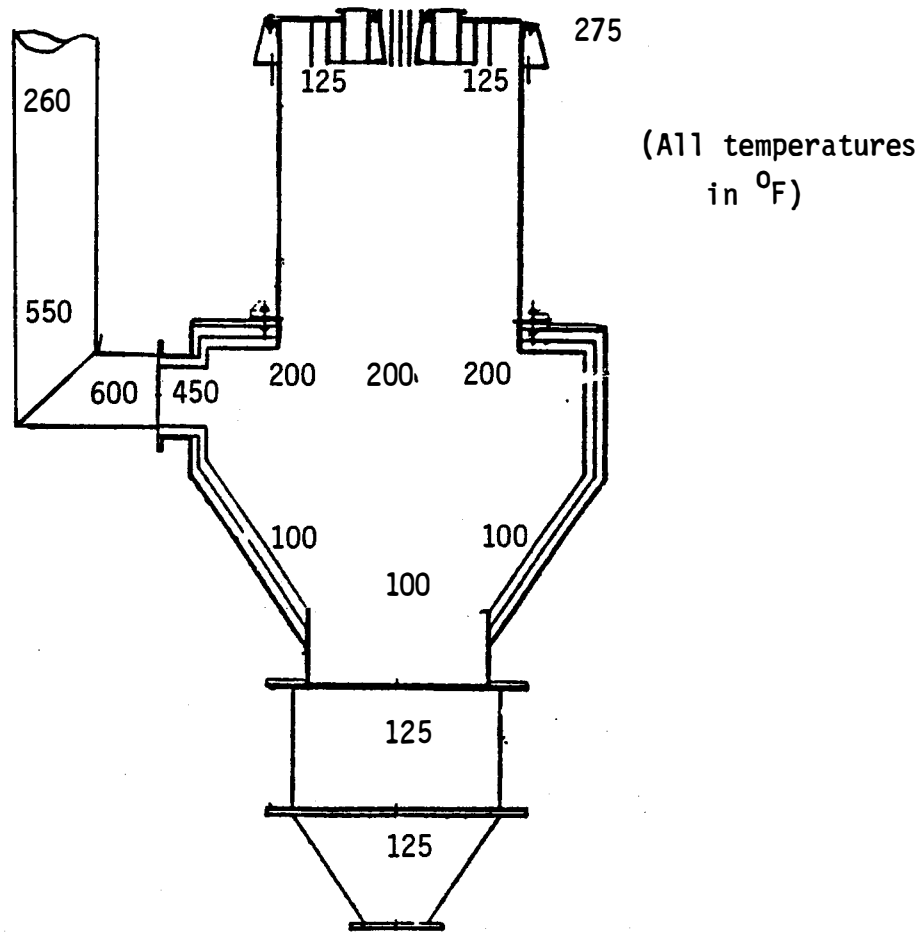

Figure 4-11. Gasifier Shell Temperature Distribution

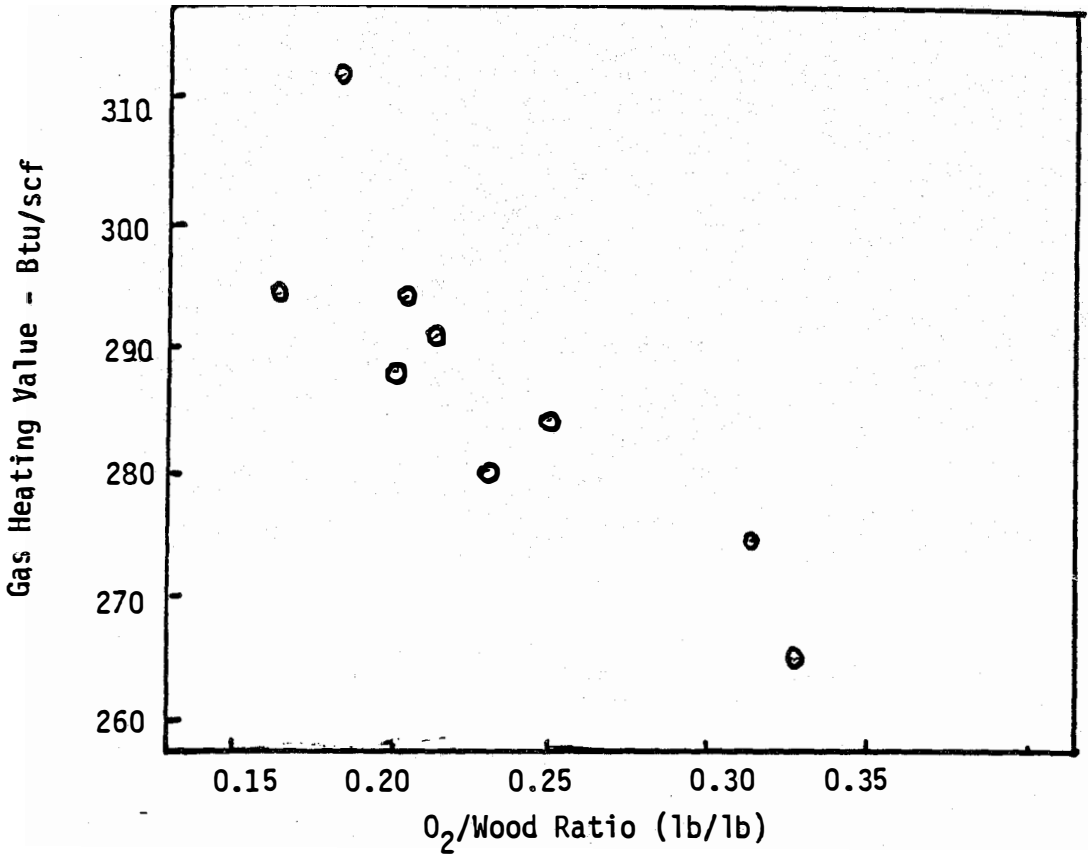

Figure 4-12. Gas Heating Value as a Function of O_2 Wood Ratio

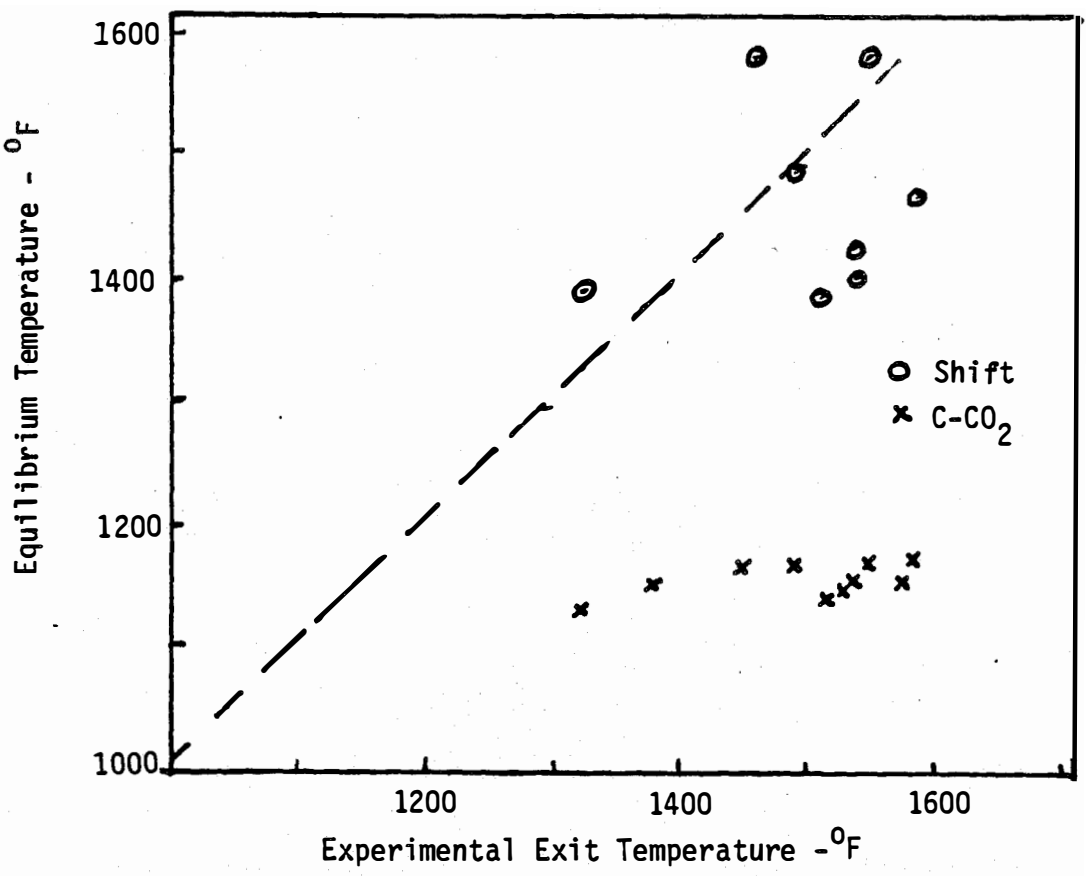

Figure 4-13. Approach to Equilibrium for Gasification Reactions

reaction is essentially at equilibrium. However, the carbon-carbon dioxide gasification reaction is far from equilibrium, and significant potential for char gasification remains.

Table 18 shows that the gasifier offgas temperature during oxygen operation was typically 1550°F. In comparison, the offgas temperature for air operation is approximately 1350°F. Observed carbon conversions are higher in air operation. It is not clear why there is such a difference between air and oxygen.

Table 18 indicates that the required pressure drop to sustain high throughput exceeds 100 in. wc. This is generally higher than that required for air operation even though the product gas volume with air is twice that for oxygen. Experimentally, all the pressure drop is located against the perforated disengaging plate. The layer of fine charcoal deposited against the plate must be less porous with oxygen than with air. It is observed that the charcoal produced during oxygen operation is finer than charcoal produced using air. No size distribution data is available. It is possible that the heating of the wood chips is rapid enough in oxygen that the chips explode, producing considerably more char dust.

4.13 DISCUSSION

The test program has demonstrated that medium Btu gas can be produced by oxygen blowing in the SynGas gasifier. The gas produced has a wet cold lower heating value in excess of 250 Btu/scf and a dry tar free higher heating value in excess of 300 Btu/scf. The SynGas gasifier has been designed to operate on air. The test data reported has been generated by that system with essentially no modification.

The gasifier has been operated on two very dry softwoods, a lodgepole pine and cedar. The former was 10% mc and the latter 5% mc. Testing was also successfully conducted on a 25% mc lodgepole pine fuel. On these fuels, the gasifier has been operated at up to 3 MMBtu/ft^2-h. Treating 3 MM as the maximum capacity, a 50tons per day (dry feed) reactor designed at 75% of maximum rate would be 50 in. in diameter in comparison to the 30 in. test unit. This is the size of SynGas' commercial air blown unit.

Whether operation on oxygen or air is carried out, some drying of fuel may be required. This means that the plant may require an associated fuel drying system. Depending on the application, much or all of the drying can be accomplished with waste heat.

Downdraft wood gasification requires no steam input to the reactor whether air or oxygen is used. In the particular case of oxygen gasification, while there is a premium charge for oxygen, there is no such premium charge for steam.

For the production of synthesis gas, hydrocarbon production should be minimized. Preliminary tests were conducted to vary the intensity of mixing in the gasifier headspace. Greater turbulence and mixing increased the headspace temperature and decreased hydrocarbon production. It was not possible to run the existing gasifier in this mode, however, due to inadequate headspace cooling of metal parts. Follow-on test work should address this aspect of operation.

The gasification process produces char amounting to about 5% of the wood feed

and containing 10% of the wood energy. It would be desirable to increase the consumption of the char to enhance the process economics. Additionally, consumption of char in the reactor will mean that a greater oxygen consumption has been effected. This should enhance the degree of cracking of the gas.

The grate is the single most important component of the gasifier. With adequate grate action, high gasifier throughput can be maintained. In the test program, bed pressure drop was higher for oxygen operation than for air operation at the same wood feed rate. To maintain throughput, a higher grate speed and thus a greater char extraction rate was required. Follow-on test work should address methods to provide the necessary pressure drop in the gasifier to increase carbon conversion and hence reduce hydrocarbon production. Tar production is greater for operation than for air. This is a direct result of the lower carbon conversion using oxygen.

REFERENCES

1. Fluor Technology Inc., *Evaluation of the Production of Methanol from* Biomass," Prepared for Southern California Edison, 1986.

2. Desrosiers, R, "Thermodynamics of Gas-Char Reactions," in *A Survey of Biomass Gasification,* SERI TR/33/239 Vol (2) Ch. 6, Golden, CO: Solar Energy Research Institute, 1979

3. ASTM Method D 3588-81, "Calculating the Calorimetric Value and Specific Gravity of Gaseous Fuels", *The American Society for Testing Materials,* Section 5.05, 1986.

Table 4-18. Operating Data from Oxygen Run 10.

Date Time	5/29/86 20:23	5/29/86 21:10	5/29/86 22:13	5/29/86 23:15	5/30/86 3:18	5/30/86 4:29	5/30/86 5:16	5/30/86 20:24	5/31/86 1:23	5/31/86 4:44
Variable										
Wood Feed Rate	1136	1171	1210	554	988	1199	1344	1232	466	1045
Oxygen Rate	56	53	51	36	39	49	49	44	29	34
Reactor P	131.4	107.9	136.9	141.8	114.9	135.6	133.7	43.3	31.7	21.5
Toff (Level 6)	1540	1536	1521	1330	1587	1496	1459	1590	1556	1389
Grate Speed	4	4	4	6	5	6	5	6	4	5
O_2/Wood lb/lb	0.249	0.229	0.213	0.329	0.200	0.207	0.184	0.181	0.315	0.164
Gas Btu/SCF	284	280	291	265	288	294	312	320	274	294
% CH_4	4.94	4.69	5.71	5.55	5.42	5.81	6.71	6.81	5.04	6.66
COMMENTS	Fine Char	Fine Char	Fine Char	Grate Failure	Grate Repaired	---	---	---	---	---

Table 4-19. Gas Composition Data for Run 10.

Date Time	5/29/86 20:23	5/29/86 21:10	5/29/86 22:13	5/29/86 23:15	5/30/86 3:18	5/30/86 4:29	5/30/86 5:16	5/30/86 20:24	5/31/86 71:23	5/31/86 4:44
Component										
CO	30.92	27.70	28.54	28.85	30.33	32.72	33.88	35.71	33.98	32.75
CO_2	29.00	28.76	31.97	39.32	31.61	30.44	31.80	31.43	32.89	37.69
H_2	30.60	29.07	27.51	22.45	25.46	27.06	22.55	19.34	21.81	15.48
CH_4	4.94	4.69	5.71	5.55	5.42	5.81	6.71	6.81	5.04	6.66
Ethane	0.28	0.24	0.35	0.40	0.28	0.34	0.49	0.50	0.30	0.56
Ethylene	0.82	0.86	1.47	1.18	1.38	1.29	1.83	2.07	1.05	1.77
Acetylene	0.07	0.07	0.18	0.15	0.23	0.16	0.41	0.54	0.07	0.43
Propylenes	0.32	0.28	0.38	0.45	0.34	0.34	0.51	0.57	0.31	0.64
Nitrogen	3.05	8.33	3.88	1.65	4.93	1.84	1.82	3.03	4.56	4.01
TOTAL	100.00	100.00	100.00	100.00	100.00	100.00	100.00	100.00	100.00	100.00

CHAPTER 5

BASIC STUDIES OF GASIFIER DESIGN AND OPERATION

5.1 PRINCIPLES OF BIOMASS GASIFIER DESIGN

While the gasifier was being constructed, we were able to operate other, smaller research gasifiers to determine the principles of operation of the new stratified downdraft gasifier. Some of this work was reported at contractors' meetings [1]. The findings are summarized in this chapter.

From this experience, the following guidelines were derived for biomass gasification and gasifier design. A number of other gasifiers were constructed, embodying these principles; they are described in the next section.

5.1.1 Fuel Considerations

Coal and biomass gasifiers have sufficiently different properties so that they must be designed quite differently. When biomass is pyrolysed, 70%-90% of the biomass is vaporized, forming primarily tars, and oils that must be converted to gas [2]. By contrast, when coal is pyrolyzed, only 20%-30% of coal is volatilized. Furthermore the charcoal resulting from biomass is highly reactive while the coke resulting from coal has perhaps 1/50th the reactivity at the same temperature. Thus the main function of a biomass gasifier must be partial oxidation of the tars and oils to gas, while the main function of a coal gasifier must be to convert coke to gas.

5.1.2 Low Tar Production

Updraft, fixed bed gasifiers produce very hot gases by oxidizing, then gasifying the charcoal in the lowest zone; these gases then pyrolyze the incoming biomass, producing 5%-20% tars and oils. These require impractical levels of cleanup for any use except immediate combustion. Updraft gasifiers can be recommended for co-production of gas and tar, but not clean gas.

Downdraft gasifiers were initially developed to produce low-tar gas to operate engines. In a downdraft gasifier the incoming oxidant burns most of the pyrolysis products in flaming pyrolysis and some may crack subsequently in the char bed. The SERI oxygen gasifier produces gases with typically 0.1-1% condensible organic materials, provided char levels are less than 5%.

In **fluidized bed and entrained flow gasifiers** the oxidant may contact either charcoal or biomass in the primary reaction. Therefor the levels of tar are intermediate to those of downdraft and updraft gasifiers.

5.1.3 Thermodynamic Temperature Stabilization:

In a well mixed biomass reactor, gasification requires 0.3-0.45 lb of oxygen per pound of biomass to produce an equilibrium gas free of carbon and tar. Less oxygen than this allows some char and tar to escape with the gas; more oxygen consumes the bed and burns product gas. This equilibrium amount of oxygen produces a temperature of 700°-800°C in the gas as it leaves the char bed. This gas temperature is relatively stable because although the energy and water content of the biomass varies considerably and the energy content

of the gas varies widely, the temperature is "buffered" in this range by the water gas and Boudouard chemical equilibria, that can absorb large energy changes with only a small change of off-gas temperature (though wider variations can occur at various points in the bed and below the grate).

5.1.4 Kinetic Temperature Stabilization:

Two kinetic factors operate to balance the temperature throughout the bed in downdraft gasifiers. As the biomass reaches surface temperatures above 200°C, volatile oils are evolved that would produce very high temperatures if burned stoichiometrically in air, (approximately 2000°C) or oxygen (3000°C). However these temperatures are not reached in practice because the oxidant is not well mixed with the vapors and the combustion occurs in close proximity with the pyrolyzing biomass. Instead, the potential high temperature transfers heat to the pyrolyzing particle and accelerates the pyrolysis reactions. These absorb and convert this thermal energy to chemical energy in the gas. Thus, surface temperatures are stabilized in the range 500°-800°C even though gas temperatures may be considerably higher and the biomass particles may still be at room temperature internally.

These thermodynamic and kinetic factors lead to temperature stabilization throughout the reactor, provided that the gases are in intimate contact with the solid at all points. Bridging and channels, however, can lead to hot spots or unreacted gases, tars, and oils.

5.1.5 Oxidant/Fuel Distribution

The flaming pyrolysis reaction will tend to propagate through a bed of biomass toward the incoming oxidant. If the oxidant is injected at specific points through nozzles (tuyerres), the reaction will be stabilized at the nozzles and high temperatures may be generated at these points with possible slag formation. If the oxidant enters the biomass uniformly with the feed, the pyrolysis/gasification reaction will be uniformly spread over the reactor cross section, producing the most uniform reaction and providing the highest average and the lowest peak temperatures and the most uniform contact between fuel and oxidant. The stratified downdraft gasifier is based on obtaining uniform introduction of the oxidant to the reaction zone. We can't stress too much the need to keep the feed uniformly mixed with the oxidant, both in time and space.

5.1.6 Reaction front stabilization

If the gasification reaction zone is not constrained, it will usually tend to move toward the oxidant entry point, i.e., the top of the biomass bed for the stratified gasifier or to the nozzles for the Imbert gasifier [3]. With air in dry fuel, the pyrolysis front can propogate in the biomass against the air stream at several cm/min and with oxygen it propogates at 10-20 cm/min . If the velocity of the oxidant is too high or the fuel is too wet however, the flame cannot propagate from particle to particle fast enough, and the zone may move away from the oxidant. Eventually then, the zone will approach the grate, where it may be stabilized by combustion of some of the char or may be extinguished. The flame front velocity is one factor that determines the maximum gasification rate [3].

With oxygen the flaming pyrolysis front moves at a rate of 10-20 cm/min toward the oxygenand rapidly reaches the top of the bed where combustion of

pyrolysis vapors can occur in the gas phase. This "hot top" operation favors faster pyrolysis of the incoming biomass. However, it requires an insulated refractory top on the gasifier with some form of lock hopper to reduce radiation losses and provide a pressure seal for the burning gases.

5.1.7 Planar Flame Front Stabilization

When biomass is gasified with oxygen there is a fourfold increase in volume because of the production of gas. There is also a threefold increase due to the increase in temperature to around 600°C. Thus there is overall a 12-fold increase in the volume of gas because of the generation of gases and the temperature increase. When biomass is gasified with air, there is a fivefold increase in gas volume due to the reaction and temperature increase.

Therefore, the principal resistance to gas flow is in the pyrolysis and char zones. The oxidant can be introduced through a fairly thick bed of biomass at room temperature with very little pressure drop. As a corollary, a flat reaction zone will tend to be stable, since small perturbations in a flat zone are unstable.

5.1.8 Insulation

Heat losses from the pyrolyzing/gasifying bed are to be avoided because although the gasification reaction is buffered against temperature changes, energy loss from the gasifier is reflected in lower heat content of the gas produced, and the reduced temperatures reduce the rate of cracking the tars and oils. These heat losses may be a small fraction of the energy throughput at high gasification rates, but they become dominant at low rates and determine the maximum turndown ratio that can be achieved. One of the greatest improvements made on World War II gasifiers was the addition of insulation in the hot zone, that increased turndown ratio from 5 to 15 [4].

5.2 OTHER STRATIFIED DOWNDRAFT GASIFIERS

5.2.1 A Simple Laboratory 5-20 kW Gasifier

We learned the above principles slowly and painfully over the period of the oxygen gasifier project. As they became apparent, we built a number of other gasifiers primarily for research purposes.

During the period while the phase II modifications were being made, a small gasifier was built to test some of the above principles that had been learned on the oxygen gasifier.

The gasifier was built inside a 5-gal solvent can and is shown in Fig. 5-1. (The same principles can be used to make larger or smaller gasifiers.) The gasifier vessel is shown made from a piece of 4-in. pipe welded to a flat cover made from 12-gauge steel. The cover of the solvent can is cut out, leaving a thin 1 cm rim. The flat plate fits over this rim and is sealed with silicone sealant.
The gasifier is operated slightly below atmospheric pressure so that the cover is held to the can rim. A number of 1 cm diameter holes are cut into the bottom 4 inch length of the pipe to allow the char-ash and gas to pass through. We also used vertical slots 1 cm wide at the bottom tappering to a point 10 cm above the bottom equally spaced around the perimeter. The holes

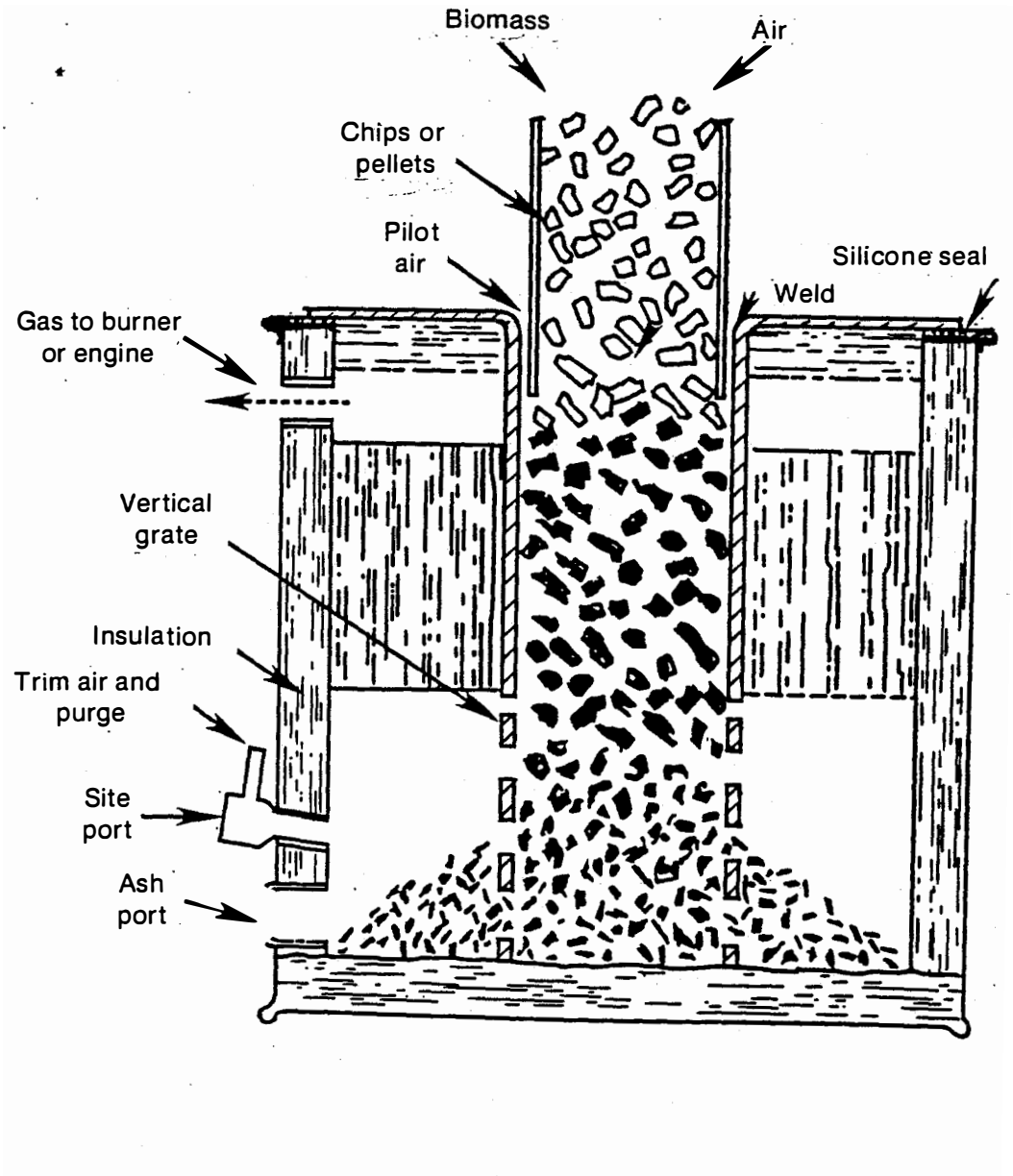

Figure 5-1. Five Gallon Stratified Downdraft Gasifier

or slots allow the gas to pass laterally through the char-ash. The inside lateral surface of the can is insulated with a 12-in. diameter riser sleeve [5]. The bottom and top surfaces are insulated with fibrous refractory. A coarse filter of fibrous insulation was sometimes mounted between the pipe and can as shown in Fig. 5-1 to prevent char-ash from passing out with the gas.

In operation, the gasifier is started using a charge of charcoal (typically remaining from the previous run). The charcoal is lit with a torch with a low air throughput, the resulting gases pass to a flare (see below). After several minutes the char bed will become incandescent, and biomass can be added to the filling tube either from a hopper or from a feeder. When the gases have burned a few minutes in the flare, the gasifier could be converted to engine operation. We did not operate an engine since an external cyclone and tar cleanup filter would be required for engine operation.

After cooling, gas is pulled through the gasifier with a high speed blower capable of generating 20-in. of water pressure vacuum. The experimental system was similar to that shown in Fig. 5-2 (b) for a different gasifier. The gas from the blower was flared during tests. The gas was injected tangentially near the bottom of a flare, made from another 5-gal solvent can lined with a riser sleeve. A propane torch was inserted tangentially into the flare opposite the gas entry point. Air could pass upward through the center through a 5-cm-diameter hole that could be covered with a movable flap to give the optimum flame. Once the flare was hot, the propane torch could be turned off as long as the gas flowed continuously to keep the surfaces hot.

The gasifier was operated for long periods on wood chips and a number of observations and measurements were made on the rate of heating individual particles. However, the flaming pyrolysis zone gradually approached the top of
the iron pipe and would go into the top stabilized mode with a deep bed of char. We were able to stabilize the pyrolysis zone below the bed top by inserting a tube a few mm smaller (made from a coffee can) loosely into the top. This tube acted as an additional magazine to hold reserve fuel; in addition, air passed through the annular space and stabilized the pyrolysis zone at the bottom of the tube.

A 4-in. pipe is shown in the gasifier in Fig. 5-1. However, we also used six and eight inch pipes for higher throughput. We did not measure consumption on this gasifier, but similar gasifiers generate typically 0.5 -1 MMBtu/h-ft^2 of gas. With wood chips having a bulk density of 12 lb/ft^3, this corresponds to a linear wood consumption rate of 1-2 in./min. The energy production and wood consumption predicted on this basis are shown in Table 5-1.

H.LaFontaine has since built a 7 kW gasifier based on modifications of this design for the Federal Emergency Preparedness Program (FEMA) of the U.S. Department of Defense [6]. A manual for the construction of simple gasifiers out of readily available materials will be placed in libraries around the country for possible use in case of emergency.

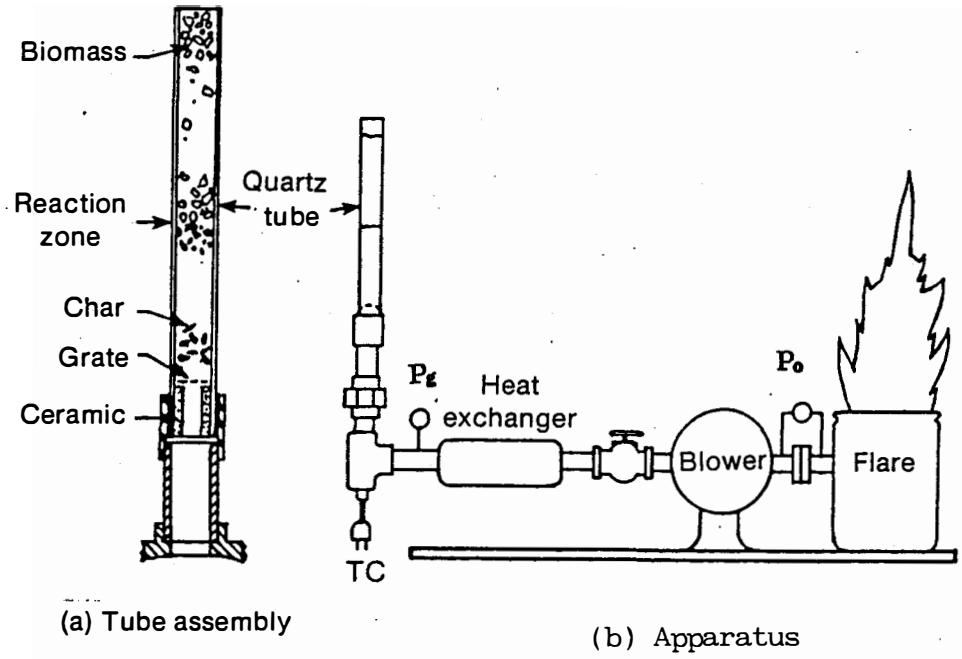

Figure 5-2. Transparent Gasifier for Measuring Motion of Flaming Pyrolysis Zone

Table 5-1. Projected Wood Consumption and Electric Power Generation for 5 Gal Gasifier

	Pipe Size - in.			
	4	6	8	
Wood Chip Consumption	7	16	27	lb\h
Energy Production	55	125	220	X 10^3 Btu/h
Electric Power[1]	3.2	7.3	13	kW

[1] Assumes heat rate of 17,000 Btu/kWh

5.2.2 Transparent Laboratory Gasifiers

A major problem in improving gasifiers is that it is not usually possible to see inside the gasifier to determine the position of the various zones. Vitreous-quartz tubes have the advantage that they are transparent, relatively poor heat conductors, shock resistant, and available in a wide variety of sizes at costs not much above steel. We have constructed a number of transparent gasifiers using quartz and used them for studying the operation of the gasifier and the formation and destruction of tars.

In 1982 the transparent gasifier shown in Fig. 5-2 was built to study the rate of motion of the flaming pyrolysis and char reaction zones [2].

The gasifier of Fig. 5-2 was used to study the rate at which the reaction zone moved with or counter to the flow of air or oxygen. The velocity of motion is reported for a variety of conditions. In particular, it was found that there were a number of ways to influence the motion of the zone with or against the flow. Decreasing the air velocity, insulating the tube, using metal walls, or using oxygen all caused the flaming pyrolysis zone to move more rapidly against the oxidant stream. Unfortunately, the factors influencing the motion of the zones are some of the most difficult to understand so that these results should be regarded as semiquantitative [2].

The principal heat loss mechanism from a bed of hot biomass or charcoal is by radiation; unfortunately, the quartz increases this loss relative to steel or ceramics. A relatively well insulated gasifier can be made by surrounding the quartz tube with a riser sleeve of fibrous high temperature ceramic and cutting a small slot or small holes in the tube.

One of the authors (T. Reed) developed a novel insulation at MIT composed of a layer of gold 2000 nm thick deposited on the inside of a Pyrex tube. This gold layer reflects more than 98% of the infrared but transmits the visible radiation. The insulation value of the gold at high temperature is equivalent to that of a 2.5 cm layer of asbestos. In addition, the gold provides excellent insulation without a corresponding high thermal mass to heat.

The transparent gold insulation was originally developed for crystal growth. Commercial laboratory electric furnaces that utilize this principle are made by a company, Trans-Temp, under an MIT patent. These furnaces are used primarily for semiconductor processing but also for a wide variety of other applications. The tubes can be purchased separately for other high temperature insulation uses [7].

We have used these gold insulating tubes to make several sizes of well-insulated, transparent gasifiers [8]. A typical transparent furnace is shown in Fig. 5-3. The gasifier is built using a 9-cm ID quartz tube 30-cm long as shown in Fig. 5-3. It is insulated by an 11-cm ID Pyrex tube with the transparent layer of gold deposited on the inside surface. The two tubes are separated by a 3-mm air space. The two tubes are held concentric by a steel adaptor at the top and bottom to which the glass and quartz are cemented with silicone cement. The bottom adaptor carries a support for a wire mesh grate fitting up into the quartz tube a distance of 5 cm to keep excessive heat from the cement.

A photograph of the assembled furnace and cracking unit is shown in Fig. 5-4. Figure 5-5 is a photograph of 1-in. diameter dowels being gasified. In this case the charcoal bed is too short to complete the gasification process,and pyrolysis flames are seen below the grate.

For air gasification the upper adaptor was left open for feeding of chips. Thermocouples and probes were used to take temperatures and samples of gas at intervals down the bed. For oxygen gasification the upper adaptor was connected to a vibratory feed system sealed to a fuel hopper as shown in Fig. 5-6.

For the studies of thermal and catalytic tar destruction, two tubes were connected to a 19-liter (5-gal) steel cylindrical vessel, which contains the tar reformer/cracker as shown in Fig. 5-3. This reactor was insulated with 5 cm layer of mineral fiber insulation to give a 10-liter inner volume and provided a 5-10 s residence time for the producer gas that flows through.

Oxygen and/or propane can be injected through six nozzles, 1.5 mm in diameter built into the top of the tar reactor. The nozzles are directed tangentially downward to form a hexagonal pattern to provide good mixing in the reactor.

Accurate control of feed rate is necessary for establishing a steady state for making measurements of tar production and other parameters. We found that we could control bed level from the temperature at the top of the pyrolysis zone, since the temperature is at a local maximum at the surface of the pyrolyzing/burning bed. In operation with the sealed system of Fig. 5-6, the bed level is maintained constant by using two vertical thermocouples, 1 cm apart, located in the top of the bed, 1 cm from the wall. The feed rate is controlled by maintaining the bed level such that the temperatures at the two thermocouple levels are equal.

The bed level is maintained between the two thermocouples by a standard proportional/integral control algorithm. As the bed level rises, the upper thermocouple measures a higher temperature than the lower thermocouple. The controller then lowers the feed rate to bring the bed level down. As the level falls, the temperature of the lower thermocouple is higher, and the feed rate is increased to bring the bed up.

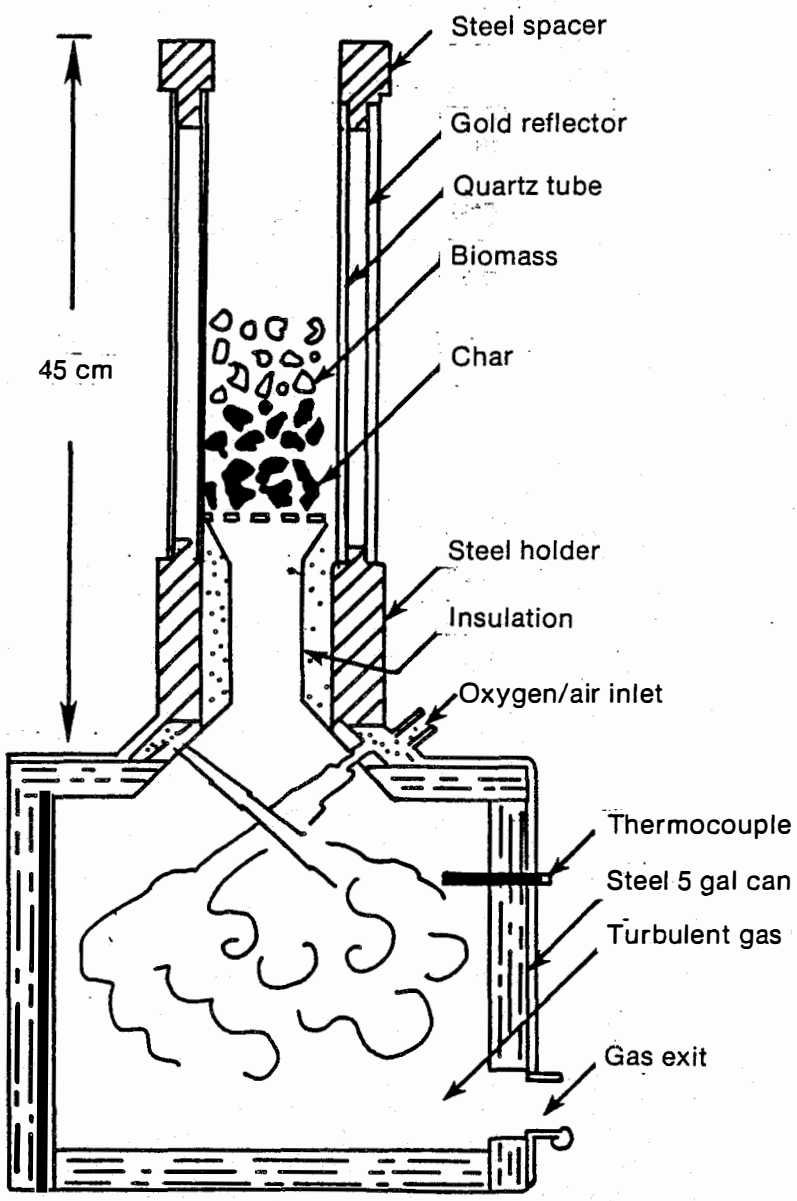

Figure 5-3. Gold Insulated Transparent Gasifier and Tar Cracking Chamber

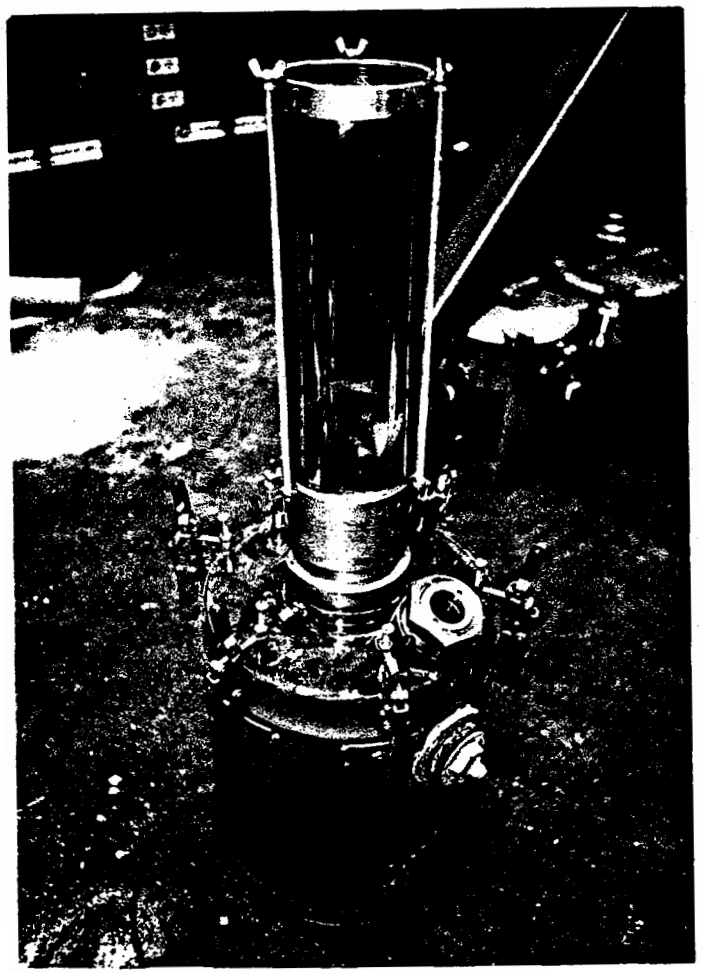

Figure 5-4. Photograph of Gold Insulated Gasifier and Cracking Chamber

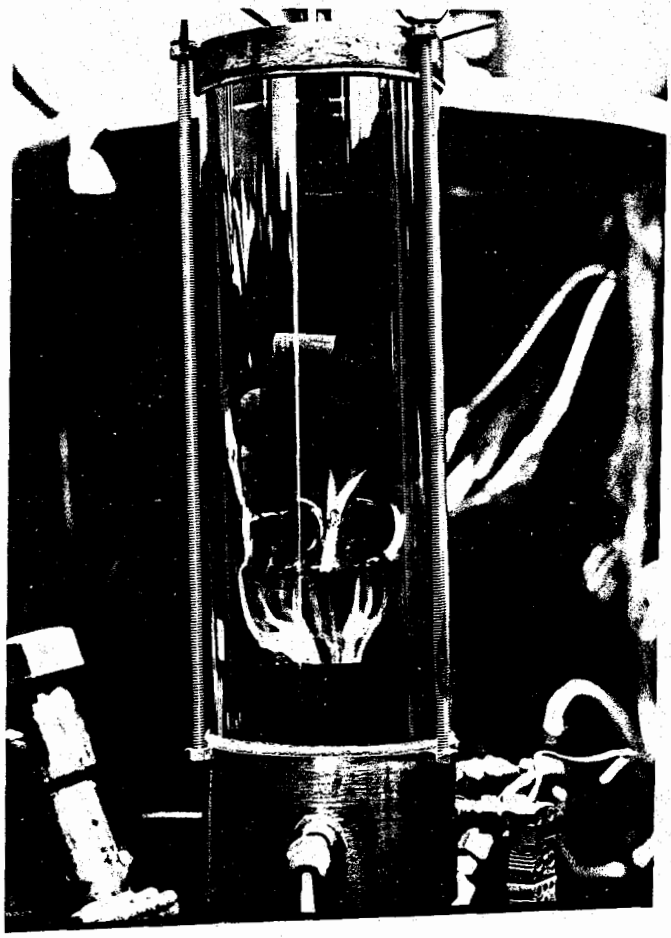

Figure 5-5. Photograph of 1-in. diameter birch dowells burning in transparent gasifier, showing pyrolysis flames burning below grate

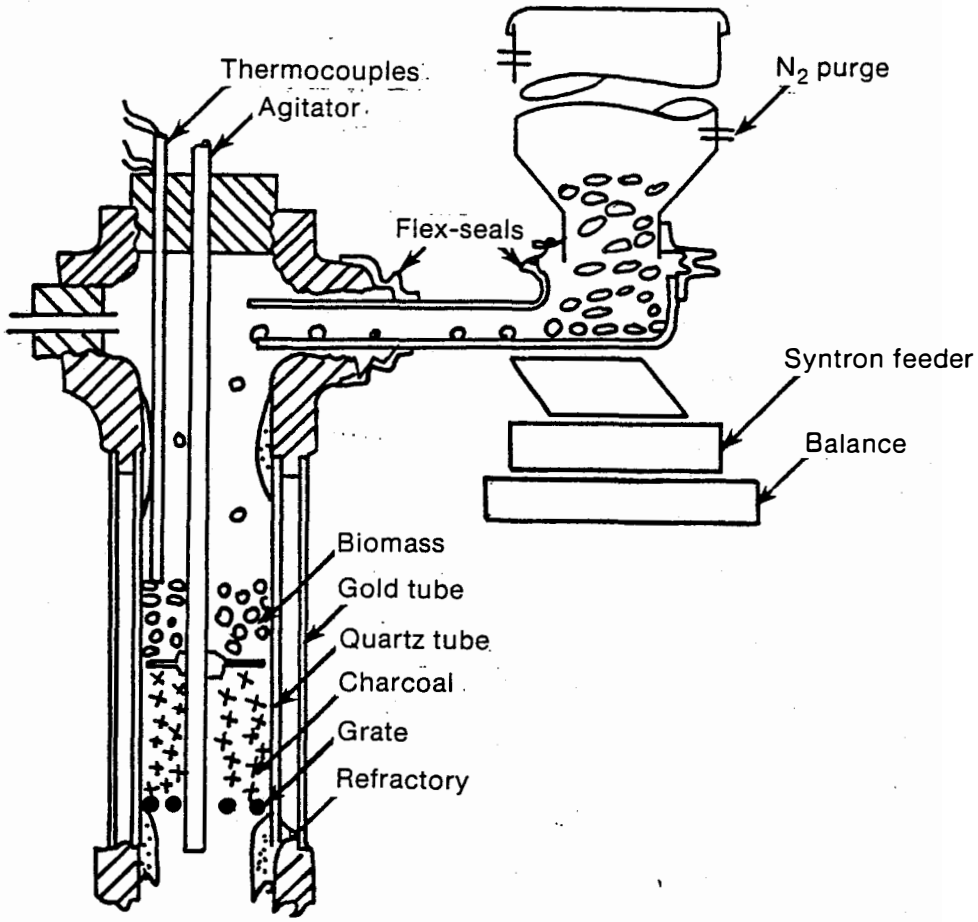

Figure 5-6. Closed feed modification of gold-insulated gasifier for oxygen operation

A number of photographs and video tapes of the gasification process have been made using the transparent gasifier. They are illuminating and thought provoking. In the video tapes one can see the unburned fuel at the top of the bed, the fuel beginning to burn, the cessation of combustion, and the final breakup of the char as it is gasified. Anyone wishing to design other gasifiers or model gasifiers would benefit by watching this process, normally hidden from view in metal gasifiers. These tapes have been collected and edited and can be seen by contacting the authors.

5.2.3 The "Upside-downdraft Gasifier"

We have developed a new form of gasifier, shown in Fig. 5-7 (a), that we call the "upside-downdraft" because it has many of the features of the conventional downdraft gasifier, except that the gases move up rather than down.

Moving bed (fixed bed) gasifiers are generally classified as downdraft (co-flow) and updraft (or counter-flow) as shown in Fig. 5-7 (b) and (c). Downdraft gasifiers are characterized by partial combustion (flaming pyrolysis) of the volatile materials by the incoming oxidant. The name "downdraft" comes from the fact that the oxidant and gas are drawn down over the feed that moves down under the force of gravity. A better name, occasionally used is **co-flow.** Updraft gasifiers are also sometimes called counter-flow gasifiers, since the solid fuel moves in the opposite direction from the gas.

In one form of the upside-downdraft gasifier, the fuel is fed by an auger from below and moves up with the gas through the gasifier. Alternatively, the gasifier can be operated in a batch mode in which a bed of charcoal is ignited on top of a reservoir of biomass. Because natural convection causes the hot gases to rise, this geometry is particularly simple and permits operation without external means to move the gas or fuel.

In conventional downdraft gasifiers, the downward motion of the hot gas must overcome natural convection, that would tend to move the hot gases up. This is probably one of the factors that sets a lower limit on stable operation and an upper limit on the turndown ratio of the Imbert or stratified downdraft gasifiers.

The upside-downdraft mode permits construction of a particularly simple gasifier that can be connected in the laboratory to the molecular beam mass spectrometer (MB-MS) operated by Milne and Evans [9]. A 2.5-cm-inside diameter quartz tube was fitted with an air supply and a quartz wool grate as shown in Fig. 5-8 (a). The tube was insulated with vacuum formed insulation (riser sleeve) with slots cut to permit observation. Air was flowed through the bed at 4 L/min, and the top of the bed was ignited.

On first lighting the bed operated in a combustion mode, but as the char bed developed, the gas became combustible and the gasifier operated for about 5 minutes, producing gas, high-temperature tars and low temperature pyrolysis oils. After ignition, a small, porous, ceramic plug and some quartz wool were placed on top of the bed to compact the char and prevent fly ash from entering the MB-MS. The sampling port of the MS is shown above the tube.

The total ion current, a measure of the amount of tar formed in the gasifier,

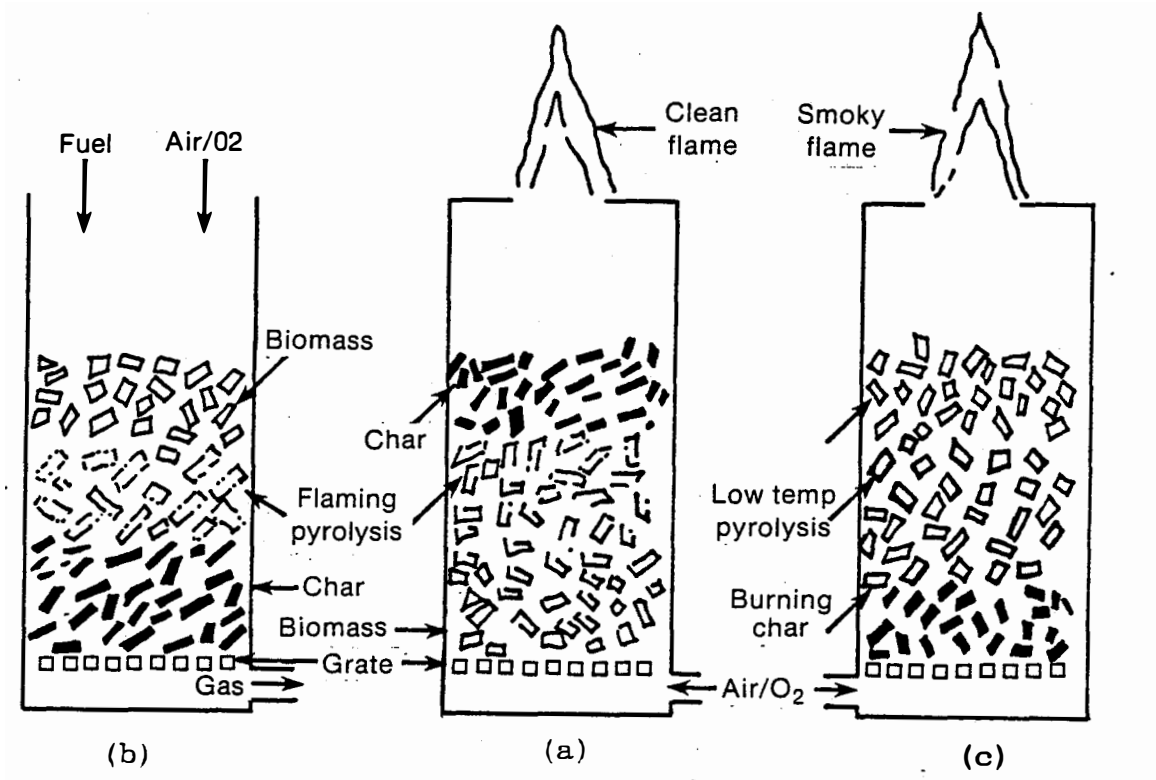

Figure 5-7. Upside-downdraft gasifier (a) contrasted with conventional stratified downdraft (b) and updraft (c).

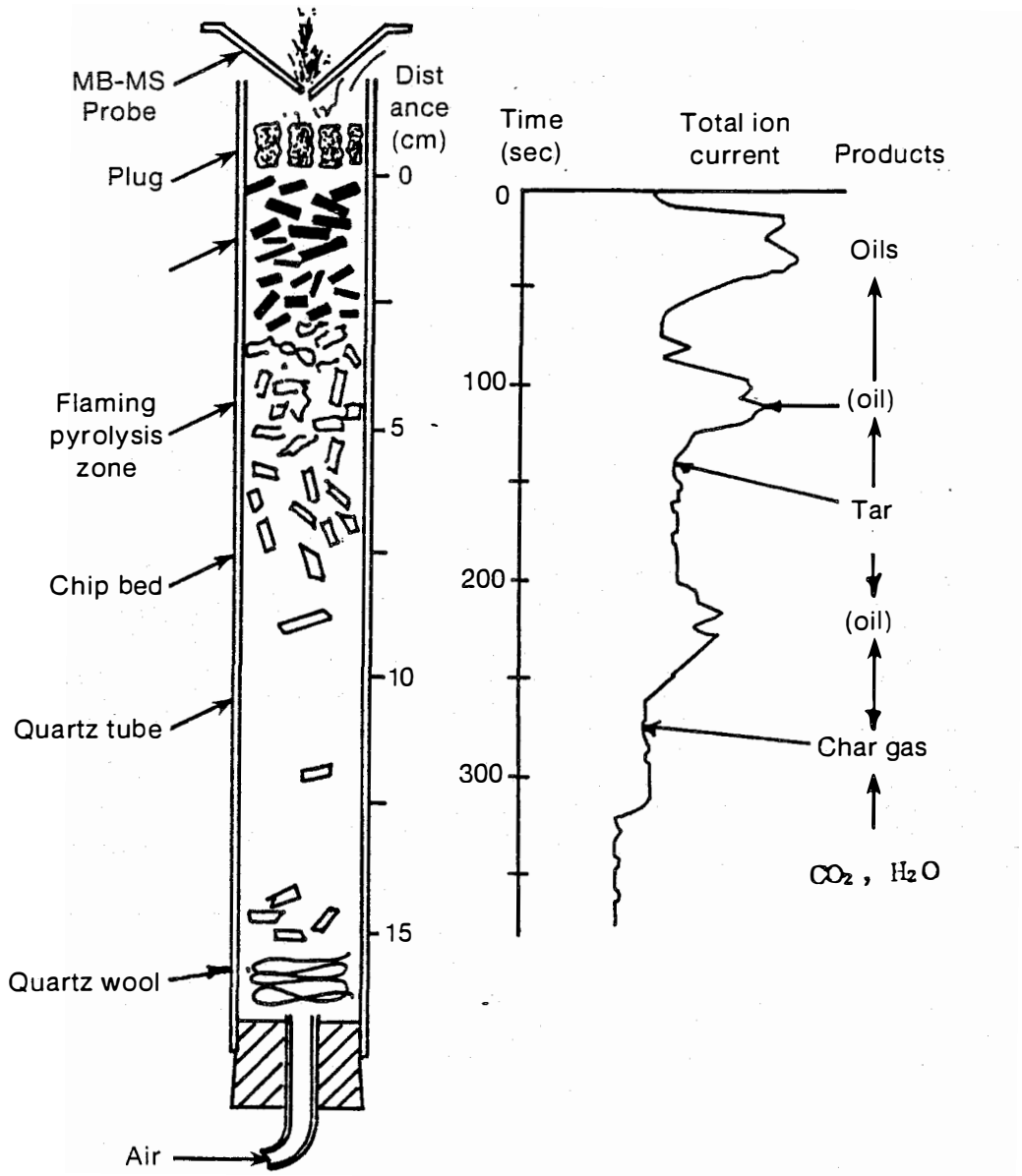

Figure 5-8. (a) Laboratory upside-downdraft gasifier and (b) total ion current observed in molecular beam mass spectrometer.

is shown in its physical relation to the gasifier bed in Fig. 5-8 (b) After an initial high level burst of low temperature pyrolysis oils (10-70 s), the gasifier settled down to production of a lower level of the high-temperature tars. Twice during the run there was a holdup of the bed followed by collapse; this caused bursts of oil to appear (100- 130 s and 230-270 s). When pyrolysis was completed at 270 sec, the remaining char was gasified. Finally, at 320 s the only products were CO_2 and H_2O.

We were able to operate the same gasifier in the updraft mode by igniting a 5 cm bed of charcoal in the gasifier of Fig. 5-8 (a) and then filling the tube with wood chips. This produced large amounts of low temperature "wood oil" that had a different chemical nature than the aromatic tars produced by the higher temperatures of the (upside-) downdraft mode.

5.3 A SINGLE PARTICLE REACTOR

The operation of large industrial oil and entrained coal furnaces is based on a thorough knowledge of the interaction of gas velocity, material properties and heat transfer in these furnaces. Unfortunately this knowledge does not exist for biomass for either combustion or gasification. Construction and successful operation of a fixed bed gasifier or a wood- or MSW-fired furnace are based on experience and application of empirical rules.

In 1983 we constructed a two-zone model for stratified downdraft gasifiers consisting of a "flaming pyrolysis zone" followed by a "char gasification zone." We found that there was adequate kinetic information available for modeling the char gasification zone. However, there was little scientific information available on which to base a model of the pyrolysis zone. Fortunately, we found an empirical study by Huff that predicted times for **flaming combustion,** and we have used that information to formulate some of the models in Chapter 8 [10].

It seems reasonable to assume that one cannot understand the behavior of an assemblage of particles without knowing the behavior of a single particle relative to the above variables. Therefore we have built a **single particle reactor** in which to study the effect of the above variables on the time required for pyrolysis and gasification. These times in turn determine the shape and dimensions of the equipment that is built. This work is being done primarily by Ben Levie as a PhD thesis at the University of Colorado at Boulder.

The time required for pyrolysis of a biomass particle depends only on the rate of heat transfer to the surface. The heat is transferred primarily by radiation and convection. Our current knowledge of these forms of heat transfer is probably sufficient to construct a model of updraft gasification. However "flaming pyrolysis" and "flaming combustion" are much more complex phenomena since a fraction of the heat comes from conduction through the evolving vapors to the surface from a flame a few millimeters away as shown in Fig. 5-10. As pyrolysis rates increase, this boundary layer becomes thicker, tending to reduce the rate. **This flaming pyrolysis and combustion is fundamental to all biomass combustion and downdraft gasification.** Yet we have no present model explaining the interaction of these factors. The single particle reactor has been built to obtain these data.

The single particle reactor is shown in Fig. 5-9. The reactor consists of three sections. An upper preheater section is filled with nickel turnings

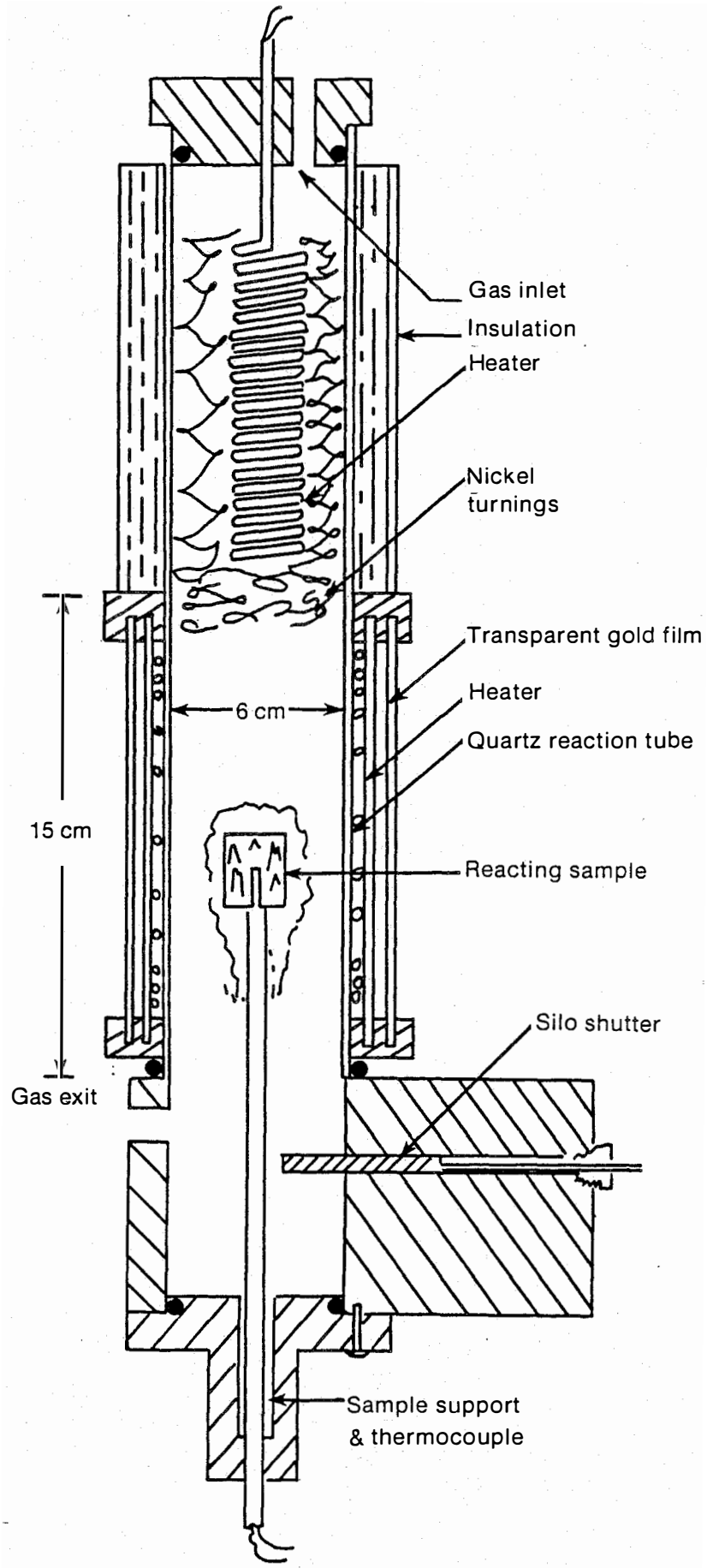

Figure 5-9. Single particle pyrolysis-combustion reactor

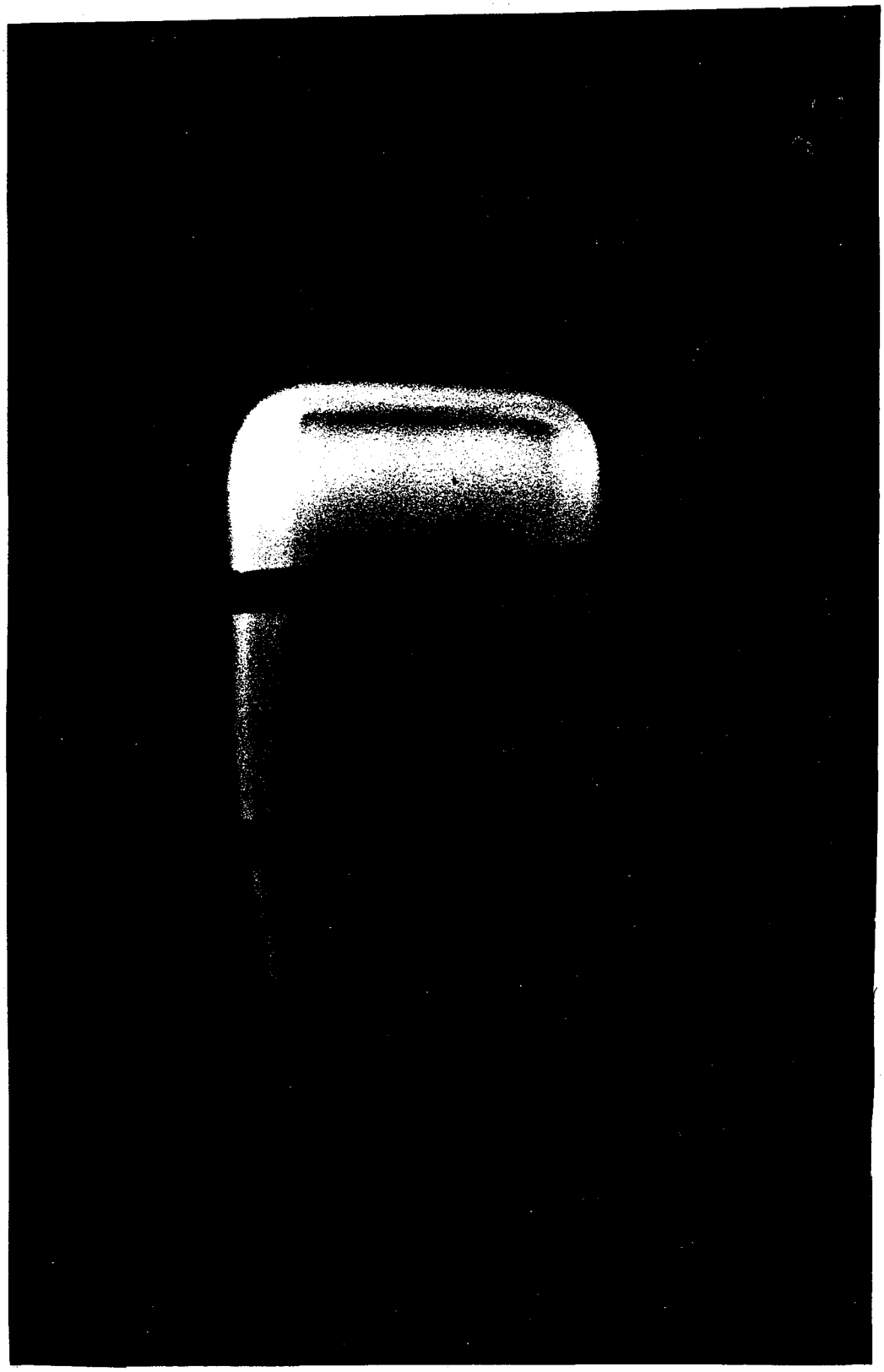

Figure 5-10. Photograph of 1-in. birch dowel burning in air in the single particle reactor

that preheat the incoming gas (eg N_2, O_2 or air) to between 200° and 1000°C. This permits measurement of the effect of convective heat transfer on pyrolysis (using N_2) and flaming pyrolysis and combustion (using O_2 or air).

The central section is a transparent furnace that provides a uniform bath of radiant heat corresponding to a black body at 200°-1000°C. This is a necessary part of the reactor because the radiant heat from surrounding particles in a gasifier is probably the primary source for pyrolysis and convective heat transfer alone is not sufficient to maintain a level of pyrolysis high enough to support combustion.

The bottom section consists of a "missile silo" in which we maintain the sample below a shutter in order to keep it at room temperature until the start of pyrolysis. This section also contains an exit port for the pyrolysis and convective gas.

A calorimeter is attached to the port in the lowest section to measure the heat for pyrolysis. The sample is mounted on a thermocouple that rests on a balance. In a typical run the temperature of the furnace, the gas, the surface of the sample, and the axis of the sample are monitored with thermocouples. The data are collected using a Data Acquisition System (DAS) made by Keithley, Inc. [11], and the data are selected and displayed using Lotus 123.

The modeling portion of this work is being performed on wood dowels. A 2.5-cm wood dowel burning in air is shown in Fig. 5-10. The system is calibrated by using a porous firebrick soaked in a heat transfer liquid with known properties. A major part of the work will focus on the pyrolysis/combustion of refuse-derived-fuels (RDF). This work is still in progress and will be reported at a later date.

5.4 GAS TRANSPORT THROUGH PACKED BED GASIFIERS

5.4.1 Introduction

It is by no means obvious that the method of moving the gas through the gasifier can affect the stability of the operation of the gasifier. Yet we have found that there are subtle differences between different methods, and we offer an explanation of these differences here.

5.4.2 Practical Gas Transport Devices

Gases can be pulled or pushed through the gasifier bed by a variety of means such as blowers, ejectors, or compression of the oxidant. The device must generate enough pressure to overcome the bed resistance and move the gas through the bed [typically requiring 0.25-2.5 kPa (1-10 in. water)]. The device must also overcome pressure drops typically of the same magnitude as those in the bed, piping, cyclone, scrubbers, etc.

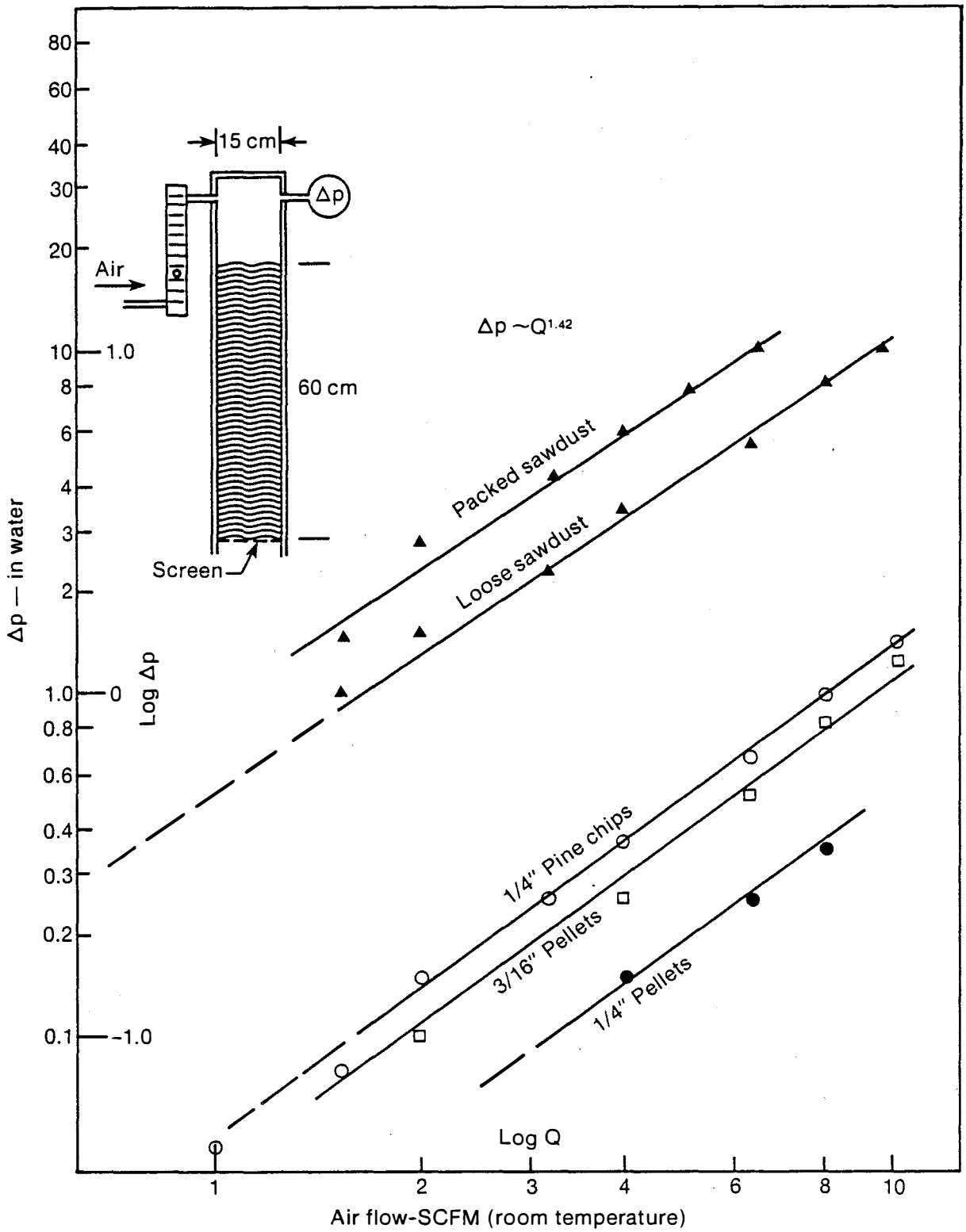

Figure 5-11. Pressure drop vs flow for several biomass feeds

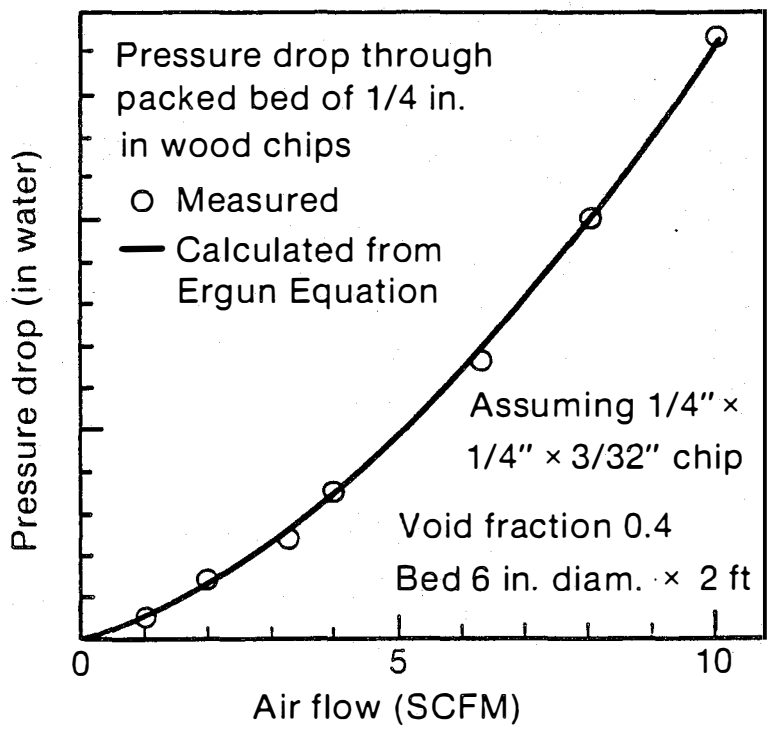

Figure 5-12. Comparison of theoretical and measured pressure drop in a packed bed

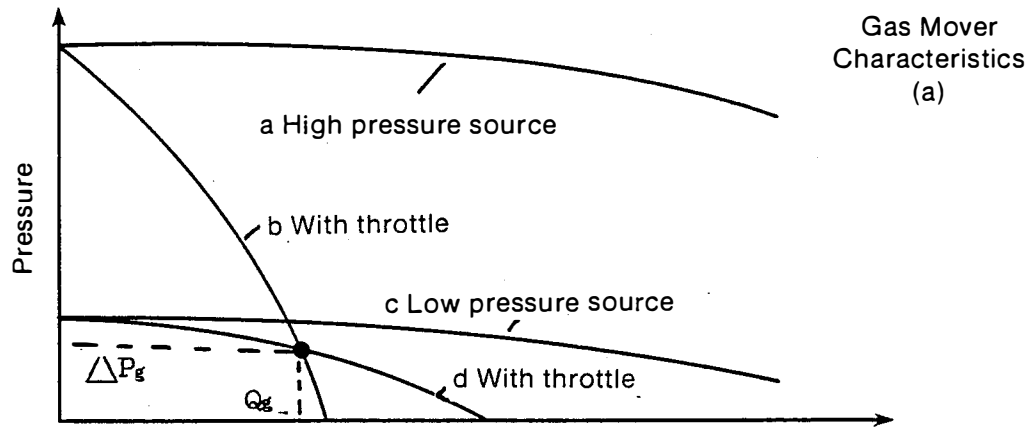

(a) Flow Variation For Various Gas Moving Devices

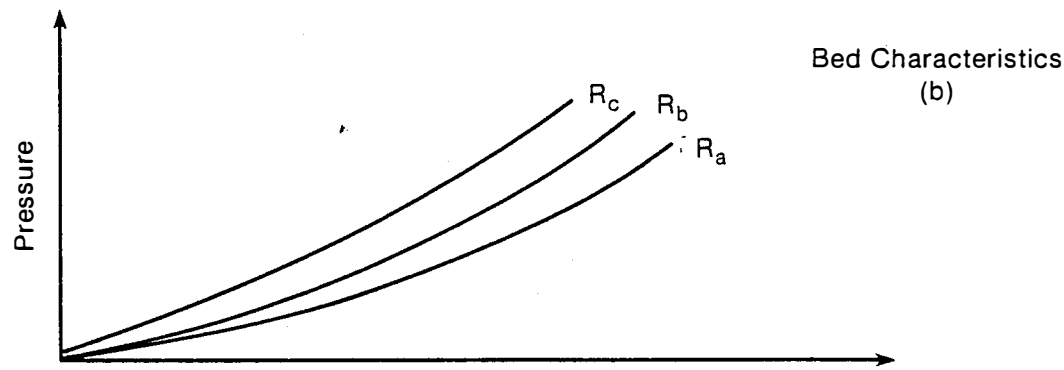

(b) Flow Variation for Various Bed Resistances

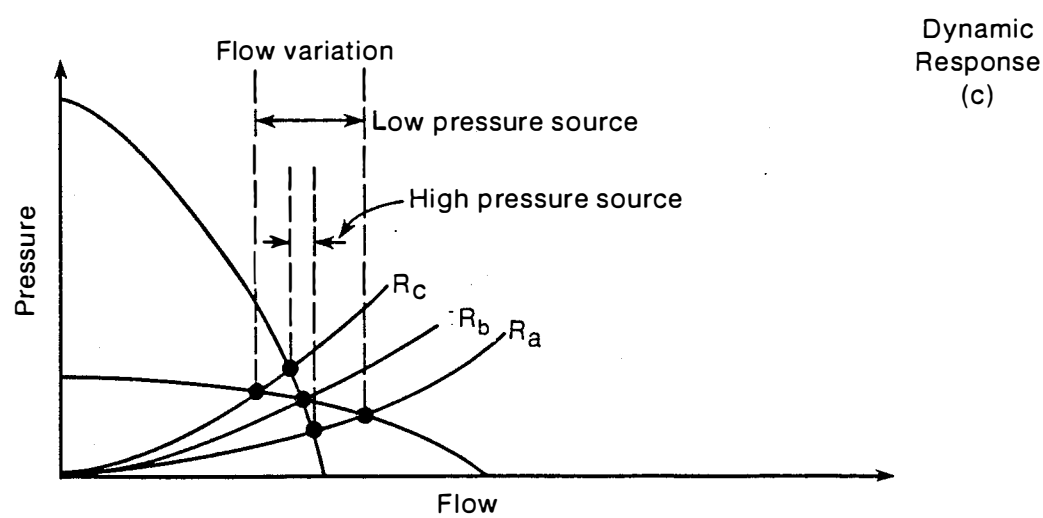

(c) Dynamic Response of Bed to Low and High Pressure Gas Moving Device

Figure 5-13 Flow variation in fixed beds because of pressure-flow relationship for Gas Moving Devices and Various Bed Resistances

In Phase I testing, oxygen was supplied at pressures of 500-5000 kPa and had more than enough pressure to move the oxygen through the bed, even though it was tightly packed. In Phase II we initially used a low-pressure blower to generate a pressure of 0.25-2.5 kPa (1-10 in. water) to operate the 1 ton/day downdraft gasifier. The most satisfactory gas transport method for atmospheric testing was a gas or steam ejector, shown in Fig. 2-6, used to generate a vacuum of 10 kPa (40 in. water) to move gas to the flare in the test setup. This had the advantage that even when the gas had high tar levels, the tar could be burned if the piping was kept hot.

5.4.3 Pressure Drop In Packed Beds

The pressure drop and gas output in a moving bed gasifier depend on the bed length and cross section, the particle size of the biomass and char, the packing and void fraction, and the temperature and composition of gas in the bed. The pressure drop through the bed can be calculated, for instance, using the Ergun equation if the flow characteristics through the feedstock are known [1, 12]. We decided to test the flow characteristics of several of our feedstocks in order to establish a baseline and check the validity of the Ergun equation.

A simple cold flow test device, shown in Fig. 5-11, was set up to simulate the oxygen gasifier. It consisted of a transparent plastic tube 15 cm in diameter, 80 cm long, with a screen near the bottom. The tube was filled with biomass to a depth of 60 cm, air was metered through a rotometer and passed down through the bed. The pressure drop was measured with a Dwyer gauge.

The pressure drop for several biomass materials of potential interest are shown as a function of flow in Fig. 5-11 (note logarithmic scale). The lines appear to be parallel with a slope of 1.42, as in the equation

$$\triangle P = kQ^{1.42} \qquad (5\text{-}1)$$

where $\triangle P$ is the pressure drop, Q is the air flow, and k is a proportionality factor. Note that the pressure drop for a flow of 16 nm/h air through a 61 cm bed ranges from 0.02 to 2.5 kPa (0.1-10 in. of water) for the biomass tested. These are the magnitudes of flows and pressures we observe in the oxygen gasifier.

The pressure drop through packed beds can be calculated from the Ergun Equation [12] or from variations of this equation given in the Handbook of Chemical Engineering [13]. The pressure drop per unit length of column is given by an equation of the quadratic form

$$\triangle P/L = aU + b\rho U^2 \qquad (5\text{-}2)$$

where U is the superficial velocity of the gas, ρ is the gas density, and $\triangle P/L$ is the pressure drop per unit length. The first term on the right side of the equation is the inertial resistance of the bed and the second term is the kinetic resistance to flow that dominates at higher flows; a and b are proportionality constants depending on the fluid and solid properties. Working with various materials Ergun found excellent agreement between measurement and the derived equation:

$$\triangle P = [150(1-e)2\mu U/e^3 D^2 + 1.75(1-e)\rho U^2/e^3 D)L/g \quad (5\text{-}3)$$

where e is the fraction of voids in the bed, g is the gravitational constant and μ is the viscosity. D is the effective particle diameter given by

$$D = 6\ V_p/A_p \quad (5\text{-}4)$$

where V_p is the particle volume and A_p is the particle surface area. (D needs to be a weighted average when there is a distribution of particle sizes.

As an example of the use of this equation, the pressure drop was calculated for air [viscosity = .0174 centipoise (11.7 x 10^{-6} lb/s-ft)] passing through a 0.6 m (2 ft) bed of 6 mm (1/4-in.) chips (approximate dimensions 6 mm x 6 mm x 3 mm) in a 15-cm diameter gasifier. The calculated results are compared to the measured results in Fig. 5-12. Excellent agreement was obtained with an assumed void fraction of 0.4.

From this it can be seen that the Ergun equation predicts the pressure drop with satisfactory accuracy in the range measured, and that the pressure drop through cold biomass is relatively small. Similar calculations could be used to predict the pressure drop profile along a working gasifier. In order to do so it would require temperature, particle size, and molecular weight data along the bed (data not currently available), and the differential form of the equation should be used. However, the form of the equation shows the trends to be expected.

Three factors combine to make the pressure drop in the hot char bed at least ten times that in the cold biomass: (1) high temperatures will increase gas viscosity and gas velocity; (2) in the reaction of biomass with oxygen or air, the quantity of gas (and hence velocity) increases by a factor of 4.2 and 1.6 respectively; (3) as biomass is converted to char there is some shrinkage, and as the char breaks up during gasification there is production of smaller particles. Thus one can expect the primary pressure drop to occur primarily in the active gasification bed.

In Phase I we found that we needed to agitate the bed in the 15 cm gasifier to prevent bridging and channeling in the biomass and plugging of the charcoal bed. In Phase II it was recommended that agitation of the grate be controlled separately from agitation of the bed. We found that on the 75-cm gasifier we needed to agitate the grate, but not the bed.

Agitation of the bed serves the purpose of keeping the biomass charge from bridging and channeling, and the amount of agitation depends primarily on the original form of the biomass. The agitation of the grate is required to remove the fine char-ash resulting from charcoal gasification. These two effects are independent and should be controlled independently.

5.4.4 Influence of Gas Transport Device on Gasifier Behavior

The device used to move the gas can greatly influence the performance of the gasifier. For instance, when using high pressure oxygen is supplied at 1000 kPa with flow controlled by a throttle valve, the flow through the bed is essentially independent of bed pressure drops up to 100 kPa and it was possible to operate with a bed almost totally plugged by char-ash. A low pressure oxygen supply would not have permitted this buildup. The shape of the pressure-flow curve for the gas transport device can also have unexpected

influence on the dynamic stability of the gasifier, as discussed below.

These relationships can be made clear from several diagrams. In Fig. 5-13 (a), the pressure-flow relationships are shown as at a and c for a high pressure (such as oxygen) and low pressure (such as a blower) gas transport system. These can be called the "operating line" of the device. Assume that we want to operate the gasifier at a flow Q of gas. This will require a pressure drop in the gasifier, Pg, as shown (typically 0.25-2.5 kPa (1-10 in. water). To reach this point with a high pressure device, it is necessary to "throttle" the flow with a valve to produce a new operating line such as b and d in Fig. 5-13 (a).

It may at first seem unimportant whether the operating point is established with a high- or low-pressure device. However, the system will operate very differently (and generally more reliably) with a high pressure device. The pressure drop across the gasifier depends on particle size, bed length, temperature, and char-ash buildup. The bed resistance fluctuates continually during operation. The operating characteristics for several different bed conditions are illustrated in Fig. 5-13 (b) where the line R_a might represent a well stirred or shaken bed, the line R_b might represent an average bed, and the line R_c might represent a bed with char-ash buildup.

The variation of flow with bed resistance for a low and high pressure source is shown in Fig. 5-13 (c). As the bed resistance swings from R_a to R_c with a low pressure source, there is a large change in flow to accommodate the bed pressure drop. As the bed resistance changes with a high pressure source, there is a much smaller variation in flow.

Thus a high pressure approximates a constant flow device; a low pressure device permits wide variations in flow. Since it is generally desirable to produce a constant gas flow, the higher pressure device is preferable. On the other hand, energy is expended in compressing gases to a high pressure, so that the operating pressure should not be too great and all efforts should be made (such as agitation or stirring) to keep bed resistance constant.

REFERENCES

1. *Annual Proceedings of the Biomass Therrmochemical Conversion Contrators' Review Meeting;* Edited by Pacific Northwest Laboratory, Richland, Wash. These proceedings, describing work supported by the U.S. Department of Energy, are available from the National Technical Information Service (NTIS), U.S. Department of Commerce, 5285 Port Royal Rd., Springfield, VA 22161.

2. Chan, W. R., Kelbon, M. and Krieger, B. B., "Product Formation in the Pyrolysis of Large Wood Particles", *Fundamentals of Thermochemical Biomass Conversion: An International Conference. Estes Park,* Colorado, October 18-22, 1982. Proceedings edited by R.P. Overend, T.A. Milne, and L. Mudge. Elsevier, London 1985.

3. Reed, T. B. and Markson, M. "Reaction Velocities in a Downdraft Gasifier," Fundamentals of Thermochemical *Biomass Conversion: An International Conference. Estes Park,* Colorado, October 18-22, 1982. Proceedings edited by R.P. Overend, T.A. Milne, and L. Mudge. Elsevier, London 1985.

4. "Gengas: Svenska Erfarenheter Fran Aren 1939-1945", Stockholm, 1950; Translated as "Generator Gas: The Swedish Experience from 1939-1945" by M. Geuther (T. Reed and D. Jantzen, eds.) by the Solar Energy Research Institute, SERI/SP-33-140, 1979; reissued as Gengas with index added by A. Das, TIPI Workshop Books, P.O. Box 84, Allenspark, CO, 1982.

5. Western Refractories, 7001 W. 117th Av., Broomfield, Co (303-460 0707).

6. LaFontaine, H., "Emergency Use of Simple Inexpensive Gasifiers for Farm Machinery, Truck and Fishing Boats", *Energy from Biomass and Wastes XI,* Institute of Gas Technology seminar in Orlando, Fl, 16 March, 1987.

7. Transtemp Co., 155 6th St., Chelsea, MA 02150 (617-884 2620).

8. Reed, T. B., Levie, B., Scahill, J., Evans, R. and Milne, T. "Moving-bed Air and Oxygen Gasification", *Proceedings of the 1985 Biomass Thermochemical Conversion Contractors' Meeting*, PNL-SA-13571, Feb. 1986.

9. Evans, R. J. and Milne, T. A., "Applied Mechanistic Studies of Biomass Pyrolysis", *Proceedings of the 1985 Biomass Thermochemical Conversion Contractors' Meeting*, PNL-SA-13571, Feb. 1986.

10. Huff, E. R. "Effect of Size, Shape, Density, Moisture and Furnace Wall Temperature on Burning Times of Wood Pieces", *Fundamentals of Thermochemical Biomass Conversion: An International Conference. Estes Park,* Colorado, October 18-22, 1982. Proceedings edited by R.P. Overend, T.A. Milne, and L. Mudge. Elsevier, London 1985.

11. Keithley Instruments, Inc., 28775 Aurora Rd., Cleveland, OH 44139.

12. Ergun, S. "Fluid Flow through Packed Columns", Chem. Eng. Prog., 48, 89, 1952.

13. Perry, R. H. and Green, D. W., "The Chemical Engineer's Handbook-6th Edition", McGraw Hill, N. Y. 1984.

CHAPTER 6

TAR CONVERSION

6.1 INTRODUCTION

6.1.1 The Tar Problem in Gasification

The word "tar" is loosely used to cover a wide variety of materials having a range of chemical compositions. It is used specifically in gasification to indicate a material of medium to high viscosity produced in gasifiers which tends to line the cooler piping. While sometimes a solid at room temperature, it is a liquid at the temperature of collection. It interferes with all uses of the gas except combustion. Much has been learned about biomass tars in the last decade, so we can be much more specific now about particular forms of tar [1-8].

Updraft gasification of biomass can produce up to 20% of an oil or tar, which can be liquid or solid, depending on conditions. The production of oils and tars in gasifiers is the single largest technical problem to overcome in gasification.

If the producer gas is required for heat only, it can be burned with high tar levels, provided that temperatures in all distribution lines are maintained above the dew point of the oils and tars. However, if the gas is to be compressed, piped any distance or used in an engine, oils and tars must be removed to a level below 50-500 ppm (0.005-0.05%) or they will foul the compressor, pipes or engine [9].

This problem is not new; gas was produced from coal and distributed to individual houses in the major cities of the world by the middle of the last century. There are two steps required in making clean gas: (1) The gas should be produced with the minimum amount of impurities; and (2) whatever residual impurities remain must be removed in a cleanup train. Obviously, the cleaner the gas produced initially, the simpler the cleanup job. Today it is particularly important to produce clean gas because it is difficult to dispose of the impurities in an environmentally acceptable manner.

Fortunately, the downdraft gasifier produces much less tar than other gasifiers, typically less than 5000 ppm or (0.5%) of the feedstock, and as little as 500 ppm (0.05%). This results from the volatiles being largely burned in the flaming pyrolysis front and then passing through the hot char gasification zone. However, even these small amounts of tar in the product gas are above the acceptable level and will eventually cause problems.

We have found that the methods of operating the downdraft gasifier can make a considerable difference in the tar production. In particular a high char-ash removal rate favors high production because it reduces the oxygen/fuel ratio, lowers the temperature of the pyrolysis flame and reduces the partial combustion of the volatiles. These factors are discussed in more detail in Chapters 3 and 4.

One commonly used gas cleaning process is wet scrubbing. However this leaves a dirty, probably carcinogenic residue that must be disposed of. If the oils and tars can be destroyed thermally or catalytically in or near the gasifier

while the gas is hot, the complexity and cost of gasifier systems will be greatly reduced. Therefore we have been investigating both the effects of gasifier conditions, such as rake speed and char production on **tar production,** and the **thermal and catalytic destruction** of the tars.

The work reported in this chapter on the 1 ton/day oxygen gasifier was interspersed with other tests and modifications, so the data are less conclusive than we could wish. We have chosen the best data. The work on the transparent gasifier was specifically undertaken to test cracking catalysts. Unfortunately, it was cut short by a 6-month modification of the test area ventilation system, after which other projects took priority over the catalyst work. We report the work as far as it went.

6.1.2 The Nature of Gasifier Tars

Historically **wood tars** were widely used as a wood and rope preservative, a source of medicinal chemicals, etc. However, in gasification, the term "tar" is used as a pejorative term to indicate a viscous material that lines pipes and coats the valves of gasifiers and downstream equipment. The term "tar" covers a wide range of materials and we need to understand the nature of "tar" better if we wish to limit its production and destroy it thermally or catalytically.

Analysis of the results of MB-MS basic studies on various "tars" collected from a variety of gasifiers showed that there were two types of "tars," often physically similar but chemically quite distinct [4-6]. The kinetic studies of Antal and Diebold related these chemical differences to the temperature of production [7,8].

We now know that the initial steps in pyrolysis of the polymer biomass (a co-polymer of cellulose, hemicellulose and lignin) occur well below 500°C. They result in production of a medium viscosity, somewhat acrid, water soluble oil. The mass spectrometer shows that most components of this oil are monomers, oligomers, and fragments of the original wood polymers. We can call this oil "**primary pyrolysis oil, "wood oil"** for short, to distinguish it from the less specific term "tar."

If wood oil vapors are heated for any length of time to temperatures above 600°C the highly oxygenated molecules are largely converted to ethylene and other olefins. However some of these light, active molecules then condense further to form polynuclear aromatics such as napthalene and anthracene. These **secondary pyrolysis tars** are very similar to the tars resulting from high temperature coking of coal. We suggest calling them **"wood tars"** by analogy.

In practice, tars from gasifiers may consist primarily of either wood oil or wood tar or a mix, depending on the temperature-time exposure of the vapors. Tar often contains char dust or soot as well, that can give the mixture a consistency anywhere from that of molasses to that of pitch.

6.2 IN SITU MASS SPECTROMETRIC STUDIES OF UP- AND DOWNDRAFT GASIFIER TARS

6.2.1 Direct Measurement of Tar and Oil Spectra

The upside-downdraft gasifier described in Chapter 5 is particularly simple to construct and convenient to use in the laboratory. It was connected to the SERI MB-MS, and the spectra of the gas was measured in both the downdraft and updraft modes. This work was originally reported at the Thermochemical Contractors Meeting in Nov. 1985 [9].

6.2.2 Measurement of Downdraft Tar Composition

Air flowed through the bed at 4 L/min, and the top of the bed was ignited. Initially the bed operated in a combustion mode, but as the char bed developed, the gas became combustible and the gasifier operated for about 7 minutes, producing gas and a minor amount of tars. After ignition a small, porous ceramic plug and some quartz wool were placed on top of the bed to compact the char and prevent fly ash from entering the MB-MS.

The spectra of the hot gases was recorded approximately every 10 s. A computer data acquisition system permits display of individual spectra and also of the intensity of single masses as a function of time. The total ion current is shown in Fig. 5-4 (b) juxtaposed to a schematic of the actual gasifier, so that the vertical position of the spectra corresponds approximately to the position of the reaction in the tube. The total ion current and an averaged spectrum taken over 60 s is shown in Fig. 6-1(a) and (b). Tentative identification of the compounds is given in Table 6-1. (The total ion current is analogous to the operation of a flame ionization detector (FID), and shows relative response of the mass spectrometer, depending on the ions collected. It is particularly sensitive to the larger ions because of their greater cross section.) The molecules shown in the spectrum correspond primarily to those produced by high temperature cracking of pyrolysis vapors.

The varying flows of oxygen, benzene, and carbohydrate derived species (such as acetic acid, mass 60) with time is shown in Fig. 6-2. The changing operation of the gasifier is clearly shown by reference to the total ion current and the individual ions plotted against time. Upon first ignition some oxygen leaks through the bed, producing an initial oxygen response (mass 32) in Fig. 6-2. (b). Oxygen begins to leak through the bed again at about 370 s after the final fuel is consumed. As the reaction proceeds, a bed of char is built up and starting at about 20 s primary oils (typified by mass 60) and tars (typified by benzene at mass 78) begin to come through in quantity.

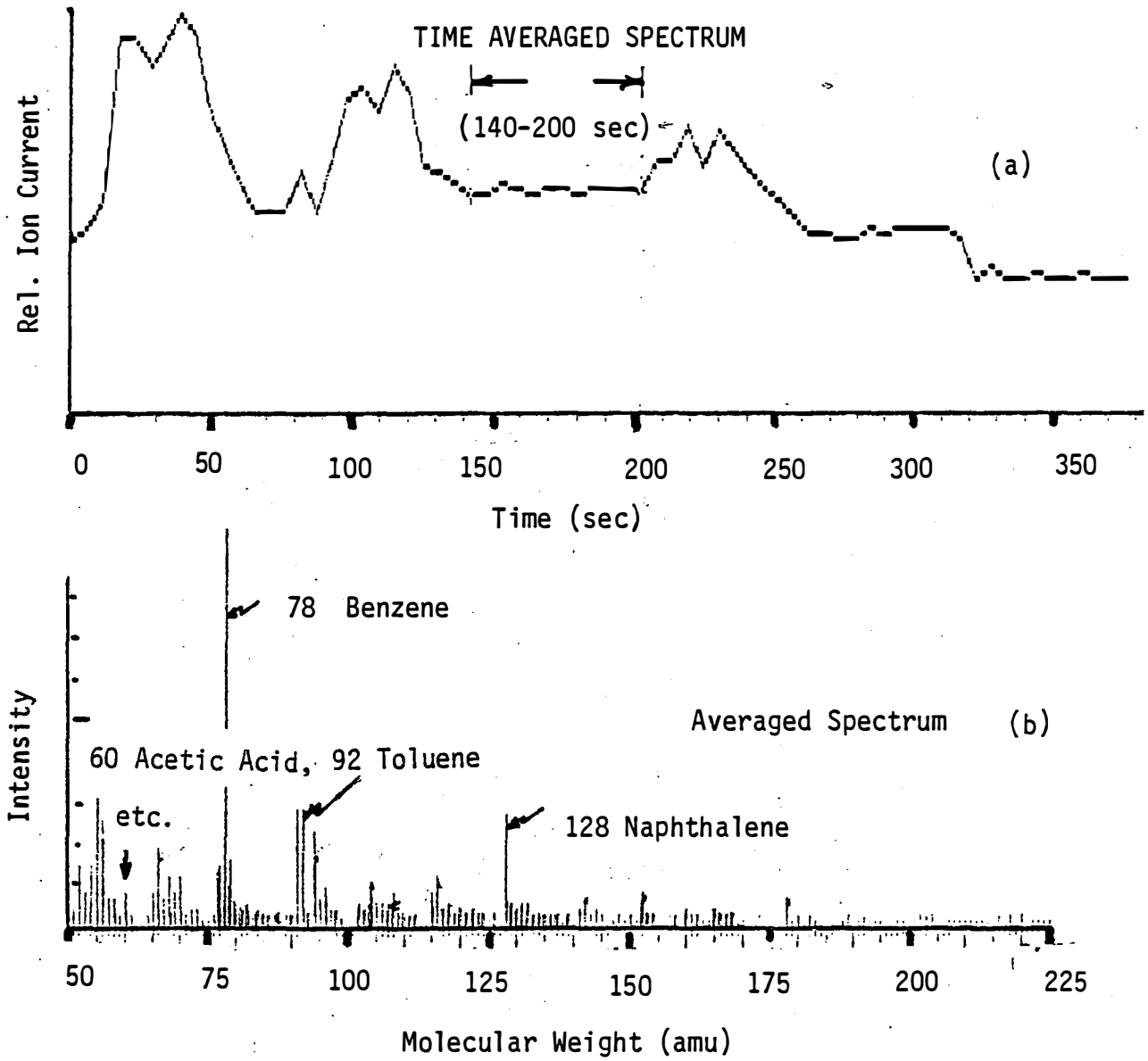

Figure 6-1. Total Ion Current (a) and Mass Spectrum (b) from Upside-downdraft Gasifier

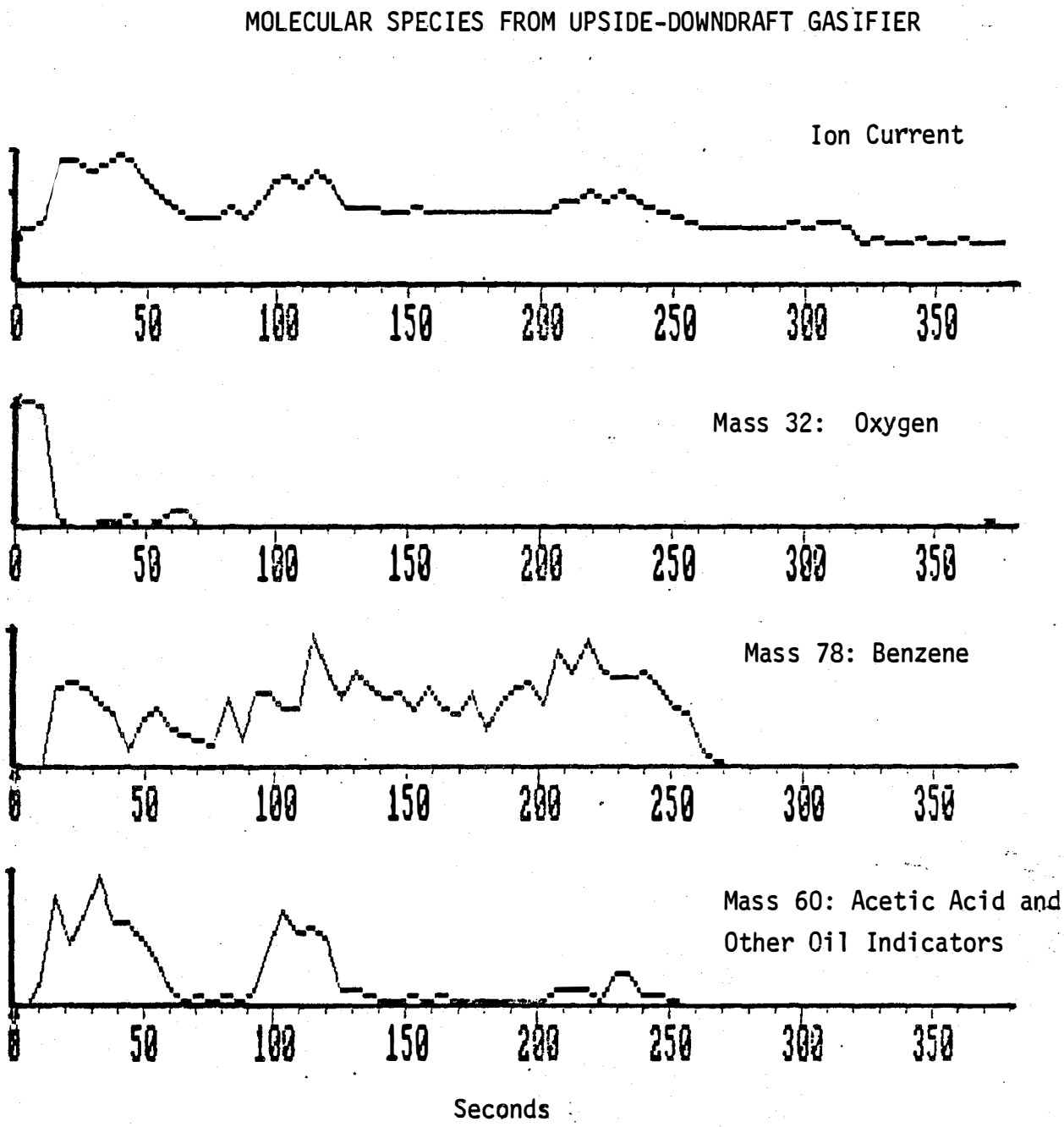

Figure 6-2. Time-intensity of Selected Ions from Upside-Downdraft Gasifier

Table 6-1 Compounds identified in MBMS Spectra of Downdraft Gasifier

Compound	Identified[1]	Gasifier[2] Intensity[3]
66 Cycloheptene		18
78 Benzene	X	100
92 Toluene	X	25
94 Phenol	X	20
104 Styrene		10
106 Ethylbenzene	X	5
108 Methyl-methoxyphenol	X	8
108 Cresol	X	8
110 Dihydroxybenzene	X	-
116 Indene	X	12
124 Methoxy phenols	X	4
128 Naphthalene	X	28
142 Methyl naphthalene	X	8
152 Acenaphthelene	X	10
154 Biphenyl	X	-
166 Fluorine	X	-
168 Phenyl toluenes	X	-
178 Anthracene, Phenanthrene	X	10
180 Dimethyl biphenyl	X	4
192 Methyl anthracene etc.	X	3
202 Pyrene	X	4

(1) Previously identified in studies of Milne and Evans [4-6] and Beckman [2]
(2) Reported in [9].
(3) Intensities estimated visually from spectra. Assignments from previously identified compounds or from cracking chemistry

*****

At about 60 s the gasifier becomes sufficiently stable so that the primary oils are largely cracked, as indicated by the disappearance of mass 60, characteristic of primary wood-oil vapor. Mainly primary tars, characterized by mass 78, come through until all the fuel is pyrolyzed at about 270 s. Some oil (60) comes through also at 110-130 s and 200-250 s, probably because of the irregular motion of the hot char bed dropping down on fresh biomass. Finally, pyrolysis ends at about 260 s and no more tars or oils appear. However the gasifier continues to operate as a char gasifier, producing primarily CO until about 370 s, when the char is exhausted and oxygen comes through unreacted.

In particular it is seen that along with the conventional wood tar compounds previously seen, there are even larger amounts of the volatile compounds benzene, toluene, cyclopentadiene, and styrene, that are normally not seen in condensed wood tars because their high volatility allows them to leave before detection. Compounds (such as mass 60) associated with primary wood oil are at a very low level, except when a momentary interruption in the fuel supply followed by a sudden drop of fuel into the pyrolysis zone causes a momentary influx of fuel. This instability could be avoided by adding a mechanical vibration to keep the fuel moving.

6.2.3 Measurement of Updraft Tar Composition

This same gasifier was operated in the updraft mode by establishing a bed of burning charcoal at the **bottom** of the tube and pouring biomass on top of the charcoal. The hot gases produced by char gasification rise through the biomass, producing mostly primary pyrolysis oils. The total ion current is shown in Fig. 6-3 for updraft operation along with an averaged spectrum taken between 40 and 230 s. Here the spectrum of primary oils is seen. The peak for benzene at 78 has only a very small relative intensity, indicating that little or no high temperature tars are produced in the updraft gasifier.

We believe that this is the first real time examination of the products of downdraft and updraft gasification that includes all the tar and oil species. This method can shed new light on the relationship between gasification conditions and the products emitted (eg, effects of periodic feeding and sudden collapse of "bridges"). This increased understanding can help to eliminate the unwanted products and improve gasification and combustion processes.

It is clear from the above discussion that updraft gasifiers produce condensates of mostly primary oils, and downdraft gasifiers produce condensates primarily of tars. The primary oils can be rapidly destroyed by heat alone at temperatures above 700°C [4-8], but this destruction produces small quantities of tars that persist for long periods at temperatures above 800°C because of to the relatively high stability of aromatics.

Most earlier papers on tar/oil cracking do not clearly distinguish between **primary oils,** that crack easily below 700°C, and **tars,** that only begin to form at this temperature. We believe that until this distinction is clearly made, the kinetics of tar/oil cracking will be confused and controversial. The reported reductions of "tar" in earlier publications and in our earlier work does not take this distinction into account and must be viewed as tentative until the level of oil in the tar is determined.

6.3 FACTORS AFFECTING TAR PRODUCTION

It has been widely observed that tar-oil production is very high (5-20%) in updraft gasifiers where the incoming biomass is pyrolyzed by the hot rising gases generated by burning charcoal at the grate [3,10].

The downdraft gasifier reduces tars typically to 0.5%, and sometimes to 0.05% because the incoming oxidant reacts with a major portion of the vapors produced and creates a high temperature that exposes the remaining vapors to severe cracking conditions. It is important to recognize the factors that control the range of tars. Since tar destruction is due to oxidation of the pyrolysis vapors it is to be expected that the degree of destruction is related to the oxygen/fuel ratio at which the gasifier operates.

In the overall balance of biomass gasificationthe carbon requires a disproportionate amount of oxygen to make the CO portion of producer gas. The amount of char-ash byproduct has been found to be an important variable in gasifier operation by ourselves and others [9,11]. At low char-ash removal rates the oxygen/fuel ratio is high, and the flaming pyrolysis temperature is correspondingly high. At high char-ash removal rates the amount of oxygen in the final gas is reduced and therefore the temperature of flaming pyrolysis is reduced and tars increase.

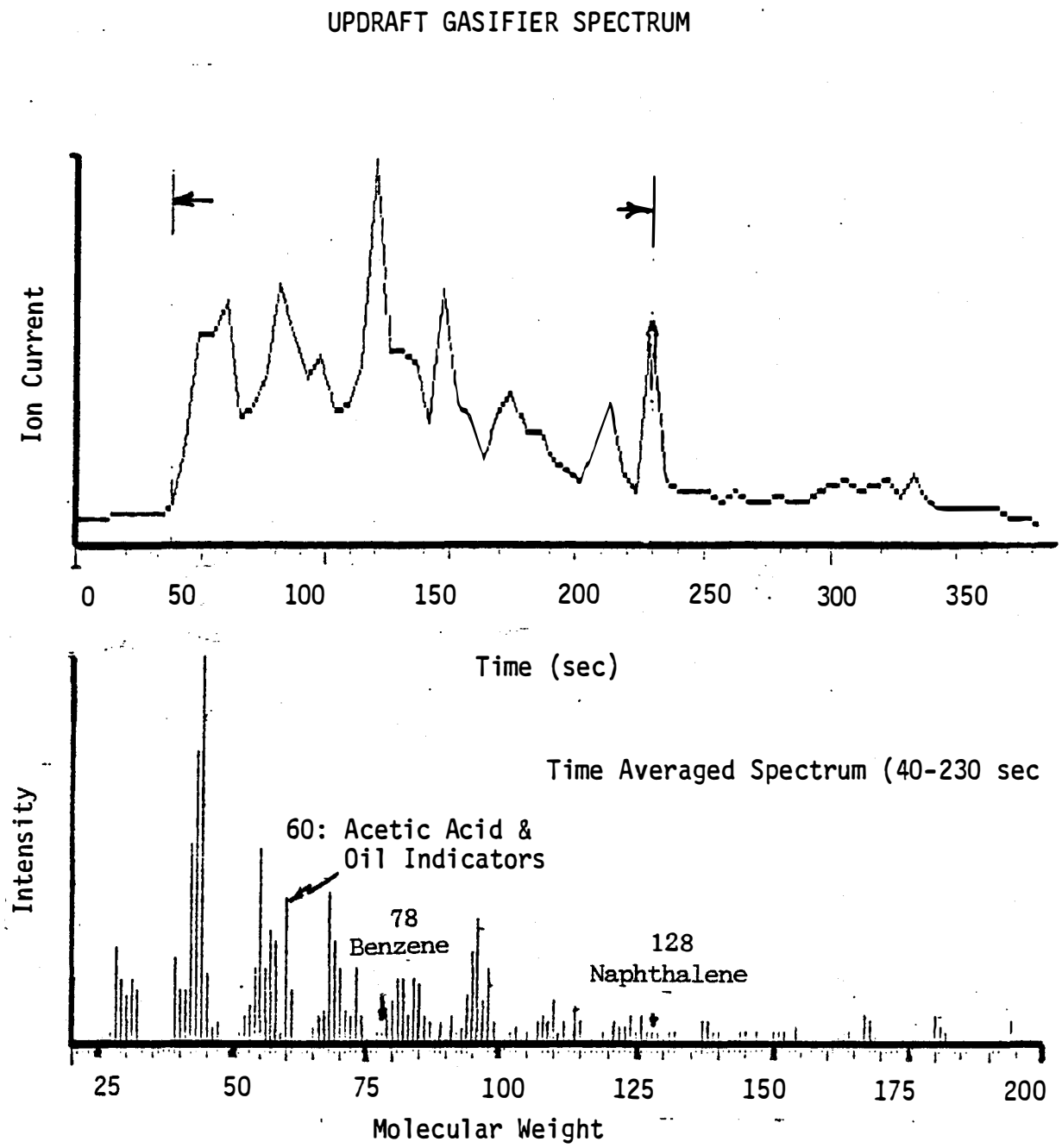

Figure 6-3. Total Ion Current and Averaged Mass Spectrum from Updraft Gasifier

We found that we could generate gas with a 5 % tar content by operating at high stirring rates that produced 10% char-ash. In this way the operation of the gasifier approaches the operation of a pyrolyzer, the quality of the gas is improved by higher olefin content, but the quantity of tars and oils is also increased.

In Phase II it gradually became obvious that grate rotation was an important variable in the amount of char and tar produced. While tar-char production with grate rotation was never studied directly, Table 6-2 contains sample data that shows the increase of tar from 3600 ppm to 10,000 ppm as rotation is increased from 7 to 120 RPM.

Table 6-2 Dependence of Tar Production on Grate Rotation Rate

RUN	B2-3	B1-4	B1-5
Moisture (Wt %)	1	1	1
Feed rate (kg/hr, dry)	7.2	10.25	14.2
Gasifier oxygen (kg/hr)	3.96	5.54	5.54
Grate rotation (rph)	7	26	120
Gasifier Tar (% of feed)	0.36	0.45	1.01

Note: From Run B1 and B2 on 5 mm pine chips.

*****

6.4 MEASUREMENTS OF PRODUCER GAS TAR LEVELS

6.4.1 Phase I Tar Production

In the Phase I gasifier tests an estimate of the tar level was made by analyzing the scrub water for chemical oxygen demand (COD). This was a rough estimate because the water-tar level changed continuously as run conditions changed and some of the "tars" were probably not soluble in the water. In these tests we found tar levels of 0.041% of the feedstock [10]. This low level is consistent with the fact that we were not removing char at the grate and so had a relatively high O_2/fuel ratio [11-13].

6.4.2 Phase II Tar production

In Phase II we used the gas sampling train shown in Fig. 6-4 to measure tars. A weighed 40 mm Gelman glass-fiber absolute filter was mounted in a filter holder heated to 60°-80°C to prevent water condensation. A measured amount of gas was drawn through the filter. The filter was then extracted with a mixture of 50% acetone-50% methanol and weighed again. The weight loss corresponds to the tars condensed from the gas stream. Note that materials of higher volatility such as benzene and toluene will not be included in this tar analysis even though they may have similar or higher concentration in the gas phase (see above).

The level of tar production in Phase II was generally much higher than in Phase I because of the higher rate of removal of char-ash at the grate. Levels measured are shown in the tables of Chapter 3 and Tables 6-2 to 6-4. They ranged from 0.1% to 5%, depending primarily on grate rotation rate.

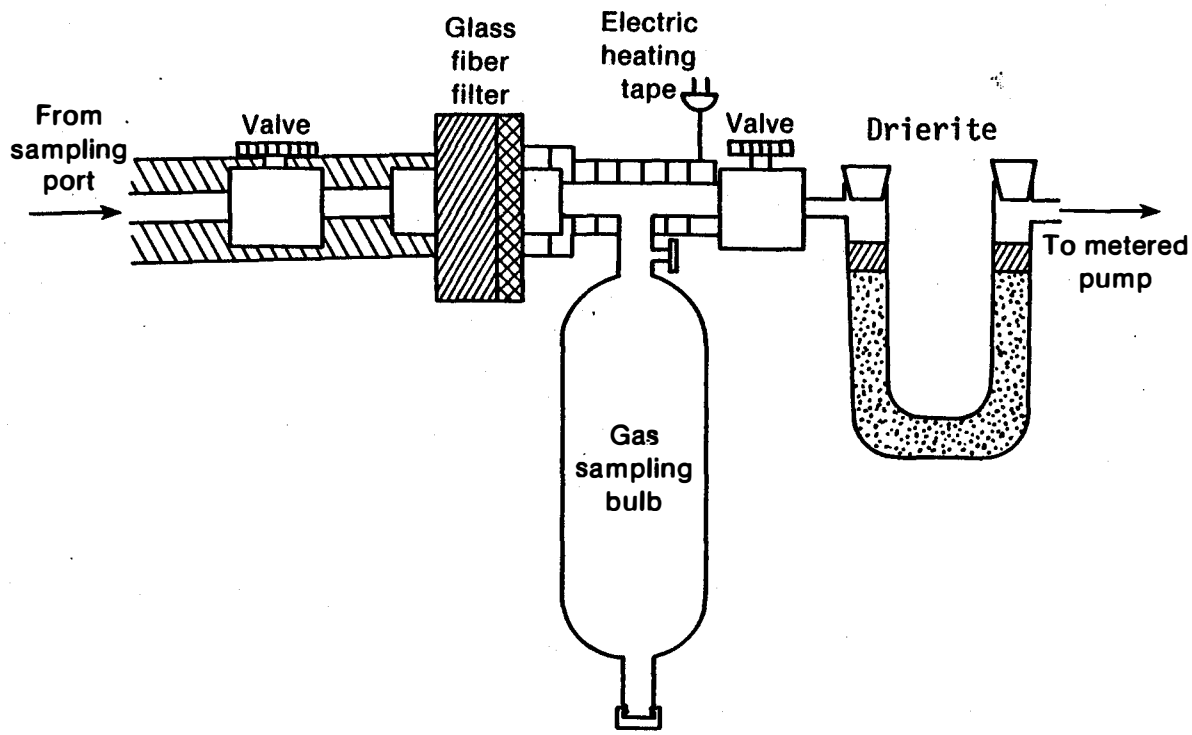

Figure 6-4. Gas and Tar Sampling Train

6.5 THERMAL TAR DESTRUCTION

6.5.1 Previous Studies on Thermal Tar Destruction

A number of papers have appeared recently discussing the kinetics and technology of cracking wood tars and oils [4-8]. However, as noted earlier, in the literature there is a lack of differentiation between the wood oils and the wood tars that may cause the results of various studies to be inconsistent.

There has been an active program in oxygen blown fluidized bed gasifiers for making synthesis gas for methanol production in Europe under the aegis of the International Energy Agency [14-18]. It is a characteristic of fluidized bed gasifiers that they produce more tars and methane than the fixed bed downdraft gasifier. The French Croissot Loire gasifier uses a reforming chamber maintained at 1300°C to destroy tars and reform methane [15]. The Swedish Mino Process on the other hand uses a conventional methane reforming catalyst at about 1000°C for methane and tar destruction [18]. These results were not available when we began our tar destruction studies, but are consistent with our findings. Again there is no analysis of these "tars" to determine whether they are tars or oils or a mix.

6.5.2 Tar Destruction Experiments in the 1 Ton/day Gasifier

When the oxygen gasifier was first designed, it was believed that tars, remaining in the gas after flaming pyrolysis is completed, could be destroyed by passage through a sufficiently long bed of hot charcoal. After our studies of charcoal gasification kinetics, we now believe that the endothermic H_2O and CO_2-charcoal reactions can quench a very hot gas down to less than 900°C in a fraction of a s. **Thus it is impossible to maintain a charcoal** bed in excess of 900°C in presence of H_2O and CO_2 and so it seems unlikely that the charcoal bed is effective in tar cracking.

It would be desirable if the tars could be cracked in a reasonable residence time at high temperature. This could be accomplished with little loss of energy using a very small amount of oxygen to raise the gas to a high temperature, recovering this excess heat with a counterflow heat exchanger. We therefore decided to test the effect of a high temperature zone on tar destruction.

The 1 ton/day gasifier discussed in Chapters 2 and 3 was modified to provide a small injection of oxygen below the grate to explore the use of a burner in reforming and cracking the tar in the producer gas. The producer gas diffuses into the oxygen and spontaneously combusts or is ignited by glowing char to produce a luminous flame. The results of this secondary combustion are shown in Table 6-3. They show that the tar level was decreased by a factor of 2-6 by the addition of oxygen although the measured temperature rise was only 590°C. (The temperature measurement is suspect here.) The residence time of the gas through this flame was less than a half second in the 5 liter combustor. In subsequent runs the grate was moved up in the gasifier 30 cm to provide a larger volume for secondary combustion to occur below the grate. Since the smaller biomass feedstocks require only 5 to 16 cm of bed for pyrolysis and gasification, the loss in bed height by moving the grate is an advantage in terms of reducing pressure drop and heat loss. Two opposing oxygen lances were then used for the secondary combustion

reforming below the grate. The residence time was thereby increased in the 10 liter volume section to over one second, allowing more complete mixing. The results are shown in Table 6-4. The tars were reduced by a factor of about 1/3, not very dramatic, even though the burner temperature was a more reasonable 855°-890°C. However the starting levels of tar were not as high.

Table 6-3 Tar Conversion with Short Burner Below Gasifier G+ate

RUN	M5-3	M5-2	M5-4	M5-5
Moisture (Wt %)	1	1	15	15
Feed rate (kg/hr, dry)	6.15	7.13	4.97	7.57
Gasifier oxygen (kg/hr)	2.83	3.78	2.78	3.41
Grate rotation (rph)	6.0	6.0	6.0	6.0
Burner Oxygen (kg/hr)	0	0.63	0	0.63
Burner Temperature (C)	300	590	500	590
Gasifier Tar (% of feed)	4.43	0.64	1.01	0.45

Note: Run M5 on 5 mm pine chips.

*****

Table 6-4 Tar Conversion with Long Burner Section Below Gasifier Grate

RUN	B2-2	B2-1	B2-4	B2-3
Moisture (Wt %)	1	1	1	1
Feed rate (kg/hr, dry)	8.60	10.40	8.60	7.20
Gasifier oxygen (kg/hr)	3.35	4.37	2.75	3.96
Grate rotation (rph)	7.0	7.0	7.0	7.0
Burner Oxygen (kg/hr)	0.00	0.76	0.00	0.76
Burner Temperature (C)	815	890	880	0.36
Gasifier Tar (% of feed)	0.73	0.40	0.77	0.36

Note: From Run B2 on 5 mm pine chips.

*****

6.5.3 Thermal Tar Destruction in the Transparent Gasifier

It became evident in these runs that our "retrofit" burner did not adequately test the hypothesis that additional oxygen would crack the tars, probably because insulation and mixing were inadequate. It was obvious that we needed better understanding and control of the gasifier and burner to make meaningful measurements. It was also clear that the 1 ton/day gasifier would require a major investment of labor and capital to build a satisfactory cracking device and was too cumbersome for making tests.

In order to more thoroughly study tar conversion with an after-burner, the improved transparent gold insulated quartz tube gasifier, shown in Fig. 5-3 was built. It is described in more detail in Chapter 5. In this gasifier, oxygen and/or propane can be injected through 6 nozzles, 1.5 mm in diameter through the top of the after-burner reactor. The nozzles are directed tangentially downward to form a hexagonal pattern to provide good mixing in the reactor.

For thermal tar destruction measurements, gas and tar samples were taken from a point just before the point where the gases enter the tar reactor and from another point at the exit from the reactor. The reactor temperature was varied from 600°-1200°C by varying the bed length of the gasifier and the oxygen flow to the tar reactor. A propane/oxygen mixture is burned to heat the tar reactor to cracking temperature before starting the gasifier. After the reactor reaches 700°C or more, the gasifier can be lit and the propane turned off. The oxygen will automatically burn some of the producer gas to give a flame to maintain the selected temperature.

The tar cracker/reformer has removed up to 94% of the tar coming in from the gasifier. In some cases tar contents were reduced below 200 ppm, but it was found that temperatures above 900°C were required to achieve significant cracking. In addition, the reactor conditions were not sufficiently steady to clearly differentiate between changes in the gasifier and changes produced by the cracker.

A major problem that was encountered in the thermal cracking experiments was the difficulty of generating a gasifier stream with a constant level of tar in order to determine the effect of thermal or catalytic cracking. During periods of overfeeding, the gasifier behaved as a pyrolyzer, producing high tar and oil levels. Periods of underfeeding caused the gasifier to behave like a char gasifier with very low tar levels, but with increased production of heat by charcoal combustion and relatively weak gas from char gasification. Therefore,a number of improvements were made on the gasifier before studying catalytic tar conversion.

6.6 CATALYTIC TAR CONVERSION

6.6.1 Introduction

Catalysts are widely used for destruction of heavy hydrocarbon vapors in the oil industry. They have also been tested in some gasification projects [10-16]. It has been found that catalysts can remove tars at much lower temperatures than those required for thermal cracking. We believe that much of the above work did not sufficiently distinquish between the cracking of the primary pyrolysis oil compounds and the high temperature tar compounds, so that the results are specific to each process. Our work on cracking catalysts took place during the same time period as the above studies and compliments many of their results.

6.6.2 Apparatus for Catalytic Tar Cracking Tests

In order to make meaningful measurement of tar destruction, it is necessary to have a constant production of tars. The transparent gasifier was modified as shown in Fig. 6-5 to operate on oxygen with a continuous chip feed level to produce a steady state with a constant tar level. The bed level was maintained constant in the laboratory gasifier using the proportional-integral control system described in Chapter 5.

The majority of the gas produced passes to the flare. During sampling some of the gas is passed through a catalyst contained in a furnace. A typical temperature profile of the furnace is shown in Fig. 6-6. A sample train is attached to both the inlet and outlet of the furnace and permits taking samples of the gas before treatment in the furnace and after treatment for

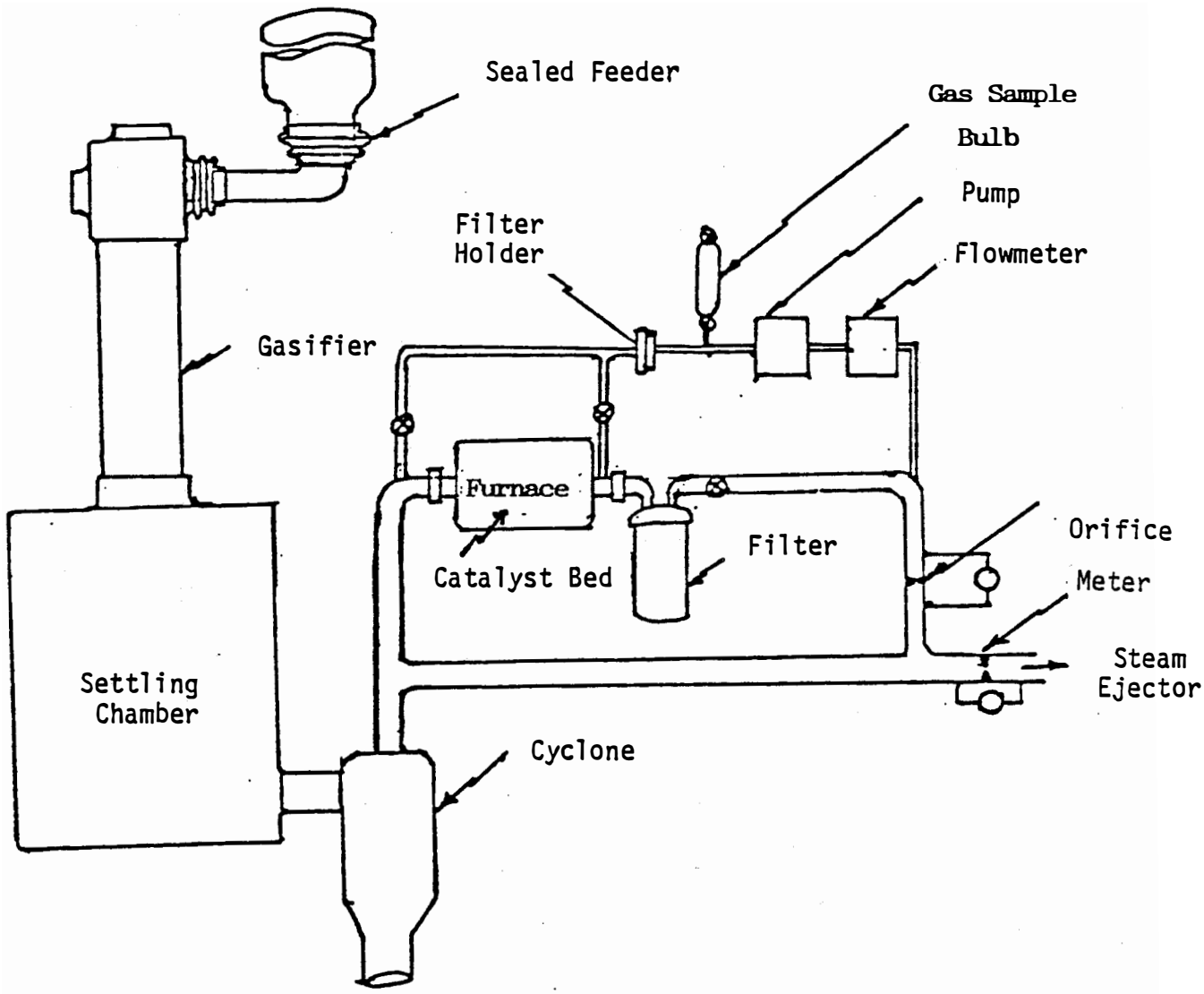

Figure 6-5. Modification of Transparent Gasifier for Tar Cracking Tests

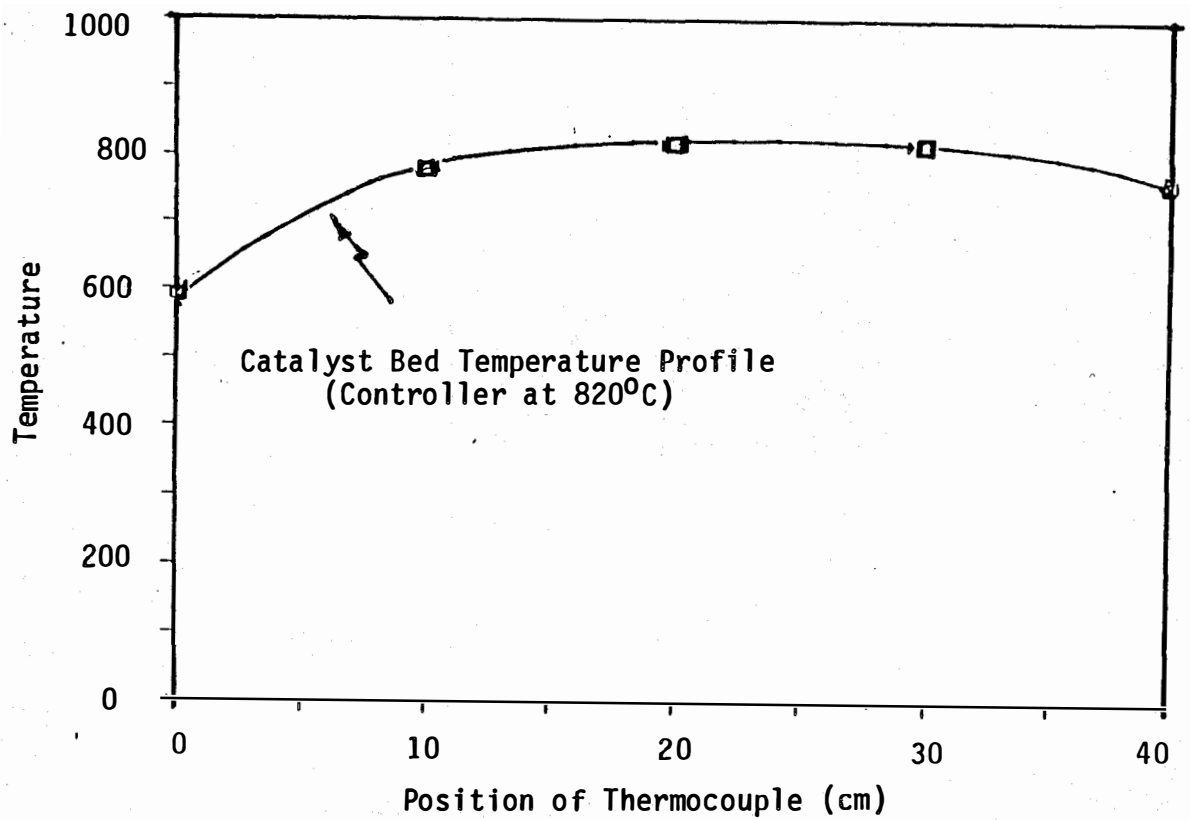

Figure 6-6. Temperature Distribution in SERI Tar Cracking Reactor

direct comparison during the same time period.

Before each run the catalyst charge (typically 500-1000 g) was weighedand loaded into a stainless steel tube 20 mm in diameter. In operation the furnace was raised to the temperature of the test, the gas flow was started through the catalyst by a vacuum pump, and the flow at the outlet of the pump was measured with a wet test meter.

The gasifier was operated typically at a rate of 1.6 kg/hr to generate gas containing tars using 1 cm pine chips. The effect of temperature was measured by making runs at several temperatures while maintaining a constant flow rate of 0.36 kg/hr through the catalyst. The residence time was also varied at a constant temperature.

It should be emphasized that the catalyst never reached a steady state of coke coverage. Hence it is not surprising that there is considerable scatter in the data.

6.6.3 Results of Catalytic Tar Cracking Tests

The first catalyst tested was dolomite limestone. Dolomite had been reported by Ekstrom to be effective in the MINO process [17] and in other tests by D'Eglise and Black [19,20]. It is widely available and low in cost. The results are shown in Table 6-5. The gas phase residence time was varied, at a constant temperature of 750°C, and the results are shown in Table 6-6. The results in these two tables show the quantity of tar entering the gasifier and the quantity remaining after the stated residence time, as well as the degree of tar reduction. From these results it is seen that both higher temperature and increased residence time are effective in reducing the tars.

The gas analysis at 820°C, and a flow of 0.36 kg/hr, is shown in Table 6-7.

Table 6-5. Effect of Temperature on Tar Cracking Over Dolomite Catalyst

Temp** C	Residence time s	<----tar level---> Before mg/Nm³	After mg/Nm³	Reduction Ratio	k (s)⁻¹
600	0.86	8421	3164	2.7	1.14
820	0.68	15904	2352	6.8	2.81
960	0.61	7341	979	7.5	3.30

Catalyst: 1.03 kg Dolomite*
Gas Flow: 0.36 kg/h
Space Velocity: 0.35 g/g-hr

*****

Table 6-6. Effect of Residence Time on Tar Cracking Over Dolomite Catalyst

Gas Flow Rate kg/hr	Space vel g/g-hr	Residence time s	<---Tar Level---> Before mg/Nm3	After mg/Nm3	Reduction Ratio	k (s)-1	
0.80	0.78	0.30	2787	1138	2.5	2.99	
0.22	0.21	1.11	2787	176	16.0	2.49	
0.44	0.43	0.56	6630	2118	3.1		2.04

Notes:
* 1.03 kg of dolomite lime contained in a 20 cm length of 5 cm ID stainless steel pipe. Bulk density = 3345 kg/m3; void volume = 0.25 cm3/g. Dolomite limestone decomposes to dolomite lime in the range of 600-1000 C so th state of the catalyst is unknown at this time
** Average temperature over a 20 cm length of furnace

*****

Table 6-7. Analysis of Gas Before and After Cracking at 820- C over Dolomite

Component	Before Vol %	After Vol %
Hydrogen	19.1	21.7
CO_2	33.9	44.3
Ethylene	1.4	1.4
Ethane	0.2	0.1
Acetylene	0.3	0
Nitrogen	1.5	0.1
Methane	4	7
CO	38.6	25.4
LHV, Btu/sc	241	227

*****

It can be seen that the gas composition was significantly altered: CO decreased, while CO_2, H_2 and CH_4 all increased. This suggests that the dolomite catalyst was effective in establishing the water gas shift at this temperature, but more tests would be required to confirm this conclusion. The above experiments were performed with uncalcined dolomite limestone (limestone that has not lost CO_2 by heating), but at higher temperatures the limestone was partially converted to lime as evidenced by a 20% weight loss in the catalyst weight after the highest temperature experiment, (960°C).

The catalyst was held for an hour at each temperature before measuring the conversion rate. The experiments were performed in the order shown in Table 6-5 so that it is not clear what the degree of conversion to lime was in each experiment.

The behavior of all catalysts tested is tabulated in Table 6-8. Details of the catalyst and the experiments are given in the footnotes. We believe the tars decompose according to

$$\text{rate} = dC/dt = -kC \qquad (6\text{-}1)$$

A reaction rate constant for each run was calculated from the measured data according to

$$k = -\ln(C_1/C_2)/t_r \qquad (6\text{-}2)$$

where C_1 is the initial concentration of tars in the gas and C_2 is the concentration after a residence time t_r in the catalyst bed. The results are listed for each run. The value of log k is plotted against $1/t_r$ in Fig. 6-7 for the dolomite runs.

Olivene chips 1 cm on a side were tested because they contain nickel, are thermally stable and are potentially low in cost. A plot of log k vs 1/T is shown in Fig. 6-8 for the olivene runs. It can be seen that olivene produces a relatively small reduction of tars at high temperature.

A Si-Al cracking catalyst from Davison Chemicals was tested and proved to be very effective as shown in Fig. 6-9. This was one of the most effective catalysts tested. A silicalite cracking catalyst from Union Carbide was tested and the results are shown in Fig. 6-10. These two catalysts had the highest reduction of tars at quite low temperatures as shown in Table 6-8.

Results for the LZY-62 cracking catalyst, a Y type molecular sieve, were confusing. Three successive tests were performed at 15 minute intervals at 350°C to test catalyst lifetime. The rate decreased from 1.5 to 0.89 in this time. A run at 463°C did not increase the rate. The catalyst was reactivated by pulling air through the bed at 500°C for 6 hours. This did not increase the catalyst activity, even at 600°C. When the catalyst was removed from the furnace there was evidence of some coking only at one end. Thus we have no explanation at present for the rapid degradation of this catalyst.

6.6.4 Discussion of Results

A summary of the catalyst kinetic data is shown in Fig. 6-11. While there is considerable scatter in the data, the general trends are shown and differ considerably among the catalysts. These catalyst tests were not as extensive as we would have liked but certainly give an indication that catalysts are effective in destroying tars at much lower temperatures than are required for thermal destruction. We think it probable that catalysts can be found that will give even more effective tar reduction.

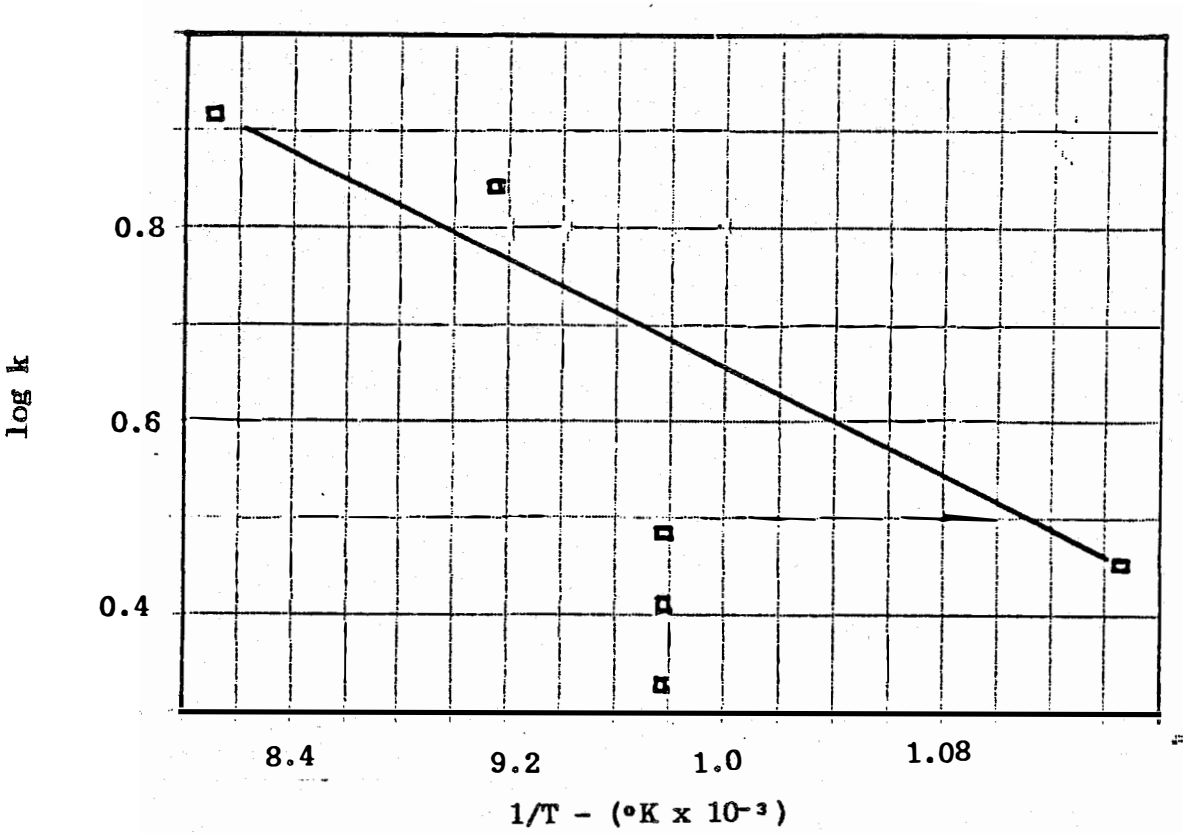

Figure 6-7. Dolomite Tar Cracking Rate vs Temperature

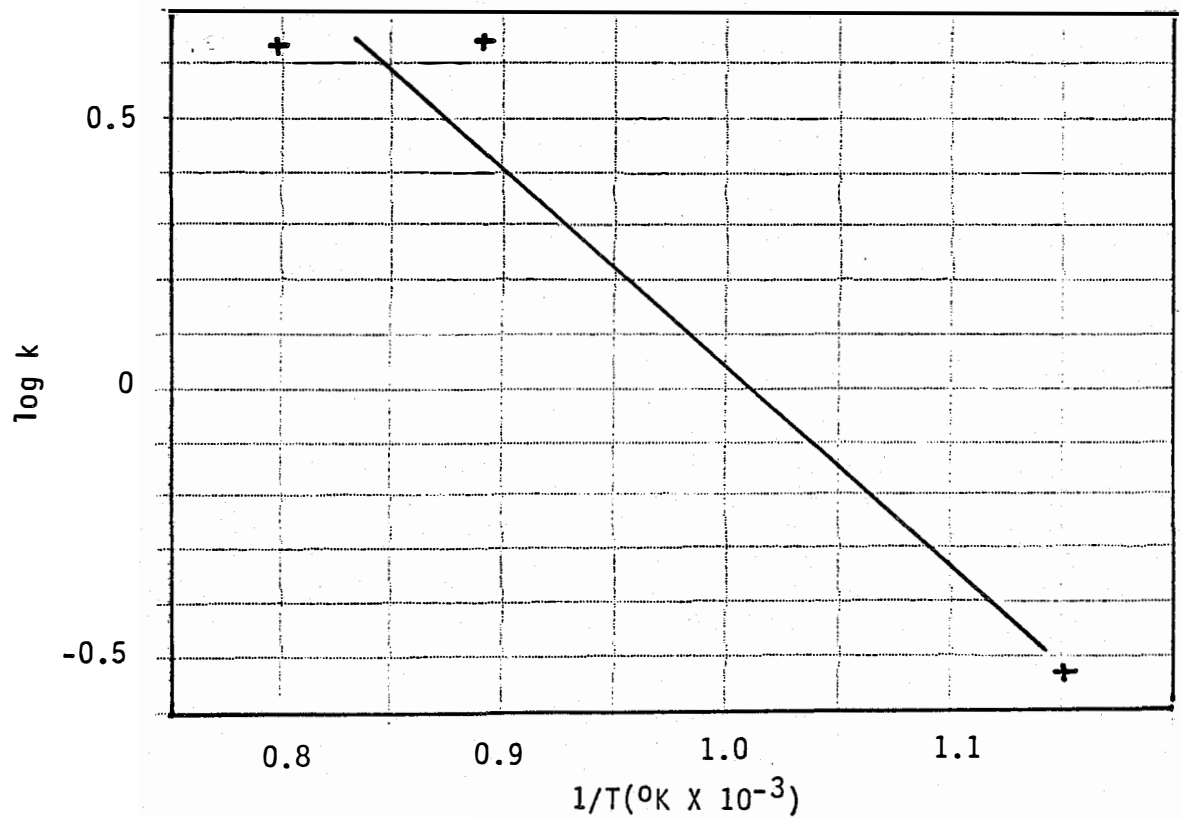

Figure 6-8. Olivene Tar Cracking Rate vs Temperature

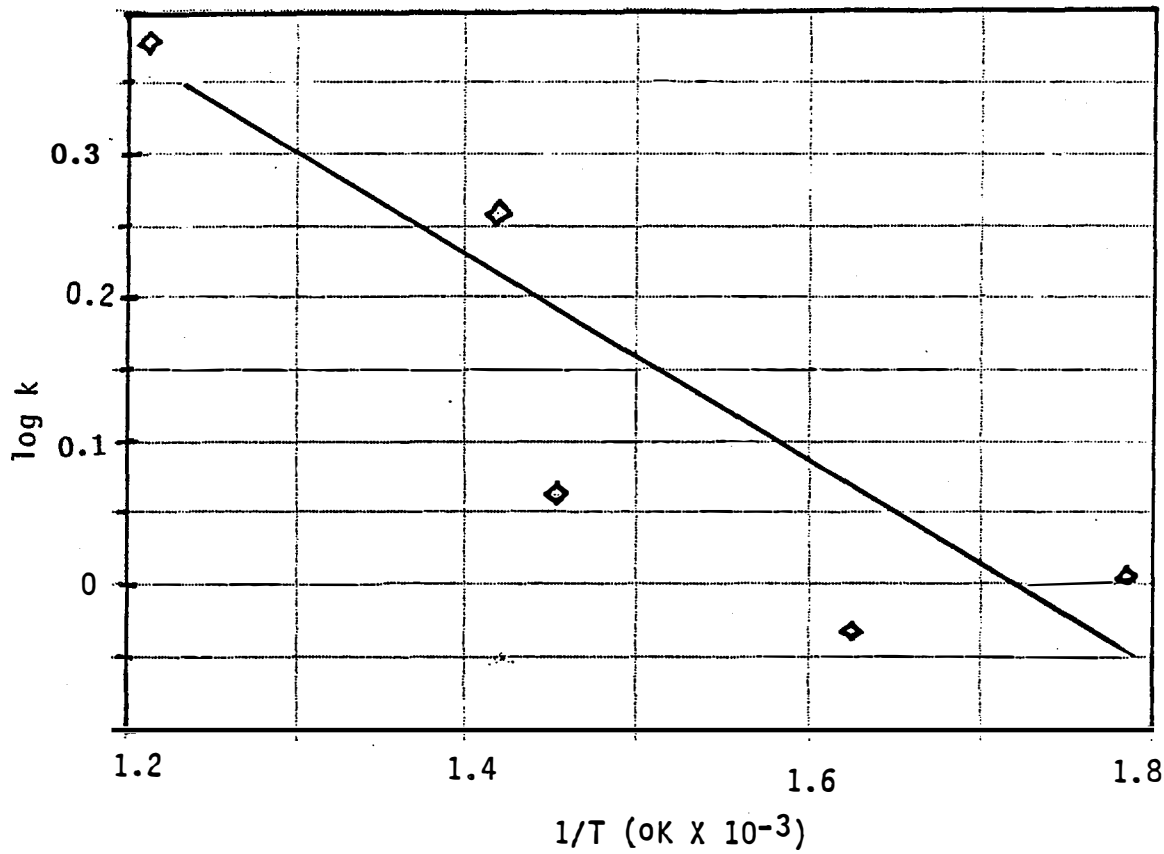

Figure 6-9. Si-Al Cracking Catalyst Rate vs Temperature

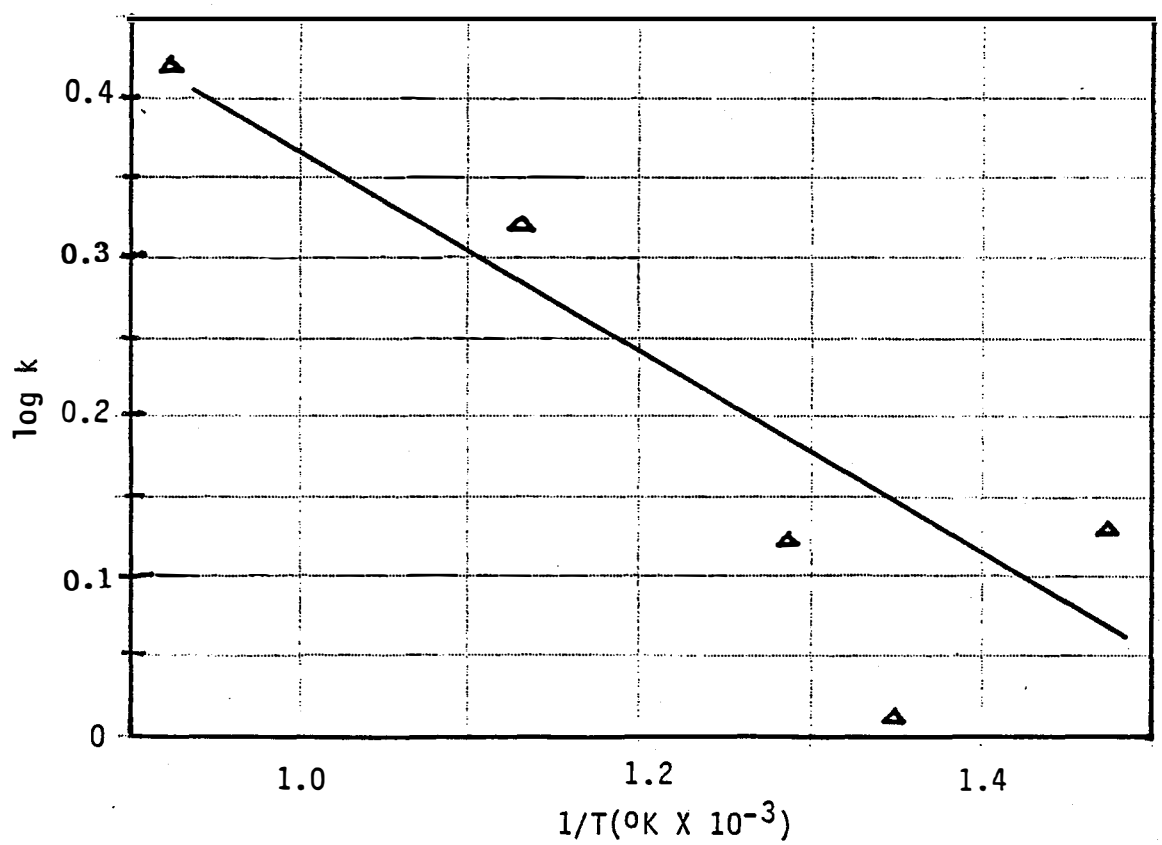

Figure 6-10. Silicalite Tar Cracking Rate vs Temperature

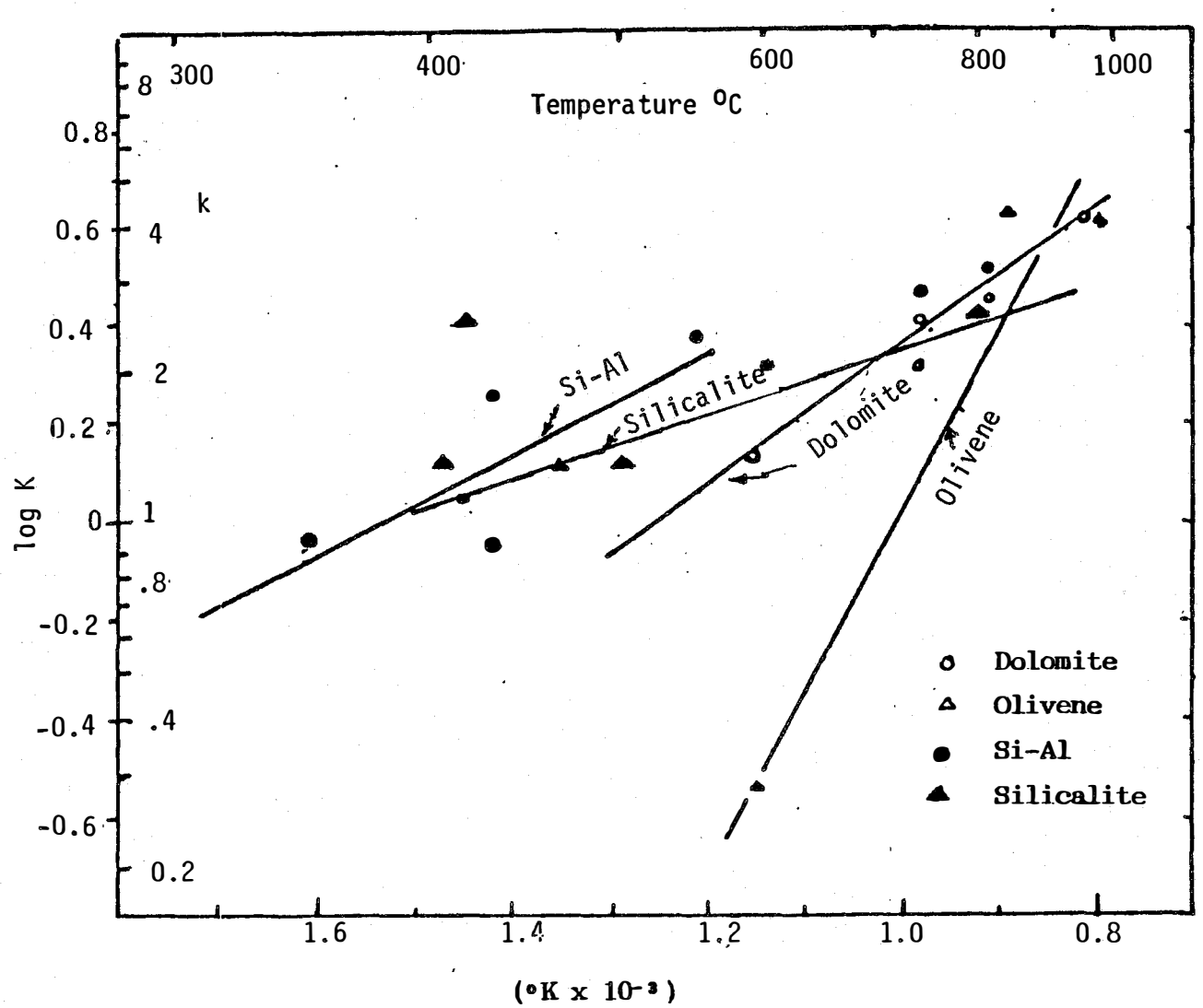

Figure 6-11. Summary of Catalytic Tar Cracking Data

Table 6-8 Summary of Catalytic Tar Cracking Runs

RUN CONDITIONS				TAR REDUCTION			
Temp °C(1)	Flow Rate	Residence Time-s	Space Vel g/g-hr	Before mg/Nm³	After mg/Nm³	Rate-k 1/s(2)	log k
Catalyst: Dolomite (3)							
600	0.73	0.34	0.33	9574	3597	2.84	0.454
750	0.73	0.29	0.29	3169	1294	3.05	0.484
820	0.73	0.28	0.27	18082	2674	6.95	0.842
960	0.73	0.24	0.24	8346	1113	8.26	0.917
750	0.20	1.07	1.04	3169	200	2.58	0.411
750	0.40	0.54	0.52	7537	2408	2.13	0.328
Catalyst: Olivene (4)							
595	0.42	0.66	0.63	11915	9821	0.29	-0.531
850	0.42	0.51	0.49	19843	2160	4.37	0.640
980	0.42	0.45	0.44	5862	818	4.33	0.636
Catalyst: Si-Al Catalyst (5)							
432	0.51	1.54	2.02	18082	4654	0.88	-0.055
432	0.51	1.54	2.02	22070	1313	1.83	0.263
552	0.56	1.20	1.57	5929	333	2.40	0.380
415	0.48	1.68	2.19	4863	695	1.16	0.064
343	0.49	1.84	2.40	4654	847	0.93	-0.033
287	0.51	1.94	2.54	5605	780	1.02	0.007
Catalyst: Crystalline Silica S-115 (6)							
416	0.59	0.91	1.68	8280	790	2.58	0.412
406	0.39	1.40	2.57	15237	2303	1.35	0.131
469	0.34	1.47	2.70	15189	3359	1.03	0.012
505	0.48	0.99	1.83	11725	3131	1.33	0.125
613	0.47	0.89	1.64	25305	3930	2.10	0.321
812	0.42	0.81	1.50	9184	1075	2.64	0.422
Catalyst: Y zeolite (LZY-62)(7)							
350	0.43	1.65	4.04	13581	1142	1.50	0.175
350	0.43	1.65	4.04	13800	2389	1.06	0.026
350	0.43	1.65	4.04	15979	3654	0.89	-0.050
463	0.44	1.37	3.34	13990	4121	0.89	-0.049
Catalyst reactivated 6 hr @ 500°C with air							
476	0.5	1.18	2.89	11411	5025	0.69	-0.159
605	0.44	1.15	2.80	17425	6671	0.84	-0.077

Notes to Table 6-8:

(1) Average temperature over a 20 cm length of furnace.

(2) Rate calculated from $k = -\ln(C_1/C_2)/t_d$

(3) 1.03 kg of Dolomite lime contained in 20cm length of 5 cm id stainless pipe. Bulk density = 3346 kg/m³; void volume = .25 cm³/g. Dolomite limestone decomposes to dolomite lime in the range 600-1000 C. Particle size 5 mm.

(4) Olivene sand, (1.04 kg; 1701 kg/m³). Particle size ~1mm Bulk density 1701 kg/m3; Void volume .27 cm³/g

(5) Si-Al cracking catalyst (Davison Chemicals, Gr 980-13) 510 g sample, bulk density 7655 kg/m³; void volume .85 cm³/g Particle size 1mm d X 5 mm long cylinders

(6) Crystalline silicalite catalyst S-155 (Union Carbide) 543 g charge; bulk density .76/g/cm³; Void vol 0.80 cm³/g

(7) LZY-62 (Union Carbide) Y type molecular sieve, ammonium cations, heated to 550 C over 4 hrs, then held 2 hours. Charge 409.2 g; Bulk density 0.61 g/cm³; Void vol 1.27 cc/g

6.7 Recommendations for Future Tests

The catalyst runs are instructive but preliminary in nature. More runs were planned, but the laboratory was shut down for a period of four months to install improved ventilation. This prevented our running a few more catalyst candidates and determining catalyst lifetimes on the better catalysts.

We would recommend that more work be done to:

- o Find other better and cheaper cracking catalysts
- o Determine the rate of coking of the best catalysts
- o Determine the ease of removing coke
- o Determine mechanical properties of the catalysts
- o Operate a catalyst bed continuously with a gasifier
- o Determine the optimal conditions for cracking tars and oils
- o Evaluate cost of catalytic gas cleanup relative to scrubbing

6.8 Application of Catalytic Tar Conversion to Commercial Gasification

The above studies show that it is possible to achieve one to two orders of magnitude of tar destruction using either thermal (with oxidation by steam and CO_2) or catalytic cracking. Thermal cracking can be implemented by heating the producer gas to a temperature above 1000°C in a vessel downstream of the gasifier. Counterflow heat exchange and high quality insulation would minimize the need for external energy input.

Catalytic cracking is effective in the temperature range 400°-800°C, typical of the gas temperatures leaving a gasifier, and so catalytic cracking is more attractive than thermal cracking. However, it would be necessary to employ either a fluidized or a circulating bed system to permit regeneration of the catalyst, as the catalyst will gradually coke up. Further studies will be necessary to determine coking levels on the various catalysts.

In a practical gasifier cleanup system the catalyst could be contained in a moving bed under the grate to take advantage of the high temperature of the gas at that point. A recirculating side arm can be provided to permit steam stripping or oxidative removal of coke as it formed and deliver fresh catalyst to the top of the bed.
A gasifier with moving catalyst bed and a steam/oxidant stripper is shown schematically in Fig. 6-12. The ratio of steam to oxidant could be used to control temperature in the stripper and catalyst bed. (Alternatively a fluidized bed system could be attached to a gasifier to achieve the same results, but this could only be justified for a large gasifier.)

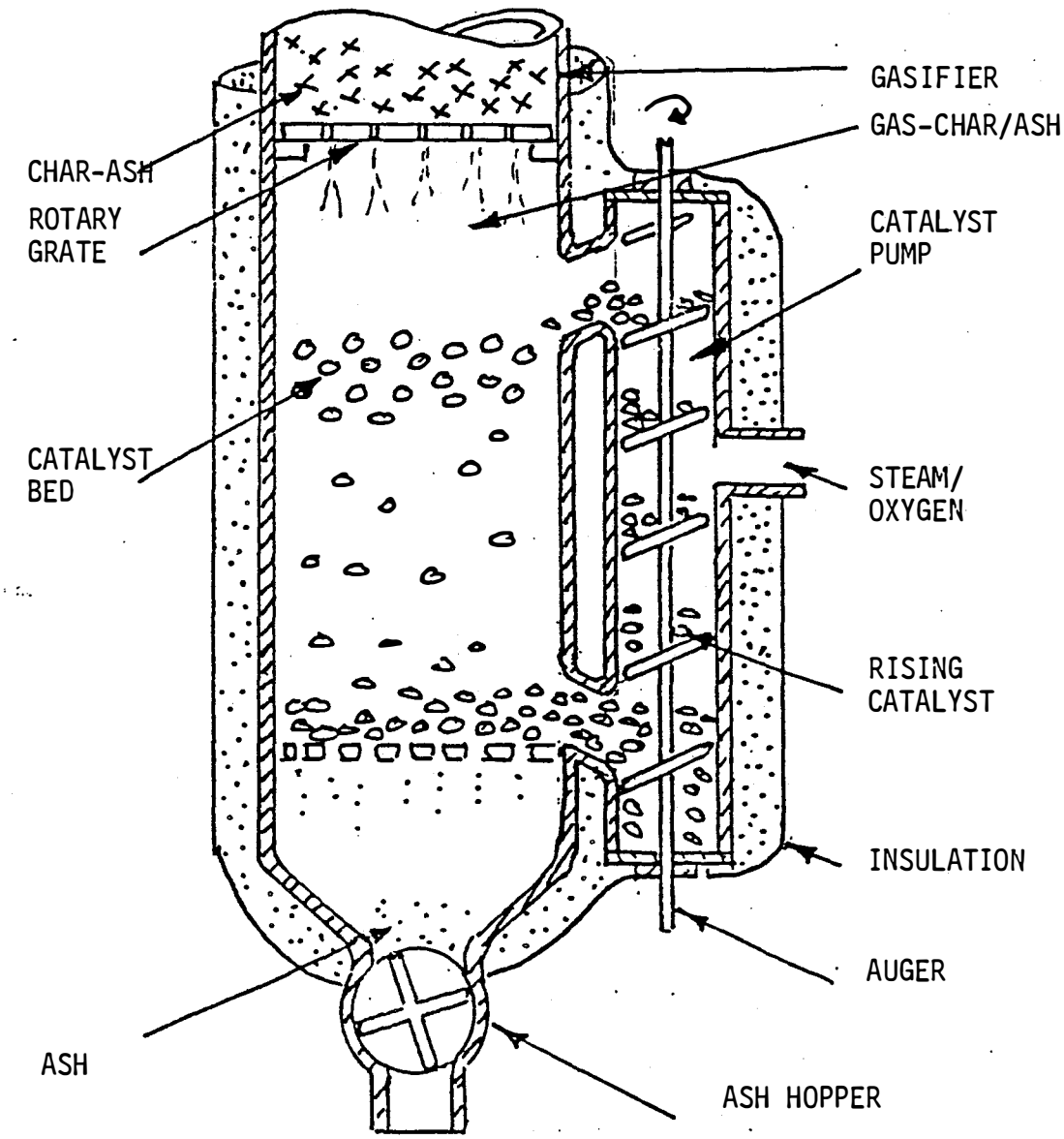

Figure 6-12. Schematic of Catalytic Cracking Apparatus Attached to Gasifier

REFERENCES

1. Elliott, D. C., *Analysis and Comparison of Biomass Pyrolysis/Gasification Condensates* - Final Report PNL-5943, Richland WA: Pacific Northwest Laboratory, 1985.

2. Beckman, D. and Elliot, D. C., "Comparisons of the Yields and Properties of the Oil Products from Direct Thermochemical Biomass Liquefaction Process," *Canadian Journal of Chemical Engineering,* Vol. 63, 1985, pp. 99-104.

3. Baker, E. G.,, Brown, M. D., Moore, R. H., Mudge, L.K., and Elliott, D. C., *Engineering Analysis of Biomass Gasifier Product Gas Cleaning Technology*, PNL-5534, Richland, WA: Pacific Northwest Laboratory, 1985.

4. Milne, T. A., Evans, R. E. and Soltys, M. N. "Characterization of Biomass Pyrolysis Oils by Flash Evaporation and Direct, Molecular-Beam Mass Spectrometry", *Energy from Biomass and Wastes VIII*, (Klass, ed.) Lake Buena Vista, Fla., Jan 30, 1984, (IGT, 1984).

5. Evans, R. J., Milne, T. A. and Soltys, M. N. "Fundamental Pyrolysis Studies", *Proceedings of the 16th Biomass Thermochemical Conversion Contractors'Meeting,* Portland, Ore May 8, 1984, PNL-SA-12403, 1984.

6. Evans, R. E. and Milne, T. A., "Molecular Characterization of the Pyrolysis of Biomass. I Fundamentals" *Energy and Fuels* Vol. 1, 1987.

7. Antal, M.J.,Jr. "The Effects of Residence Time, Temperature and Pressure on the Steam Gasification of Biomass," *ACS Symposium Biomass as a Nonfossil Fuel Source,* Honolulu Meeting, 1 April 1979. See also Antal, M. J., Jr., "Biomass Pyrolysis: A Review of the Literature, Part I - Carbohydrate Pyrolysis", *Advances in Solar Energy,* ed K. W. Boer and J. A. Duffie, American Solar Energy Society, Boulder, CO Vol. 1, pp 61-112 (1982).

8. Diebold, J. P., *The Cracking Kinetics of Depolymerized Biomass Vapors in a* Continuous Tubular Reactor*, Master's thesis, Colorado School of Mines,* Golden, CO 1985.

9. Reed, T. B., Levie, B., Scahill, J., Evans, R. and Milne, T., "Moving-Bed Air and Oxygen Biomass Gasification", *Proceedings of the 1985 Thermochemical Conversion Contractors' Meeting,* (Oct 15, 1985), PNL-SA-13571, Richmond WA: Pacific Northwest Laboratory, Feb. 1986.

10. Reed, T. B., Markson, M. and Graboski, M. "The SERI High Pressure Oxygen Gasifier", *Biomass-to-Methanol Specialists Workshop,* Tamarron, CO 3-5 March 1982, ed by T. B. Reed and M. Graboski, SERI/CP-234-1590 (Solar Energy Research Institute, Golden, CO 1982)

11. Desrosiers, R., *Fundamental Air Gasification Engineering Parameters,* SERI/PR-234-1470, (February 1982). *Also Gasification Engineering--Quarterly Report,* SERI/PR-622-1348, (December 1981) and SERI/PR-622-1153 (April 1981).

12. Chern, Shyh-Ming, *The Gasification of Biomass in Commercial Downdraft* Gasifiers, *Masters Thesis, Kansas State University, 1985.*

13. Wallawender, W. P., Chee, C. S. and Fan, L. T., "Operating Parameters Influencing Downdraft Gasifier Performance", *Symposium Papers, Energy from Biomass and Wastes XII,* Institute of Gas Technology, Chicago, 1987.

14. Strub, A., "The Commission of the European Communities R & D programme 'Energy from Biomass'", *Thermochemical Processing of Biomass* , A. V. Bridgwater, Ed., Butterworths, London (1984).

15.Selected papers on the results of the programs described are found in the proceedings of the conference *BioEnergy '84, Proceedings of a World Conference,* Goteborg, Sweden, June 21, 1984, edited by H. Egneus and A. Ellegard. Elsevier, London, 1985.

16. Beenackers, A.A.C.M.and van Swaaij, W.P.M.,"Advanced Gasification:Methanol Production from Wood - Results of the EEC Pilot Programme", Vol 8, Series E in *Energy from Biomass,* D. Reidel Co., Boston (1986).

17. Ekstrom, C., Lindman, N. and Petersson, R., "Catalytic Conversion of Tars, Carbon Black and Methane from Pyrolysis/Gasification of Biomass", *Fundamentals of Thermochemical Biomass Conversion*, ed Overend et al, Elsevier, London, 1985.

18. Strom, E. et al, "Gasification of Biomass in the Mino Process", *Bio-Energy '84,* H. Egneus, Ed., p. 57, Vol 3 (Elsevier, 1985).

19. Black, J. W. *Evaluation of Reforming as a Practical Technology for Elimination of Water Pollution from Wood*, ENFOR Project No. C-166Z, DBC Engineering Research Ltd., Markham, Ontario, Canada, Oct. 1983.

20. D'Eglise, X. et al "Wood Tar Cracking in Gasifiers: Kinetic Data", *Proceedings of Forest Products International Symposium* Vol. 5, CSIR, Pretoria, South Africa, p. 13-12 (1985).

21. Morita, Y. "Calcined Dolomite", *J. Japan Petrol. Inst.* Vol. 21, 1978 p. 1.

22. Mudge, L. K. et al "Catalytic Generation of Methanol Synthesis Gas from Wood", *Proc.Biomass To Methanol Specialists Workshop,* Ed. T. Reed, Durango, CO March 3, 1982; SERI/CP-234-1590.

CHAPTER 7

CHEMISTRY AND THERMODYNAMICS OF GASIFICATION

7.1 CHEMISTRY OF BIOMASS COMBUSTION AND GASIFICATION

7.1.1 Composition of Biomass, Charcoal and Pyrolysis Oil

The chemistry and thermodynamics of biomass thermal conversion processes have generally been considered to be closely related to those of coal and many books on biomass merely quote the conventional results for coal. Only recently have the basic scientific properties of biomass been considered separately from coal. The reader is referred to some of these works for a more complete treatment (1-7).

Reactions of solid fuels are more difficult to describe than reactions of liquids and gases, in part because solids have a wide range of composition. Fortunately, the range of chemical variation and energy content for most biomass is quite small when given on a moisture- and ash-free basis. For purposes of discussion, some approximations must be made.

The measured compositions of a variety of biomass species, of charcoals and pyrolysis oils are given in Table 7-1. The compositions are expressed in weight percent, atomic percent and as a ratio formula. The heats of combustion of the various species are also given. These will be discussed below.

In making calculations on gasification reactions, it is necessary to convert the weight fraction found by analysis to a molecular formula. An average formula for wood can be expressed by the ratio formula $CH_{1.4}O_{0.6}$. The theoretical equivalent formulas for cellulose and lignin are $CH_{1.66}O_{0.83}$ and $CH_{1.23}O_{0.36}$ respectively. This type of representation is convenient for writing chemical reactions.

The compositions of various fuels can be shown graphically in relation to conversion processes in the ternary diagram of Fig. 7-1. The figure also shows the wide variation of char compositions, overlapping the composition (but not the physical structure) of coals. Chars formed below 800 C have a significant hydrogen and oxygen content.

The principal chemical elements contained in all fuels--carbon, hydrogen and oxygen--are shown as the vertices of a triangle. The elemental compositions of some biomass, coal, and char samples are plotted in the figure where the hatched areas define the practical range of variation of these solid fuels.

In this diagram, **synthesis gas (CO plus H_2)** and **producer gas (CO plus H_2 plus N_2)** lie on or to the right of the line defined by the composition CO and H_2. At temperatures above 1100°C, only CO and H_2 are stable. However, at lower temperatures, CH_4 and other hydrocarbon gases become stable and CO becomes unstable, so there is no exact position for the line separating gaseous fuels from other fuels unless thermodynamic and kinetic conditions are specified. Hydrocarbons, alcohols and other liquid fuels lie in the upper left half of the diagram with H/C ratios generally >1.

Table 7-1. Analyses and Heats of Combustion of Biomass, Charcoals and Pyrolysis Oils[a]

NAME	Temp o C	REFERENCE[b]	COMPOSITION c-h-o basis, Wt% c	h	o	HEAT OF COMBUSTION Measured HHV-kJ/g	Calculated[c] HHV-kJ/g	ERROR (Meas-Calc) Meas
BIOMASS COMPONENTS								
Cellulose (Avicel)		Mok et al	43.3	6.3	50.4	NA	17.14	NA
Lignin (Indulin)		Mok et al	66.8	5.5	27.7	NA	26.77	NA
BIOMASS								
Pine sawdust		Diebold	51.3	6.0	42.7	20.21	20.40	0.009
Maple		Tillman	51.5	6.1	42.4	20.28	20.59	0.015
Douglas Fir		Tillman	52.8	6.4	40.9	21.22	21.56	0.016
Paper		Survey	46.4	6.2	47.4	18.82	18.41	0.022
Maritime Pine		Bourgeois	52.6	6.2	41.2	20.59	21.23	0.031
Chestnut & Oak		Bourgeois	50.1	5.6	44.3	19.20	19.27	0.004
"Typical biomass"		Reed	52.2	6.1	41.7	NA	20.89	NA
					Avg abs error			0.015
PRIMARY OILS								
Primary Oils R 35CS		Diebold	54.5	5.7	39.8	20.3	21.44	0.055
Primary Oils R 40CS		Diebold	57.6	5.9	36.5	22.9	23.11	0.010
Primary Oils R 40PS		Diebold	57.1	5.6	37.2	22.3	22.53	0.011
Poil popler77% yield	500	Scott	55.2	6.1	38.8		22.28	
					Avg abs error			0.026
CHARS								
Torrefied Pine	280	Bourgeois	60.8	5.7	33.5	23.90	24.30	0.017
Torr. chestnut & oak	275	Bourgeois	57.8	5.3	36.9	22.70	22.36	0.015
Charcoal		Tillman	84.8	3.3	11.9	32.81	31.85	0.029
Fir Bark Char		Survey	63.6	5.1	31.3	24.49	24.75	0.011
Grass Straw Char		Survey	68.5	5.0	26.5	25.93	26.82	0.035
Rice Hull Char		Survey	71.6	5.2	23.3	28.18	28.50	0.011
Redwood Charcoal	549	Survey	77.7	3.4	18.9	29.62	28.75	0.029
Oak Charcoal	571	Survey	78.6	2.6	18.9	28.02	27.96	0.002
Oak Charcoal	641	Survey	80.1	2.8	17.0	29.32	29.07	0.008
Redwood Charcoal	941	Survey	82.5	3.7	13.8	31.88	31.37	0.016
FP Char, Run 53	625	Diebold	87.7	3.8	8.4	34.40	33.98	0.012
FP Char, Run 338-1	880	Diebold	92.6	1.9	5.5	33.42	33.47	0.002
					Avg Abs error			0.021
SECONDARY TARS								
Sec Tars - Run 56	730	Diebold	85.4	5.0	9.6	34.08	34.60	0.015
Sec Tars - Run 59	825	Diebold	79.3	5.9	14.8	33.92	33.09	0.024
					Avg abs error			0.025

Notes: (a) From Reference [8]

(b)Based on IGT/Dulong formula [9]:

$HHV = \Delta h_c = 0.341\ c + 1.322\ h - 0.12(o + n) - 0.0153\ a + 0.0686\ s$ kJ/g

$HHV = 14658\ c + 56878\ h - 5153\ (o + n) - 658\ a + 2945\ s$ Btu/lb

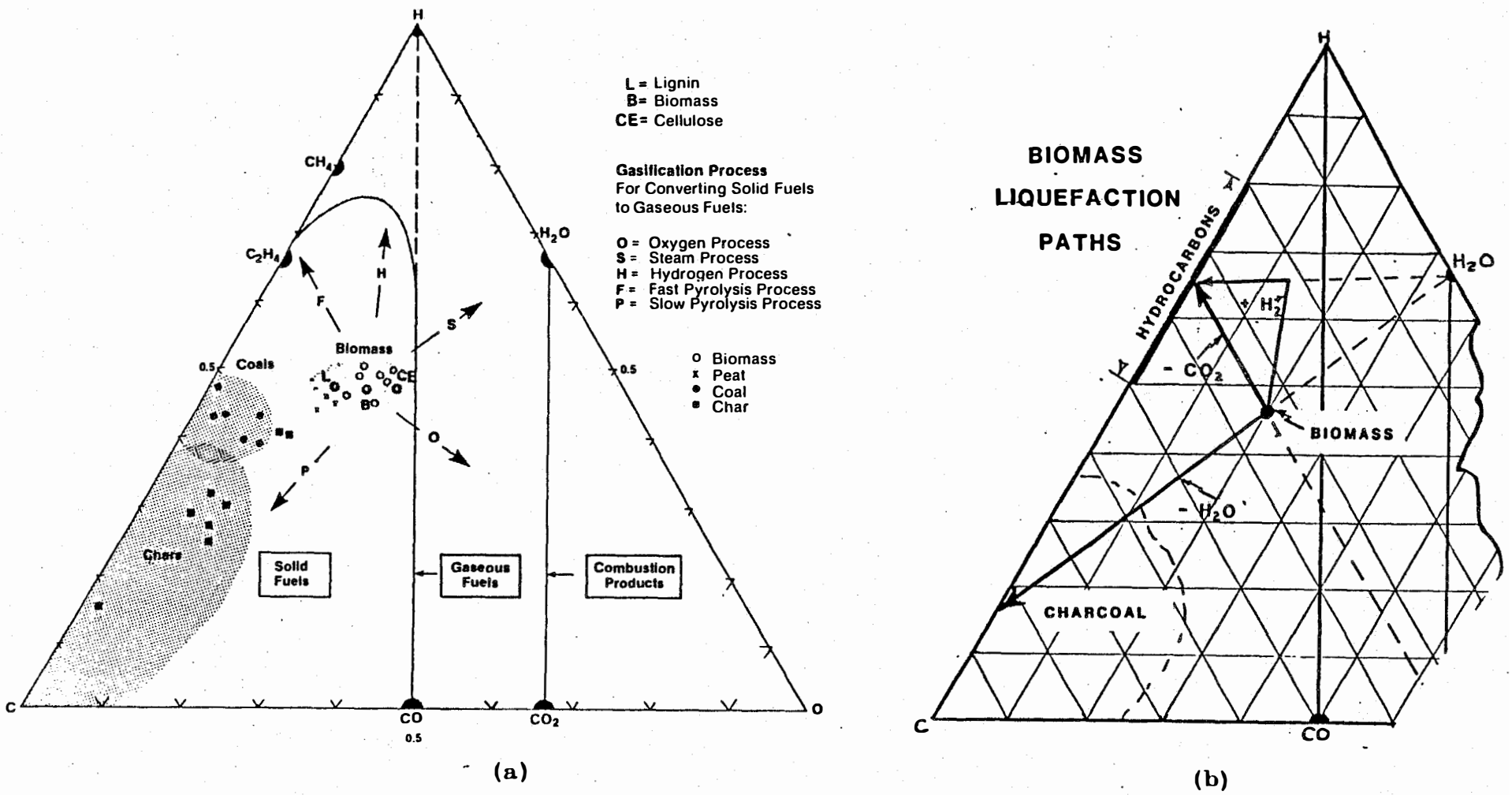

Figure 7-1. (a) Ternary diagram showing mole fraction of C, H and O in various solid and gaseous fuels. Position of the solid fuels coal, char, biomass and peat indicated at left; the synthesis gas line H_2-CO at center; the combustion line H_2O-CO_2 at right. (b) Portion of diagram showing route of primary pyrolysis to charcoal, oil, water and gas as well as secondary cracking of oil to hydrocarbon gases.

7.1.2 Biomass Thermal Conversion Reactions

The products of complete combustion lie on the line connecting CO_2 and H_2O. Combustion with oxygen or air then can be represented by the arrow O joining the fuel and oxygen and ending on this line. Final compositions to the right of this line represent combustion with excess air or oxygen. Compositions slightly to the left represent incomplete combustion.

Pyrolysis is the disproportionation of biomass to yield char (arrow P), gases and oil as shown in Fig. 7-1 (b). Pyrolysis starts at about 250°C and is essentially complete by 500°C. Combustion and char gasification occur at higher temperatures. Therefore, pyrolysis is a fundamental step in all high temperature processes, combustion, gasification and pyrolytic gasification.

Gasification can be defined chemically as any reaction that shifts the composition of the solid fuels on the left side of Fig. 7-1 (a) along one or more of the arrows to a gaseous composition. Oxidative gasification processes use air or oxygen to move along the arrow marked O to shift primarily to gases rich in CO and H_2. Oxygen/air gasification is mechanically the simplest method of producing gas because the overall reaction can be exothermic if some CO_2 and H_2O are also formed. The majority of gasifiers use this method, and in this work "gasification" will be used to mean oxidative gasification unless otherwise specified.

Pyrolytic gasification uses an external heat source to pyrolyze biomass and crack the oxygenated oil vapors to hydrocarbon gases, plus CO and H_2. The resulting gas then has a relatively high energy content. However, it is necessary to use an external heat source and a heat transfer medium to supply the heat of reaction [10-13].

Steam can be used alone for biomass gasification, producing a gas high in methane as indicated by the arrow S. The temperature of operation must be kept relatively low to favor the equilibrium, and so, long residence times or the use of catalysts is required [13]. Pyrolytic gasification and steam gasification will not be discussed further in this report.

The stoichiometric combustion of biomass with oxygen (or air) for combustion purposes can be ideally represented by:

$$CH_{1.4}O_{0.6} + 1.05\ O_2 \text{--->} CO_2 + 0.7\ H_2O \qquad (7\text{-}1)$$

Gasification can be thought of as incomplete combustion. An "ideal gasification" using a minimum about of oxygen would be represented by

$$CH_{1.4}O_{0.6} + 0.2\ O_2 \text{---->} CO + 0.7\ H_2 \qquad (7\text{-}2)$$

Unfortunately, this reaction is about 20 kJ/mole endothermic at 800 C, so that external heat would have to be added to the system to accomplish this "ideal gasification."

Adiabatic gasification converts biomass to fuel by a partial internal combustion using oxygen in excess of the ideal amount according to, for instance,

$$CH_{1.4}O_{0.6} + 0.45\ O_2 \text{--->} 0.7\ CO + 0.3\ CO_2 + 0.55\ H_2 + 0.2\ H_2O \qquad (7\text{-}3)$$

(The exact amount of oxygen used and the products formed depend on final temperature, heat loss, water content, and the degree of approach to equilibrium. See discussion below.) Note that in this case almost a third of the carbon and hydrogen have been burned to CO_2 and H_2O to supply the heat for the reaction, so that reaction (7-2) requires no external heat input. Variations of this reaction form the basis of all oxygen/air gasifiers, and provide for high efficiency and mechanical simplicity since no external heat is required. However, the energy content of the gas is lowered by the presence of CO_2 and H_2O. If external heat can be supplied, less biomass is consumed. (A gasification process using an electrically heated pyrolysis zone is being developed in Brazil [14]).

The reactions (7-1) and (7-3) represent the overall "global" reactions of gasification or combustion, but in practice the reactions occur in several steps, since biomass must undergo pyrolysis to vapor and charcoal before oxygen can contact these materials.

7.1.3 Thermochemistry of Biomass Compounds

The measured heats of combustion for the various biomass and related materials are shown in Table 7-1. These are useful for calculating the energies required for various reactions since the energies are additive.

Values of the heats of combustion are also shown, calculated from the modified IGT equation

$$\Delta h_c = 0.341c + 1.322h - 0.12(o + n) - 0.0153a + 0.0686s \text{ kJ/g} \qquad (7\text{-}4)$$

where Δh_c is the high (gross) heat of combustion, c, h, o, n, a, and s are the weight fractions of carbon, hydrogen, oxygen, nitrogen, ash, and sulfur respectively.

This formula was originally derived for coal [9], but was used by Graboski to estimate the heats of combustion for biomass materials [2]. He found that the agreement between measured and calculated values for biomass was within 1%-2%, probably within the experimental error for single measurements. It is seen in this table that the error is quite low for the other biomass derived of the materials in Table 7-1 as well.

A large collection of "Thermodynamic Data for Biomass Conversion and Waste Incineration" has been recently published by SERI and the ASME [8]. This compilation of materials lists thermochemical properties for over 700 materials from alfalfa seeds to sandbar willow. A casual examination would suggest that the heat of combustion of biomass materials varies from as low as 2.8 to more than 25 J/g. This variation is largely illusory because samples have as high as 82% moisture. When calculated on a moisture- and ash-free basis, the heats of combustion have a variation similar to that shown in Table 7-1.

7.2 THERMODYNAMICS OF BIOMASS GASIFICATION

7.2.1 Value of Thermodynamic Calculations

Thermodynamics is the "Sybil" of biomass high temperature conversion. Like the original Sybils, Thermodynamics only speaks the truth, but often one can

only understand the prophecy after hard experience or when it is too late.

Thermodynamics cannot predict the course and products of all possible reactions in a given situation, but it does limit possible pathways and products and prevents us from attempting the impossible. Thus it is useful for understanding old and new processes, and in the case of downdraft gasification, comes close to predicting the final gas composition. In this chapter we will discuss several important concepts in gasification: The role of oxygen/fuel ratio in determining the degree of gasification and the role of carbon saturation in determining the final gas composition.

7.2.2 Thermodynamic Calculation of Gasification Temperature and Gas Composition

For any chemical reaction,

$$aA + bB + \ldots \longrightarrow mM + nN + \ldots \qquad (7\text{-}5)$$

the equilibrium constant K is given (for ideal gases) by

$$K = p_M{}^m . p_N{}^n / p_A{}^a . p_B{}^b \qquad (7\text{-}6)$$

where p_A is the partial pressure of gaseous component A etc. and a etc. is the number of moles of component A. Thus a value of $K_p \gg 1$ indicates that the reaction proceeds to completion as written; a value of $K_p \ll 1$ indicates that very little reaction occurs; a value close to 1 indicates that the reaction proceeds only partially.

The equilibrium constant is calculated in turn from the standard Gibbs free energy of reaction ce, $\Delta G_R{}^\circ$, by

$$\Delta G_R{}^\circ = - RT \ln K_p \qquad (7\text{-}7)$$

These equations, combined with the molar balance equations and the total pressure equation, provide a set of equations that can be solved to give the partial pressure of each component for a specified total pressure and temperature. For low order equations, they can be solved explicitly, but for higher order equations they are generally solved numerically.

The principal reactions of C, H, and O to make producer gas at high temperatures are listed with numerical values for the free energy and equilibrium constant in Table 7-2. The data have been taken from the JANAF Thermochemical Tables [7] and fitted to a linear equation for ΔG over the region 800°-1600°K. (The formulas for ΔG use the effective values of ΔH and ΔS listed over this range. This simplifies calculations for these reactions. Greater precision for free energy data is not justified by the accuracy of the original measurements [16,17]).

Table 7-2. Thermodynamics of Gasification Reactions

Reaction Name:	Boudouard[a]	Steam Carbon	Steam Reforming	Water Gas Shift[b]
Reaction	$C+CO_2 \rightarrow 2CO$	$C+H_2O \rightarrow CO+H_2$	$CO+3H_2 \rightarrow CH_4+H_2O$	$CO+H_2O \rightarrow CO_2+H_2$
ΔG_r(kJ) =	170.72 - 0.175T	135.9 -0.143T	-225.6 + 0.252T	-34.83+0.0328T

Temperature K	C	$K_p=p_{CO}^2/p_{CO_2}{}^{2M}a_c{}^c$	$K_p=p_{CO}p^2/p_{H_2O}a_c$	$K_p=p_{CH_4}p_{H_2O}/p_{H_2}{}^3Mp_{CO}$	$K_p=p_{CO}p_{H_2O}/p_{CO_2}p_{H_2}$
800	527	0.0099	0.0394	36.9	3.639
900	627	0.171	0.382	0.852	2.033
1000	727	1.673	2.349	0.042	1.277
1100	827	10.8	10.4	3.54E-03	0.872
1200	927	51.3	35.8	4.54E-04	0.635
1300	1027	191.3	102.2	7.96E-05	0.485
1400	1127	591.2	250.8	1.79E-05	0.386
1500	1227	1571.9	546.3	1.59E-06	0.265
1600	1327	3698.4	1079.5	4.92E-06	0.316

Notes:
(a) Linearized fit of data in the region 800<T<1600K to the equation $\Delta G_R = \Delta H_R - T\Delta S_R$. The Constants are the effective values of ΔH and ΔS in this range.
(b) This data can be derived from the first three reactions and is not mathematically independent. It is included here for convenience.
(c) The activity of solid carbon is generally taken as 1.

The pressure equilibrium constant for each of these reactions, K_p, calculated from the free energy data, is tabulated in Table 7-2 as a function of temperature. The values shown here are based on the most recent thermodynamic data available, [15-17] but differ only slightly from those published more than 30 years ago [1].

The free energy change for the gasification reactions are plotted in Fig. 7-2. Here it is seen that all the reactions cross the line $K_p=1$ between 1000 and 1200K, indicating that major changes in composition at equilibrium can be expected for small changes in temperature in this range, but that above or below these temperatures only minor changes in composition will occur.

7.2.3 Calculation of "Adiabatic Reaction Temperature"

The "adiabatic reaction temperature," T^*, is a very important concept in gasification. In effect it is the temperature that the reaction would produce if it came to equilibrium and there were no heat losses. It is evaluated by solving the energy balance

$$-\Delta H_c = \sum_{i=1}^{n} n_i \int_{T_o}^{T^*} c_i \, dT - \sum_{i=1}^{n} n_i \, \Delta H_{c,i} - n_w \Delta H_w \qquad (7\text{-}8$$

for T^*, where ΔH_c is the standard heat of combustion of the biomass, $\Delta H_{c,i}$ is the standard heat of combustion of the ith fuel gas component formed in gasification, and c_i is the heat content of the ith component. (n_i is the number of moles of the ith product, c_i is the heat capacity of each component, n_w is the number of moles of water (or other condensed materials) formed, and

ΔH_w is the heat of combustion of water.) Unfortunately, T* is an implicit variable and must be determined by iteration. Evaluation of T* and gas composition would be a tedious process without a computer. Methods of solution are discussed by Gumz and others [1-4]. Some values for the thermodynamic data can be taken from Tables 7-1 and 7-2. Heat capacity and other data can be found in Refs 15-17.

The equilibrium reaction temperatures and gas compositions for wood of varying moisture content were first calculated by Gumz and his results are shown in Table 7-3 [1]. The magnitude of the gas compositions calculated agree quite well with the observed gas compositions measured in downdraft gasifiers and more recent calculations [2-4,18,19].

Table 7-3. Gumz Calculation of Wood-Gas Composition[a]

Moisture %	0	10	20	30
Net heating value (kJ/kg)	18540	16440	14330	12230
Reaction Temp. C	661	631	600	555
		Gas Analysis (wet)		
CO	21.0	16.5	12.0	6.8
CO2	10.0	12.7	15.2	17.9
H2	18.2	18.7	18.9	17.5
H2O	4.7	6.7	9.4	13.7
CH4	0.7	1.1	1.7	2.7
N2	45.5	44.3	42.7	41.5
Gas Net Heating Value (kJ/Sm³)	4860	4480	4150	3710

(a) From Ref. [1].

The "equivalence ratio", Φ, is a very important concept in measuring the degree of pyrolysis, gasification, and combustion. The mass oxidant/fuel ratio controls the degree to which the fuel is oxidized. However, the specific value of this ratio depends on the composition of the fuel, moisture content, etc. so it is not possible to write chemical equations using a mass basis. For purposes of discussion the equivalence ratio is defined as the ratio of the amount of oxidant used to that required for complete combustion.

We will see that an equivalence ratio of 1 corresponds to stoichiometric combustion; a Φ of about 0.25 corresponds to gasification and a Φ of 0 corresponds to pyrolysis. We could not make such a general statement about the corresponding mass oxidant/fuel ratio. Complete combustion requires 1.05 moles of oxygen for each mole of biomass, so the number of moles for gasification can be found by multiplying the equivalence ratio by 1.05. Complete combustion requires mass ratio of 1.47 for O_2 or 6.36 for air for each mass of a typical biomass. The mass ratio is then found from the equivalence ratio by multiplying by these ratios.

Several computer programs have been written to explore more fully the equilibrium energy relations of the equations in Table 7-2. Desrosiers has presented data for a wide variety of conditions using oxygen, air and steam [2]. The adiabatic reaction temperature of biomass with oxygen or air is shown in Fig. 7-3. as a function of equivalence ratio Φ. The equilibrium compositions associated with these temperatures are shown in Fig. 7-4. The energy contents of the gas and char are plotted in Fig. 7-5. The low heating value for dry equilibrium gas produced by air or oxygen gasification is shown

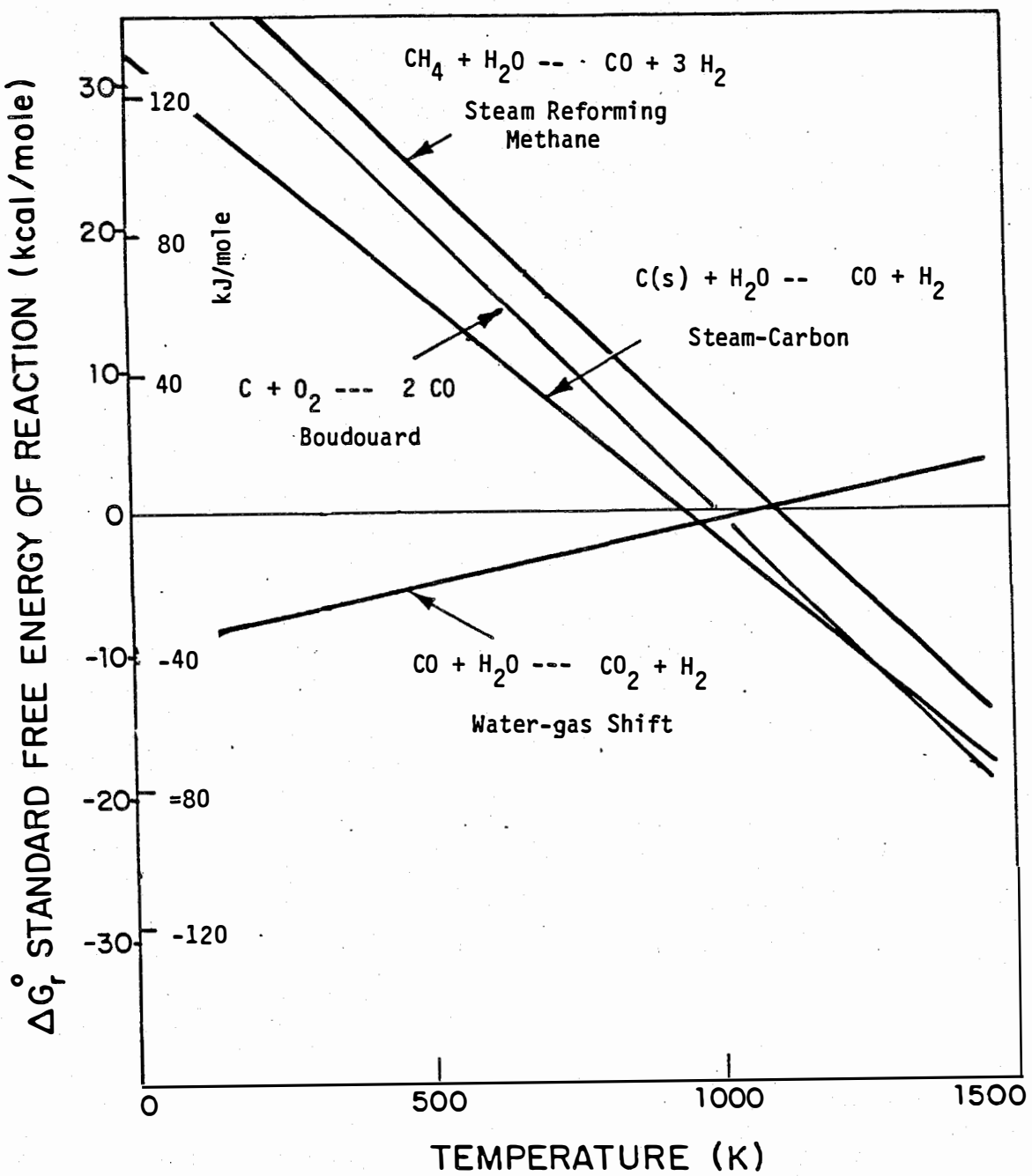

Figure 7-2. Free Energy of Gasification Reactions

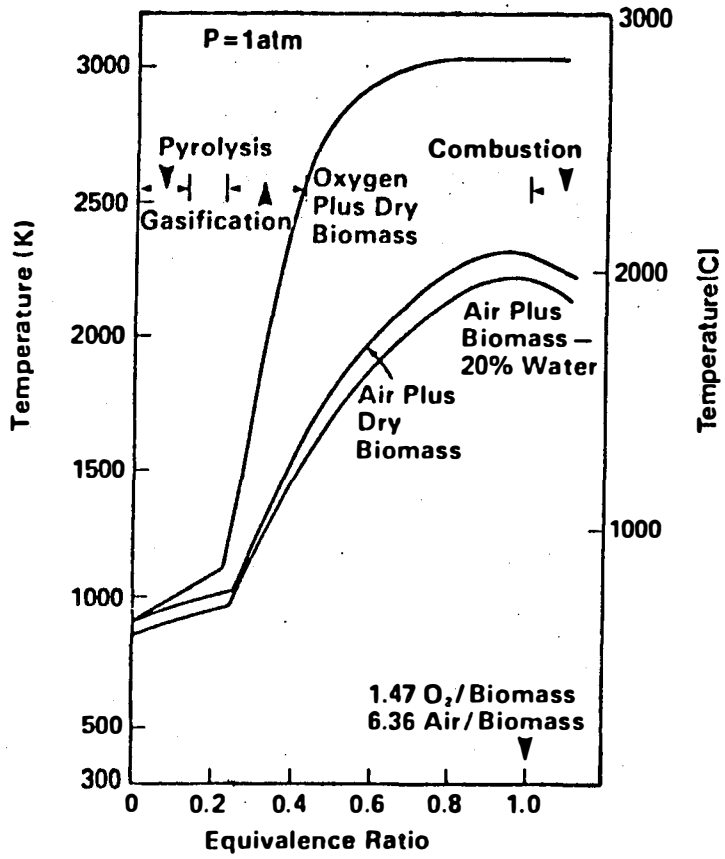

Biomass Adiabatic Reaction Temperatures

Figure 7-3. Biomass adiabatic reaction temperatures, showing pyrolysis, gasification and combustion regions as a function of equivalence ratio ϕ

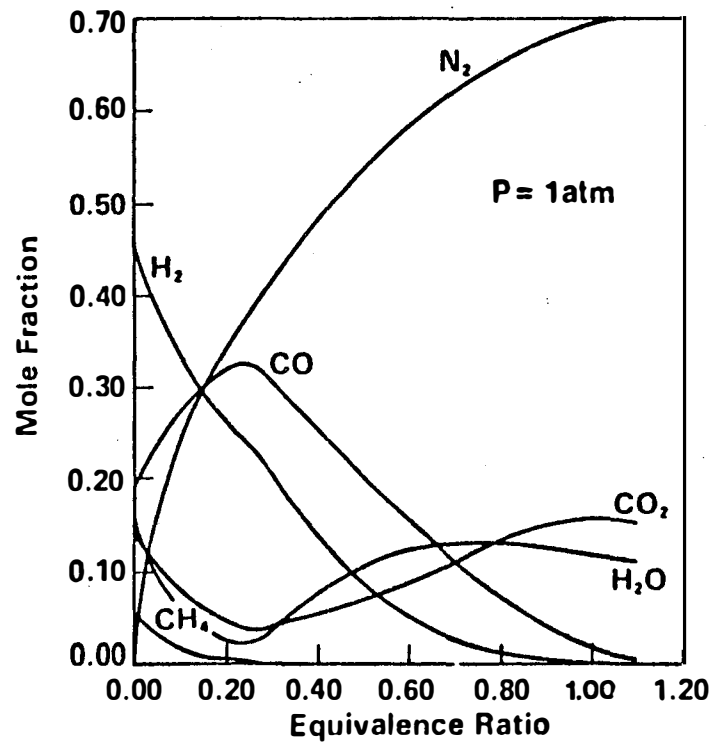

Equilibrium Composition for Adiabatic Air/Biomass Reaction

Figure 7-4. Equilibrium gas composition for adiabatic air-biomass equilibrium

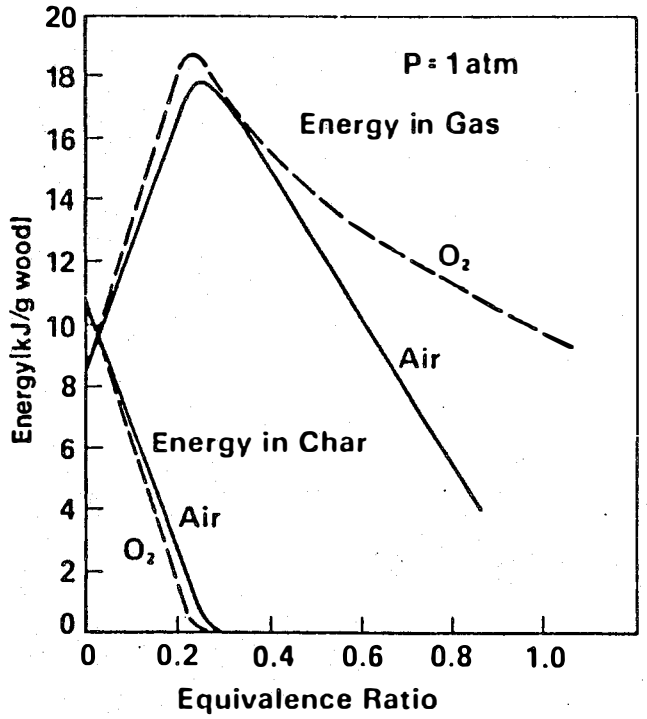

Figure 7-5. Gas and char energy content for oxygen and air-biomass equilibria

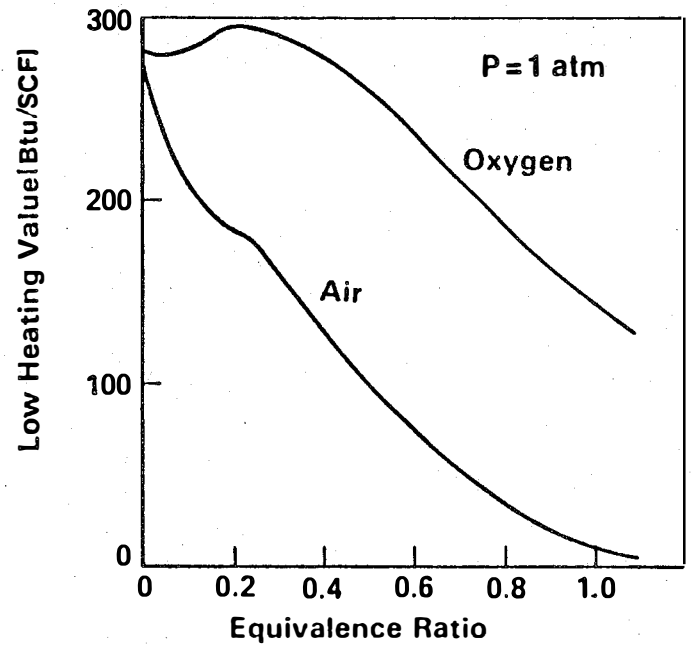

Figure 7-6. Low Heating Value for dry equilibrium gas for air/O_2 - Biomass reaction.

in Fig. 7-6.

The distinction between **pyrolysis, gasification,** and **combustion** is easily seen in Figs. 7-3 to 7-6. **Pyrolysis** is the destructive breakdown of biomass in the absence of oxygen, and so would be represented by $\Phi = 0$. Note in Fig. 7-4 that if pyrolysis can bring biomass to equilibrium, a gas rich in methane results. However, as shown in Fig. 7-1 and 7-5, the composition of biomass does not contain sufficient hydrogen or oxygen to produce all gas, so pyrolysis alone also produces a sizable fraction of charcoal as shown in Fig. 7-5.

In **downdraft gasification** the hot gases pass through a bed of hot charcoal before leaving the gasification zone. This establishes an approach to equilibrium between the gas and carbon at about $\Phi = 0.25$ and temperatures in the range 700°-900°C. Finally, the use of stoichiometric oxidant ($\Phi = 1$) results in complete combustion and temperatures of approximately 2000°C for air combustion and 3000°C for oxygen.

Calculations similar to those of Desrosiers were performed for the oxygen gasifier and are reported in the first oxygen gasifier report [18]. Compositions calculated for a variety of conditions to show the effect of pressure, use of steam, and heat loss are shown in Table 7-4.

Table 7-4 Calculated Equilibrium Gas Temperature and Gas Composition for 5-mm Pellets

Case	P (atm)	Heat Loss (%H_c)a	Steam Rate (Mass Steam)/(Mass Biomass)	Moisture	O_2 Consumption (Mass oxygen)b/(Mass biomass)	Temp[c] °C	Composition (Vol %) CO	CO_2	H_2	H_2O	CH_4
1	1	0	0	3.6	0.352	731	46.2	9.9	37.2	5.5	1.1
2	1	5	0	3.6	0.409	709	42.7	13.3	35.5	7.1	1.3
3	1	0	0	20	0.356	660	29.8	18.2	37.5	11.9	2.5
4	1	10	0.2	3.6	0.436	642	25.9	22.3	34.8	14.1	2.5
5	1	0	0.2	3.6	0.327	672	31.8	16.4	38.5	10.8	2.3
6	10	0	0	3.6	0.358	878	46.2	10.0	32.5	8.3	2.9

(a) From Reference [8]
(b) Calculated dry basis.
(c) Adiabatic reaction temperature.

Compositions measured in the SERI oxygen gasifier are compared to predicted compositions in Table 7-5. These predicted compositions also agree qualitatively with the observed compositions listed in Chapter 3 for oxygen and air downdraft gasification. However, the agreement may be in part fortuitous since it depends on the measured off-gas temperature in the vicinity of the grate. Under conditions of steep gradient and high radiation, the measured off-gas temperature may differ significantly from the effective thermodynamic gas temperature.

Overend has examined these reactions for air and oxygen using the Gumz model over a wide range of conditions, and his results are shown in Fig. 7-7 for downdraft gasification [3]. The work on equilibrium calculations is by no means complete, and it would be desirable to have a universal computer model able to calculate gas compositions simply for a wide range of conditions.

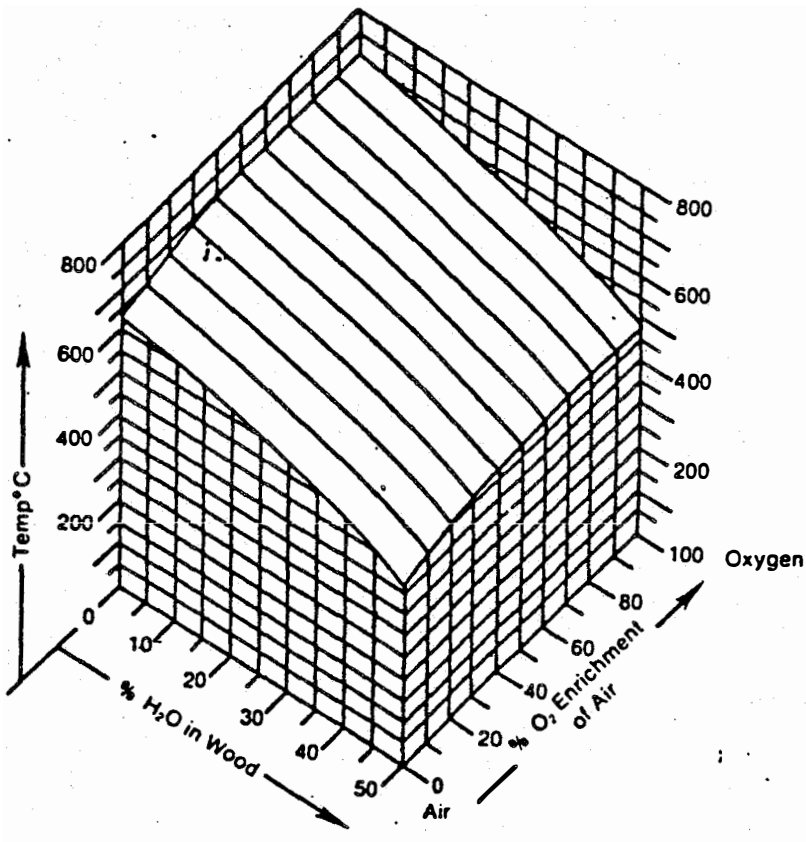

Figure 7-7. Adiabatic reactor temperatures calculated from Gumz model by Overend (Ref 4)

Table 7-5. Comparison of Calculated and Experimental Gas Compositions[a]

	O_2/Fuel Ratio	Temp °C	Composition (vol %) CO	CO_2	H_2	CH_4
Calculated						
0% heat loss	0.339	731	48.9	10.5	39.4	1.2
10% heat loss	0.445	690	42.8	18.4	36.9	1.6
Experimental Run 14A[b]	0.430	800	42.8	19.2	33.3	4.1

(a) From Ref. [19]
(b) Nitrogen free basis

In summary, the results of the above calculations suggest that downdraft gasification produces a gas composition that can come close to the equilibrium values predicted by thermodynamics. Downdraft gasifiers are constrained to operate near the discontinuity of slope at $\Phi = 0.25$ of the curve in Fig. 7-3.

7.2.4 Gasifier Operating Point

A gasifier must supply sufficient oxidant to bring as much solid as possible into the gas phase but to burn as little of that gas as practical and minimize oxygen use. How is it possible to operate a gasifier near this optimum?

The oxygen/fuel or air/fuel ratio or the equivalence ratio Φ at which the gasifier operates is the most important characteristic of a gasifier. However, it is important to understand that Φ is in practice not an independent variable for downdraft gasifiers. It can be measured from a mass balance when the gasifier is in a stable operating mode.

It is seen in Fig. 7-3 to 7-6 that the molar equivalence ratio for complete gasification of dry biomass is about 0.25. Since the mass oxygen/fuel ratio for complete combustion is 1.05, a Φ of 0.25 corresponds to an oxygen/fuel mass ratio of (0.25x1.05) 0.26. The presence of moisture and heat losses can increase this value so that each set of gasifier conditions will have a somewhat different operating point.

In a fixed bed gasifier, operation at low values of Φ would cause charcoal to be produced (as shown for low Φ in Fig. 7-5), and it would build up in the reactor unless it is augered or shaken out. Operation at high values of Φ consumes charcoal, oxygen, and product gas, and the temperature goes up rapidly. At the correct value of Φ, the bed level remains constant.

7.2.5 Downdraft Gasifier Control Mechanisms

The question of gasifier control is intimately bound up with the thermodynamics of the reactions occurring in the gasifier, and a knowledge of this relationship is necessary to understanding the control of various gasifiers. In the Imbert gasifier of Fig. 1-1, air is injected at the interface between the incoming biomass and the charcoal bed. If the char level is too high in the gasifier, the incoming air burns more char and less biomass thus bringing fresh biomass back into the combustion zone. If the char is consumed too fast, more biomass enters the combustion zone and generates charcoal at a higher rate. Thus the Imbert gasifier is self regulating.

The SERI gasifier (Fig. 1-2) has two modes of operation. In oxygen operation the flaming pyrolysis zone is at the top of the bed. It is generally operated with a fixed flow of oxygen,and biomass is added faster or slower to maintain a fixed bed level. Alternatively, biomass could be added at a fixed rate and oxygen flow controlled to maintain constant bed level. When operating with air the flaming pyrolysis zone is generally stable beneath the surface of the incoming biomass. A small fraction of the air can be introduced through rotating nozzles to maintain the zone at the nozzle level. This method is also used in the "Buck Rogers" gasifier [22].

The actual operating point of downdraft gasifiers can be to the left of the theoretical point in Fig. 7-3 if there is char removal or oil production, both of which reduce the oxygen consumption. The operating point can be shifted to the right if the bed is too short or the throughput too high to reach equilibrium.

A gasifier can be operated on purpose at values of $\emptyset$ below the theoretical 0.25 required for gasification by augering charcoal out of the char zone. Since a disproportionate fraction of the oxygen is required to gasify the charcoal, this reduces oxygen consumption. It also produces charcoal--a potentially valuable by-product--and makes a gas with a higher heating value. Such operation is not a true gasification, but should be though of as "gas-charification."

In updraft gasifiers the incoming air passes through the burning charcoal and approaches the charcoal-oxygen equilibrium at the top of the charcoal bed. The pyrolysis step then produces tar vapors at low temperatures, that do not come to equilibrium as they exit the pyrolysis zone. Updraft gasifiers operate at equivalence ratios significantly below $\Phi = 0.25$ because they produce 5%-20% of pyrolysis oil. Pyrolysis oil is similar in composition to unpyrolyzed biomass as shown in Table 7-1, and its production is equivalent to not gasifying some of the biomass.

Fluidized and suspended bed gasifiers are not constrained to operate at the discontinuity of Fig. 7-3, since the rate of feed and the ratio of biomass to oxygen can be varied independently. In this case Φ is an independent variable and must be set, typically by monitoring temperature and flows. This requires an exact control of both oxidant and biomass inputs, typically in time periods of a few seconds. Gas compositions in suspended and fluidized bed gasifiers can approach thermodynamic equilibrium, given sufficient time and temperature.

7.2.6 Kinetic Approach to the Operating Point

It is also important to examine the manner in which various gasifiers approach their operating point. Updraft and downdraft gasifiers are plug-flow reactors so that the reactions occur in sequence. In the downdraft gasifier all of the oxidant is available to burn the pyrolysis oils during the pyrolysis stage, since the gases have not yet reacted with the 10%-25% charcoal formed during the pyrolysis stage. Thus the volatiles are first overoxidized and then re-reduced. The sequence is reversed in an updraft gasifier. The charcoal is overoxidized with consequent high temperatures; then no oxygen is available for combustion of the volatiles.

A fluidized bed gasifier is a well stirred reactor. The oxidant surrounds each particle while pyrolysis is in progress. However, as smaller particles finish pyrolyzing, their char can compete with the remaining particles for available oxidant. Thus tar levels are intermediate to downdraft and updraft gasifiers.

7.3 CARBON-GAS EQUILIBRIUM

7.3.1 The Role of Carbon Saturation in Gasification

The breaks in the adiabatic reaction curves of Figs. 7-3 to 7-6 are caused by the fundamental change in the reaction mechanism because of the disappearance of carbon as a reaction product as oxidant is increased. The break occurs at an equivalence ratio, Φ, that can be called the "carbon saturation point", Φ_s. The variation of the location of this point with temperature produces a "carbon saturation line."

The concept of carbon saturation plays a role of major importance in understanding gasification. For instance, if a gasifier produces a high level of char-ash, the problem can either be thermodynamic or kinetic. If the temperature in the char-ash bed and the equivalence ratio indicate that there is insufficient oxygen to remove more char, the problem is thermodynamic, and more oxygen or higher temperatures must be provided. If they indicate that there is sufficient oxygen to remove char at the temperature of the bed, the problem is kinetic, and the bed can be extended or smaller fuel particles used.

The importance of the role of carbon saturation in gasification is analogous to the importance of the role of water-air saturation in terrestrial events. Just as the psychrometric charts enable us to determine humidity, air-conditioning requirements, weather behavior,etc., the extent of carbon saturation determines whether carbon is formed or consumed under any given thermal processing (combustion, gasification, pyrolysis) condition. A more complete discussion of the methods, calculations, and results are given in Ref. 20.

If a gas in equilibrium with carbon contains both H_2 and O_2, it will have the following dominant species at temperatures above 800K: CO, CO_2, H_2, H_2O and CH_4. (At lower temperatures other gaseous species such as ethane, and propane begin to have significant thermodynamic stabilities of fractions of 1% concentration levels.)

7.3.2 Location of the Carbon Saturation Line

Determination of the gas composition at the carbon saturation line requires the numerical solution of simultaneous linear and quadratic equations that cannot be solved explicitly. They are solved using, for instance, the Newton-Raphson optimization.

7.3.2.1 Equilibrium of Carbon

As an example of these calculations, the equilibrium concentrations of gases containing C, H and O in equilibrium with solid carbon can be calculated as follows. The concentrations of the five species are determined by solving the following five equations:

(Boudouard) $C + CO_2 \longrightarrow 2\ CO$ $\quad K_B = (p_{CO})^2/p_{CO_2}$ (7-9)

(Methanation) $C + 2\ H_2 \longrightarrow CH_4$ $\quad K_M = p_{CH_4}/(p_{H_2})^2$ (7-10)

(Steam-Carbon) $C + H_2O \longrightarrow CO + H_2$ $\quad K_W = p_{H_2}p_{CO}/p_{H_2O}$ (7-11)

$$p_{CO} + p_{CO_2} + p_{H_2} + p_{H_2O} + p_{CH_4} = P \quad (7\text{-}12)$$

$$R_{O/H} = (p_{CO} + 2p_{CO_2} + p_{H_2O})/[2(p_{H_2} + p_{H_2O}) + 4P_{CH_4}] \quad (7\text{-}13)$$

where $R_{O/H}$ is the oxygen/hydrogen ratio in the reactants, and p_i is the partial pressure of the gaseous components.

As an example of the utility of Eqs. 7-9 to 7-13, the equilibrium composition for a mixture of gases with an oxygen/hydrogen = 1 is shown in Table 7-6. From this it is seen that at low temperatures, CO, CO_2, H_2, H_2O and CH_4 are all relatively important components, but that above 1100K, CO and H_2 constitute more than 94% of the total.

7.3.2.2 Equilibrium of Biomass

The same methods can be used to calculate the concentrations of species in equilibrium with carbon in biomass or coal gasification and to find the oxygen or steam needed to just reach this equilibrium. The equation for complete gasification can be written:

$$CH_aO_b + R_{o,s}O_2 + c\ H_2O + (3.76\ R_{o,s})N_2) \longrightarrow$$
$$mCO + nCO_2 + pH_2 + qH_2O + rCH_4 + (3.76\ R_{o,s}N_2) \quad (7\text{-}14)$$

where $R_{o,s}$ and c are the moles of oxygen and steam used to reach carbon saturation and m...r are the moles of each gaseous product. The values of $R_{o,s}$

Table 7-6 C-H-O Equilibrium Composition for R O/H = 1
P = 1 Atm

Temperature °K	°C	Composition (vol %) p_{CO}	p_{CO_2}	p_{H_2}	p_{H_2O}	p_{CH_4}
800	527	6.1	36.0	21.2	30.6	6.5
900	627	22.4	28.4	29.9	16.5	2.9
1000	727	47.0	12.8	32.7	6.1	1.0
1100	827	61.3	3.4	32.9	1.8	0.4
1200	927	65.5	0.8	33.2	0.6	0.2
1300	1027	66.0	0.2	33.2	0.2	0.1
1400	1127	66.3	0	33.2	0	0.1
1500	1227	66.3	0	33.2	0	0

and c are fixed by the requirements:

- o the gas must be in equilibrium with solid carbon
- o no solid carbon remains

To determine $R_{o,s}$ it is necessary first to calculate the relative concentrations m...r for the gas at equilibrium with carbon by solving the equilibrium equations and total pressure equation (7-9) to (7-12). These values are then used in the hydrogen/carbon elemental ratio equation:

$$H/C = (a + 2c)/1 = (2p + 2q + 4r)/(m + n + r) \quad (7\text{-}15)$$

and the oxygen/carbon elemental ratio equation

$$O/C = (b+2R_{o,s}+c)/1 = (m + 2n + q)/(m + n + r) \qquad (7\text{-}16)$$

to calculate $R_{o,s}$ for a specified pressure and steam input. These equations determine a composition corresponding to that of the carbon saturation line.

Sample results for such a calculation are shown for a steam/biomass ratios of 0 for typical biomass in Table 7-7. The heat of combustion of the biomass and gas is also calculated. The equivalence ratio Φ is calculated from the oxygen consumed relative to that required for complete combustion. Carbon saturation lines are shown in Figs 7-8 and 7-9, and in the phase diagram of Fig. 7-10 for the gasification of dry biomass.

Table 7-7 Gas Composition at Carbon Saturation

For the Reaction Equation:

$CH_aO_b + R_{os} \cdot O2 + c\ H2O \text{ ----> } m\ CO + n\ CO_2 + p\ H_2 + q\ H_2O + r\ CH_4$

Input Conditions

Fuel: Typical Biomass — Ultimate Analysis (Wt %, MAF)

			C	H	O
H/C Ratio	a =	1.4	0.522	0.061	0.417
O/C Ratio	b =	0.6	H2O/Fuel ratio = 0		
H2O/C Ratio	c =	0			

H_c = -474 kJ/mole (= -8972 Btu/lb)

Pressure (atm) P = 1

		<----Gas Composition (vol %)----->						
T-°K	T-°C	X_{CO}	X_{CO2}	X_{H2}	X_{H2O}	X_{CH4}	$R_{o,s}$	$\Phi_{o,s}$
700	427	1.2	56.6	8.3	30.7	3.2	0.889	0.855
800	527	6.8	48.7	19.3	22.6	2.6	0.793	0.762
900	627	22.3	31.3	31.1	13.5	1.8	0.589	0.567
1000	727	40.9	11.0	40.7	5.5	1.9	0.347	0.334
1100	827	49.5	2.5	45.8	1.7	0.5	0.236	0.227
1200	927	51.3	0.6	47.4	0.5	0.2	0.209	0.201
1300	1027	51.7	0.1	47.9	0.2	0.1	0.203	0.195
1400	1127	51.7	0.1	48.1	0.1	0.1	0.201	0.193
1500	1227	51.8	0.0	48.1	0.0	0.0	0.101	0.193

Notes: From ref [20]. Mole fractions of species calculated from molar ratios and equilibrium constants, assuming carbon saturation.

*****

Note that in Table 7-1, for no steam input ($H_2O/C = 0$) that at a temperature of 1181°K (by interpolation) or 908°C, the heat of combustion of the gas equals that of the biomass fuel so that this would be the adiabatic reaction temperature in the absence of heat loss or input. The equivalence ratio at this point is 0.206.

A number of calculations of this nature were made to determine the effect of moisture and pressure on the position of the carbon saturation line in biomass gasification. The effect of pressure is shown in Fig. 7-8. The effect of moisture is shown in Fig. 7-9.

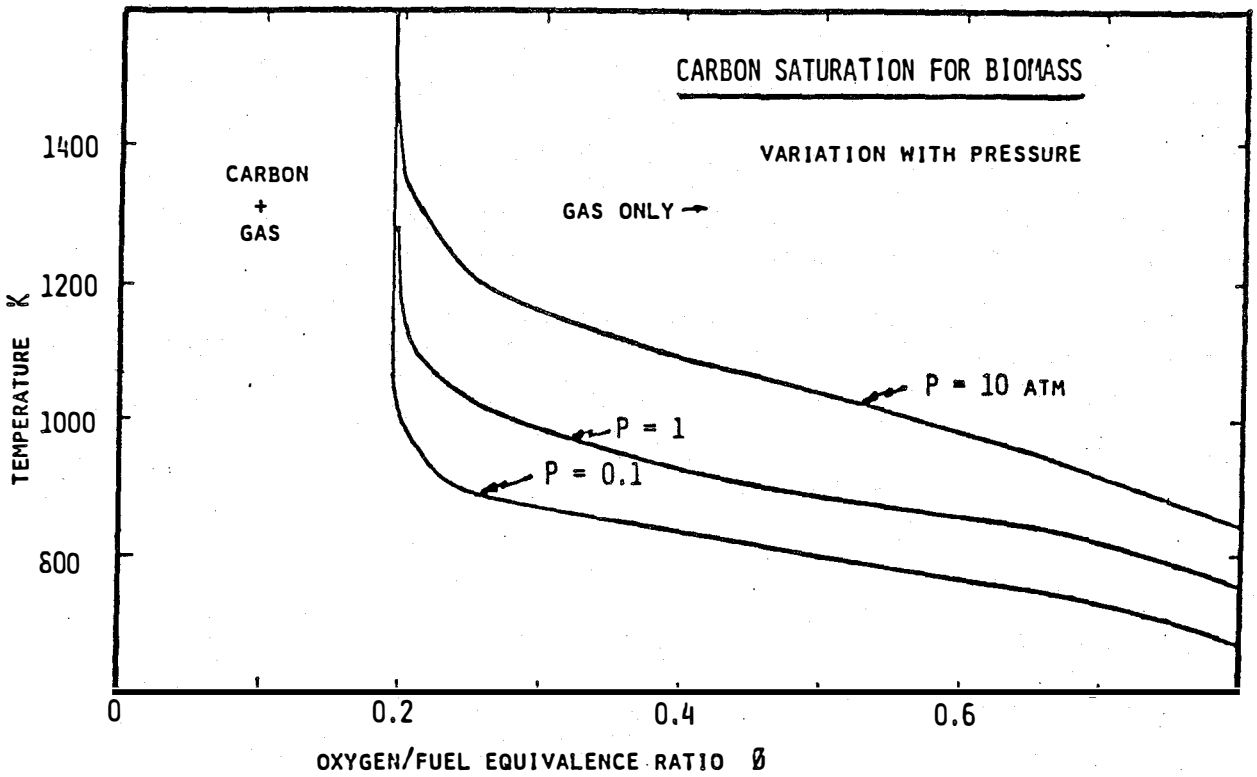

Figure 7-8. Variation of carbon saturation boundary with pressure

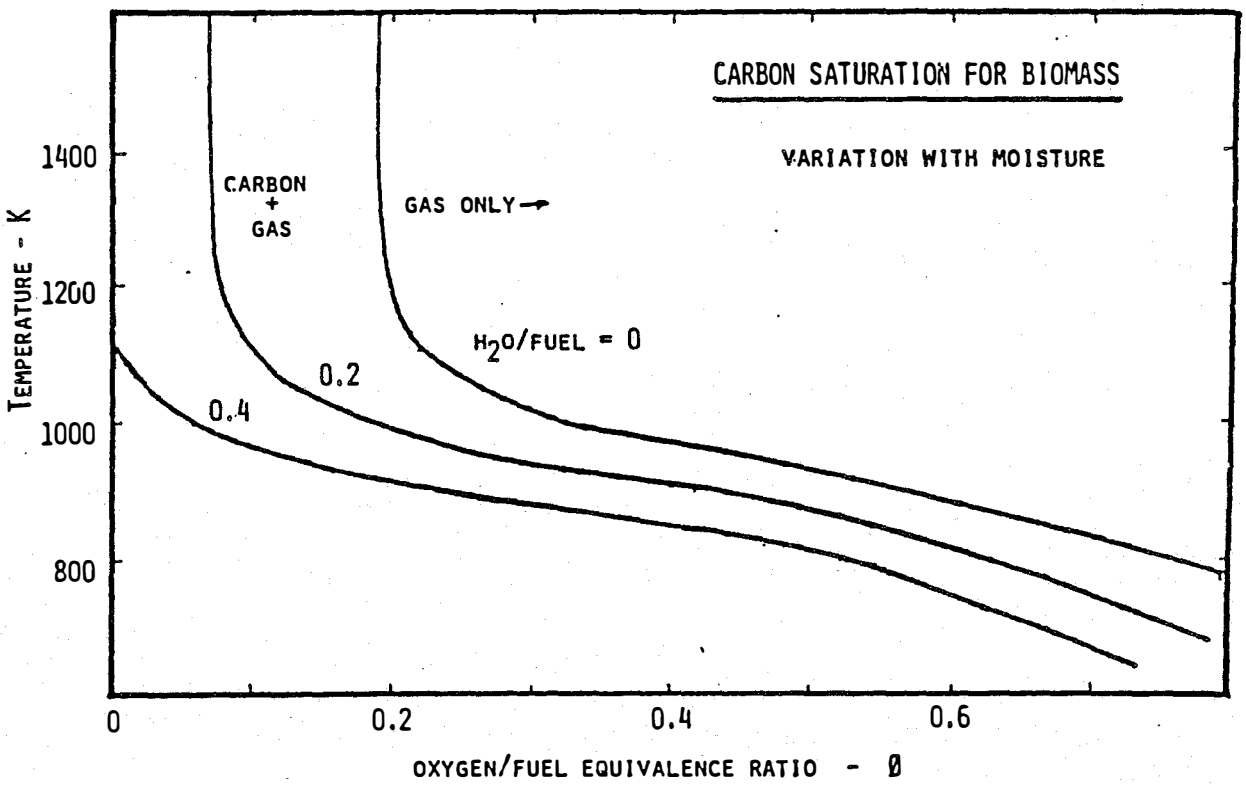

Figure 7-9. Variation of carbon saturation with moisture content

It should be realized that the calculations given above are complementary to those made by Desrosiers and presented in Figs. 7-3 to 7-6. In those calculations a value of ϕ was assumed and the temperature varied to reach equilibrium. In the carbon saturation calculations, it is assumed that carbon is in equilibrium with the gas and the compositions corresponding to this equilibrium are calculated. From these compositions the gas energy can be calculated and the adiabatic reaction temperature or other temperature involving heat loss or gain can be found.

7.3.3 A Pseudo Gas-Char-Oil Phase Diagram for Biomass Pyrolysis/Gasification

We have shown that the operating point of a gasifier can be found by either (1) locating the break in the adiabatic flame temperature calculated as a function of equivalence ratio, or (2) calculating the Φ of the carbon saturation line and the adiabatic flame temperature on that line. A pseudo-phase diagram of gasification can be constructed by combining these two methods of calculation as shown in Fig. 7-10. This diagram shows the adiabatic char gasification line running vertically near the center of the figure. It also shows the adiabatic reaction temperature line intersecting the carbon saturation line at a temperature of 770°C. Regions to the right of the saturation line correspond to a single gas phase. Regions to the left of the line correspond to two phase regions of carbon plus gas.

At low temperatures it is also possible to have non-equilibrium wood oil. This gives a possible three phase region at temperatures below about 700 C, depending on the history of the mixture. However, these tars are not in thermodynamic equilibrium with the gas, hence the designation "pseudo" phase diagram for the gas-char-oil mixture at these temperatures, since a true phase diagram implies a true equilibrium. This diagram shows the effect of changing oxygen equivalence ratios or temperature (by insulation, drying, etc.) at the operating point.

7.4 SUMMARY

In summary, it is necessary to understand the chemistry of biomass gasification to design and operate gasifiers. It is also useful to understand the thermodynamic factors affecting gas composition and the effect of change of these variables on the thermodynamic behavior of the system.

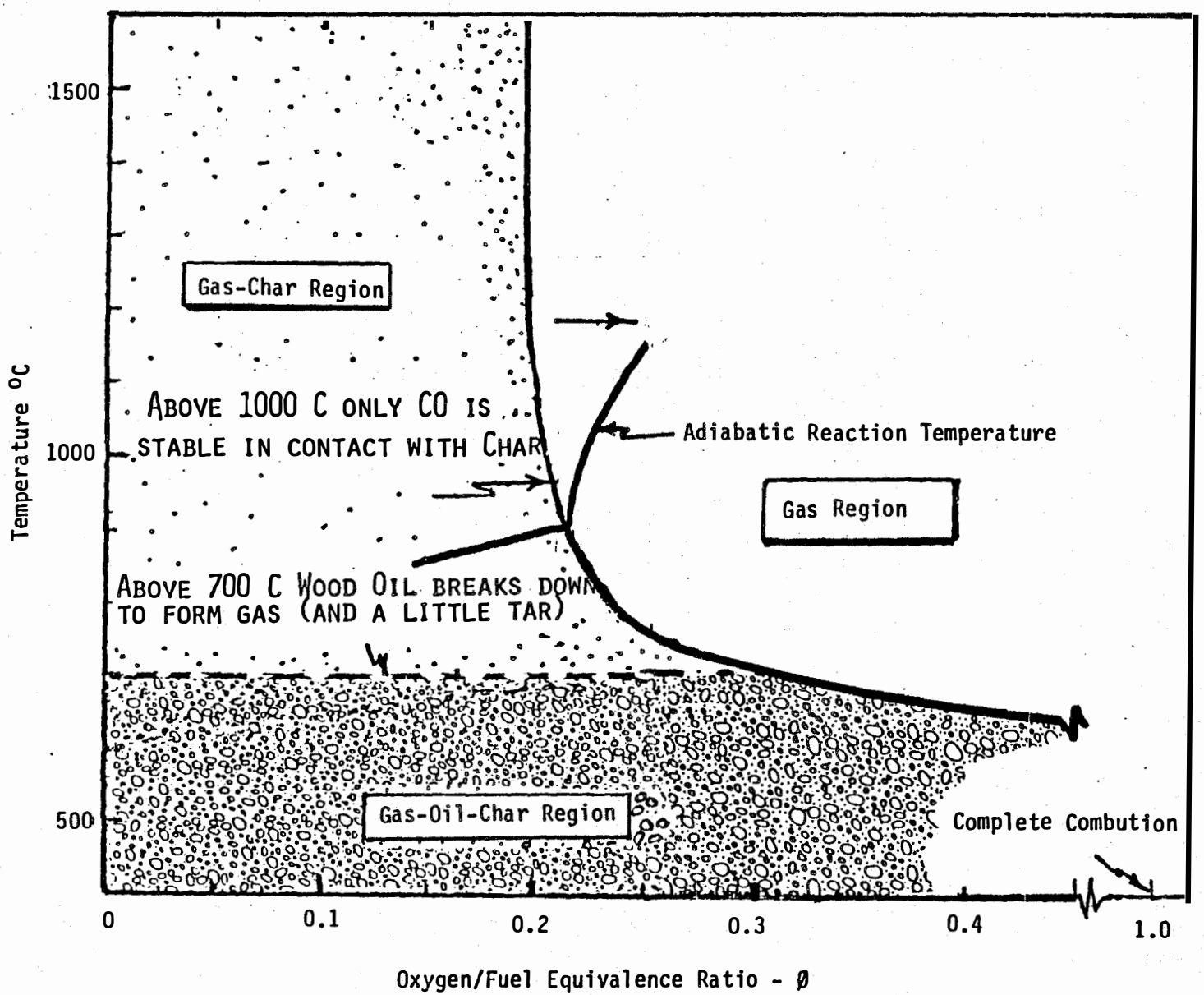

Figure 7-10 Gas-Char-Oil Phase Diagram for Gasification and Pyrolysis, showing Possible Products, Depending on Equivalence Ratio and

REFERENCES

1. Gumz, W., *Gas Producers and Blast Furnaces,* J. Wiley and Sons, New York, 1950.

2. *A Survey of Biomass Gasification, Vol. I-III,* SERI/TR-33-239, edited by Solar Energy Research Institute, Golden, CO, 1979. In particular see chapters by Desrosiers, R., "Thermodynamics of Gas-Char Reactions", and Graboski, M. "Properties of Biomass Relevant to Gasification". These volumes are also published in hard cover as *"Biomass Gasification: Principles and Technology,"* T. Reed, editor, Energy Technology Review No. 67 Park Ridge, NJ: Noyes Data Corp, 1981.

3. Overend, R. "Wood Gasification--Review of Recent Canadian Experience", *National Research Council (Canada) Report NRCC 20094,* March 1982.

4. Reed, T.B., "Principles and Technology of Biomass Gasification" in *Advances in Solar Energy*, Vol. 2, pp ed. by K. W. Boer and J. A. Duffie, (American Solar Energy Society, Inc. and Plenum Press, (1985), pp 125-174.

5. Antal, M. J., Jr., "Biomass Pyrolysis: A review of the Literature, Part 1-Carbohydrate Pyrolysis", *Advances in Solar Energy*, Vol 1, ed. by K. W. Boer and J. A. Duffie (American Solar Energy Society, Boulder, CO) 1982, pp 61-112.

6. Antal, M. J., Jr., "Biomass Pyrolysis: A review of the Literature, Part 2-Lignocellulose Pyrolysis", *Advances in Solar Energy,* Vol. 2, ed. by K. W. Boer and J. A. Duffie, (American Solar Energy Society, Inc. and Plenum Press, 1985, pp 175-255.

7. Evans, R. E. and Milne, T. A., "Molecular Characterization of the Pyrolysis of Biomass. I Fundamentals", *Energy and Fuels* Vol. 1, 1987.

8. Domalski, E. S., Jobe, T. L., Jr., and Milne, T. A., "Thermodynamic Data for Biomass Conversion and Waste Incineration", *SERI/SP-271-2839,* the Solar Energy Research Institute, Golden, CO. 1986). Also published as "Thermodynamic Data for Biomass Conversion and Waste Components", same authors by American Society of Mechanical Engineers, N. Y., 1987.

9. "Coal Conversion Systems Technical Data Book", *DOE Contract EX-76-C-01-2286,* Institute of Gas Technology (IGT). (1978). Available from NTIS, (National Technical Information Service, U.S. Department of Commerce, 5285 Port Royal Rd., Springfield, VA 22161.)

10. Coffman, J. A., "Steam Gasification of Biomass", *Proceedings of 13th Biomass Thermochemical Conversion Contractors Review Meeting,* Pacific Northwest Laboratories, PNL-SA-10093, CONF-8110115, 1981..

11. Diebold, J. P. and Scahill, J. W., "Ablative, Entrained-Flow Fast Pyrolysis of Biomass", in *Proceedings of 16th Biomass Thermochemical Conversion Contractors Review Meeting,* PNL-SA-12403, CONF-8405157, Pacific Northwest Laboratories, 1985.

12. Feldman, H. F., Paisley, M. A. and Appelbaum, H. R., "Conversion of

CHAPTER 8

DOWNDRAFT GASIFIER MODELLING

8.1 INTRODUCTION TO PROCESS AND GASIFIER MODELLING

A **model** of a system, phenomenon, process or device (eg the universe, the atom, petroleum cracking, or a gasifier) relates the important variables in such a way that one can **predict** the effect of changing any one variable on the other variables. The variables can be dimensions, flow rates, input, output etc. The model is based on an understanding of the relationships between the variables. The Copernican-Newtonian model of the universe, the Bohr-Schroedinger model of the atom, the Crick-Watson spiral helix model of DNA are examples of successful models.

More recently, models have also become useful for **controlling** processes. A quantitative understanding of a complex process or device (eg an oil refinery or an automobile) permits design of feedback loops that can keep the output (eg product mix or exhaust emissions) within specified limits. With the advent of low cost microprocessors, such control will become commonplace for processes. However, such control depends on having an adequate understanding of the process.

The design of furnaces for burning pulverized coal is an excellent example of a field highly dependent on modelling. Several interesting works are available describing the fundamentals and their use in modelling of furnaces [1-3]. Some of this work is applicable to modelling of gasification and biomass combustion.

We note a less fortunate development in this area. In recent years the verb "modelling" has come into fashion as a substitute for "investigating". Many papers mention modelling in the titles but the information presented does not in fact permit one to model either a part or all of a process, (though the investigation may cast some light on questions needing answers before modelling starts). For this reason we have used the redundant term "predictive modelling" to emphasize the true function of "modelling" [4]. This is not to say that models of subsets of the whole are not very useful - but they should not be labelled "gasifier models". However, while there are no satisfactory complete system models for biomass gasification, a large amount of work has been conducted in modelling the subsystems of **pyrolysis** and **char gasification** [5-16].This is at present a very active field and is continuing to evolve.

A successful model of a gasifier should permit one to relate the desired output of gas to the dimensions of the gasifier and the fuel. It should start with a qualitative understanding of the major phenomena involved in the gasifier and proceed to a quantitative mathematical description of the phenomena that relate all important variables.

Over the last five years we have studied the downdraft gasifier, both experimentally and theoretically. From this work we have developed the two-stage model described initially in Ref. 4 and amplified in Refs. 15-16. We summarize this work in this chapter and present new work. While far from perfect, we believe this is the only gasifier model that predicts gasifier zone lengths and required gasifier dimensions, based on particle size and properties and gasifier throughput.

8.2 QUALITATIVE DESCRIPTION OF DOWNDRAFT GASIFIER

8.2.1 Physical Basis of 2-Stage Model

It is important to have a qualitative understanding of the separate steps of a model before trying to make each step quantitative. Our model is based on our observation that for a single particle, **pyrolysis** and **gasification** are sequential reactions.

The two stage nature of gasification and combustion can be understood by looking closely at a burning match as shown in Fig. 8-1. While we often speak of "burning" wood, a close examination of the burning match shows that wood does not burn; rather pyrolysis at the surface produces gases that burn several mm away from the surface. This process is called **flaming combustion**.

Meanwhile, charcoal can be seen forming at the wood surface inside the flame. The charcoal is not burning because the surrounding envelope of pyrolysis gases prevents oxygen from reaching it. The charcoal will burn after the flame has passed to the unburned match. The charcoal combustion is called "**glowing combustion**" and is familiar in charcoal and coke fires. (The wood is treated in many U.S. made matches so that the charcoal will not continue to burn, thus reducing fire hazard.) The processes of glowing and flaming combustion will be discussed at more length in Section 8.3.

During pyrolysis the production of the >80% volatile matter from biomass causes a thousandfold increase in volume of the gases over the volume of the solid. This evolution of gases produces a "**pyrolysis wind**", illustrated in Fig. 8-2. In an updraft gasifier the heating of the particle results from the hot gases formed by burning the charcoal at the grate. In the downdraft gasifier air burns the pyrolysis vapors to supply the heat for pyrolysis, and so results in a relatively low tar gas. The pyrolysis wind greatly complicates the analysis of heat transfer during pyrolysis, flaming combustion and flaming pyrolysis and we believe that it is the primary source of difficulty in the modelling studies mentioned above and the reason why there is no single satisfactory model of the flaming combustion and flaming pyrolysis of wood and biomass.

More direct evidence for the two-stage model comes from the temperatures measured in a gasifier, as shown in Fig. 8-2. A particle-probe was made from three 2.5 cm diameter birch dowels 2.5 cm long wired together to form a triangular assembly enclosing a 1 cm diameter gas space [4]. A thermocouple was placed at the center of one dowel at the surface of a second dowel and in the middle of the gas space. The assembly was placed on the surface of the chip bed of the 5 gallon gasifier described in Chapter 5 and allowed to move down with the chips into the flaming pyrolysis zone.

It can be seen in Fig. 8-3 that at 2.5 min the surface temperature, T_s, rose rapidly to about 700°C. The temperature on the axis, T_a, only began to rise 5 min later, as pyrolysis was completed. The flame temperature, T_f exceeded the surface temperature most of this time, but dropped to the surface temperature as pyrolysis ended. Finally when pyrolysis was complete, all three temperatures climbed about 100°C as the hot combustion gases heated the charcoal [4]. (While the thermocouple in the gas space registered up to 1000°C, the actual gas temperature was probably much higher, as the flame temperature of hydrocarbons in air is about 2000°C.)

BA-G0201715
571

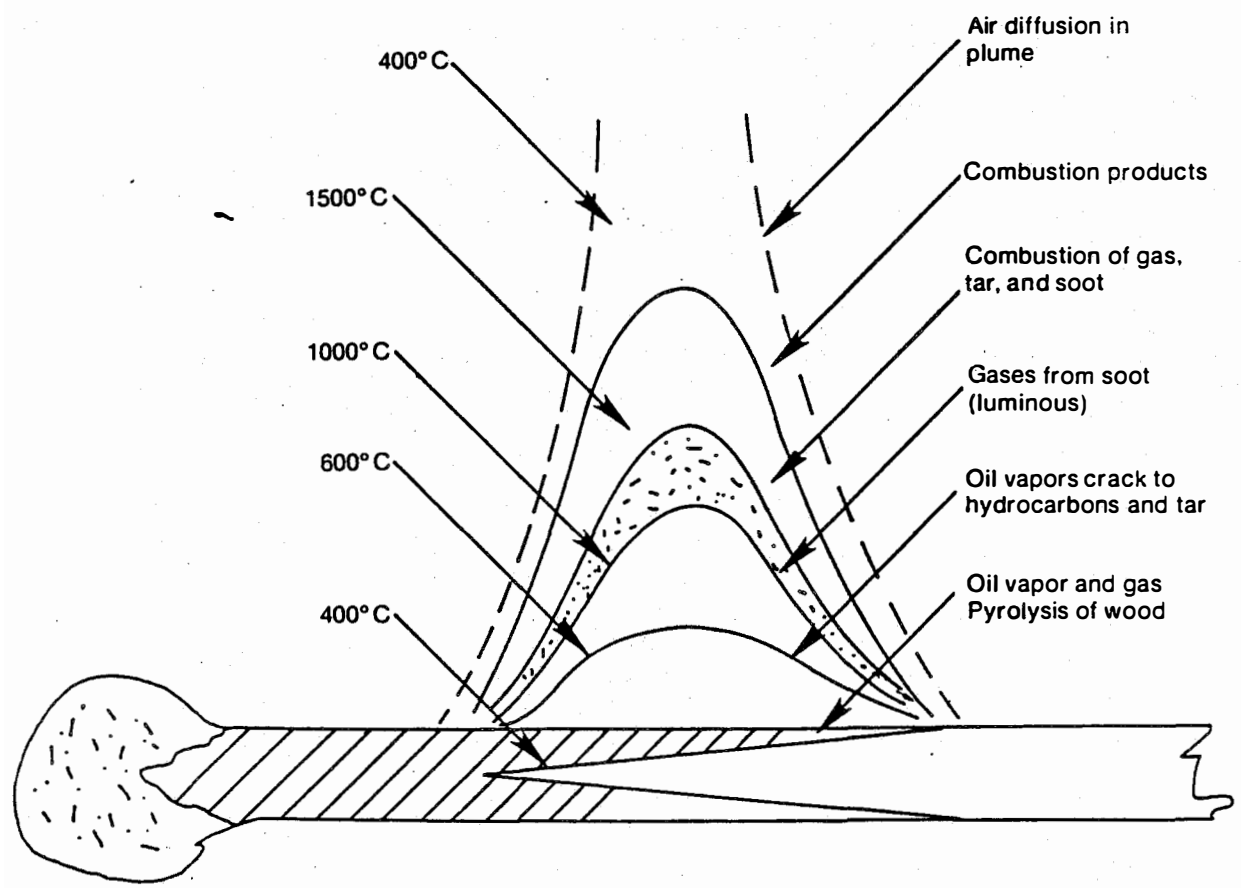

Figure 8-1. Pyrolysis and Combustion Zones seen in Flaming Match

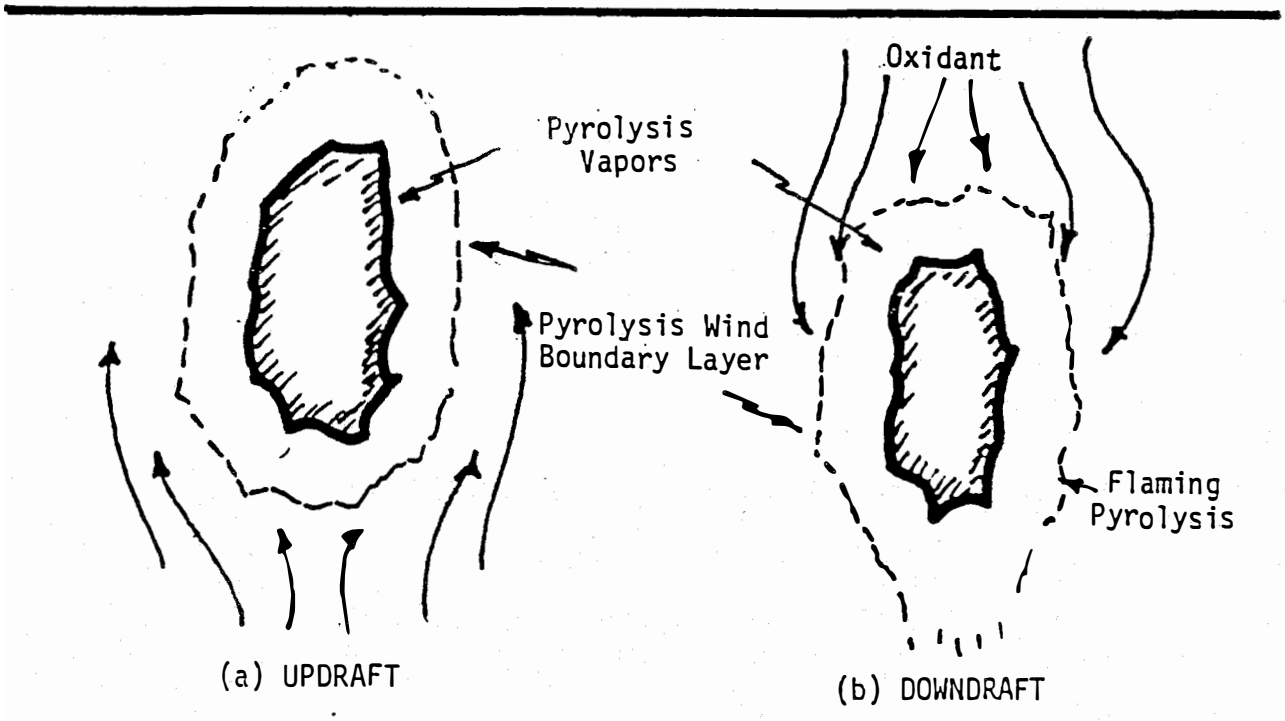

Figure 8-2. Diagram of "Pyrolysis Wind" Forming a Boundary Layer Around a Particle which Prevents Char Reactions During Pyrolysis. (a) in Updraft Gasifier with External Heat Transfer and (b) in Downdraft Gasifier with Heat Transfer from Flaming Pyrolysis.

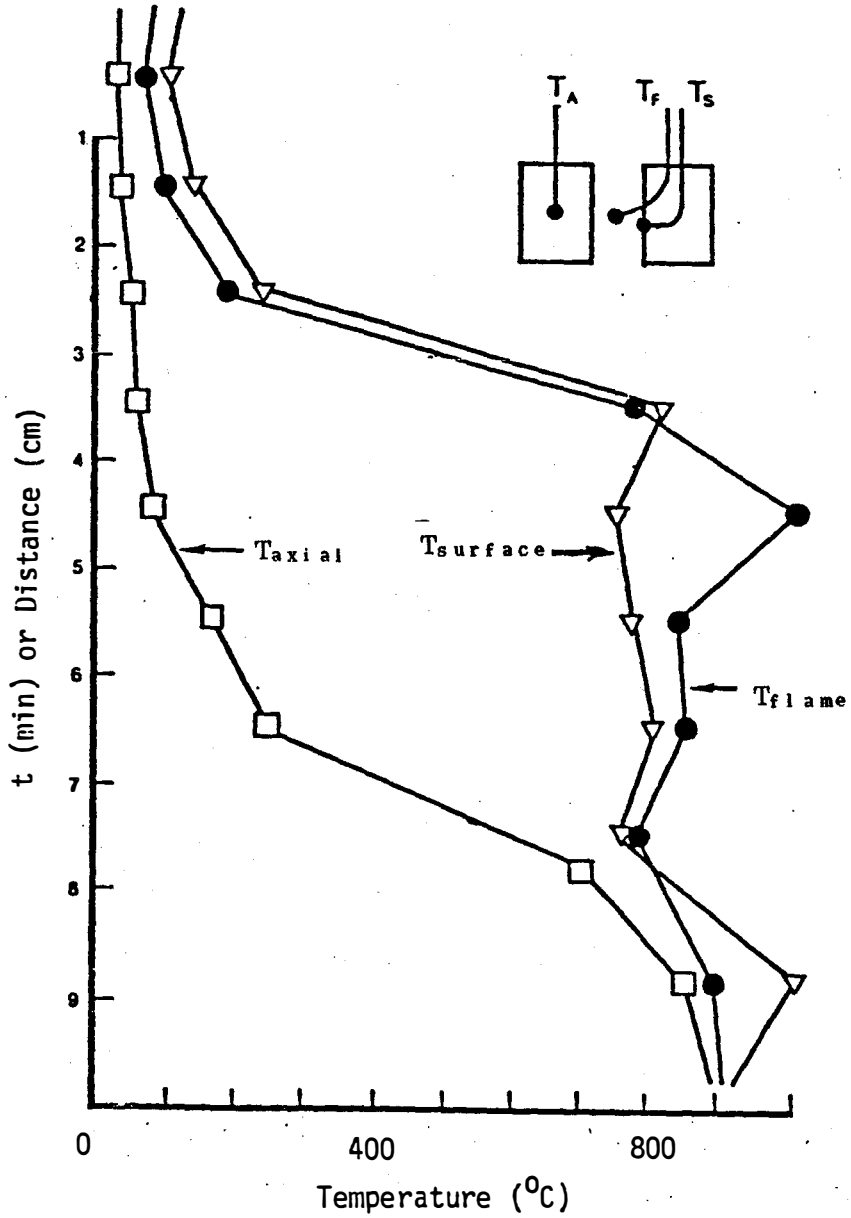

Figure 8-3. Temperatures Measured at the Axis, the Surface and in the Gas Space of a 2.5 cm Diameter Birch Dowel Undergoing Progressive Flaming Pyrolysis in a Downdraft Gasifier.

The four minute period between about 2.5 min and 7.5 min in Fig. 8-3 represents the pyrolysis stage for this fuel. Charcoal gasification reactions only begin at temperatures above about 800°, so that the second gasification stage can begin only after pyrolysis is complete at 7.5 min.

8.2.2 Diagram of Stratified Downdraft Gasifier Model

In our six years of observing and photographing the downdraft gasifier, especially in the gold insulated transparent furnace, we have arrived at the qualitative description of the gasifier operation in terms of the temperatures, compositions and reactions shown in Fig. 8-4 for the air gasifier and Fig. 8-5 for the oxygen gasifier. The figures are based on the sequential reactions of flaming pyrolysis followed by char-gasification. It should be understood that these two figures are compatible with all our observations, but that they are oversimplified. Some of the features shown, that would be very difficult to measure experimentally, are deduced from general experience in combustion chemistry

A stratified downdraft gasifier is shown schematically for air in Fig. 8-4(a). It consists of an insulated cylindrical vessel closed at the bottom end with a perforated grate through which small particles of char-ash can pass, but which supports the charge of charcoal and wood. At steady state there will be found up to four parallel, horizontal strata in the gasifier - hence the name **stratified downdraft gasifier**. The incoming oxidant is drawn or forced down through the four strata or zones and emerges at the grate as producer gas.

The top strata in air gasification consists of cool **biomass fuel** (BF) and the depth of this strata is largely a matter of convenience. In this stratum the temperature (Fig. 8-2(b) is that of the incoming fuel and air. The gas composition is that of air. This zone acts as a fuel reservoir and permits batch feeding of the gasifier through the open top. It also acts as insulation and the incoming fuel prevents heat from leaving the gasifier at the feed point. The incoming fuel should be evenly distributed across the gasifier.

The second zone, B, is the **flaming pyrolysis** zone. We define "flaming pyrolysis" to mean a pyrolysis caused by partial combustion of the products in an insufficient supply of air. (We will discuss the phenomenon of flaming combustion at greater length below.) In oxygen operation the flaming pyrolysis zone, B, moves up into unburned fuel so fast that there is no reservoir of unburned fuel in zone A. Instead, there is oxygen combustion of the incoming fuel and the pyrolysis vapors in the burner section marked BU in Fig. 8-5.

In the **flaming** pyrolysis zones of Figs. 8-4 and 8-5, the oxidant burns the fuel and converts it to partially oxidized gas and charcoal. At the beginning of the zone the biomass surface rapidly reaches a temperature of 500°-700°C. However the surface is also cooled by the pyrolysis gases, maintaining a relatively stable temperature as shown in Figs. 8-2(b) and 8-3(b), so it can't go higher in temperature. The temperature at the center of the particle is initially room temperature, and seconds or minutes may elapse before it changes temperature, depending on particle size. The time required for the heat to completely pyrolyze the particle determines the time for pyrolysis and therefore the length of the flaming pyrolysis zone.

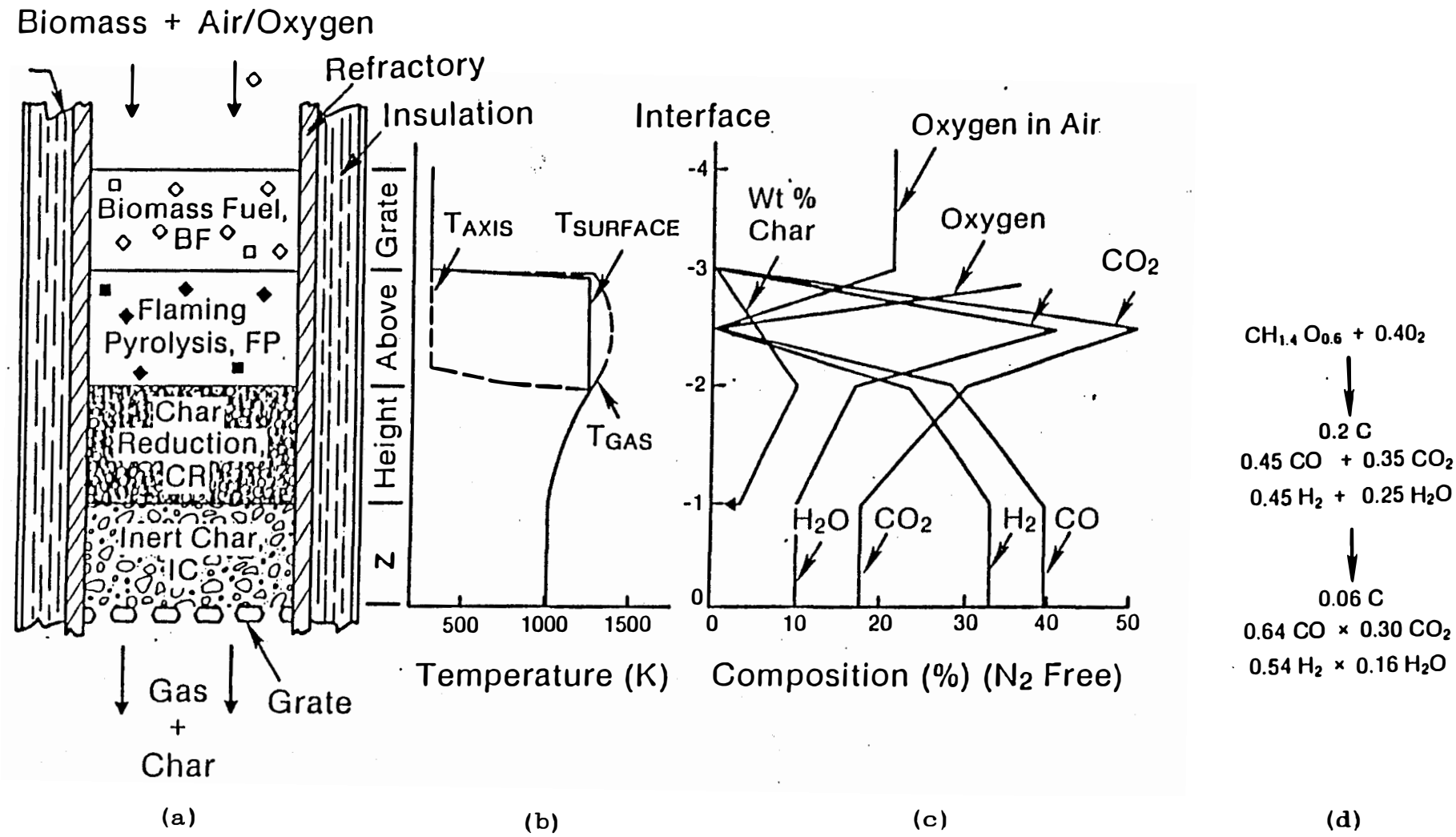

Figure 8-4 Qualitative Diagram of Stratified Downdraft Air Gasifier Showing (a) Geometry of Gasifier Showing Four Zones; (b) Temperature History of Particles and Gases; (c) Composition of Gas; (d) Chemical Reactions in Each Zone.

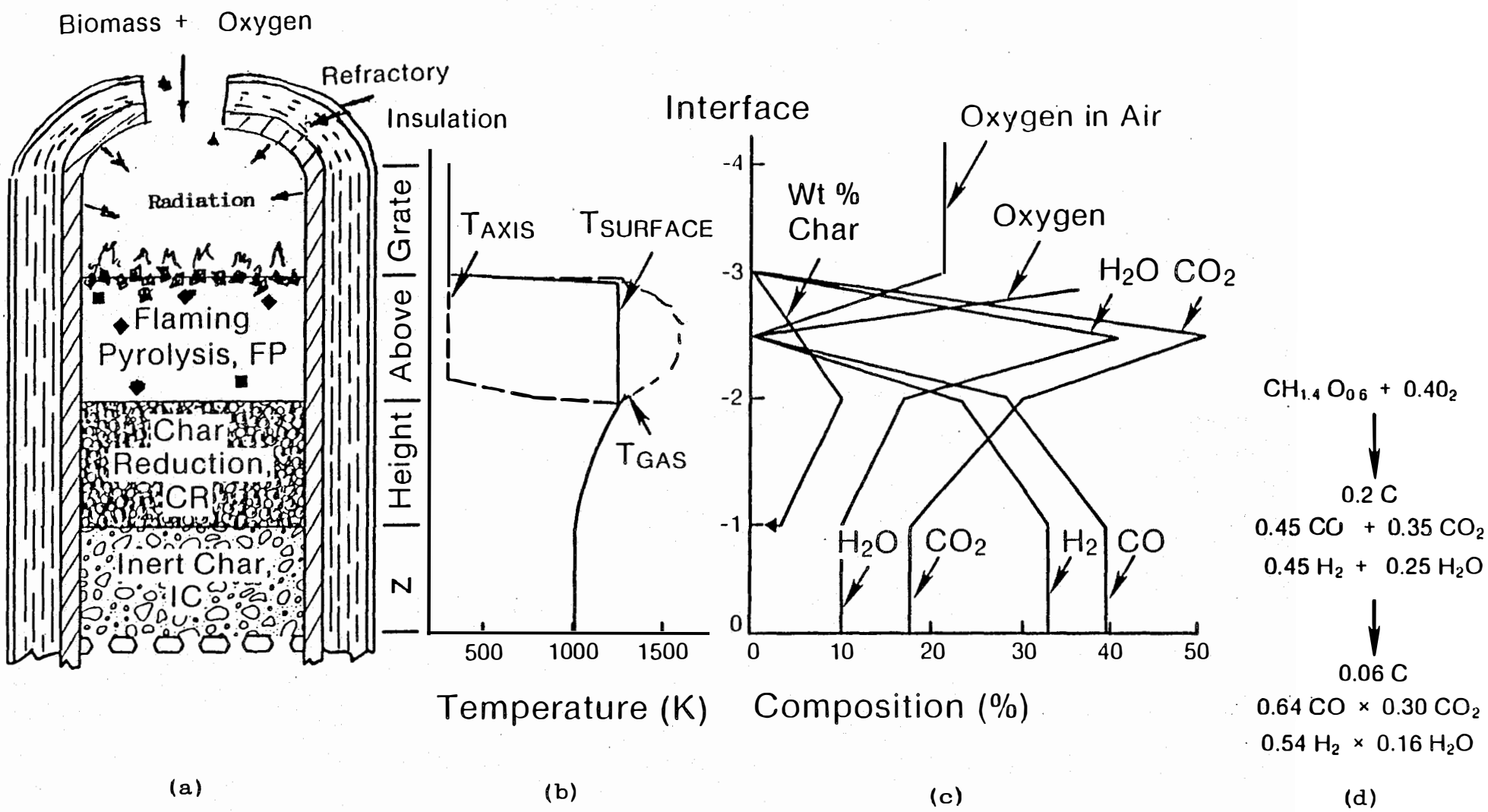

Figure 8-5 Diagram of Zones in an Oxygen Gasifier, Showing (a) Geometry of gasifier Showing Four Zones; (b) Temperature History of Particles and Gases; (c) Composition of Gas; (d) Chemical Reactions in Each Zone.

In an air gasifier all of these reactions occur in the flaming pyrolysis zone, (FP), as shown schematically in Fig. 8-4. However, in the oxygen gasifier some of the flaming pyrolysis occurs in the burner section (BU) above the bed as shown diagramatically in Fig. 8-5. It is particularly hard to define a temperature in the burner section of the oxygen gasifier due to the non-equilibrium conditions caused by convection from the flame, by radiation from the hot, luminous flames and by re-radiation from the hot walls to the top of the pyrolysis zone.

At the upper part of the flaming pyrolysis zone, the gas is relatively high in oxygen as shown in (c), but as the gas passes down, the volatiles burn, and consume all the oxygen and eventually generate CO and H_2 by partial oxidation. These reactions can be represented chemically by

STAGE I: FLAMING PYROPLYSIS ZONE

$$CH_{1.4}O_{0.6} + 0.4\ O_2 \longrightarrow 0.2\ C + 0.45\ CO + 0.35\ CO_2 + 0.45\ H_2 + 0.25\ H_2O \quad (8\text{-}1)$$

as shown in (d) of Figs. 8-4 and 8-5. Note that at this stage there are still 0.2 moles of carbon in the form of charcoal (about 10% by weight). This reaction represents a combination of pyrolysis of the biomass to oil vapors and char, followed by partial oxidation of the oil vapors. It converts over 80% of the biomass to a low grade producer gas and so is <u>**the principal reaction in the downdraft gasifier.**</u> (The inert nitrogen is omitted from these equations, but must be taken into account in heat and mass balances.)

The third zone, zone C in Figs. 8-2 and 8-3 is the **adiabatic char reduction** zone, CR. In this zone some, (but not all) of the hot, oxidizing CO_2 and H_2O containing gases react with the charcoal according to the equations 7-12 and 7-13 to give the partial reaction:

STAGE II: ADIABATIC CHAR REDUCTION

$$0.2\ C + .05\ CO_2 + 0.09\ H_2O \longrightarrow .06\ C + .19\ CO + 0.09\ H_2 \quad (8\text{-}2)$$

In this zone no further heat is added, hence the name "**adiabatic char reduction**". Calculations described below suggest that the temperature of the gas at the end of the pyrolysis zone is on the order of 1400 K for air and 1550 for oxygen gasification. This excess sensible heat contained in the products of Eq. 8-1 is consumed in the endothermic char gasification reactions of equations 7-9 - 7-11. This produces rapid cooling of the gas and char; hence the name "**adiabatic char reduction**" that we apply to this zone. We will discuss this in more detail below.

Since the reaction in zone (C) is self-quenching, it reaches a temperature at the bottom of the zone where essentially no further reaction occurs. However, physically there is generally a final bed of **inert char-ash,** (IC), on the grate. While not necessary for the chemistry of gasification, it serves the purpose of insulating the active zone from heat losses at the grate and provides a buffer to any dynamic change in the upper zones. It can also increase pressure drop if smaller particles are allowed to accumulate. It is very important to control the thickness of this zone.

The reactions 8-1 and 8-2 can be added to give the **overall reaction**

OVERALL GASIFICATION REACTION

$$CH_{1.4}O_{0.6} + 0.4\ O_2 \longrightarrow 0.06\ C + 0.64\ CO + 0.30\ CO_2 + 0.54\ H_2 + 0.16\ H_2O \quad (8\text{-}3)$$

(This equation differs from the idealized adiabatic gasification equation 7-3 because it contains about 5% unreacted carbon as found in practical gasifiers. We will see below that the amount of this char-ash plays an important role in determining the gasifier performance.)

It should be stressed that all the chemical reactions occur in zone B and C. The remainder of this chapter will focus on describing these two zones. The model assumes that all particles are the same size and require the same time for pyrolysis and gasification. In practice of course there will be some - or a great deal - of variation from this ideal, producing overlap of the zones.

8.3 PYROLYSIS, FLAMING COMBUSTION, FLAMING PYROLYSIS AND GLOWING COMBUSTION

The above description qualitatively describes the reactions occurring in the stratified downdraft gasifier. It now remains to quantify the behavior of the **flaming pyrolysis** and **char reduction** zones since a successful model of the whole depends on having a successful model of each of the parts. In particular, the model for the stratified downdraft gasifier should relate the time and bed length required for completion of **flaming** pyrolysis and for char reduction to the process conditions.

We present in Sections 8.3.1 and 8.3.2 a discussion of the phenomena and kinetics of conventional pyrolysis, ie heating biomass without oxygen. We will then discuss "flaming combustion" and "flaming pyrolysis" in Sections 8.3.3 and 8.3.4. The energies required for pyrolysis are discussed in Sections 8.3.5 and 8.3.6. The heat transfer required for pyrolysis is estimated in Section 8.3.7.

The kinetics of char gasification will be discussed in section 8.4. We then combine these two submodels in section 8.5 into a "predictive model" that we have used to design gasifiers for various purposes.

8.3.1 Pyrolysis vs Flaming Pyrolysis

"Pyrolysis" is the breaking down of materials, eg biomass, by heat. Generally pyrolysis is taken to signify a process in that no oxidant is present unless otherwise specified, but in practical processes some of the heat may arise from oxidation. Pyrolysis is the first step in all thermal conversion processes, since combustion and gasification occur at temperatures over 600°C. The pyrolysis step in the updraft gasifier of Fig. 2(a) is **pure** pyrolysis because all the oxygen has been removed from the hot gases by the charcoal burning at the grate.

We define **"flaming pyrolysis"** as the pyrolysis of biomass by a flame with insufficient oxidant as shown in Fig. 2(b). **We distinguish flaming pyrolysis** from **conventional pyrolysis** processes because the principal source of heat is the combustion of the volatiles at the outside of the particle-gas boundary layer. We distinguish **flaming pyrolysis** from **flaming combustion** because there is only a limited access to oxidant in the gasifier bed, while in ordinary wood fires there is excess oxidant available at all times. Thus flaming pyrolysis is intermediate in all senses between pyrolysis and flaming combustion.

While the products of conventional combustion are CO_2 and H_2O, the lack of oxidant yields significant quantities of CO and H_2 in flaming pyrolysis, as shown in Eq. 8-1.

8.3.2 Flaming Pyrolysis Modelling

The slow pyrolysis of wood was the foundation of charcoal manufacture over the last ten millenia, and was a major chemical industry in the last century and through World War II. Early tests give detailed lists of the products and show the effects of temperature and pressure on the distribution of products in amazing detail [17].

The literature on pyrolysis was recently reviewed by Antal [18,19]. The chemistry of the products has been investigated extensively especially by Evans and Milne at SERI using the Free Jet Molecular Beam Mass Spectrometer (FJMBMS) [20,21]. Compositions of the oils and tars from various gasifiers have been measured by Elliott and Beckman [22,23].

A number of papers have appeared that attempt to model the pyrolysis process (without combustion) based on the fundamental properties of wood or other biomass (thermal conductivity, diffusivity, heat of pyrolysis, etc.) and the temperature or heat transfer at the surface [5,6,8,9,24-26]. Unfortunately, the pyrolysis process is sufficiently complex so that most of these papers do not predict the time required for pyrolysis of a particle of arbitrary dimensions and properties though they all shed some light on specific aspects of the pyrolysis process. None of the papers discuss flaming pyrolysis.

Because flaming pyrolysis is central to operation of the downdraft gasifier and has not been previously described in detail before, we will spend a good deal of space on it here, adding recent work and further discussion to our original papers [4,15,16].

8.3.3 A Quantitative Formula for Flaming Combustion

Flaming combustion (FC) is even more difficult to model than conventional pyrolysis [24,26,27]. In FC the heat for pyrolysis is provided by combustion of the pyrolysis products and radiation from adjacent particles or a surrounding furnace. This heat must be transported to the particle surface through the "pyrolysis wind" as shown in Fig. 8-2. This process is self adjusting in part. Any factor that increases heat transfer also increases the rate of streaming and the thickness of the boundary layer. This in turn tends to reduce the heat transferred by convection across the boundary layer (but not that due to radiation). The process of flaming combustion accounts for most of the energy production from wood in the world; yet we do not even have a satisfactory analytical model for a single particle of wood, and particularly we do not have a model for flaming combustion in a bed of particles.

Because of the difficulty of making an analytical model of this process, E. Huff made a large number of factorial designed tests in which he measured the time required for flaming combustion of a wood particle in a furnace of controlled temperature as a function of particle size, shape, density, moisture content, and furnace temperature [28,29]. In this experiment the time for flaming combustion was measured visually since the pyrolysis "end point" is easily distinguished by the extinction of the flame. From this he derived an

empirical formula that describes flaming combustion, in terms of the above"practical" variables.

According to Huff, the time required for flaming combustion of a wood particle, t_{fc}, is given by

$$t_{fc} = 0.12\ \rho D(1 + 0.61D)F_s(1 + 1.76F_m)\exp(4370/RT) \qquad (8\text{-}4)$$

where t_{fc} is the time (in min) required for flaming combustion of a particle of density ρ (g/cm^3), average dimension D in cm (equal to the cube root of the volume, $V^{1/3}$), sphericity F_s, and moisture content F_m (dry basis). (The sphericity is defined as the ratio of particle surface area to that of a sphere of equivalent volume. A sphere has a sphericity of 1.0; a piece of paper might have a sphericity of 0.1). R is the gas constant and T(K) is the furnace temperature.

This formula predicts the burning time for the particles studied within 3% of the measured values. (Huff has more recently investigated the effect of velocity and low oxygen concentrations on pyrolysis times, and expects to publish this in the future [29]).

Note that in this formula those terms that involve the mass of the wood and water (moisture content, density) increase time for pyrolysis in a linear fashion. The dependence of time on size of the wood, D, is also linear for small particles where $D \ll 1$. The dependence becomes quadratic for $D > 1$ where the resistance to heat flow depends on heat flow resistance in the wood as well as in the gas boundary layer.

The data of Huff applies to a single particle burning in excess air, while in the gasifier there are many particles burning in a diminishing stream of oxidant. Ultimately data will have to be collected to permit modelling on the basis of diminishing oxidant supply in a multi-particle bed. The experiments described in section 5.4 on the single particle reactor are an attempt to fill this need.

(In addition Huff observed the time required for glowing combustion of the charcoal remaining after the completion of flaming combustion. He also gives data and a similar formula for glowing combustion).

8.3.4 Modification of Huff Equation to Estimate Time For Flaming Pyrolysis

To a first approximation Eq.8-4 has the proper functional dependence on particle size, shape, density etc. to describe flaming pyrolysis in a fixed bed. The times predicted could be too short because oxygen is not present during part of the pyrolysis. On the other hand the hot gases from early combustion are in more intimate contact with the particle because of the narrow gas passages in the bed. The answers obtained from the model are consistent with measured gasifier dimensions.

Unfortunately, Huff did not measure the effect of oxygen concentration on flaming combustion time. In order to account for this we have modified the Huff equation to include the effect of oxygen using the functional dependence found by Simmons and Ragland to give [25]:

$$T_{fp} = 0.207\ \rho F_s(1 + 1.76F_m)D(1 + 0.61D)\exp(4369/RT)/(1 + 3.46F_{O_2}) \qquad (8\text{-}5)$$

where F_{O_2} is the initial fraction of oxygen in the ambient gas.

There are a large number of variables in this equation. Table 8-2 shows the time calculated for flaming combustion by this equation for a wide variety of particle sizes and input conditions with biomass particles varying by more than 10^5 in volume and t_{fc} varying from 0.053 to 10 minutes.

8.3.5 The Heat of Pyrolysis

In modelling the flaming pyrolysis zone of the gasifier it is essential to know the amount of energy that is required for pyrolysis. The "heat of pyrolysis", Δh_p is a quantity that has been discussed, measured and argued about for many decades [17,30]. A major reason for the different results is that the heat of pyrolysis depends on the products of pyrolysis and the conditions of the measurement.

It is not surprising that the energy required is very dependant on conditions and products. Yet one finds discussion of the "heat of pyrolysis" in the literature as if it were a fixed quantity to be measured, like the heat of vaporization of water. While there is some similarity to a true phase change, pyrolysis occurs over a range of temperatures.

In the slow destructive distillation of wood during charcoal manufacture it was observed that at a temperature of 270°C the reaction became exothermic ($\Delta h_p < 0$) and the temperature of the charge would exceed that of the surroundings, carrying the temperature up to 400°C spontaneously. (The Stafford wood distillation unit uses this effect to minimize energy inputs [17].

Others have measured the heat of pyrolysis however, and find the reaction to be endothermic, ($\Delta h_p > 0$). (See review of heat of pyrolysis in thesis of Cowdery [30]). Most recently Antal has measured the heat of pyrolysis for cellulose as a function the amount of charcoal formed and found that it varies from +270 J/g at 10% char production to -125 j/g at 22% char production, as shown in Fig. 8-6 [18]. (The degree of char formation was varied by changing the pressure at which pyrolysis occurred). Desrosiers modelled the pyrolysis of a wood cylinder with internal reaction and found a value of +368 J/g for the heat of pyrolysis at 350°C with a surface temperature of 700°C [26]. Herman modelled pure pyrolysis, including the effect of transpirational cooling. She obtained good agreement with experimental data using a value of +334 J/g, but found that the model predicted excessively long pyrolysis times when she used a value of 1256 J/g [15].

Thus it is seen that the heat of pyrolysis has no single value, but varies with degree of char produced, and certainly with heating history and product changes. In general, the slow conversion of wood to charcoal and relatively small quantities of vapor is exothermic, while the fast pyrolysis of wood to high vapor yields is endothermic. (The heat of vaporization of most materials is of much larger magnitude than heats connected with changes in solid structure.) Again more work needs to be done in this field.

8.3.6 The Heat for Pyrolysis

We define the "heat for pyrolysis at Ts", $h_p(T_s)$ as the sum of (a) the heat required to bring wood (or other biomass) from an initial temperature of T_o to the pyrolysis temperature, T_p; (b) the heat required for the pyrolysis reaction and (c) the heat required to raise the gaseous products to the

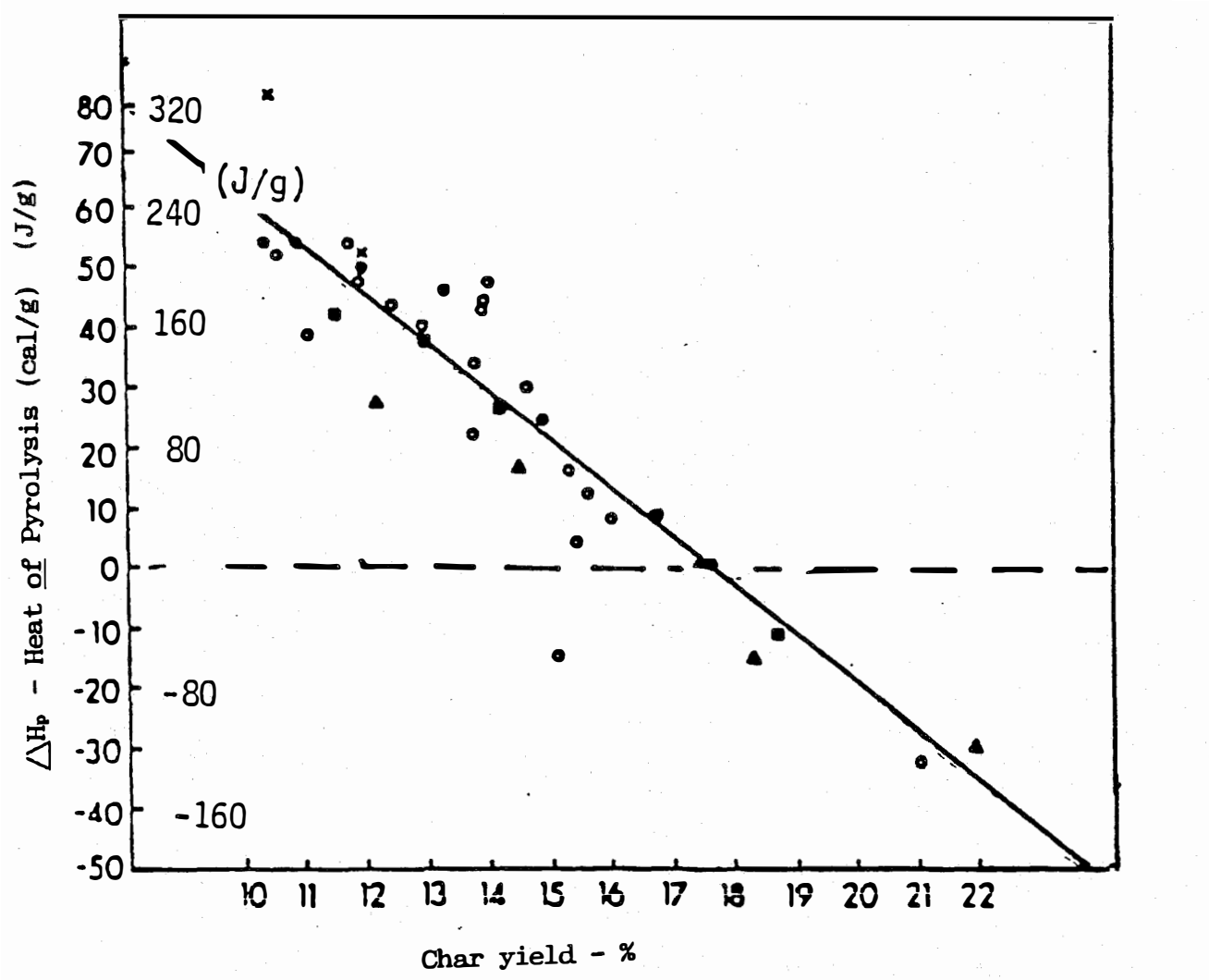

Figure 8-6. Heat of Pyrolysis of cellulose, ΔH_p, vs Char Formation as Measured by Antal [18].

particle surface temperature, Ts, ie

$$h_p(T_s) = \int_{T_o}^{T_p} C_{p,w}dT + \triangle h_p + \sum_{i=1}^{n} n_i \int_{T_p}^{T_s} C_{p,i}\,dT \qquad (8\text{-}6)$$

where $c_{p,w}$ is the heat capacity of the wood at constant pressure, $\triangle h_p$ is the heat of pyrolysis and $c_{p,i}$ is the heat capacity of the ith product of pyrolysis. The distinction between "heat of pyrolysis" and "heat for pyrolysis" is shown in Fig. 8-7(a) and (b) for slow and fast pyrolysis.

The average heat capacity of wood ranges from about 1.2 to 1.6 J/g. Heating wood to 400 C for pyrolysis will then consume 480 to 640 J/g. The heat capacity of the gas and vapors produced is of similar magnitude. From this it can be seen that the sensible heat terms in Eq. 5 are larger than the positive or negative value of $\triangle h_p$. An error in the value of $\triangle h_p$ makes a smaller error in h_p. We have measured the heat for pyrolysis in a "heat flux concentrator" used for producing pyrolysis vapors [30].

We found values of the heat for pyrolysis, h_p ranging from 640 to 1840 J/g for pyrolysis occurring in the temperature range 473°-600°C. From this data, the heat of pyrolysis, $\triangle h_p$, was calculated from Eq. 5 using sensible heat data. $\triangle h_p$ ranged from -440 to 190 J/g over this temperature range [30].

For instance at 600°C the heat for pyrolysis was 1840 J/g. The sensible heat of the wood at the pyrolysis temperature of 466°C was 1046 J/g. The heat required to raise the char, vapors and gas to 600°C was 418, 132 and 56 J/g respectively. Subtracting these from the total gave a heat of pyrolysis of +189 J/g. heat

8.3.7 Heat Transfer in Flaming Combustion

Knowledge of values for the heat for pyrolysis permit calculation of the magnitude of heat flux to the particle during flaming combustion from the data of Huff. The time for flaming combustion is related to the heat flux by

time = energy required/energy supply rate

$$t_{fc} = (h_p(T_s) + F_m h_w)V\rho/qA \qquad (8\text{-}7)$$

$$q = (h_p(T_s) + F_m h_w)V\rho/At_{fc} \qquad (8\text{-}8)$$

where V is the volume of the particle, h_w is the heat of vaporizatio of water, and A is the surface area. This equation permits the calculation of the average heat flux, q, during flaming combustion. Values of q were calculated from the particle properties, assumning a representative value of h = 2000 J/g. They are shown for the various particles and conditions represented in Table 8-1. Note that the average heat transfer to the particle varies between 2 and 15 W/cm², only by a factor of 8, while the mass of the particle varies by 10^5.

This equation can also be used to calculate the time for pyrolysis if the heat transfer can be calculated in other ways. This was the basis of our "simplified model" for calculating flaming pyrolysis time [16].

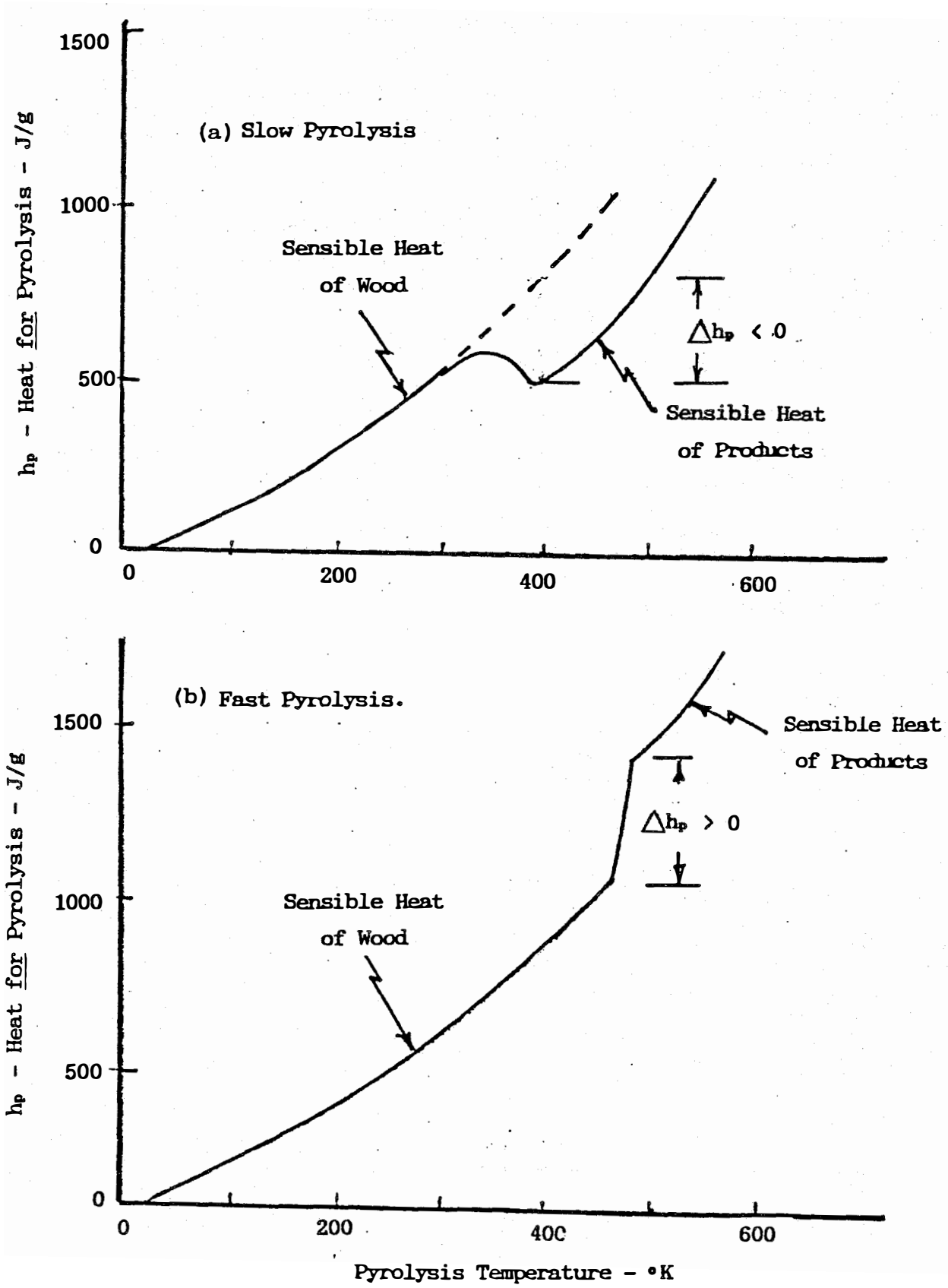

Figure 8-7 Schematic Diagram Showing Negative (a) or Positive (b) contribution of Heat of Pyrolysis, Δh_p, to the Heat for Pyrolysis, h_p

Table 8-1. Time and Heat Flux in Flaming Pyrolysis Calculated from Modified Huff Equation, $T_{fp} = 0.2072\ \rho F_s(1 + 1.76F_m)D(1 + 0.61D)\exp(4369/RT)/(1 + 3.46F_{O2})$

	INPUT CONDITIONS							RESULTS	
	VOLUME V_{cm^3}	TYPICAL DIMENSION D(cm)	SPHERICITY F_S	DENSITY ρ	MOISTURE F_m	TEMP T°C	OXYGEN FRACTION F_{O2}	FLAMING PYROLYSIS TIME t_{fc}-min	HEAT FLUX q-W/cm²
		EFFECT OF VARYING DIMENSION - PINE CUBES							
SMALL	0.001	0.10	0.81	0.41	0.00	600	0.21	0.053	4.51
!	0.13	0.50	0.81	0.41	0.00	600	0.21	0.323	3.67
!	1.00	1.00	0.81	0.41	0.00	600	0.21	0.798	2.97
!	3.38	1.50	0.81	0.41	0.00	600	0.21	1.423	2.50
!	8.00	2.00	0.81	0.41	0.00	600	0.21	2.199	2.16
LARGE	125.00	5.00	0.81	0.41	0.00	600	0.21	10.031	1.18
		EFFECT OF VARYING TEMPERATURE - 1 CM PINE CUBES							
COOL	1.00	1.00	0.81	0.41	0.00	600	0.21	0.798	2.97
	1.00	1.00	0.81	0.41	0.00	800	0.21	0.499	4.75
HOT	1.00	1.00	0.81	0.41	0.00	1000	0.21	0.361	6.56
		EFFECT OF VARYING MOISTURE - 1 CM PINE CUBES							
DRY	1.00	1.00	0.81	0.41	0.00	900	0.21	0.419	5.66
	1.00	1.00	0.81	0.41	0.20	900	0.21	0.566	5.66
	1.00	1.00	0.81	0.41	0.50	900	0.21	0.787	5.66
WET	1.00	1.00	0.81	0.41	1.00	900	0.21	1.155	5.66
		EFFECT OF VARYING DENSITY - 1 CM SELECTED SPECIES							
BALSA	1.00	1.00	0.81	0.14	0.00	900	0.21	0.143	5.66
PINE	1.00	1.00	0.81	0.41	0.00	900	0.21	0.419	5.66
OAK	1.00	1.00	0.81	0.66	0.00	900	0.21	0.674	5.66
PELLETS	1.00	1.00	0.87	1.10	0.00	900	0.21	1.206	5.27
		EFFECT OF OXYGEN - 1 CM PINE CUBES							
INERT	1.00	1.00	0.81	0.41	0.00	900	0.00	0.723	3.28
AIR	1.00	1.00	0.81	0.41	0.00	900	0.21	0.419	5.66
OXYGEN	1.00	1.00	0.81	0.41	0.00	900	1.00	0.162	14.62
		EFFECT OF VARYING SPHERICITY - VARIOUS SHAPE PINE							
CUBE 1X1X1	1.00	1.00	0.81	0.41	0.00	900	0.21	0.419	5.66
FLAT 1.8X1.8X.4	1.00	1.00	0.62	0.41	0.00	900	0.21	0.320	7.40
FLATTEST 3.4X3.4X.13	1.00	1.00	0.25	0.41	0.00	900	0.21	0.129	18.34
STICK 4.5X.7X.57	1.00	1.00	0.57	0.41	0.00	900	0.21	0.295	8.05

INPUT DEFINITIONS: D = typical dimension = $V^{1/3}$; F_s = sphericity; F_m = fraction moisture; F_{O2} = fraction oxygen; T= Temperature of test (K); ρ = density

OUTPUT DEFINITIONS: T_{fp} = time required for flaming combustion (min); V_f = fuel velocity

8.3.8 Heat Transfer Mechanisms in Flaming Pyrolysis and Flaming Combustion

The heat transfer to each particle in the flaming pyrolysis bed is by conduction through the boundary layer from the combustion interface to the surface; by convection from the gases streaming outside the boundary layer; and by radiation from other particles, from the furnace walls, and by the luminous flame. We do not have at present sufficient understanding of the processes in flaming combustion to accurately predict heat transfer in a given situation (see Sec. 5-4), but we can estimate the magnitudes of the heat transfer from these mechanisms.

8.3.8.1 Conductive heat transfer

The magnitude of the boundary layer size can be judged from the boundary layer in a match such as shown in Fig.8-1 or from the boundary layer around the burning 2.5 cm birch dowel in the photograph in Fig. 5-10. Visual estimate shows that the (non luminous) boundary layer beneath and at the sides of a horizontal 2 mm square kitchen match is 1-1.5 mm thick. (The luminous burning plume above the match may be several cm thick so we presume very little heat is transferred through the gas to the top.). Combustion in the match is controlled by natural convection.

Scaling the birch dowel photograph in Fig. 5-10 shows that the boundary layer on the upstream side is 3.5 mm thick, while that at the sides averages 5.3 mm in thickness.

Heat flux through this layer can be estimated from Newton's equation of heat conduction,

$$q_c = k\ dT/dx \qquad (8\text{-}8)$$

where q is the heat flux per unit area, k is the thermal conductivity of the gas and dx is the thickness of the boundary layer.

The magnitude of the thermal conductivity of the combustion gases in the boundary layer is 400×10^{-6} J/cm^2°C-s. Combustion produces peak temperatures of about 1600°C at the outer edge of the boundary layer and the pyrolyzing surface is approximately 600°C so that the temperature difference will be 1000°C. From this we estimate that the heat flux through the 1-1.5 mm boundary layer to the burning match will be 2.7-4 W/cm^2. The heat transfer to the upstream side of the birch dowel will be 1.1 W/cm^2 and to the sides will be 0.75 W/cm^2. These values are comparable to the 2.16 W/cm^2 calculated from the modified Huff equation for a 2 cm particle in Table 8-1.

8.3.8.2 Convective Heat Transfer

A major mechanism by which convection increases heat transfer over that of conduction is by reducing the size of the boundary layer. In the above estimate the boundary layer thickness was taken into account, so that it includes the contribution of the convective heat transfer.

The analysis of convective heat transfer in a situation where gases and vapors are generated by the heat transfer is a very complex situation and has not yet been attempted for large biomass particles.

8.3.8.3 Radiative Heat Transfer

Radiation heat transfer can occur from solids or gases. The radiation from gases is relatively small because of their low emissivity. (One can hold a finger parallel to a candle flame without discomfort. However, long path lengths or high pressure can make gas emissivity appreciable.)

Radiation is transferred from a flat surface at a temperature T_2 to a parallel surface at T_1 according to

$$q_r = \epsilon\sigma(T_2^4 - T_1^4) \qquad (8\text{-}9)$$

where ϵ is the surface emissivity and σ is the Stefan-Boltzmann radiation constant, 5.67×10^{-12} W/cm²-(K)⁴.

We have made preliminary measurements of the surface temperature of pyrolyzing or burning particles in the single particle reactor using thermocouples and an infra-red optical pyrometer. The temperatures are 450-700°C. For purposes of discussion we will use a surface temperature of 600°C.

The radiation to or from a particle at 600°C according to Eq. 9 is 2.8 W/cm². This has the same magnitude as the conductive heat flux. Therefore, it is not surprising that radiative heat loss makes it difficult to burn large single particles of wood. In a match the thin boundary layer enhances the conductive heat transfer, barely supporting burning (if the matches are dry, there is no wind and the match is held "head down"). In a fireplace or stove, radiation from adjoining logs compensates in part for radiation losses. In the single particle reactor, the furnace permits adjusting the radiation loss or gain. Even very dry wood does not easily burn without some radiative heat input.

In a gasifier all the particles undergoing flaming pyrolysis are approximately at the same temperature. While no heat is gained by radiation, no heat is lost either, so radiation is a passive phenomenon in the bulk of the bed. However, at the surfaces of the bed a significant amount of heat can be lost and radiation should be taken into account.

While this discussion outlines the magnitude of heat transfer to be expected from these mechanisms, the heat transfer in a gasifier bed is a complex phenomenon not currently understood in detail. We are now using a single particle reactor to measure the relative contribution of each mechanism [32]. Meanwhile we will use the modification of the equation of Huff to model the flaming pyrolysis section of the gasifier below.

We will use Eq. 8-5 to predict the length of bed required for pyrolysis in the downdraft gasifier, as discussed below. We realize that the equations need to be altered in detail in the future as we learn more.

8.4 ADIABATIC CHAR GASIFICATION

8.4.1 Introduction

Coal pyrolysis produces typically 80% fixed carbon (coke) and hence the principal reactions of coal gasification are those that convert coke to gas,

ie.

$$C + O_2 \longrightarrow CO_2 \quad (8\text{-}10)$$

$$2\ C + O_2 \longrightarrow 2\ CO \quad (8\text{-}11)$$

$$C + CO_2 \longrightarrow 2\ CO \quad (8\text{-}12)$$

$$C + H_2O \longrightarrow CO + H_2 \quad (8\text{-}13)$$

The elucidation of first the chemistry, then the thermodynamics and finally the kinetics of the char reduction reactions was one of the early triumphs of fuel chemistry and put the gasification of coal on a relatively sound theoretical basis. The time spent in these studies may exceed that devoted to any other chemical reactions with the possible exception of the reduction of iron oxides in steel manufacture.

Many volumes have have been written in which coal science is discussed in great detail. One of the best summaries of coal gasification - and some biomass gasification - is that of Gumz, written just after the period of World War II in which the gasification of coal and synthesis of gasoline reached its height in Germany [14]. Since then work has continued but has primarily added detail to what was previously discovered.

Unfortunately, the unravelling of these puzzles for coal did not add much to the understanding of wood gasification. At that time coal received the lion share of attention from scientists because of its commercial importance. Wood only became important during World War II because it could be gasified in small gasifiers for transportation purposes. In the turmoil of World War II it was understandable that the knowledge developed for coal-coke was applied uncritically to wood-charcoal. Yet the quantity of charcoal resulting from wood pyrolysis is typically less than 20% as much as the coke resulting from coal gasification, and it is up to 100 times as reactive as coke. As a result the char reactions are relatively less important in a biomass gasifier as compared to a coal gasifier.

A further problem not faced at that time was that coal was generally gasified in updraft gasifiers where combustion of coke with oxidant and steam provided surplus energy to pyrolyze the coal bed. This coal technology could be applied with little change to charcoal gasification. However, wood was gasified in downdraft gasifiers where the oxidant was consumed by the pyrolysis vapors. No combustion of the charcoal occurred and no steam was added (though steam is generated in the drying and flaming pyrolysis reactions above the char bed.)

We have developed an **adiabatic char reduction** model to apply specifically to downdraft gasification and will discuss it in the following sections.

8.4.2 Char Reaction Chemistry

Freshly devolatalized char is highly reactive. The reactions with CO_2 (Boudouard reaction) and H_2O (steam carbon reaction) are endothermic (heat absorbing) while the reaction with hydrogen to form methane (methanation reaction) is exothermic. The reaction of CO with H_2O to form CO_2 and H_2 is mildly endothermic. These reactions are discussed in Chapter 7 and data is given in Table 7-2 on the thermodynamics.

SERI/PR-234-2571

8.4.3 Charcoal Reaction Kinetics

Thermodynamics permits one to calculate the equilibrium concentrations of the gas components at any temperature, given sufficient time to establish equilibrium, and sets a bound to the limits of reaction. However, kinetic data is required to determine to what degree the reactions will actually proceed in a given time lapse at a specified temperature.

A vast amount of research has examined the kinetics of coke gasification, and most of the charcoal kinetics work has taken this as a starting point. Considerable work has also been done on the kinetics of charcoal gasification. For a general review on coke and charcoal reactions, see Ref. 33.

Char gasification rates are typically measured by recording the weight W of a particle of charcoal remaining at time t and temperature T in a flowing gas of CO_2, H_2O, or mixtures of these. The rate is then given by:

$$r = k\ dW/dt \qquad (8\text{-}14)$$

where W is the mass of material remaining at time t and k is the reaction rate constant. As in pyrolysis studies, the results are often fitted to an Arhennius equation where k has the form:

$$k = A(\exp\text{-}E/RT) \qquad (8\text{-}15)$$

where A is the pre-exponential factor and E is the activation energy for the reaction occurring at a temperature T.

At sufficiently high temperatures (above 1100°C for coke and above 900°C for charcoal) these reactions are mass transport limited, and the reaction rate is determined by the rate at which the gases can diffuse to and from the external surface of a particle shown schematically in Fig. 8-8 (a) [34]. The activation energy is then quite low, a few kCal, as shown in Fig. 8-8(b). The particles then gradually shrink until they disappear. This is called the "shrinking core" model because the reaction takes place on the outer surface and the particle shrinks in size. At intermediate temperatures, pore diffusion limits the rate of reaction and the particle becomes internally more open to diffusion of the reactants.

Finally, at the lowest temperatures, the reaction rate is limited by the availability of true molecular internal surface area for reaction, and the char particle size stays constant while the density decreases. In this case the activation energy is much higher, 40-60 kCal as shown in Fig. 8-8 (b). In practice, examination of actual gasification beds shows a combination of the above mechanisms, with simultaneous shrinking of the charcoal and decrease in density.

Values for A and E for maple and jack pine gasified in several mixtures were measured by Nandi and Onischek and are shown in Table 8-2 [34].

Where gas mixtures are involved, the absorbtion step may be important, and the above model may not adequately describe the rate. In this case it may be important to evaluate kinetic data using the Langmuir-Hinshelwood rate law of the form:

$$r(T,P_i) = k_1\ pH_2O/(1 + k_2 p_{H2O} + k_3\ p_{H2}) \quad (8\text{-}1)$$

or

$$r(T,P_i) = k_4\ p_{CO}2/(1 + k_5\ p_{CO}2 + k_6\ p_{CO}) \quad (8\text{-}2)$$

where the partial pressures of the various species involve separate rate constants [33,35].

Edrich et al measured rate constants on freshly pyrolysed biomass and found that the temperature of pyrolysis was also a major factor in determining the activation energy [35]. The rate equation

$$R = -f\ K_1\ p_{CO2}/(1 + K_2\ p_{CO} \quad (8\text{-}18)$$

where

$$f = \exp[-9970(1/T-1/T_p)] \quad (8\text{-}19)$$

$$K_1 = \exp(-17141/T + 12.309) \quad (8\text{-}20)$$

and

$$K_2 = \exp(34021/T - 28.43) \quad (8\text{-}21)$$

was developed to fit the data. The values for rate constants that they found are shown in Table 8-3.

Edrich et al measured gasification rates for CO_2 on freshly prepared chars of the order of 0.1 g/g-min with a true activation energy of 54 kcal/mole. However, if the biomass was pretreated at temperatures higher than the gasification temperature, the activation energy was lowered by about 20 kcal/mole, because of annealing effects. They concluded from data on various size particles that macropore structure did not affect the reaction rate up to the highest temperature studied (1135°C). Measurements on char from densified (pelletized) biomass showed similar activation energies.

While formally similar to coke gasification, examination of reported rate data on coke and charcoal suggests that the rates for charcoal are about 50 times faster than those for coke [34]. This is probably because of the very low density of the charcoal (due to the high volatile content of biomass, typically 0.05-0.1 g/cm^3), the much larger internal surface area of the charcoal (typically 10-100 m^2/g), the low ash content of the charcoal, and the non-graphitic nature of freshly formed charcoal. In addition, char reactivities are even larger in freshly prepared chars than in those exposed to air after preparation [35]. One should be cautious in comparing data on charcoals taken under different conditions.

8.4.4 Models of the Adiabatic Char Reduction Zone

8.4.4.1 Simple Adiabatic Cooling Model.

The above data form the basis for construction of a simple model of behavior in an actual char bed. In the flaming pyrolysis zone of the gasifier a gas is generated that may be at a temperature from 1000°-1400°C. It also contains a relatively high proportion of CO_2 and H_2O, so that it can be further reduced by the char zone to a producer gas containing more CO and H_2. However this reduction is very endothermic, so that the gas is cooled very rapidly at these temperatures to a temperature range where the the reaction becomes slower and slower, approaching some limiting temperature where no further reaction occurs (we will see that this is at at about 800°C.)

In our first model of adiabatic char gasification, we assumed that the hot gas and char were at thermal equilibrium at the initial conditions shown in Table 8-2 and 8-3. The char zone was divided into a number of time zones as shown in the tables. We calculated the degree of char reaction in a short period from Eqs. 15 or 18. we calculated a cooling of the reactants from their heat capacity and from the degree of reaction. Each 1% of the reaction causes a cooling of about 24°C.

The temperature in the next zone was then recalculated, and a new reaction rate calculated. The temperature and composition were thus followed as a function of time until very little further reaction occurred. The time increment was increased as shown as the reaction rate slowed. If the char bed is moving, as in gasification, the position in the bed is proportional to the time increments.

The resulting temperature-time-distance history of the gas and char is shown in Table 8-2 and Fig. 8-9 for calculations using the data of Nandi and Onischak. It is seen in this figure that initially the char is consumed very rapidly, but that below about 1150°K the rate becomes very slow. This model does not take into account the fact that at the end of the flaming pyrolysis process the char is at pyrolysis temperature (about 700°C), while the gas is much hotter (1200°-1300°C). Furthermore it presumes a knowledge of gas composition at the end of the flaming pyrolysis zone which is very sensitive to char carryover. . We now believe that char-carryover is one of the most important variables in the stratified downdraft gasifier. Therefore, a second model was constructed to include heat transfer effects.

8.4.4.2 Char Carryover/Heat Transfer Model

A more complete user interactive model of the char reduction zone has been developed. It is written in basic for an IBM PC. In this model the amount of char carryover is specified as an initial condition. Also the ultimate analysis of the fuel, water content, percent fixed carbon after pyrolysis, off-gas temperature and air or oxygen as oxidant are specified.

The program first calculates the O_2/fuel ratio required for the off-gas temperature and char carryover. It then calculates the adiabatic temperature at the end of the pyrolysis zone, along with the gas composition. Using these initial conditions for the char reduction zone, and an estimate of the initial char temperature (≈ 600°C), the heat transfer kinetics and the thermodynamic quantities are calculated down the gasificer to yield gas and char temperatures and gas compositon and char conversion.

The model has been run to simulate gasifier performance for both air and oxygen. A sample of the program inputs and outputs are shown in Table 8-4 for air an oxygen gasification. The corresponding temperature gradients and degree of conversion for air and oxygen operation is shown in Figs. 8-10 and 8-11 respectively. From the table and the figures it is seen that there is not a lot of difference in the char reduction zone between air and oxygen operation, but the oxygen pyrolysis gases are about 100°C hotter than the air gases, even though the oxygen/fuel ratio is lower, as shown in Table 8-4. In both cases, the charcoal conversion is initially very rapid in the first minute and very slow after several minutes.

Table 8-2. Temperatures in Adiabatic Gas-Char Reaction Zone Calculated from data of Nandi and Onischek [34].

For the Reaction: $C + H_2O \longrightarrow CO + H_2$ ΔH = 40 kcal/mole
Rate Equation: $R = A \exp(E/RT)$ Rate Constants

Case	Wood	Test Gas	A min-1	E kcal/mole
1	Maple	50% H2, 50% N_2	2.42E+07	39,830
2	Maple	50% H2), 25% H_2, 25% N_2	4.14E+11	62,800
3	Jack pine	50% H2, 50% N_2	1.29E+07	39,100
4	Jack pine	50% H_2O, 25% H_2, 25% N_2	4.53E+11	63,600

Initial Conditions:
Char-Gas Temp 1400 K Char bed velocity 0.0333 cm/s

Case					1	2	3	4
Zone No No.	Time s	Position Z - cm	Rate (1) g/g-min	$-\Delta T(1)$ K	Temp K	Temp K	Temp K	Temp K
1	0	0.00	-0.24	-9.7	1400	1400	1400	1400
2	1	0.03	-0.22	-8.8	1390	1357	1393	1365
3	2	0.10	-0.20	-8.0	1382	1336	1387	1345
4	3	0.20	-0.18	-7.3	1374	1322	1381	1331
5	4	0.33	-0.17	-6.8	1366	1310	1376	1321
6	5	0.50	-0.16	-6.3	1359	1301	1370	1312
7	6	0.70	-0.15	-5.9	1353	1294	1365	1304
8	7	0.93	-0.14	-5.5	1347	1287	1361	1298
9	8	1.20	-0.13	-5.2	1342	1281	1356	1292
10	9	1.50	-0.12	-4.9	1337	1276	1352	1287
11	10	1.83	-0.12	-9.3	1332	1271	1348	1282
12	12	2.23	-0.10	-8.3	1322	1262	1340	1273
13	14	2.70	-0.09	-7.6	1314	1255	1333	1266
14	16	3.23	-0.09	-6.9	1306	1249	1326	1260
15	18	3.83	-0.08	-6.4	1300	1243	1320	1254
16	20	4.50	-0.07	-5.9	1293	1238	1315	1249
17	22	5.23	-0.07	-5.5	1287	1234	1309	1245
18	24	6.03	-0.06	-5.2	1282	1230	1304	1241
19	26	6.89	-0.06	-4.8	1277	1226	1299	1237
20	28	7.83	-0.06	-4.6	1272	1222	1295	1234
21	30	8.82	-0.05	-21.5	1267	1219	1291	1230
22	40	10.16	-0.04	-16.4	1246	1204	1270	1215
23	50	11.82	-0.03	-13.2	1229	1193	1254	1205
24	60	13.82	-0.03	-11.1	1216	1185	1241	1196
25	70	16.15	-0.02	-9.5	1205	1178	1230	1189
26	80	18.81	-0.02	-8.3	1195	1172	1221	1183
27	90	21.81	-0.02	-7.4	1187	1166	1212	1178
28	100	25.14	-0.02	-6.7	1180	1162	1205	1173
29	110	28.80	-0.02	-6.0	1173	1158	1198	1169
30	120	32.80	-0.01	66.4	1167	1154	1191	1165

Table 8-3. Temperature in gasifier predicted from Adiabatic Gas/Char Model (Based on Data of Edrich & Graboski [35])

Rate Equation $R = -f\ K1\ PCO_2/(1+K_2 pCO)$ where $f = \exp[-9970(1/T-1/T_p)]$
$K1 = \exp(-17141/T+12.309)$ $K2 = \exp(34021/T-28.43)$

Initial Conditions:

Vel-cm/sec	T_o (K)	T_p (K)	Degr Rx_o	PCO_o	PCO_{2o}
0.03	1400	1400	0.32	0.48	0.52

Zone No.	Time sec	Position Z - cm	Temp oK	Rate g/g-min	-/\T °K	Degree of Rx-%	P_{CO}	P_{CO2}
1	0	0.00	1400	-0.55	-21.8	0.32	0.48	0.52
2	1	0.03	1378	-0.39	-15.7	0.33	0.50	0.50
4	3	0.20	1350	-0.25	-10.1	0.34	0.51	0.49
5	4	0.33	1340	-0.21	-8.5	0.34	0.51	0.49
6	5	0.50	1332	-0.19	-7.4	0.35	0.52	0.48
7	6	0.70	1324	-0.16	-6.5	0.35	0.52	0.48
8	7	0.93	1318	-0.15	-5.8	0.35	0.52	0.48
9	8	1.20	1312	-0.13	-5.3	0.36	0.53	0.47
10	9	1.50	1307	-0.12	-4.8	0.36	0.53	0.47
11	10	1.83	1302	-0.11	-8.8	0.36	0.53	0.47
12	12	2.23	1293	-0.09	-7.5	0.36	0.53	0.47
13	14	2.70	1285	-0.08	-6.5	0.37	0.54	0.46
14	16	3.23	1279	-0.07	-5.8	0.37	0.54	0.46
15	18	3.83	1273	-0.06	-5.2	0.37	0.54	0.46
16	20	4.50	1268	-0.06	-23.3	0.38	0.55	0.45
17	30	5.49	1245	-0.04	-14.3	0.38	0.56	0.44
18	40	6.83	1230	-0.03	-10.3	0.39	0.56	0.44
19	50	8.49	1220	-0.02	-8.0	0.39	0.57	0.43
20	60	10.49	1212	-0.02	-6.5	0.40	0.57	0.43
21	70	12.82	1206	-0.01	-5.5	0.40	0.57	0.43
22	80	15.48	1200	-0.01	-4.7	0.40	0.57	0.43
23	90	18.48	1195	-0.01	-4.1	0.41	0.58	0.42
24	100	21.81	1191	-0.01	-7.3	0.41	0.58	0.42
25	120	25.81	1184	-0.01	-5.8	0.41	0.58	0.42
26	140	30.47	1178	-0.01	-4.8	0.41	0.58	0.42
27	160	35.80	1173	-0.01	-4.1	0.41	0.59	0.41
28	180	41.79	1169	0.00	-3.6	0.42	0.59	0.41
29	200	48.45	1166	0.00	-3.2	0.42	0.59	0.41
30	220	55.78	1162	0.00	-2.8	0.42	0.59	0.41
31	240	63.77	1160	0.00	-2.5	0.42	0.59	0.41
32	260	72.43	1157	0.00	-2.3	0.42	0.59	0.41
33	280	81.75	1155	0.00	-2.1	0.42	0.59	0.41
34	300	91.74	1153	0.00	-2.0	0.42	0.59	0.41

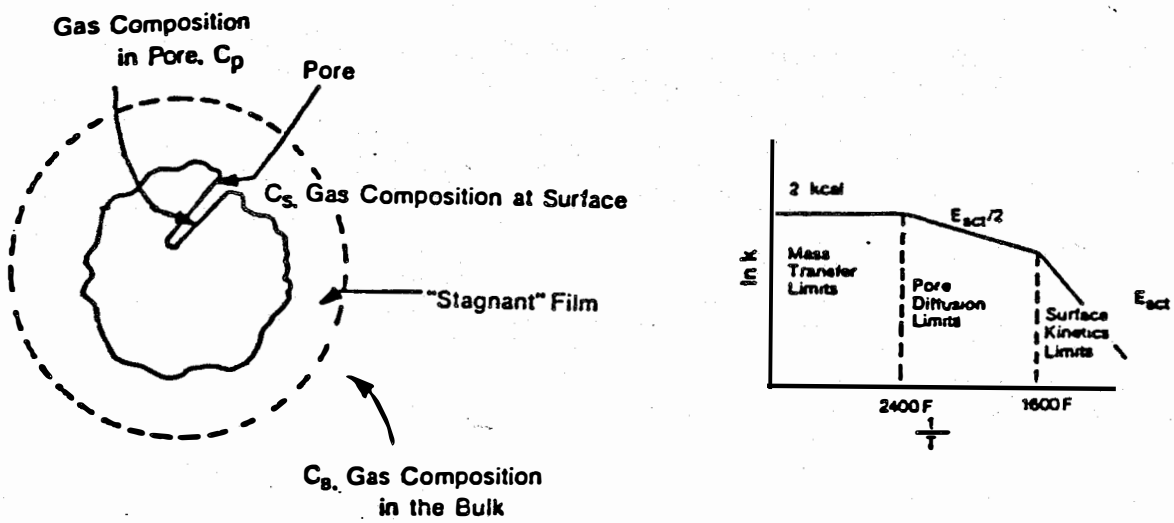

Figure 8-8 (a) Model of Porous Char Particle (b) The Effect of Temperature on Reaction Rate of Heterogeneous Processes.

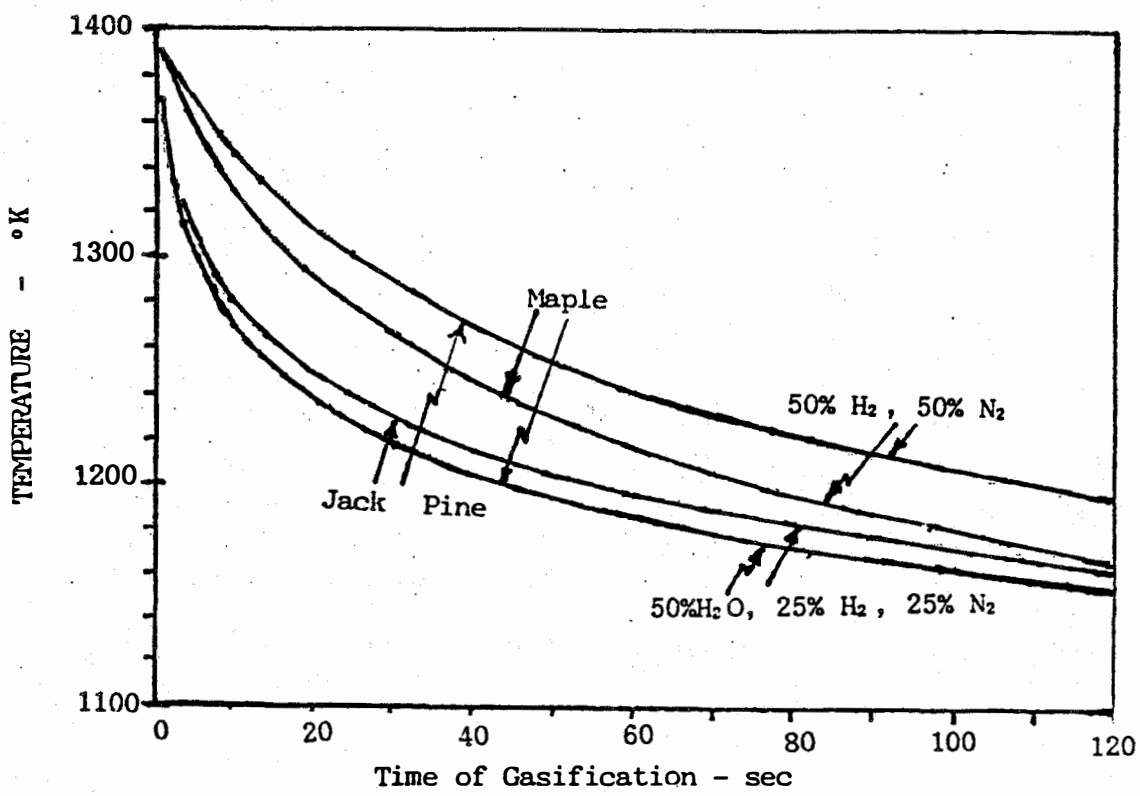

Figure 8-9 . Temperature Profiles in a Char Bed moving at 0.03 cm/sec Predicted from Kinetic Data of Nandi and Onischek for Maple and Jack Pine Charcoal.

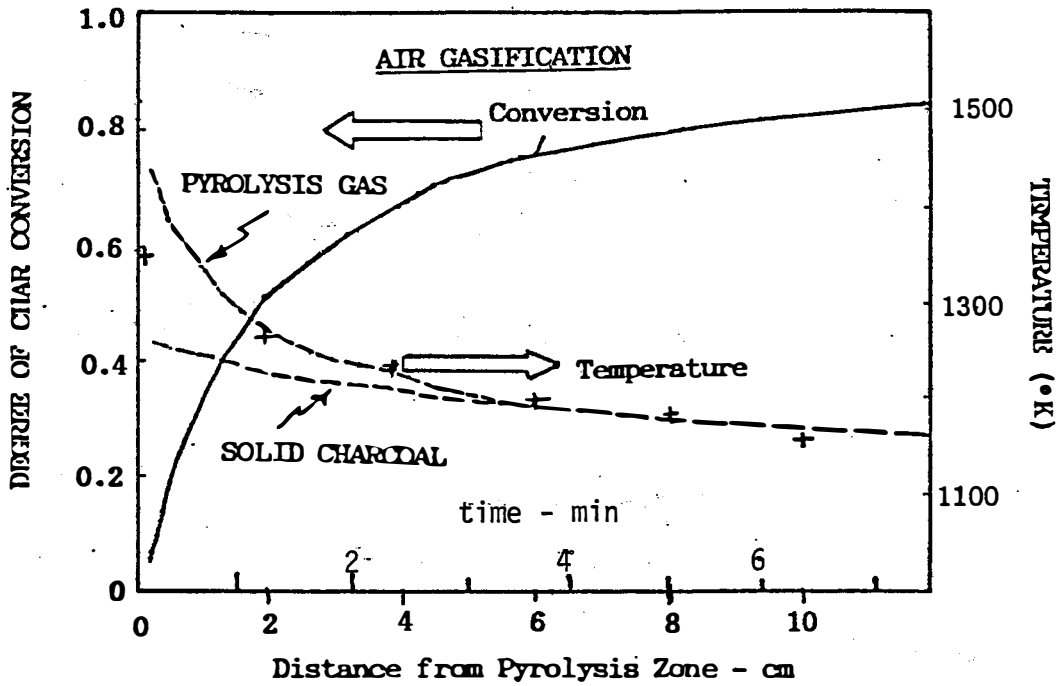

Figure 8-10. Degree of Conversion and Temperature Profile of Solid Char and Pyrolysis Gas Predicted by Char Carryover - Heat Transfer Model for Oxygen Gasification

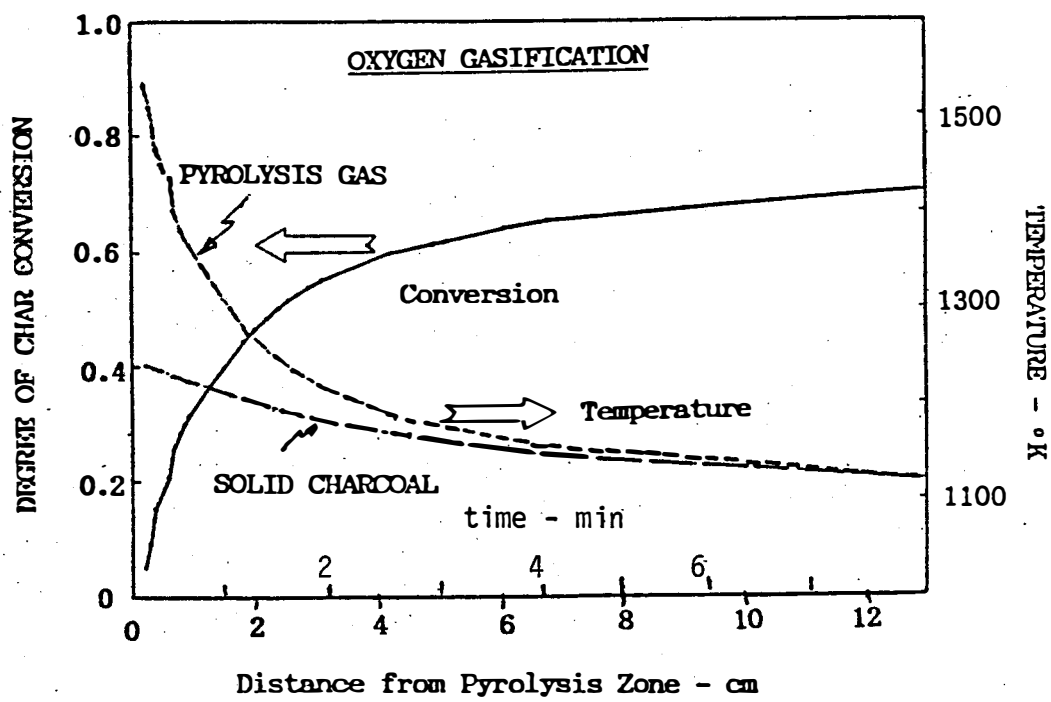

Figure 8-11. Degree of Conversion and Temperature Profile of Solid Char and Pyrolysis Gas Predicted by Char Carryover - Heat Transfer Model for Air Gasification

This model takes into account the effect of char-carryover that we have determined to be the principal variable in downdraft gasification because of its effect on the oxygen/fuel ratio. The effects of char carryover on the O_2/fuel ratio and the pyrolysis flame temperature predicted by the model are shown in Fig. 8-12. Here it can be seen that a high char carryover rate greatly reduces the oxygen/fuel ratio. This in turn reduces the temperature of the pyrolysis flame. (The effect is probably even stronger in practice; a lower flame temperature cracks fewer volatiles, so that high tar levels are associated with high char levels. This further reduces oxidant consumption even further, leading to even more tar, but this effect is not taken into account by the model.)

Table 8-4. Inputs and outputs of Char-carryover/heat transfer model for Figures 8-11 and 8-12.

Figure:	8-11	8-12
INPUTS:		
Oxidant	Air	Oxygen
Char Carryover	3%	3%
Moisture	10%	10%
Ultimate Analysis		
Carbon	50%	50%
Hydrogen	6%	6%
Oxygen.	44%	44%
Off-gas Temperature - K	1100	1100
Fixed carbon after pyrolysis	15%	15%
OUTPUTS:		
O_2/Fuel Ratio	0.52	0.42
Equivalence ratio	0.36	0.29
Gas quality - kJ/Nm^3	4610	7072
Gas temp after pyrolysis K	1475	1600

8.4.4.3 Summary of Char Gasification Models

While the results from the simple char gasification model calculations and the char carryover model differ in detail, they both predict that temperatures in will drop below 1200 K (927°C) in less than 2 min and that they will not drop below 1100 K (827°C) in a much longer period, an asymptotic approach to a temperature on the order of 800°-850°C. Thus, while the asymptotic behavior precludes establishing an exact time for char gasification, this behavior also indicates that it would require a very large increase in bed length to achieve significantly higher carbon conversions after the bed temperature has dropped to 800°C. For this reason we have arbitrarily chosen a time of 100 s for char gasification in our model below.

8.5 A PREDICTIVE MODEL OF THE STRATIFIED DOWNDRAFT GASIFIER

8.5.1 Spreadsheet Model of the Stratified Downdraft Gasifier

The Previous sections have developed models to predict the time required for the flaming pyrolysis stage and the gasification stage for a fixed bed, stratified downdraft gasifier. It now remains to combine these with the rate of fuel motion in the gasifier to predict the actual lengths required to accomplish these two stages in the final design.

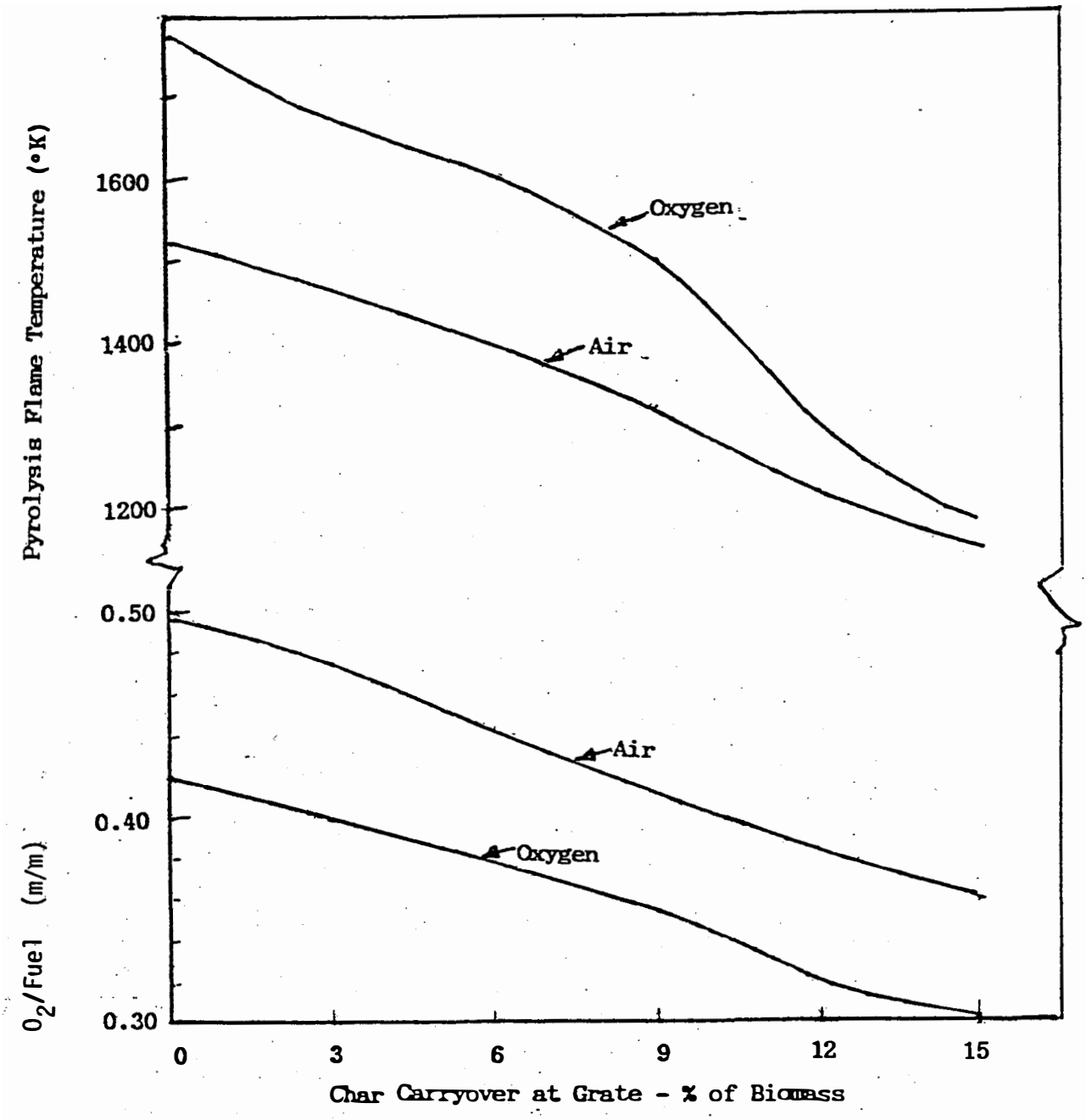

Figure 8-12 . Flame Temperature at End of Pyrolysis Zone and Oxygen Consumption for Oxygen and Air Gasification Predicted by Heat Transfer Model.

In the calculation shown in Table 8-5, the mass flow is determined from the process energy generated in the gas from relation

$$E_p = \dot{m}\, q_f\, e_d\, e_g \tag{8-22}$$

where $\dot{m}$ is the dry mass flow rate, q_f is the energy content of the biomass, e_d is the efficiency of the device using the gas for heat, power or chemical synthesis and e_g is the efficiency of the gasifier itself.

The diameter of the gasifier is determined from the maximum rating of the gasifier type. A conservative rule of thumb for the gasifier operating in the submerged mode on air is that it generates 11 GJ/m²-h (1 MMBtu/ft²-h). Operation in the top stabilized mode on oxygen or air permits ratings of 22 GJ/m²-h (2 MMBtu/ft₂-h).

The velocity of motion of the fuel in the gasifier is a function of the amount of wood being gasified and is given by

$$v_f = m/[A_g F_d\ (1 - F_v)] \tag{8-23}$$

where A_g is the cross-sectional area of the gasifier or the grate, F_d is the density of the fuel particles, and F_v is the void fraction of the chips or charcoal in the bed. The time for flaming pyrolysis is given by Eq. 8-5. (The product of $F_d(1 - Fv)$ gives the bulk density of the fuel). The length of the flaming pyrolysis zone, l_f, is then

$$l_{fp} = v_f\, t_{fp}, \tag{8-24}$$

where t_{fp} is the time for flaming pyrolysis.

The length of the charcoal gasification zone is given by

$$l_c = v_f\, t_c \tag{8-25}$$

where we take t_c arbitrarily to be 100 s.

The final gasifier design must provide at least sufficient depth for the flaming pyrolysis and char reduction zones. In practice more space must be left as a buffer zone for the grate, and, if the gasifier operates in the submerged mode, to contain the unburned fuel. Thus this model predicts minimum size for each zone at the design throughput for a specific fuel, but a larger zone may not cause problems. However, in the case of too large a char zone, the transport of spent char-ash to the grate can cause serious plugging of the bed and excessive heat loss as we found for oxygen gasifier.

The calculations in Table 8-5 can be represented graphically to scale with a spreadsheet diagram as shown in Fig. 8-13.

Table 8-5 was given as an example of calculation of gasifier design dimensions for a single fuel. Table 8-6 illustrates the design process in abbreviated form for six sets of gasifier conditions for a 2.9 MW_{th} (10 $MMBtu_{th}$) gasifier using chips or chunkwood with air (5 or 20% moisture) or oxygen. (The variables which change are in boldface to make them easier to locate.) In this case we have chosen a more conservative 2.7 MW_{th}/m^2 (500,000 Btu/h-ft₂) for air operation

Table 8-5. SIZING THE STRATIFIED DOWNDRAFT GASIFIER

This Table gives the predicted design of a gasifier using a spreadsheet (Lotus 123, etc.) model. To design any other gasifier substitute the desired values for the process and fuel requirements.

STEP I - DETERMINATION OF GAS ENERGY AND FUEL CONSUMPTION

In choosing a gasifier size for a particular process it is first necessary to determine the amount of gas and fuel required. This requires a knowledge of the process energy to be delivered, E_p, the process energy efficiency, e_p, the input process energy required in the gas, E_g, the gasifier efficiency, e_g and the fuel energy, Q_f. The following example is for a Diesel generator.

Process		Diesel Generator
Process Energy Delivered	E_p	800 kW
Process efficiency	e_p	0.25
Gas Energy Required	$E_g = E_p/e_p$	11.5 GJth/h[1]
Gasifier efficiency	e_g	0.80
Fuel energy content	Q_f	21.00 GJ/ton
Fuel Consumption	$E_g/e_g Q_f$	0.69 tons/h

STEP 2 - CALCULATION OF GASIFIER DIAMETER

The diameter of the gasifier is determined from the maximum specific power, p_{max}. This figure is derived from experience with the particular gasifier type and mode of operation. Many groups have operated the stratified downdraft gasifier with a specific power of 11.6 GJ/m$_2$-h (1 MMBtu/ft$_2$-h) in sizes from 3-30 in. This is a conservative rating, and with mechanical char removal, oxygen or other variations the specific power can climb to at least 23.3 GJ/m$_2$-h (2 MMBtu/scf-h). We include some English units for convenience.

Max spec heat rate	$p_{max} = E_g/A_g$	23.3 GWth/m^2-h[1]
(Max spec heat rate)	p_{max}	2.00 MMBtu/ft^2-h
Grate area	$A_g = E_g/p_{max}$	0.49 m^2
(Grate area)	A_g	2.25 ft^2
Diam of Gasifier	D	0.79 m
(Diam of gasifier)	D	2.59 ft

STEP 3 - CALCULATION OF BED DEPTH FOR SPECIFIC FUEL

The minimum depth of the bed required at maximum throughput is calculated from the time of pyrolysis as calculated from the modified Huff equation (Eq. 8-5) plus the time required for char gasification (100 s) multiplied by the velocity of the fuel.

[1] GJ_{th} is thermal GigaJoules, GW_{th} is GigaWatts thermal.

FUEL PROPERTIES

Fuel:
Inch pine wood chips
Proximate Analysis, (Dry basis)

Volatiles		0.84	
Fixed Carbon		0.15	
Ash		0.01	
Moisture (wet basis)		0.20	
Wood density	F_d	0.40	g/cm^3
Bulk density		0.15	g/cm^3
Void fraction	F_v	0.63	
Length	l	2.50	cm
Width	w	2.00	cm
Height	h	0.60	cm
Avg diam	d	1.44	cm
Volume	V	3.00	cm^3
Area	A	15.40	cm^2
Sphericity	F_s	0.65	
Gasifier Conditions:			
Oxidant (Oxygen 1; air 0.21)	F_o	0.21	
Pyrolysis Temperature	T	873	K
Pyrolysis zone			
Pyrolysis time	t_p	111.3	s
Fuel Velocity	V_f	0.26	cm/s
Pyrolysis zone length	l_p	28.8	cm
Pyrolysis heat flux	q	1.40	W/cm^2
Char reaction zone:			
Char Reaction time	t_c	100	s
Char zone length	l_c	25.83	cm
Total Gasifier Active Length			
Fuel transit time	t_p+t_g	231	s
Active zone length	l_p+l_g	55	cm

This program is available from the author in the form of a spreadsheet on disk. To calculate gasifier dimensions for other fuels and other processes, enter their properties and press CALC on the spreadsheet program.

Figure 8-13. Diagram of 800 kW Gasifier for Diesel Generation Showing Projected Zone Dimensions

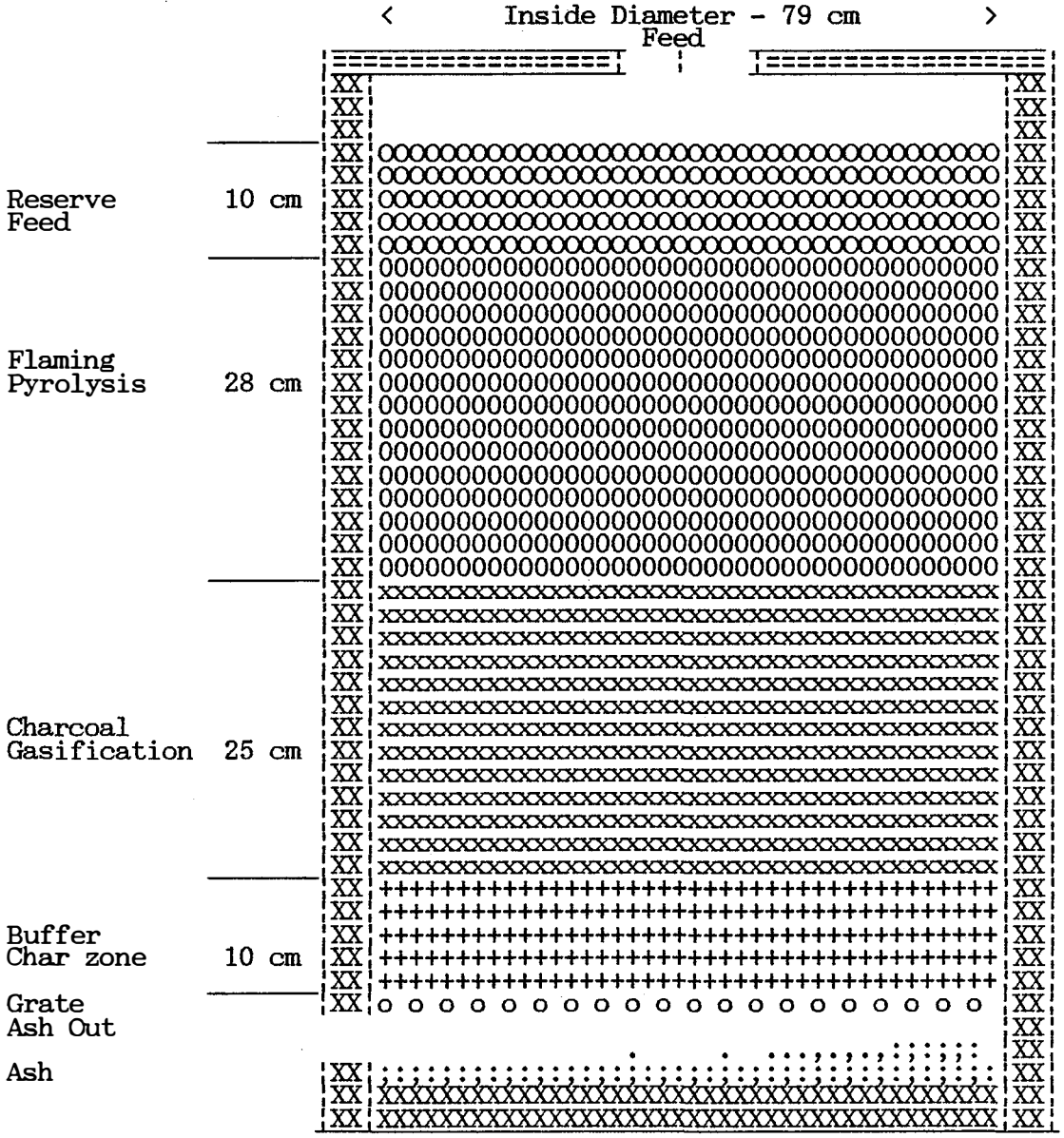

Table 8-6. DYNAMIC GASIFIER DESIGN FOR SELECTED FEEDS

INPUTS	SYMBOL	UNITS	(a)	(b)	(c)	(d)	(e)	(f)
BIOMASS PROPERTIES								
Fuel:			Inch Wood chips - Pine			Chunk wood - pine		
Density (dry basis)	Fd	tonne/m3	0.40	0.40	0.40	0.40	0.40	0.40
Bulk density	Fb	tonne/m3	0.12	0.12	0.12	0.15	0.15	0.15
Void fraction	Fv		0.70	0.70	0.70	0.63	0.63	0.63
Length	l	cm	2.50	2.50	2.50	10.00	10.00	10.00
Width	w	cm	2.00	2.00	2.00	5.00	5.00	5.00
Height	h	cm	0.50	0.50	0.50	5.00	5.00	5.00
Avg diam	d	cm	1.36	1.36	1.36	6.29	6.29	6.29
Volume	V	cm3	2.50	2.50	2.50	250.00	250.00	250.00
Area	A	cm2	14.50	14.50	14.50	250.00	250.00	250.00
Volatiles			0.74	0.74	0.74	0.74	0.74	0.74
Char			0.15	0.15	0.15	0.15	0.15	0.15
Ash			0.01	0.01	0.01	0.01	0.01	0.01
Moisture (dry basis)			0.05	0.20	0.20	0.05	0.20	0.20
OXIDANT (.21 = Air; 1.0 = oxygen)			0.21	0.21	1.00	0.21	0.21	1.00
CALCULATION OF GASIFIER DIMENSIONS - MAXIMUM RATE ASSUMPTIONS								
Max Spec heat rate	m/Ag	MWth/m2-h	2.72	2.72	8.17	2.72	2.72	8.17
(Max Spec heat rate)	m/Ag	MMBtu/ft2-h	1.00	1.00	3.00	1.00	1.00	3.00
Max spec feed rate	m/Ag	tonne/m2-h	0.57	0.57	1.71	0.57	0.57	1.71
(Max spec feed rate)	m/Ag	lb/ft2-h	125	125	375	125	125	375
CALCULATION OF GASIFIER DIAMETER								
Required thruput	W	MWth	2.93	2.93	2.93	2.93	2.93	2.93
(Required thruput)	W	MMBtu/h	10	10	10	10	10	10
Required Feed Rate	m	kg/h	568	568	568	568	568	568
(Required feed rate)	m	lb/h	1250	1250	1250	1250	1250	1250
Grate area	Ag	m2	1.08	1.08	0.36	1.08	1.08	0.36
(Grate area)	Ag	ft2	10.00	10.00	3.33	10.00	10.00	3.33
Diam of Gasifier	D	m	1.17	1.17	0.68	1.17	1.17	0.68
(Diam of gasifier)	D	ft	3.57	3.57	2.06	3.57	3.57	2.06
CALCULATION OF GASIFIER BED HEIGHT								
Pyrolysis time	tp	s	60	75	29	740	919	358
Fuel Velocity	Vf	cm/sec	0.132	0.132	0.397	0.106	0.106	0.318
Pyr Zone Length	lp	cm	7.98	9.92	11.59	78	97	114
Char Reaction time	tg	sec	120	120	120	120	120	120
Char zone length	lg	cm	15.88	15.88	47.63	12.70	12.70	38.10
Transit time	tp+tg	sec	180	195	149	860	1039	478
Total zone length	lp+lg	cm	24	26	59	91	110	152

This model should be considered a first order approximation. It takes into account the effect of particle size, density, shape and oxidant based on an empirical equation. However, it neglects the effect of interparticle effect, variations in char gasification rates, oxygen/fuel ratio and carbon carryover. An improved model could be constructed using the interactive program described above and more data from larger scale units to improve the assumptions.

8.5.2 Comparison of model with observed gasification conditions

Obviously we would like to test the predictions of the above model with measurements on real gasifiers. It is relatively easy to measure the gas composition and temperature below the grate, and such measurements are available for some gasifiers.

Measurements of gas composition and temperature were made at the grate of the 7.5 cm diameter transparent gasifier, operating with 1 cm diameter birch dowels, as a function of the distance of the top of the flaming pyrolysis zone above the grate. The results are shown in Fig. 8-14. From this it is seen that the heating value of the gas reaches a maximum at 24 cm with a grate temperature of 900 °C and then decreases.

Unfortunately it is very difficult to measure temperatures inside a gasifier. Worse yet, the measurements tend to be unreliable for a number of reasons. Probes can be used to sample the gases through the bed. However the gas sampled may represent pyrolysis gas if the probe is at the particle surface or partial combustion gas if it is in an open cavity. The temperature measurements are also highly suspect. A thermocouple which touches a solid will respond to the temperature of the solid; a thermocouple in the gas space can respond to gas temperature, but is also strongly influenced by local radiation heat transfer. A measurement of temperatures in the flaming pyrolysis zone is shown in Fig. 8-3 and 8-15.

We strongly recommend that a program be established to operate a very stable gasifier and measure the temperature, tar, and composition as a function of throughput, char carryover, oxidant etc. However, we have not yet had sufficiently stable operating conditions to do a thorough parametric study. The data of Wallawender is probably the most extensive and accurate data on an operating stratified downdraft gasifier [36]. The current work of Levie on the behavior of a single particle in flaming combustion will give valuable information for improved modelling of the flaming pyrolysis zone [31].

8.6 STABLILIZATION OF THE FLAMING PYROLYSIS ZONE

In studying the combustion of gases, the rate of flame propagation into the unburned gases is a fundamental parameter used in the modelling of flame devices.

In the air downdraft gasifier the flaming pyrolysis zone moves up through the bed toward the incoming oxidant at a constant propagation rate. The bed is moving down however, so that the position of the zone may be stable, it may move up or it may move down depending on the operating conditions of heat loss, moisture content, ignition temperature of the fuel, char removal, and throughput of the gasifier. For oxygen operation, the flaming pyrolysis zone moves to the top of the bed whose length must then be fixed for stable operation. The velocity of propagation of the pyrolysis zone into the unburned fuel is fundamental in determining gasifier throughput.

In order to understand the mechanisms governing pyrolysis zone stability, laboratory experiments were run using a 5-cm diameter quartz tube as the gasifier. The position of the flaming pyrolysis zone was easily measured. From this the velocity of propagation of the zone was measured under a variety of conditions [37]. A number of methods of stabilizing the zone position were

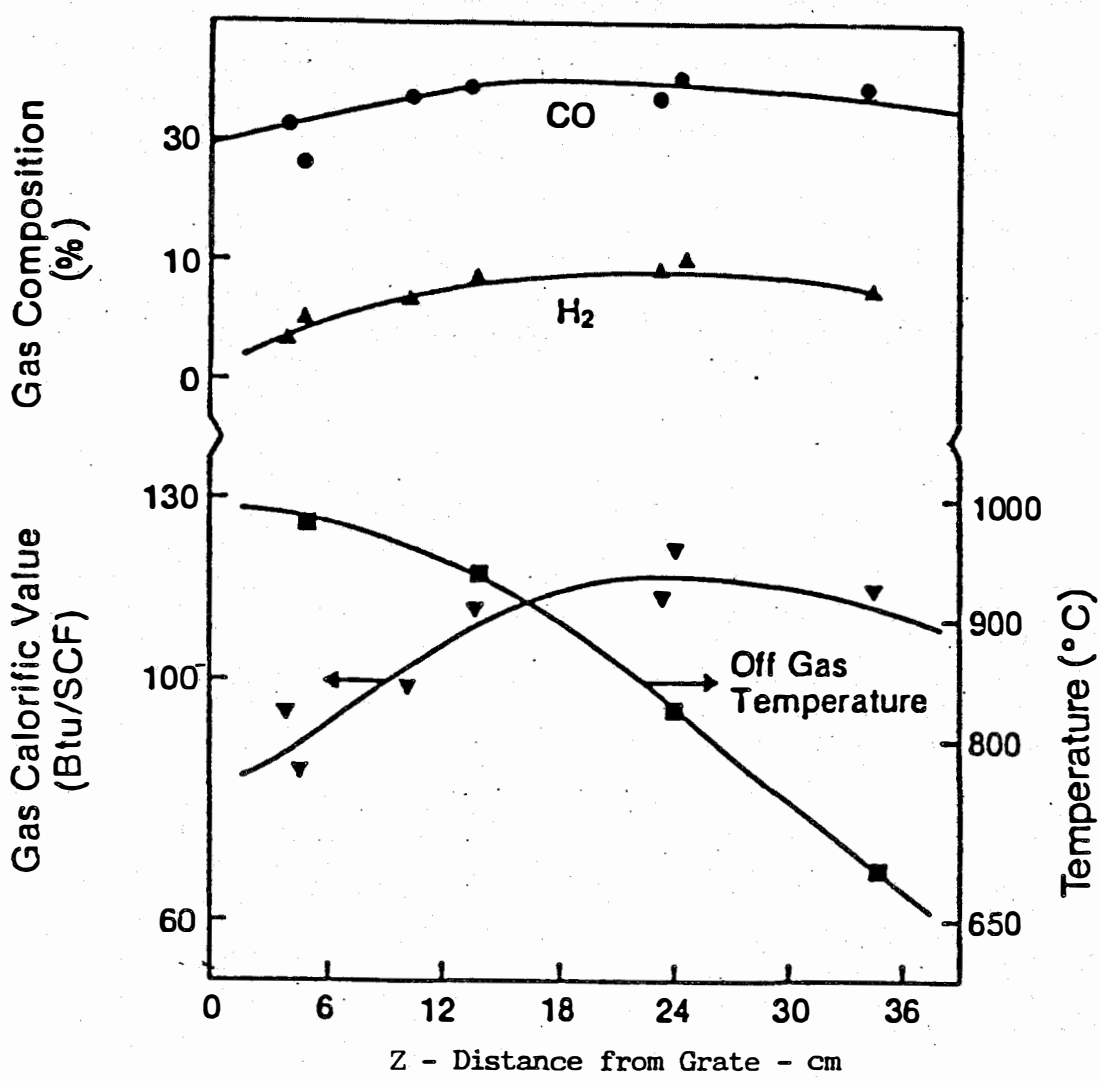

Figure 8-14 Gas Quality, Temperature (at the Grate) And composition as a Function of Distance Z Above the Grate of the Onset of Flaming Pyrolysis

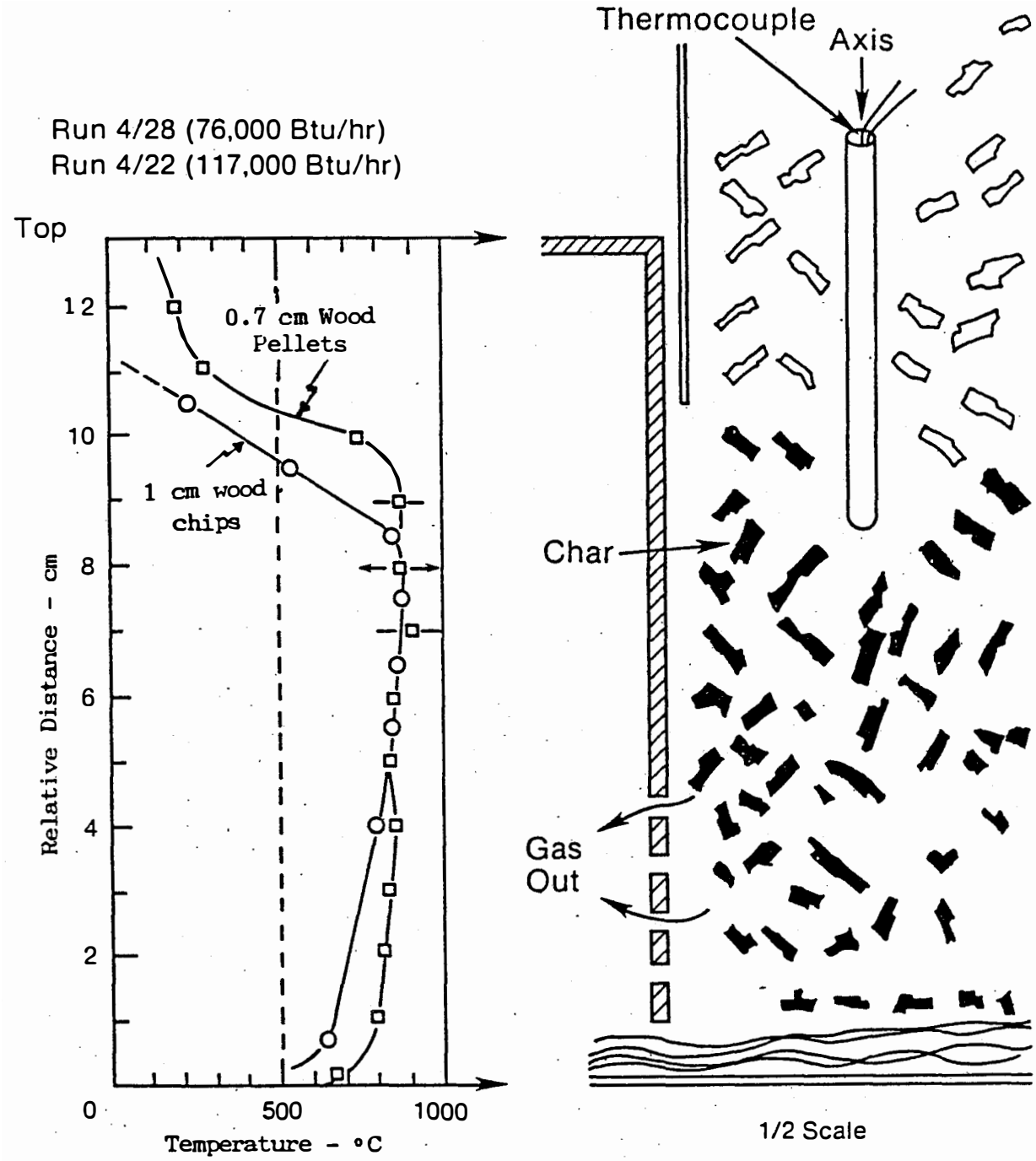

Figure 8-15. Temperatures and Compositions Measured in Downdraft Gasifier

assessed. The operation of the stratified downdraft gasifier will not be completely understood until the factors which determine propagation rate are understood.

SYMBOLS

Variables:

A - Area
C_p - Heat capacity at constant pressure
D - Effective particle size (Calculated from $V^{1/3}$)
e - efficiency
E - energy generated in gasifier
F - Fractional value (of moisture content, density etc.)
h_p - Heat for pyrolysis
Δh_p - heat change associated with pyrolysis, heat of pyrolysis
k - kinetic constant
K_n - Constants
m - mass flow rate
n_i - The nth component in a reaction
P - pressure
q - heat flux, heat per unit area
r - rate of reaction
R - Universal gas constant
t - Time (of flaming pyrolysis, char gasification etc.)
T - Temperature
v - Velocity
V - Particle volume,

Subscripts:

c - conduction
c - charcoal
d - density
d - device
f - fuel
fp - flaming pyrolysis
g - gasifier
m - moisture
o_2 - oxygen in oxidant
p - pyrolysis
r - radiation
s - sphericity
s - surface temperature of particle during pyrolysis
v - void

REFERENCES

1. Field, M. A., Gill, D. W., Morgan, B. B. and Hawksley, P. G. W., "Combustion 260 of Pulverized Coal", *The British Coal Utilization Research Association (BCURA),* 1967, republished by the Institute of Energy in 1983.

2. Mulcahy, M. F. R. and Smith, I. W. "Kinetics of Combustion of Pulverized Fuel: A Review of Theory and Experiment", *Rev. Pure and Appl. Chem.* Vol.19, 1969, p. 81.

3. Smith, I. W., "The Combustion Rates of Coal Chars: A Review", in *Nineteenth Symposium (International) on Combustion*, the Combustion Institute, 1982, pp. 1045-1065.

4. Reed, T.B., and Markson, M., "A Predictive Model for Stratified Downdraft Gasification," *Progress in Biomass Conversion,* edited by D. Tillman and E.C. Jahn Vol. 4, Academic Press, New York, 1983 p. 217-254.

5. Bacon, D. W., Downie, J., Hsu, C. C., Runaman, R. and Larish, G., "An Annotated Bibliography of Gasifier Modelling", *Dept. of Chem. Eng. Rept. K7L 3N6* Queen's University, Kingston, Ontario, 1982.

6. van den Aarsen, F.G. et al., "Wood Pyrolysis and CO2 Char Gasification in a Fluidized Bed," *Fundamentals of Thermochemical Biomass Conversion: An International Conference,* edited by R.P. Overend, T.A. Milne, and L. Mudge. Elsevier, N. Y., 1985.

7. Antal, M.J., "The Effects of Residence Time, Temperature and Pressure on the Steam Gasification of Biomass," ACS Symposium Biomass as a Nonfossil Fuel *Source,* Honolulu Meeting, 1 April 1979.

8. Buekens, A.G. and Schoeters, J.G., "Modelling of Biomass Gasification," *Fundamentals of Thermochemical Biomass Conversion: An International Conference,* Estes Park, Colorado, October 18-22, 1982. Proceedings edited by R.P. Overend, T.A. Milne, and L. Mudge. Elsevier. 1985.

9. Chan, W. C. R., Kelbon, M. and Krieger, B. B. "Modelling and experimental Verification of Physical and Chemical Processes during Pyrloysis of a Large Biomass Particle", *Fuel*, Vol. 64, (1985), p .1505.

10. Desrosiers, R., *Fundamental Air Gasification Engineering Parameters,* SERI/PR-234-1470, 1982. *Also Gasification Engineering,* Quarterly Report, SERI/PR-622-1348, (December 1981) and SERI/PR-622-1153, 1981.

11. Diebold, J.P. "The Cracking Kinetics of Depolymerized Biomass Vapors in a Continuous Tubular Reactor", *Master's thesis, Colorado School of Mines,* Golden, Colo., 1985.

12. Groeneveld, M.J. The Co-Current Moving Bed Gasifier, *PhD thesis, Twente Univ. of Technology,* the Netherlands, 1980. Also published by Krips Repro Meppel.

13. Groeneveld, M.J. and Van Swaaij, W.P.M. "The Design of Co-Current, Moving Bed Gasifiers Fueled by Biomass," *Thermal Conversion of Solid Biomass Wastes, I*, ed. Jones, J.L. and Radding, S.B., ACS Symposium Series #130,

(Am Chem. Soc., Washington, DC), 1980.

14. Gumz, W., *Gas Producers and Blast Furnaces,* J. Wiley and Sons, New York, 1950.

15. Herman, D. R., "The Rate of Pyrolysis of Densified Ponderosa Pine," *Masters Thesis (T-2525), Colorado School of Mines,* Dept. of Petroleum-Refining Engineering, 1981.

15. Reed, T.B., Levie, B., Markson, M.L., and Graboski, M.S., "A Mathematical Model for Stratified Downdraft Gasifiers," in *Symposium on Mathematical Modeling of Biomass Pyrolysis Phenomena,* Division of Fuel Chemistry, 28, 5, the American Chemical Society, Washington, D.C., 1983.

16. Reed, T.B., and Levie, B. "A Simplified Model of the Stratified Downdraft Gasifier," *The International Bio-Energy Directory and Handbook 1984,* ed Paul F. Bente, Jr. The Bio-Energy Council, 1625 Eye St. NW, Suite 825A, Washington, DC, 1984, pp. 379-389.

17. Bunbury, H. M. *The Destructive Distillation of Wood,* Benn Bros. Ltd. London, 1923.

18. Antal, M. J. Jr., "Biomass Pyrolysis: A Review of the literature, Part I - Carbohydrate Pyrolysis" *Advances in Solar Energy* ed K. W. Boer and J. A. Duffie (American Solar Energy Soc., Boulder, CO) Vol 1, pp. 61-112, 1982.

19. Antal, M. J. Jr., "Biomass Pyrolysis: A Review of the Literature, Part II-Lignocellulose Pyrolysis", in *Advances in Solar Energy* ed K. W. Boer and J. A. Duffie (American Solar Energy Soc. Inc., Boulder CO) Vol 2, pp 175-255, 1985.

20. Milne, T. A., Evans, R. E. and Soltys, M. N. "Characterization of Biomass Pyrolysis Oils by Flash Evaporation and Direct, Molecular-Beam Mass Spectrometery", in **Energy from Biomass and Wastes VIII**, (Klass, ed.) Lake Buena Vista, Fla., Jan 30, 1984, IGT, 1984.

21. Evans, R. E. and Milne, T. A., "Molecular Characterization of the Pyrolysis of Biomass. I Fundamentals" *Energy and Fuels* Vol. 1, 1987.

22. Elliott, D. C., "Analysis and Comparison of Biomass Pyrolysis/Gasification Condensates - An Interim Report", PNL-5555, Pacific Northwest Laboratory, Richland Washington, 1985.

23. Beckman, D. and Elliot, D. C., "Comparisons of the Yields and Properties of the Oil Products from Direct Thermochemical Biomass Liquefaction Process," *Canadian Journal of Chemical Engineering,* Vol. 63, 99-104, 1985.

24. Kothari, V. and Antal, M. J. Jr., "Numerical Studies of the Flash Pyrolysis of Cellulose", *Fuel*, Vol. 64, 1487 (1985).

25. Simmons, W. W. and Ragland, K. W., "Single Particle Combustion Analysis of Wood," in *Fundamentals of Thermochemical Biomass Conversion: An International Conference.* ed. R.P. Overend, T.A. Milne, and L. Mudge. Elsevier. 1985.

26. Desrosiers, R. E., and Lin, R. J., "A Phase-Change Approach to Macro-

Particle Pyrolysis of Cellulosic Materials", *ACS Fuel Symposium,* Vol 28, 1983, p. 338.

27. Reuther, J. J., Karsner, G. G. and Jack, S. T., "Plane Flame Furnace Combustion Studies of Pulverized Wood," in *Fundamentals of Thermochemical Biomass Conversion: An International Conference.* ed. R.P. Overend, T.A. Milne, and L. Mudge. Elsevier. 1985.

28. Huff, E. R.,"Effect of Size, Shape, Density, Moisture and Furnace Wall Temperature on Burning Times of Wood Pieces," in *Fundamentals of Thermochemical Biomass Conversion: An International Conference.* ed. R.P. Overend, T.A. Milne, and L. Mudge. Elsevier. 1985.

29. Huff, E. R., Personal Communication, Letters Feb, Mar 1987.

30. Cowdery, C., "Measurement of the Mass and Energy Balance in Contact Fast Pyrolysis of Wood", *Masters Thesis T-3459,* Colorado School of Mines, 1987.

31. Reed, T. B., Diebold, J. and Desrosiers, R., "Heat Transfer Perspectives", *Proceedings of the Specialists' Workshop on the Fast Pyrolysis of Biomass,* Ed. J. Diebold, SERI/CP-622-1096 (Solar Energy Research Institute, Golden, CO) 1981.

32. Levie, B., work currently in progress at Solar Energy Research Institute, Golden, Co.

33. Graboski, M., in *A Survey of Biomass Gasification, Vol. II",* SERI/TR-33-239, edited by Solar Energy Research Institute, Golden, CO, 1979. Chapter 7. Published in hard cover as T. Reed, editor, *Biomass Gasification: Principles and Technology,* Energy Technology Review No. 67, Noyes Data Corp, Park Ridge, NJ, 1981.

34. Nandi, S.P. and Onischak, M., "Gasification of Chars Obtained from Maple and Jack Pine Woods," in *Fundamentals of Thermochemical Biomass Conversion: An International Conference.* ed. R.P. Overend, T.A. Milne, and L. Mudge. Elsevier. 1985.

35. Edrich, R., Bradley, T., and Graboski, M. "The Gasification of Ponderosa Pine Charcoal," in *Fundamentals of Thermochemical Biomass Conversion: An International Conference.* ed. R.P. Overend, T.A. Milne, and L. Mudge. Elsevier. 1985.

36. Walawender, W. P., Chern, S. M. and Fan, L. T., "Wood Chip Gasification in a Commercial Downdraft Gasifier", in *Fundamentals of Thermochemical Biomass Conversion: An International Conference.* ed. R.P. Overend, T.A. Milne, and L. Mudge. Elsevier. 1985.

37. Reed, T. and Markson, M. "Reaction Velocities in a Downdraft Gasifier, in *Fundamentals of Thermochemical Biomass Conversion: An International Conference.* ed. R.P. Overend, T.A. Milne, and L. Mudge. Elsevier. 1985.

CHAPTER 9

GAS AND METHANOL PROCESS COSTS AND ECONOMICS

9.1 INTRODUCTION

During the six years covered in this report, the authors have taken part in many economic evaluations with industrial and government groups interested in economic questions relating to gasification and methanol production. We present here a simplified method for calculating approximate costs for air and oxygen gasification. We will also present here a summary of methanol production cost studies that have appeared in the last decade, including two major studies on the SERI-SGI gasifier. We will present a model for calculation of methanol manufacturing costs from a variety of feedstocks.

In this report we take the term "cost" to mean the direct costs involved in constructing a plant, operating the plant, and buying feedstock for the plant. We give in this chapter a simple method for calculating these costs based on separating the total cost into the feedstock cost and the operating cost. A major part in turn of the operating cost is the capital cost of the plant and we give methods of estimating capital costs. (We have adjusted all costs to 1987 dollars to make comparison possible.)

While the **cost** of production of gas or fuels from biomass can be assessed with some accuracy, a full scale economic evaluation of producing gas and methanol from biomass lies beyond the scope of this report, since it would also involve tax credits, return on investment, market analysis, etc.

Cost and **economic evaluation** is an essential part in the decision process leading to building a gasification or methanol plant. A single economic evaluation of a specific proposed plant performed by a reputable A&E firm can cost several hundred thousand dollars.

Cost and **economic evaluation** is also an essential part in making decisions about the sources of our future fuels in this country. Various U.S. government branches funded many studies of generalized plants to determine the cost of replacing petroleum with other fuels [1-10]. Both kinds of studies give a useful perspective on calculating plant costs and economics.

Gasification of biomass or coal to produce a low- or medium-energy gas was economically attractive and was a major industry in the United States until World War II. After the war the installation of natural gas pipelines and the low cost of oil made gasification uneconomical in most parts of the world. The equipment was dismantled and the technology forgotten.

With the advent of rising oil prices after OPEC I (1973) and OPEC II (1979), it appeared that gasification of coal or biomass would again be economically attractive as a source of process gas or synthesis gas for methane, methanol, or hydrocarbon manufacture.

The U.S. Department of Energy and other agencies have funded a number of economic studies that usually showed that production of gas or liquid feeds from alternate feedstocks was economically attractive during a period of higher oil costs or shortages [11-14]. A number of demonstration sized coal gasification plants were built and tested. Most of them are now shut down, in

part because of decreased oil prices and in part to operational difficulties. Nevertheless two major projects, the Great Plains Coal [11] gasification project and the Cool Water Power [12] generation project, have operated long enough to demonstrate technical feasibility during this period and plans are under way for further coal gasification plants of the Cool Water type.

During this period a number of biomass gasification R&D projects were also begun [13]. A few have survived the drop in oil prices, and more are being considered for special applications where biomass residues are available in sufficient supply.

9.2 COSTS OF LOW AND MEDIUM ENERGY GASIFICATION FOR PROCESS ENERGY AND SYNTHETIC FUEL PRODUCTION

9.2.1 Basis of Gas Cost Calculations

This section describes a simple generic method for calculating the magnitude of costs for gas generation using certain rules of thumb. A more accurate cost calculation would be site-specific and would require site specific estimates of costs, long range contracts, bonding costs etc. A more accurate cost estimate would obviously be mandatory before going forward with a specific cost.

If a gas is to be burned for generation of process heat, (e. g. for drying, for lime or cement kilns, glass factories etc.) a low energy gas is usually used. If the gas is to be used in turbines for power generation or distributed in pipelines, it is more important to have a higher energy gas, and preferably at high pressure. The cost of production of medium energy gas is significantly higher than the cost of low Btu gas. Thus each case must be considered separately.

Costs can be calculated on an annual basis or a unit basis. Generally we wish to know how much gas will cost per unit of energy ($/kJ or $/MMBtu) in the gas. However this depends on one time expenditures such as capital cost or annual costs such as taxes and insurance. We will represent unit costs here with a lower case "c". We will represent one time and annual costs with an upper case "C". (See Nomenclature) For purposes of approximation, we will separate the feedstock biomass cost from all the other annual costs, since this cost typically dominates total cost. We propose to calculate gas energy cost from

Cost of Gas = Operating Cost + Feed Cost

Annual Basis: $$C_g = C_o + C_f/E \qquad (9\text{-}1)$$

Unit Basis: $$c_g = c_o + c_f/E, \qquad (9\text{-}2)$$

where C_g is the annual gas production cost composed of the annual feedstock cost, C_f and the annual operating cost (exclusive of feed) C_o. (E is the efficiency of converting the energy in the biomass to gas and is typically 0.70 to 0.80.)

The largest part of the operating cost depends on the plant capital cost, C_P. The capital cost of a plant is a one-time cost, depending on design, siting etc. Depreciation and debt service of the capital cost are major parts of the

annual operating cost C_o, and will depend on depreciation rate and interest costs. The balance of the operating cost is composed of labor, utilities, supplies other than fuel, maintenance, insurance, and taxes.

We will call the ratio of operating cost to capital cost, C_o/C_p the operating cost ratio, R_o.

9.2.2 Low Energy Gas Production Cost

A typical capital cost for an air gasifier system is $15,000 per million Btu per hour (MMBtu/h) of capacity [13,16,17]. The operating cost will be about 20% of this value since an air plant has relatively low fixed costs. Thus $C_o = R_o C_p$ = $3,000/yr. On an hourly basis, this amounts to c_o = $0.34/h. (If it is planned to operate intermittently or seasonally, the cost must be adjusted accordingly.)

Wood and other biomass has typically an energy content of 8,000 Btu/lb or 16 MMBtu/ton on a 10% moisture, low ash basis. Actual analyses of the biomass to be used should be obtained and corrected to this basis for these calculation.

As an example, wood at $32/dry ton is equivalent to a feedstock cost of $2.00/MMBtu. If the gasifier is 80% efficient, the feedstock cost in the gas is $2.50/MMBtu. Adding the operating cost to the feed cost gives $2.84/MMBtu-h gas cost. Obviously this is a very rough approximation but breaks down the components so that one can make a more specific estimate as needed. In this case the feedstock constitutes 88% of the total gas cost.

A sample of these calculations is shown in the spreadsheet calculations of Table 9.1. A spreadsheet calculation can be used to explore the effect of varying the parameters on the cost of making low energy gas.

9.2.3 Medium Energy Gas from Oxygen Gasification

If the gas is to be used for synthesis of methanol, gasoline, other alcohols, natural gas, or ammonia, it is necessary to have primarily CO and H_2 in the gas (syn-gas) and usually requires the use of oxygen. (However, pyrolytic systems are also being developed for some of these uses [13].)

An oxygen gasifier requires a sealed feeding system and thus is more complex than an air gasifier. However, the high pressure feeding system permits generating the gas under pressure, an advantage for subsequent use in pipelines, engines, turbines, or for chemical synthesis, so the gas has a higher end-use value.

Capital costs for oxygen gasifiers are higher than for air gasifiers. As an example, oxygen gasifiers are expected to cost $25,000/MMBtu/h. Oxygen also adds to the operating cost, which is expected to be 30% of the capital cost (see below). The estimate of operating cost would then be $0.86/MMBtu-h as shown in Table 9-1.

Again assuming $32/ton for wood and 80% efficiency, the feedstock cost is $2.50/MMBtu of medium energy gas or synthesis gas. Adding these operating and fuel costs together, we obtain a cost of $3.36/MMBtu-h for medium energy synthesis gas made by oxygen gasification. The calculations are shown in Table 9-1.

Table 9-1. Typical Cost Calculations for Making Low and Medium Energy Gas

	Low Energy Gas (1)	Medium Energy Gas (2)	Units
OPERATING COSTS			
Capital Cost (3)	$15,000	$25,000	$/MMBtu/h
Operating Cost Factor (4)	20%	30%	
Annual Operating Cost	$3,000	$7,500	/yr
Hourly Cost	$0.34	$0.86	/h
FEED COST			
Price of Chips	$32	$32	/dry ton
Gasifier Efficiency	80%	80%	
Feed Energy	16	16	MMBtu/dry ton
Hourly	$2.50	$2.50	/h
Annual	$21,900	$21,900	/yr
TOTAL COST			
Hourly	$2.84	$3.36	/MMBtu/h
Annual	$24,900	$29,400	

NOTES:
(1) Typically 150 Btu/scf
(2) Typically 300 Btu/scf
(3) Cost shown per MMBtu/h of plant capacity; typical
(4) Typical ratio of annual cost to plant cost.

9.3 COST OF METHANOL PRODUCTION FROM BIOMASS USING THE SERI-SGI GASIFIER

A decade ago conventional wisdom dictated that methanol could be made economically only in very large plants that benefit from the economies of large scale. This limits the energy source for methanol to large natural gas wells, oil or coal, all available in highly concentrated sources. Now however, because of rising gas and oil costs, the difficulty in financing large plants and the larger number of sites potentially available for smaller biomass plants or isolated natural gas wells, it is important also to consider producing methanol from these unconventional energy sources in smaller plants.

In 1981 the International Harvester Company (now Navistar) became interested in using the SERI gasifier for production of methanol in modular plants. Several articles that detail the factors favoring small to medium scale production of methanol by members of IH appear in the proceedings of the conference "Biomass to Methanol Specialists' Workshop" [18].

In particular for biomass, the difficulty of collection of quantities over 500 tons/day mandates consideration of smaller plants. The simplicity of methanol production from wood, relative to coal permits consideration of small, skid mounted plants that can be serially produced and tested at a central location, thus decreasing production costs and minimizing construction time. An artists sketch of a plant based loosely on the IH concept is shown in Fig. 9-1.
In an effort to evaluate the profitability of selling small-scale methanol plants, IH commisioned the Applied Engineering Company (APCO, a division of

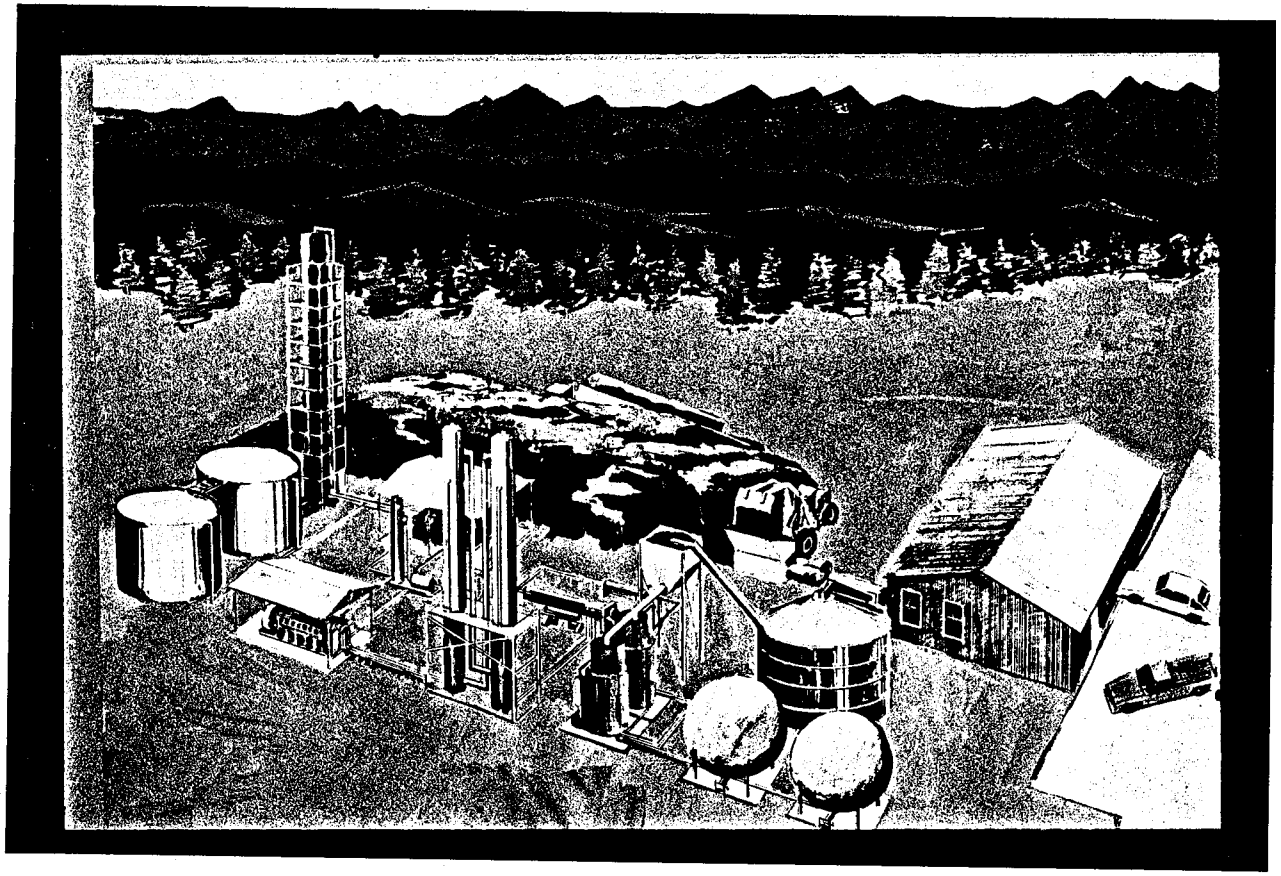

Figure 9-1. Artists Sketch of a 100 ton/day biomass based methanol plant showing (1) a front-end loader transferring wood chips or other biomass from a storage pile (2) to a drier (3). The dried biomass is stored in a silo (4) which continuously feeds one of the two gasifiers (5). Oxygen from the two storage tanks (6) enters the gasifier at several hundred pounds per square inch pressure. Raw fuel gas leaving the gasifier enters the cyclones (7) where ash and any residual charcoal are removed. The gas passes to a zinc oxide guard bed (8) where traces of sulfur are removed; then through a shift catalyst (9) which adjusts the hydrogen/carbon monoxide ratio to 2:1 as required for methanol manufacture. Excess carbon dioxide in the gas is removed in the scrubbers (10) and the gas is compressed (11). This gas is converted in the catalyst bed (12) to raw methanol, which is distilled (13) and stored in tanks (14).

Fluor Corporation specializing in small plants), to evaluate the feasibility and cost of producing small methanol plants [19]. (The report is now the property of Syn-Gas Incorporated (SGI) and further inquiries for more detailed results should be addressed to them.)

The results of the July 1981 study are summarized in Table 9.2. We have increased the costs given in that report by a factor of 1.25. (This is based on the Consumer Price Index. The Marshall and Swift index may give a basis more closely related to chemical prices.) The table shows the operating cost, the capital cost and the projected methanol cost for a 50 and 90 t/d methanol plant in 1981 and 1987 dollars. The projected 0.77-0.86 $/gal manufacturing cost (exclusive of transportation, marketing cost and profit) is not attractive in today's market where methanol can be purchased in bulk for 0.50/gal or less but would be attractive at the 1983 methanol prices, $.70-$.90/gal.

In 1983 the Department of Energy issued an RFP for evaluation of a number of processes for production of various fuels from biomass, including the production of methanol. During 1984 Stone and Webster worked cooperatively with SERI to make a projection of the feasibility and cost of producing methanol from biomass in the SERI-SGI gasifier. They examined the economics of making methanol from biomass in favorable locations in the U. S. They chose Spokane, WA as the most attractive site [20]. Table 9.2 summarizes the findings of this study on the same basis as the APCO/IHC study. The cost of $0.63/gal is also similar to that found in the APCO/IH study.

The costs found by S&W have been adjusted to 1987 dollars using a factor of 1.08. The projected cost of $0.63/ gal is not attractive in today's market without a subsidy. The report found that methanol could be competitive in Spokane (far from ocean ports and close to wood supplies) with the energy subsidies in effect at that time. A more complete summary of this study by H. Kostrin, the manager of the project appears in Appendix C.

Note that the cost of methanol production is comparable in the two studies when adjusted for inflation and size.

9.4 COMPARATIVE ECONOMICS OF METHANOL PRODUCTION FROM VARIOUS FEEDSTOCKS

9.4.1 Capital and Operating Cost Estimates For Methanol Production from Biomass, MSW, Natural Gas, and Coal

The above studies are only two of a great number of studies made on the technology and economics of alternate feedstocks and fuels during the "energy crisis" period 1974-1985 [1-10]. Most of these studies were made by reputable architectural and engineering firms and funded by DOE, but there are independent studies as well. The aggregate cost of these studies is probably 10-20 $MM. There is a great deal of information contained in these studies, but taken singly they can be confusing because each uses a different set of assumptions.

An overview of the results is presented here to give perspective on this field for those considering alternate fuel projects in the future. We present here a comparison of the cost of methanol production from various feedstocks that summarizes data from a large number of studies and gives a perspective on the interplay of feedstock cost and plant size.

Table 9-2.- APCO/Fluor and S&W Estimate of Costs in Producing Methanol from Wood Using the SERI SGI Gasifier (in original and 1977 dollars)

Manufacturer	Applied Engineering Co. (APCO) (2)				Stone & Webster		
Date	Jul 1981	Jan 1987	January 1977		1984	1987	
PLANT SUMMARY	50 ton/d		90 ton/d				Units
Output							
MeOH - t/d	50.0	50.0	90.0	90.0	77.1	77.1	tons/day
MeOH - MMg/y	5.44	5.44	9.89	9.89	7.68	7.68	MM G/y
Feedstock-Whole chips							
Moisture Content	45	45	45	45	50	50	%
Wet Basis	200	200	364	364	311	311	tons/day
Dry Basis	110	110	200	200	156	156	tons/day
Cost	20.00	25.00	20.00	25.00	30.00	32.40	$/BDT
Annual Cost	1.26	1.58	2.29	2.86	1.53	1.66	$MM/yr
Electricity	1,200	1,200	2,075	2,075	496	496	kW
Cost	0.039	0.049	0.039	0.049	0.041	0.044	$/kWh
Annual Cost	0.59	0.74	1.07	1.34	0.18	0.18	$MM/yr
Oxygen	44	44	80	80	58.20	58.20	tons/d
Cost	42.55	53.19	42.55	53.19	52.82	57.05	$/ton
Annual Cost	0.59	0.74	1.07	1.34	1.01	1.09	$MM/yr
Investment Cost	6.36	7.95	9.67	12.09	22.10	23.87	$MM
Annual Operating Cost	3.74	4.68	6.11	7.64	4.50	4.86	$MM/yr
MeOH mfg cost	0.69	0.86	0.62	0.77	0.59	0.63	$/gal

Notes:

1. Evaluations based on nth plant in a production series. All costs adjusted to January 1987 using a Consumer Price Index ratio of1.25 for the APCO (July 1981) study and 1.08 for the S&W 1984 study.

2. From "Methanol Conversion Process Economic Study", (July 1981) for International Harvester, prepared by Applied Engineering Co.

3. From "Economic Feasibility Study of a Wood Gasification Based Methanol Plant", (March 1985), for the Solar Energy Research Institute and DOE (Subcontract ZX-3-03095-1)

We also present a simplified model below for calculating methanol plant and manufacturing cost. The tables presented here were developed on a spreadsheet (Lotus 123) and so can be easily adjusted to other input conditions as they arise.

In 1980 Science Applications Incorporated (SAI) was commisioned by SERI to evaluate the costs of making methanol from various feedstocks, as reported in studies that had been made over the previous 5 years, for the SERI Survey of Biomass Gasification Chapter 13 [13]. The methanol production costs, adjusted for inflation to 1987, appear in Table 9.3. The capital costs of methanol plants based on biomass, MSW, gas and coal (1980 dollars) are plotted against plant size in Fig. 9-2.

The costs in these studies are now quite out of date and have been adjusted to 1987 dollars. . The two new studies summarized in Table 9-2 have been added to the original data base in Table 9-3. The table is divided into three major sections. In the first section, we list the various studies, their initial publication year and the process chosen for making syn-gas. The second section contains the physical scale of the plant and feed consumption. A conversion efficiency is derived from this according to

$$\text{Conversion Efficiency} = \frac{\text{Energy in Methanol}}{\text{Energy in Feedstock}} \quad \text{, or} \qquad (9\text{-}1)$$

$$E = \triangle H_{c,m} P / \triangle H_{c,f} F \ , \qquad (9\text{-}2)$$

where P is the methanol production rate (tons/day) of methanol containing 19.4 MMBtu/ton, F is the rate of feed use (dry tons/day) and $\triangle H_{c,f}$ is the heat of combustion of the dry feed (MMBtu/dry ton). (Note that this efficiency does not include plant energy consumption nor energy recovery, so is not a true plant energy efficiency. The conversion efficiency is shown for each study and an average is calculated for each feedstock. Conversion of natural gas has the highest efficiency, Municipal Solid Waste, MSW the lowest. For MSW this reflects the fact that it typically contains a high mineral content and high moisture content.) The conversion efficiencies and factors necessary for estimating plant and methanol manufacturing costs taken from Table 9-3 are listed in Table 9-4.
The projected costs for methanol plants adjusted to 1987 dollars are given in the third section. The adjusted cost of methanol production is also given, based on the feed costs shown. The projected prices have a wide variation, because of the various assumptions used in each study, but also because of varying plant size. We have removed some of this variation by scaling the plant size shown to 100 tons/day in the last column, as discussed below.

In Fig. 9-3 the SAI-SERI costs are combined with the new APCO and S&W projected costs for wood based methanol plants and plotted against size. A linear regression on the logarithmic data gives the following capital cost (in $MM) for wood based methanol plants of capacity P(tons/day):

$$C_{c,w} = 0.41\ P^{0.91} \ . \qquad (9\text{-}3)$$

(The regression gave an R squared value of 0.833. The error of the exponent was 0.014 based on the nine cases studied.)

Table 9-3. Summary of Methanol Cost Studies for Various Feedstocks Adjusted to 1987 Dollars

1-PROCESS STUDY[1-3]			2-METHANOL PLANT DESCRIPTION			3-COST IN 1987 DOLLARS (4)			
STUDY	YEAR	PROCESS	SIZE MeOH t/d	FUEL USE dry t/d	CONVERSION EFFICIENCY (5)	CAPITAL COST $ X10 6	FUEL COST $/dry ton	MeOH COST $/gal	Cost 100 t/d plant
WOOD (1)									
R. Katzen & Assoc.	1975	Moore-Can	500	1,500	0.40	$131	$69.60	$1.96	36.0
R. Katzen & Assoc.	1975	Moore-Can	2,000	6,000	0.40	$344	$69.60	$1.48	31.3
T. Reed (MIT)	1976	Purox	300	900	0.40	$65	$43.94	$0.84	27.1
Mackay and Suth.	1976	Purox	1,000	3,160	0.38	$323	$66.70	$1.39	51.2
Mitre	1977	Purox	1,340	3,400	0.48	$189	$65.25	$0.96	23.6
Mitre	1977	Purox	335	850	0.48	$67	$65.25	$1.22	25.4
Intergroup	1978	Purox	1,000	2,380	0.51	$323	$53.65	$1.10	51.2
SRI	1978	Oxygen Gasif	666	1,000	0.81	$146	$27.70	$0.74	32.1
SRI	1978	Oxygen Gasif	1,990	3,000	0.80	$390	$27.70	$0.73	35.6
APCO (2)	1981	SERI Downdr	50	110	0.55	$10	$25.00	$0.86	17.2
APCO (2)	1981	SERI Downdr	90	200	0.55	$15	$25.00	$0.78	16.4
Stone & Webster (3)	1984	SERI Downdr	77	156	0.60	$26	$32.40	$0.89	31.8
AVERAGE					0.53		$47.65	$1.08	31.60
MUNICIPAL SOLID WASTE (1)							(9)		
Math Sci. NW.	1974	Purox	275	1,500	0.27	$45	($9.28)	$0.61	20.01
Wilson et al	1977	Purox	245	1,500	0.24	$183	($20.30)	$1.04	89.21
AVERAGE					0.26		($14.79)		54.61
COAL (1)									
Exxon R&E	1977	K-T	2,000	3,436	0.43	$515	$31.61	$1.07	46.9
Exxon R&E	1977	Texaco	2,000	3,212	0.46	$457	$31.61	$0.94	41.6
Ralph M. Parsons	1977	Foster Wh	16,400	24,566	0.50	$3,045	$44.95	$0.59	51.5
Ralph M. Parsons	1977	BGC/Lurgi	16,400	22,918	0.53	$2,755	$44.95	$0.57	46.6
Ralph M. Parsons	1977	K-T	16,400	24,574	0.50	$4,205	$44.95	$0.77	71.1
Ralph M. Parsons	1977	Tex	16,400	22,100	0.55	$3,480	$44.95	$0.64	58.8
AVERAGE					0.50		$40.50	$0.76	52.74
NATURAL GAS (1)				(7)			(8)		
Exxon R&E	1977	Steam Ref	2,000	1,560	0.55	$216	$4.57	$0.93	19.7
AVERAGE					0.55		$4.57	$0.93	19.67

NOTES:
1. Based on SERI/SAI 1980 study in "Survey of Biomass Gasification"[13].
2. Based on 1981 Applied Engineering Co. study for International Harvester [19].
3. Based on 1984 Stone and Webster study for SERI/DOE [20]. All values adjusted to 1987 dollars using CPI index factors of 1.45 for 1979; 1.25 for 1981; and 1.08 for 1984 dollars
5 Conversion efficiency calculated form Eff = (Energy in methanol)/(Energy in Feedstock) assuming an energy content of wood = 16; MSW = 13; coal = 26; and gas = 43.4 MMBtu/dry ton.
6. Production cost calculated by subtracting feedstock cost from total cost.
7. 1 MMBtu of natural gas = 1000 scf = .022 tons
8. $200/ton for gas is equivalent to $4.57/MMBtu.
9 () denotes negative cost

9.4.2 Scale Factor for Methanol Plants

In designing chemical plants of various size, the cost $C_{p,x}$ for a plant of desired size P_x is generally estimated from the cost $C_{o,x}$ of a known size P_o from

$$C_{p,x} = C_{p,o} \ (P_x/P_o)^n \ , \qquad (9\text{-}4)$$

where the n is the **scale factor,** derived from previous experience with similar plants of various size. Experience with petrochemical plants assigns a value of about 0.6-0.7 to the scale factor in the absence of other information.

However, the data in the SAI-SERI compilation permit calculation of a specific scale factor for methanol plants. The costs of the methanol plants in the SAI-SERI collection and Table 9-3 were plotted against size in Ref. 13 and are shown in Fig. 9-3. The scale factors for the feed stocks considered by SAI were found to be 0.81 for gas; 0.82 for coal; 0.76 for wood; and 0.81 for MSW respectively as shown in Table 9-4.

Table 9-4. Conversion Efficiency, Scale Factor and Feed Factor for Calculating Plant costs and Methanol Manufacturing Costs from Various Feedstocks

FEEDSTOCK:	WOOD	MSW	GAS	COAL
E - Conv. Efficiency	0.53	0.26	0.55	0.50
n - Scale Factor	0.76	0.81	0.81	0.82
R_f - Feed Cost Ratio[1]	1.0	1.72	0.62	1.67

1. Plant cost relative to a wood plant

Note that the scale factor for wood using the 1980 SAI-SERI data in Fig. 9.2 was 0.76. However, addition of the more recent data as shown in Fig. 9.3 increased the scale factor to 0.91 as given in Eq. 5. This no doubt reflects the efforts of APCO and S&W to eliminate the usual effects of scale in designing serial produced small competitive plants.

We suggest that the variation in scale factors for the various feeds is not

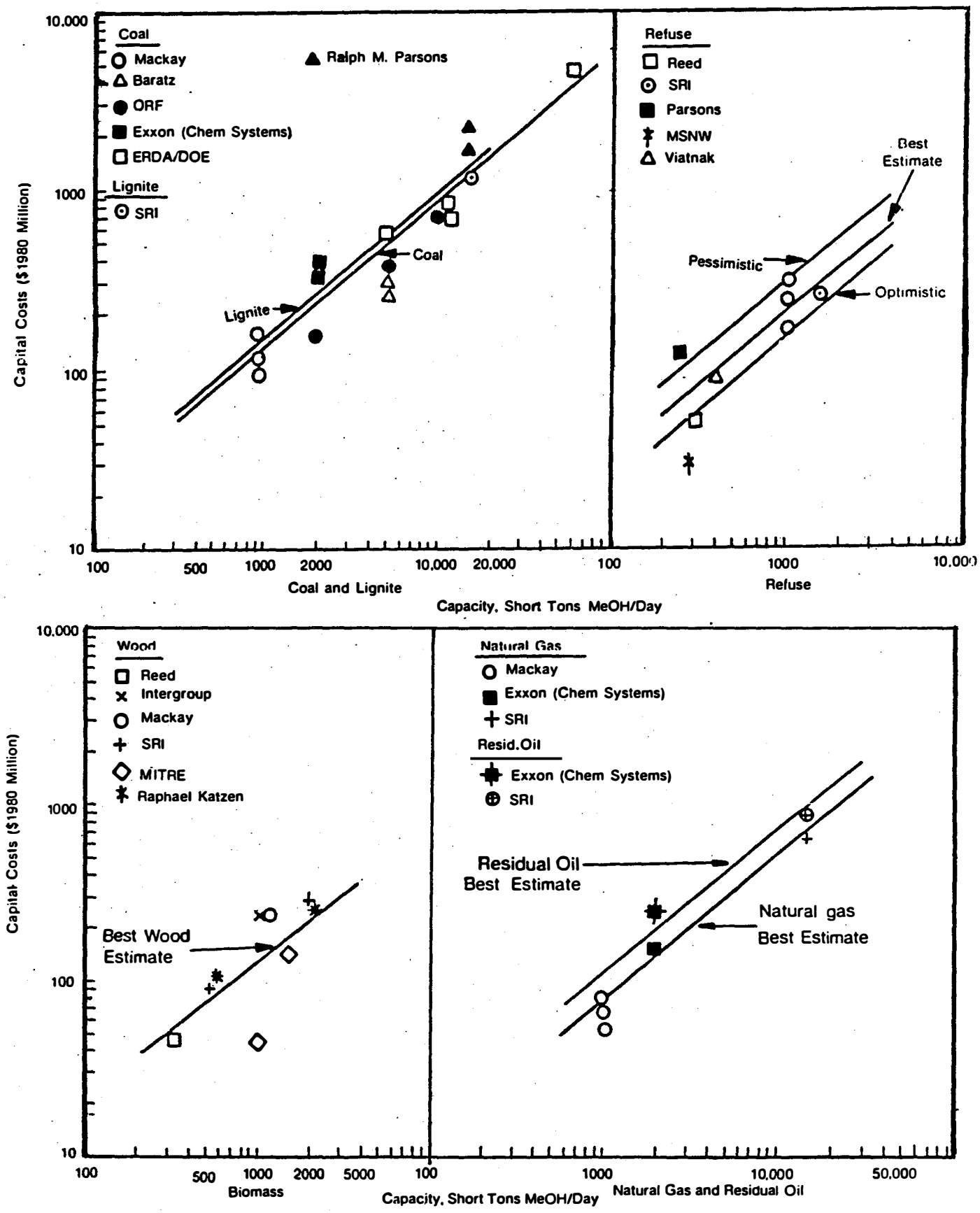

Figure 9-2. Projected Capital Costs of Methanol Plant using Wood, MSW, Natural Gas, or coal.

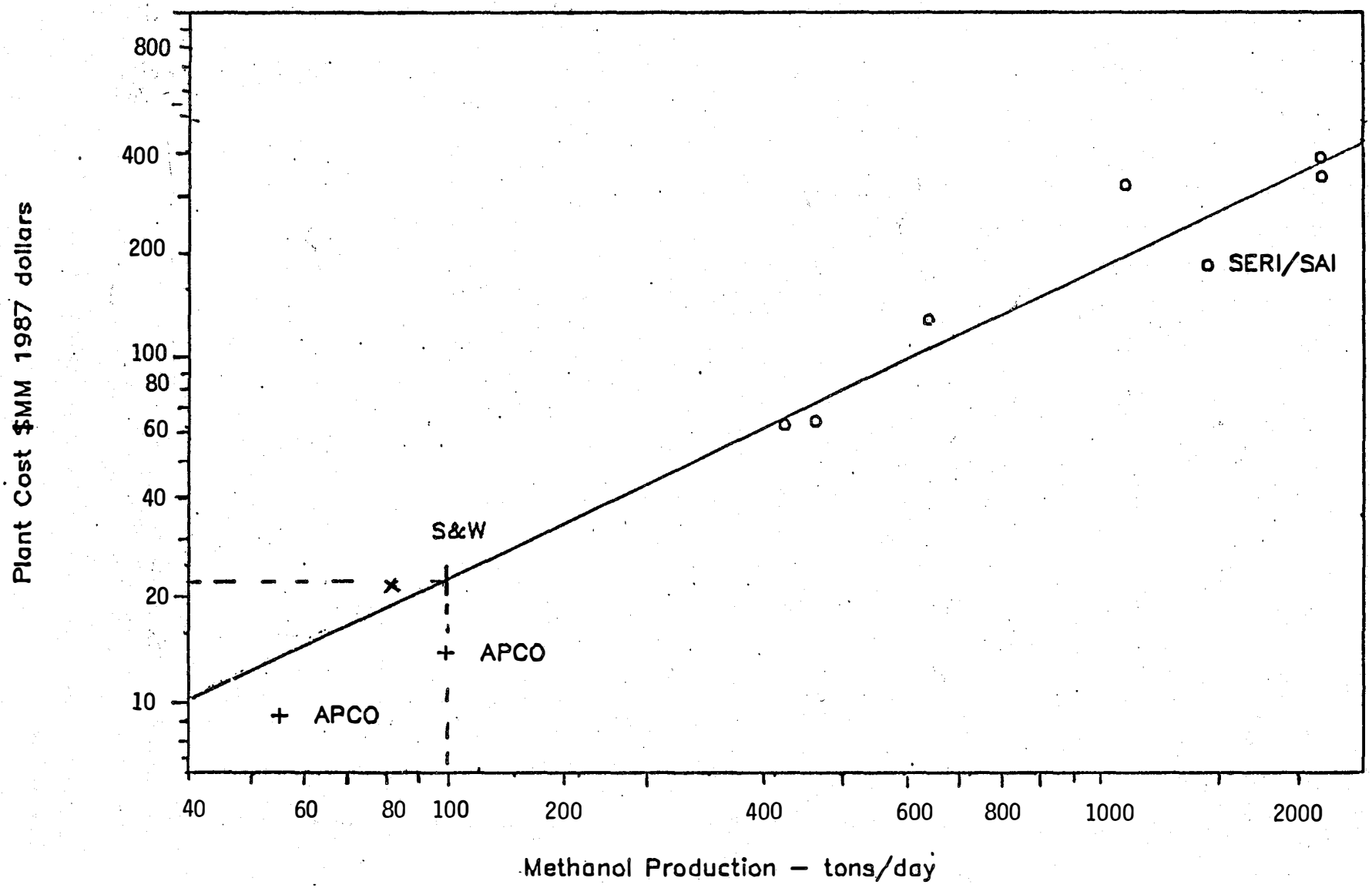

Figure 9.3 Projected Capital Costs of Methanol Plants using Wood Including the Recent APCO and S*W Studies.

statistically significant. We will arbitrarily choose a factor of 0.80 for all feeds in scaling plants in the model below.

9.4.3 Feed Factor in Methanol Plant Cost

The average costs of the plants using various feeds were scaled to 100 ton/day using Eq. 5. These costs are shown in the last column of Table 9-3. We compared production costs for different feeds at the same scale. We found the ratio of cost for plants using different feeds, R_f, shown in Table 9-4. Here one sees that MSW and coal plants cost 67% and 72% more than wood plants, while a natural gas plant costs 38% less.

The various estimates for wood plants vary by about a factor of 3 between the lowest and highest. This is not a large variation considering that no one has ever built a wood to methanol plant. The variation in cost of MSW plants is over 4. This reflects the fact that the technology was not in existence when these plants were estimated and they represent little more than educated guesses.

9.5 A SIMPLIFIED MODEL OF COST OF METHANOL PLANTS AND PRODUCTION FROM VARIOUS FEEDSTOCKS

9.5.1 Introduction

The projection of cost figures for specific processes in specified locations is a well developed science. A study of this type may cost from $50,000 to $500,000 depending on its magnitude. The final results may correspond to actual costs if the plant is built; yet overruns of 200%-1000% have been observed on larger projects (ie the Alaskan pipeline, projected to cost $900 MM and actual cost $10B). Anyone contemplating building a plant will have to go through the cost projection process. The summary of the S&W study in Appendix C illustrates this process.

Nevertheless, the collection of data presented here from many such studies permits generalizations that can be used for a simplified cost model that will permit estimation of plant and product cost, and permit comparison of various feeds for various scales in future planning.

9.5.2 Capital Cost of Various Size Methanol Plants

Combining the above factors, one can predict the cost C_p of any size methanol plant P_x, using any of these feeds from the equation

$$C_p = C_{p,o} R_f (P_x/P_o)^n \quad . \qquad (9\text{-}5)$$

To predict the cost of methanol plants using these data, we have chosen the cost of 23 $MM, taken from Fig. 9.3, as representative of the cost of a wood plant producing 100 tons/day, as the baseline cost C_o, and chosen a scale factor of 0.8. This then gives the capital cost of a methanol plant as

$$C_p = 23 \cdot R_f (P_x/100)^{0.8} \quad . \qquad (9\text{-}6)$$

9.5.3 Methanol Production Cost

In projecting costs for methanol production there are a large number of factors that are site specific that determine the final production cost of

methanol, as shown for instance in the S&W summary in Appendix C. However, the principal variables are scale and feedstock price. To a first approximation, the cost of producing methanol is given by

Annual MeOH Production Cost = Annual Operating Cost + Annual Feed Cost , or

$$C_m = C_o + C_f \quad . \tag{9-7}$$

The unit methanol cost, c_m is found by dividing the annual production cost by the annual production. If the capacity of the plant is P (in tons/day), the annual production is 365PA (in tons/yr) where A is the availability [days used/yr)/365]. There are 305 gallons of methanol in a ton, so the annual production in gallons/yr is 110,600PA.

$$c_m = (C_o + C_f)/(110{,}000\ A{\cdot}P) \tag{9-8}$$

where the upper case C refers to annual operating and feed costs and the lower case c is the unit cost of methanol, c_m in $/gal.

9.5.3.1 Operating Cost

The annual operating cost includes the cost of utilities, oxygen (if used), water, labor, maintenance, taxes and insurance, administration, sales, overhead and interest and depreciation on the debt. Annual interest and depreciation are the largest single items in the operating cost and are directly related to plant cost. They have been estimated at 8%-10% of the capital cost in the studies shown in Table 9-3. Obviously this will depend on assumed plant life, debt/equity ratio and interest rates in each specific case. (The return on the investment will add another significant quantity to the final methanol selling price, but is not considered here.)

We examined the total annual operating cost in the studies shown in Table 9-2 and 9.3 and found that the operating cost factor, R_o varied between 20% and 40% of the capital cost of the plant. We will take a value of 30% as typical. The operating cost is then given by

$$C_o = 0.30\ C_p \tag{9-9}$$

9.5.3.2 Feed Costs

Since methanol has a higher energy per mass than wood and is made with an efficiency of 0.53 (see Table 9-4), each mass of methanol $\underline{m}_m$ requires a mass of wood $\underline{m}_w = \Delta H_m/\Delta H_f E\ d\ \underline{m}_m$. The cost of feed to make methanol, $c_{f,m}$ is given by

$$c_{f,m} = \frac{\text{Feed Cost X Energy in Methanol}}{\text{(Energy in Feed)(Efficiency)}} \tag{9-10}$$

$$c_{f,m} = c_f\,\Delta H_m/\Delta H_f E \tag{9-11}$$

where c_f is the unit cost of the feed. The methanol contains 19.4 MMBtu/ton, while the wood typically contains 16 MMBtu/ton. The annual feed cost will be determined by the plant capacity (in tons/day) and the operating days per year, or

$$C_{f,m} = 365\ A{\cdot}P\ c_{f,m} \quad . \tag{9-12}$$

9.5.4 Simplified Methanol Cost Model

Substituting Eq. (10), (12) and (13) in (8)we find the total cost of operating the plant, including feed is

$$C_m = 0.30\ C_p + c_{f,m}\ (\Delta H_m/\Delta H_f E)\ A \cdot P. \qquad (9\text{-}13)$$

The unit cost of methanol is obtained by dividing this by the annual production in tons or gallons as given in Eq. 9.

This cost model has been incorporated in a spreadsheet (Lotus 123) and a sample printout is shown in Table 9-5. In operation, the required production and feedstock properties are substituted in the appropriate spaces as instructed in the footnotes and the final methanol cost and other factors are then calculated automatically.

9.5.5 Sample Costs of Methanol from Various Feedstocks

The above formulas incorporated in the spreadsheet of Table 9-5 were used to calculate a matrix of sample cases. In Table 9-6 the projected capital costs for 100 and 1000 ton/day methanol plants using wood, MSW, coal and gas are shown i the first section. These costs are then used to calculate methanol production costs from feedstocks of varying cost in 100 and 1000 ton/day plants in table 9-6.

9.6 CONCLUSIONS

Several important conclusions can be drawn from this discussion:

- o Gasification is not generally economically attractive today (1987) while oil and natural gas prices are relatively low

- o Gasification is attractive even today in situations where feed costs are low (lumber and paper mills) or there are side disposal benefits (MSW or other waste elimination)

- o Gasification is likely to become attractive when fossil energy prices increase; or when we can no longer tolerate the trade deficit because of imported oil; or when our dependence on foreign fuels forces us to pioneer domestic conversion processes

- oMethanol plants based on biomass have a lower capital cost than coal based plants at the same scale. However, methanol plants from biomass must operate at a smaller scale than coal plants because of feedstock availability and transport cost

- o The scaling factor for methanol plants derived here is 0.8, so that there is not a large penalty in building small plants

- o The relative cost of wood, waste, coal and natural gas plants are 1, 1.72, 1.67 and 0.62 respectively

- o If methanol is to be made from coal, biomass or MSW, the feedstock cost will have to be lower or the scale larger than that for natural gas, since natural gas plant capital and production costs are lower at the

same scale.

- o Early cost projections for wood/MSW plants were based on Moore or Purox gasification. Neither gasifier is suitable for methanol manufacture.

- o The cost projections for MeOH made by APCO/IH and S&W were made specifically for the SERI-SGI gasifier, and so are based on an actual, operating, prototype gasifier designed for syn-gas manufacture

- o The costs projected by APCO/IH and S&W have been shown separately in Fig. 9.1.

Table 9-5. Simplified Methanol Plant and Manufacturing Cost Model

PLANT SPECIFICATIONS		
Plant size	200	tons/day MeOH
Plant size	22.8	MM Gal/yr MeOH
Plant Efficiency (1)	0.53	
Feedstock cost ratio (2)	1	
Inflation factor (3)	1	
Plant capital cost (4)	40.0	
Annual Operating Cost (5)	12.0	
Availability	300	days/yr
FEEDSTOCK	Wood Chips	
Cost (6)	30	$/dry ton
Energy Content (7)	16	MM Btu/ton
Consumption	457.5	dry tons/day
Annual Fuel Cost	4.1	$MM
METHANOL PRODUCTION COST		
Annual	16.1	$MM/yr
Unit	0.88	$/gal

Notes: To estimate other sizes using spreadsheet, (enter tons/day of methanol)
(1) Efficiency calculated from (energy in MeOH/energy in feed.
(2) Relative Plant cost: Enter 1 for wood/ 1.72 for waste; 1.67 for coal and 0.62 for gas feedstock.
(3) Enter (current value of dollar)/1987 value.
(4) Calculated from relative plant cost and scaling at 0.8 power.
(5) Calculated assuming 0.30 times plant capital cost. Includes depreciation and interest at 10%, utilities etc., but not feed cost.
(6) (Enter cost, $/daf-ton)
(7) Enter energy content of feedstock on dry, ash free basis. . Typically, 16 MMBtu/ton for wood; 13 MMBtu/ton (but very variable) for MSW 26 MMBtu/ton for coal (but very variable); 45.5 MMBtu/ton for gas.

Table 9-6. Typical Cost of Methanol Plants and Methanol from Various Feedstocks

PLANT COST(1)	100	1000 ton/day
FEEDSTOCK		
Wood	23.0	145.1 $MM
MSW	39.6	249.6 $MM
Coal	38.4	242.4 $MM
Gas	14.3	90.0 $MM

METHANOL COST (2) - 100 ton/day plant

FEEDSTOCK	-20	-10	0	10	20	30	40	50	$/ton
Wood	0.65	0.70	0.75	0.81	0.86	0.91	0.96	1.01	$/gal
MSW	1.20	1.25	1.30	1.35	1.40	1.45	1.50	1.55	$/gal
Coal	1.16	1.21	1.26	1.31	1.36	1.41	1.46	1.51	$/gal
Gas	0.37	0.42	0.47	0.52	0.57	0.62	0.67	0.72	$/gal

METHANOL COST (2) - 1000 ton/day plant

FEEDSTOCK	-20	-10	0	10	20	30	40	50	$/ton
Wood	0.37	0.42	0.48	0.53	0.58	0.63	0.68	0.73	$/gal
MSW	0.72	0.77	0.82	0.87	0.92	0.97	1.02	1.07	$/gal
Coal	0.69	0.74	0.79	0.85	0.90	0.95	1.00	1.05	$/gal
Gas	0.19	0.24	0.29	0.35	0.40	0.45	0.50	0.55	$/gal

Notes: (1) Plant cost increases as 0.8 power of scale. Based on $23 MM for a 100 ton/day wood plant and using feed cost ratio of Table 9-4.
(2) Calculated from Cm = Co + Cf assuming Co = 0.3 Cp and using conversion efficiency in Table 9-4

NOMENCLATURE

A Plant availability (operating days/yr/365)
$c_{x,y}$ Unit cost of fuel, methanol etc.
$C_{x,y}$ Total cost of plant, yearly operation etc.
$C_{p,o}$ Cost of plant of known size, p
$C_{p,x}$ Cost of unknown plant of size p.

E Efficiency of gas or methanol production
n Scale factor in estimating plant costs
P Total production rate of plant, gal/yr or tons/d
R_f Ratio of cost of production from gas, coal or MSW to production cost from wood.
R_o Ratio of operating cost to total plant cost
$\Delta H_{c,f}$ Heat of combustion of feedstock
$\Delta H_{c,m}$ Heat of combustion of methanol

Subscripts

x General subscript, described in text
y General subscript, described in text
o Base size for extrapolation

REFERENCES

1. Blake, D. and Salo, D., Systems Descriptions and Engineering Costs for Solar-Related Technologies", Volume IX, *Mitre Report No. MTR-7485,* 1977.

2. Exxon Research and Engineering Co., "Production Economics for Hydrogen, Ammonia, and Methanol During the Period 1980-2000", *Brookhaven National Laboratory,* Long Island, N. Y., 1977.

3. Intergroup Consulting Economists Ltd., "Liquid Fuels from Renewable Resources; Feasibility Study", prepared for the Government of Canada, 1978.

4. Makay, D. and Sutherland, R., "Methanol in Ontario, a Preliminary Report Prepared for the Ministry of Energy", *University of Toronto,* Toronto, Canada, 1976.

5. Mathematical Sciences, Northwest, Inc. "Feasibility Study: Conversion of Solid Waste to Methanol or Ammonia", *MNSW 74-243-1,* the City of Seattle, 1974.

6. Ralph M. Parsons, "Screening Evaluation: Synthetic Liquid Fuels Manufacture", *EPRI AF-523* Electric Power Research Institute, 1977.

7. Raphael Katzen Associates, "Chemicals from Wood Wastes", *R.K.A. N441* Forest Products Laboratory, Madison, WI., 1975.

8. Reed, T. B., "A Survey of Our Primary Energy Sources and the Fuels We Can Make from Them," *Capturing the Sun Through Bioconversion,* Washington, D.C., March 1976.

9. Schooley, F. A. et al., "Mission Analysis for the Federal Fuels from Biomass Program", *Quarterly Progress Report to DOE,* Second Annual Symposium on Fuels from Biomass; Rensselaer Polytechnic Institute, 1978.

10. Wilson, E. et al., "Engineering and Economic Analysis of Waste to Energy Systems", *Ralph M. Parsons Co., Report No. 5495-1,* Pasadena, CA, 1977.

11. Mujaden, M. J., "Experience in Starting Up the Great Plains Coal Gasification Plant", *Thirteenth Biennial Lignite Symposium, DOE/METC-86/6036 (Vol.1),* Morgantown Energy Technology Center, Grand Forks, ND (1986).

12. "Integrated Gasification-Combined-Cycle (IGCC) Phase Construction for Flexible Growth", *EPRI Journal*, Vol. 11, 5 (1986)

13. "A Survey of Biomass Gasification, Vol. I-III," *SERI/TR-33-239,* Reed, T. B. editor , (Solar Energy Research Institute, Golden, CO, 1979). Published in hard cover as , "Biomass Gasification: Principles and Technology, *Energy Technology Review No. 67,* Noyes Data Corp, Park Ridge, NJ, 1981.

14. Bridgwater, A.V., Double, J. M. and Earp, D. M., "Technical and Market Assessment of Biomass Gasification in the UK", *Report to Energy Technology Support Unit,* Technical Appendix, Agreement No. E/5A/CON/1167/1333, Vol. 2, 1986.

15. Schroeder, R. J., Ege, H. D. and Hunt, F. E., "Biomass Gasification for Electric Utitilty Diesel Generating Units", *EPRI AP-3865,* the Electric Power Research Institute (EPRI), 1985.

16. Brogan, T. at SynGas Inc., Golden, CO. private communication, 1987.

17. See for instance "Proceedings of the 1985 Biomass Thermochemical Conversion Contractors' Meeting" *PNL-SA-13571,* Pacific Northwest Laboratory, 1986. Also Ref. 3.

18. T. B. Reed and M. Graboski, editors "Biomass-to-Methanol Specialists Workshop," SERI/CP-234-1590, the Solar Energy Research Institute, Golden, Co., 1982.

19. (APCO, 1981) "Methanol Conversion Process - An Economic Study", *project No. ED-3852* Applied Engineering Co., Orangeburg, SC, July 1981.

20. (S&W, 1985) "Economic Feasibility Study of a Wood Gasification Based Methanol Plant", *Sub-Contract ZX-3-03095,* Prepared by Stone & Webster Engineering Corp., Boston, MA for The Solar Energy Research Inst., 1985. A Summary of this report was presented by H. Kostrin, & D. A. Himmelblau at the 1986 IGT Conference and is included in Appendix D.

CHAPTER 10

FUTURE DIRECTIONS FOR FIXED BED DOWNDRAFT GASIFIERS

The energy crystal ball has been particularly cloudy over the last decade. We have experienced some actual energy shortages, greatly exaggerated perception of energy shortage, and embarrassing surpluses of energy. We continue to work in the field of gasification in spite of these viscissitudes because we believe that in the long run - we believe in our lifetimes - we will come to depend on producing high grade fuels from wood and coal. At present gasification to synthesis gas followed by conversion to methanol or gasoline is the simplest route to a high grade liquid synthetic fuel. It is in this light that we present the following recommendations for continuing work in air and oxygen gasification. Gasification with air to make producer gas for generation of power or high grade process heat is also an attractive option.

It is ironic that there existed a well developed gas manufacturing industry from 1850-1950 based on coal; yet in the last decade very little progress has been made in establishing a gas industry based on either coal or biomass. In spite of extensive development work there are only a few gasifiers operating on coal and biomass now in the U.S. There are still many areas that must be developed further if gasification is to become a mature industry and take its place in converting solid fuels to the gas or liquid fuels that our civilization requires today.

The SERI-SGI gasification program has achieved the aims set initially and reached a pre-commercial level on air and oxygen. SGI is now marketing a commercial gasifier system for generation of power based on the gasifier described in this report. They are currently obtaining permits for construction of a 10 MW power plant in Port Jefferson, Long Island using demolition wood, manufacturing wastes transportation waste and clearings. A number of projects of similar scope are in negotiation.

To be successful in this age, gasification must become reliable, automatic, and clean. We believe this can only happen if we understand the technical processes involved to the same degree that we understand the operation of an oil refinery or an automobile. A step in this direction, now in progress, is the understanding of the role of heat transfer in the pyrolysis and combustion of wood and biomass at a fundamental level. The single particle reactor work at SERI will make useful contributions to this understanding.

A natural extension of the single particle work is modification of the models developed in Chapter 8 to fit the existing gasifiers such as the SGI gasifier. To date there has been little interaction between the modeling results of Chapter 8 and the real-world experience of Chapter 4.

Development of economic gas cleanup systems are a high priority if gasifiers are to be environmentally acceptable. There are a number of approaches to gas cleaning. The preliminary catalytic tar conversion work discussed in this report was encouraging as far as it went. A decision should be reached as to whether catalytic conversion can compete with conventional gas cleanup. If so, further studies are necessary to optimize the catalyst in the real world of carbon buildup and catalyst attrition. The analysis of oils and tars that is continuing at SERI and elsewhere will form a necessary

foundation to this work.

The future course of gasification work is obviously dependent on the degree to which the United Statesperceives a need for domestic gaseous and liquid fuels. In the present climate of indifference to the implications of high oil imports and the resulting negative balance of trade, it is difficult to propose an extensive program in biomass, coal, or shale research and development. As events unfold it will be more obvious what steps will be required to maintain our energy supplies.

CHAPTER 11

SUMMARY AND CONCLUSIONS

Between 1980 and 1985 a 1 ton/day stratified downdraft gasifier was designed, constructed and operated on wood chips, peat, corn cobs, and paper cubes. The results showed that this new type gasifier could

- o Make a low (<0.5%) tar producer gas (with air) with an energy content of 140-160 Btu/scf.
- o Make a low tar synthesis gas with an energy content of 250-320 Btu/scf. This synthesis gas could be converted to methanol and behaved essentially like the gas produced in commercial coal gasifiers.
- o Operate at a pressure of 10 atmospheres to produce a similar gas, but with considerably more mechanical difficulty.

In 1985 the gasifier was scaled up to 25 tons/day by Syn-Gas Systems. The new gasifier showed that the stratified downdraft gasifier could

- o Be scaled by a factor of 20 with primarily a change in grate design
- o Operate on air for a period of 100 h at atmospheric pressure
- o Make a low-tar (<0.5%) producer gas with an energy content of 140-160 Btu/scf
- o Operate on oxygen for a period of 60 h at atmospheric pressure
- o Make a low tar synthesis gas with an energy content of 250-320 Btu/scf.

A number of smaller gasifiers were made and used to provide basic data on gasifier operation. It was found that

- o A small stratified downdraft gasifier could be built from a 5 galcan, useful for research studies and capable of making gas for a 5-10 kW generator.
- o A transparent gasifier could be used to study the factors controlling the propagation of the gasification reactions.
- o A gold insulated, transparent gasifier was very useful for studying gasifier operation and catalytic tar destruction.
- o A quartz tube "upside-downdraft gasifier" could produce gas in the laboratory in simulated downdraft and updraft modes for analysis of gas and tar vapors or for use in biological experiments.

During this period a number of basic mechanical studies were made of gasifier operation. It was found that

- o A steam ejector could move large quantities of hot, tarry gas to an incinerator and provide clean, quiet conditions for testing

- The pressure drop in various fuel beds correlated well with that predicted by the Ergun equation.

The gold insulated, transparent gasifier was operated on air and oxygen to provide a gas for testing thermal and catalytic tar destruction. It was found that

- Temperatures greater than 900 °C with residence times of several seconds were required to achieve significant tar reduction without catalysts

- Significant tar reduction could be achieved below 700 °C using silica alumina cracking catalysts or molecular sieve catalysts

The chemistry and thermodynamics of downdraft gasifiers was investigated. It was found that

- Downdraft gasification occurs in two sequential stages: In the first stage, an initial partial oxidation of the volatile matter converts approximately 85% of the biomass to a low energy fuel gas and the balance to charcoal; in the second stage the char reacts with the CO_2 and H_2O in the gas to increase the CO and H_2.

- The gas leaving the char bed corresponds approximately to the equilibrium that would be predicted at 700°-750°C except that it is high in methane

- The "adiabatic reaction" values of temperature and composition are useful for predicting the operating point, products and oxygen/fuel ratio of a downdraft gasifier.

- The position of the carbon saturation line is useful in predicting the possible products of an operating gasifier and in analyzing corrective actions to improve operation.

The kinetics of flaming pyrolysis and char gasification were investigated and used to construct several models of the stratified downdraft gasifier. The models

- Predict the times required for flaming pyrolysis

- Predict the times and temperatures encountered in the char bed as a function of oxidant and char carryover

- Predict the size of the gasifier as a function of fuel properties and throughput

- Are hard to compare to experiment because of the problems of measuring temperature and gas composition in a packed bed.

The costs of making producer gas and methanol were examined. It was found on the basis of some simplifications that

- The cost of making producer gas and methanol was determined primarily by the operating and feed costs. Plant cost is the major component of operating cost.

- The cost of making low energy gas from wood chips costing $32/dry ton is typically $2.84/MMBtu.

- The cost of making medium energy gas from wood chips costing $32/dry ton is typically $3.36/MMBtu.

- The cost of making methanol in a SERI-SGI gasifier is typically $0.77-$0.89/gal (1987 dollars) according to studies by Applied Engineering and Stone and Webster.

- The cost of methanol plants using wood, MSW, gas or coal varied as the 0.8 power of size, not the 0.65 power as found for other chemical plants.

- A simple model could be made predicting methanol manufacturing costs from feed and plant size considerations.

ACKNOWLEDGMENTS

This work was initially made possible by the financial support of the Department of Energy's Office of Alcohol Fuels, and more recently, by their Biofuels and Municipal Waste Technology Division.

Gary Schiefelbein and Mark Gerber at the Pacific Northwest Laboratories have given us critical reviews each year which helped us to satisfy DOE requirements. We appreciate the work of our external reviewers whose suggestions greatly improved the final report. Si Friedrich at the US Department of Energy has also provided continual support.

The authors would like to thank all those who have contributed so much to the technical aspects of this program. At SERI Tom Milne and Helena Chum have been continually supportive and usefully critical. We have been very fortunate in our colleagues at SERI and Hazen Research who have contributed many ideas in private discussion.

We wish to recognize major contibutions to the project by Mike Markson and Mark Kindig who were directly involved on the project for a number of years. Our thanks to Agua Das for help with gas and tar analysis. At Hazen, Tim Goens provided good management of the project until his tragic death, after which Ric Kenney continued to manage the Hazen part of the project.

APPENDIX A

UNITS AND CONVERSIONS

Although it was our intention to present the collected data within a consistent framework of acceptable metric units, this goal could be only partially achieved. The still widespread use of English units did not in all cases allow transfer of the reported data to metric units. The internationally established gram (g), meter (m), second (s), and joule (J) system (SI) is therefore occasionally replaced by units that may be more familiar and more convenient to the reader. Conversion factors are from the *Handbook of Chemistry and Physics*, 67th edition, CRC Press.

Weight

1 kg = 2.204 lb = 15,432 grains = 32.105 oz (troy)
= 0.984×10^{-3} ton (long) = 1.1023×10^{-3} ton (short)

Pressure

1 atm = 1.0133 bar = 101.33 kPa = 14.7 psia = 29.921 in. Hg = 1419 in. H_2O = 760 mm Hg

Velocity

1 m/s = 3.281 ft/s = 3.6 km/h = 2.237 mph

Energy

1 Btu = 1.055 kJ = 252 Cal = 778.2 foot-pound-force

kWh = 3.6 MJ = 3413 Btu

1 Cal = 4.187 J

Density

1 g/cm^3 = 1000 kg/m^3 = 62.43 lb/ft^3

1 lb/ft^3 = 0.01602 g/cm^3 = 16.02 kg/m^3

Power

1 watt = 1 J/s = 3.43 Btu/h = 0.2389 Cal/s = 3.6 kJ/h = 1.341×10^{-3} hp

Temperature

K = °C + 273.15

°R = °F + 459.67 = 1.80 K

°F = 1.8°C + 32

Concentration

1 $grain/ft^3$ = 2.571 g/m^3

Length

1 in. = 2.54 cm

1 micron (micrometer) = 1 μm = 10^{-6} m

Volume compressible gas (1 atm dry)

1 Nm^3 (0°C) = 38.55 scf (77°F) = 37.32 scf (60°F) = 37.90 scf (68°F)

Volume noncompressible

1 m^3 = 35.315 ft^3 = 1000 liters

1 ft^3 = 0.02831 m^3 = 7.48 gal

1 gal (U.S.) = 3.785 liters = 0.1336 ft^3 = 231 $in.^3$

1 liter = 0.353 ft^3 = 0.2642 gal = 33.82 fl oz = 61.02 in^3

Flow gas

1 Nm^3/h = 0.632 scfm (68°F)

Area

1 m^2 = 10.76 ft^2 = 1550 $in.^2$ = 1.30 yd^2

Hearth Load (for 130 Btu/scf gas)

0.9 $Nm^3/h\text{-}cm^2$ = 537 $scfm/ft^2$ = 3.73 $scfm/in.^2$ = 4.2 $MBtu/h\text{-}ft^3$

Gas Energy Content

1 Btu/scf (68°F) = 9.549 $kCal/Nm^3$ (0°C) = 39.98 kJ/Nm^3 (0°C)

Fuel Energy

1 Btu/lb = 0.5555 Cal/g = 2.326 J/g

1 Cal/g = 1.8 Btu/lb = 4.187 J/g

Gasification Rules of Thumb - approximately true

Fuel Consumption

1 hp-h ≈ 2 lb biomass = 2 scfm gas

1 kWh ≈ 3 lb biomass

1 ppm ≈ 1 mg/m^3

Standard conditions for gas measurements vary widely depending on the organization setting the standards. Since gas properties can be measured to a precision considerably finer than the error introduced by a misunderstanding in standard conditions, expressions of gas volume and heating value must specify the measurement conditions.

Two often-used references (Kaupp 1984a; Gengas 1950) use gas measurement conventions different from common gas practice. The following table is provided to indicate the sources of gas measurement conventions. However, the reader should exercise extreme caution in all conversions using the term "scf." If the gas measurement conditions are not specified or cannot be safely presumed, then gas heating value is subject to 3% uncertainty.

We have used 1 atm = 101.32 kPa = 760 mm = 29.92 in. Hg for a standard pressure and a temperature of 20°C = 68°F in our data reporting.

Standard Measuring Conditions for Gases

Unit	Where Used	Standard Conditions Pressure	Temperature	Reference
scm/scf	EPA Method 5	Dry gas 760 mm = 1 atm	68°F = 20°C	(1)
scf	American Gas Association	762 mm = 30 in. Hg dry gas	60°F = 15 5/9°C	(2)
scf	Compressed Gas Institute	760 mm - 1 atm 29.92 in. Hg	68°F = 20°C	
Nm^3	NTP = STP	760 mm = 1 atm dry gas	0°C	
Nm^3	Standards Council of Canada	1 atm dry	15°C	(3,4)
ft^3	Environment Canada Air Pollution Control Directorate	29.92 in. Hg	537°R 78°F	(5)
scf	ANSI Standard Z132.1 for gas calorific value	Saturated with water 14.73 psia	60°F	(6)
	Molecular weight standard conditions	29.92 in. Hg = 101.325 kPa 760 mm = 1 atm Dry gas	0°C = 32°F	(7)
scf	Kaupp & Goss	1 atm	77°F = 25°C	(8)
Nm^3	*Generator Gas*	1 atm dry	0°C dry	(9)
scf		1 atm dry	70°F = 21.11°C	

(1) Environmental Protection Agency, "Determination of Particulate Emissions from Stationary Sources," Codified Federal Register 40, Pt. 60, Appendix A, Method 5.

(2) *Dictionary of Scientific and Technical Terms*, 3rd Ed. New York: McGraw-Hill, 1984.

(3) International Standards Organization, *Measurement Conditions for Gaseous Fuels*, ISO STD 5024-TC28, 1979.

(4) ENFOR Project C172, DDS File No. 41SS, KL229-1-4117, 1979.

(5) Environment Canada Air Pollution Directorate, EPS 1 AP.74-1, 1974.

(6) *Calorific Value of Gases in Natural Gas Range by Continuous Recording Calorimeter*, ASTM D 1826, 1977.

(7) *Determining the Properties of Fine Particulate Matter*, ASME PTC-28, 1965.

(8) Kaupp, A. and Goss, J.R. *State-of-the-Art for Small (2-50 kW) Gas Producer-Engine Systems.* Final Report to USDA, Forest Service, 1981.

(9) *Generator Gas: The Swedish Experience from 1939-1945.* SERI/SP-33-140, 1979 (Solar Energy Research Institute, Golden, CO).

APPENDIX B

CHEM SYSTEMS INC.
One Evans Street, Fairfield, N.J. 07006
Telephone (201) 575-8820 Telex 138178

July 13, 1981

Dr. Thomas G. Reed
Solar Energy Research Institute
1617 Cole Boulevard
Golden, Colorado 80401

Dear Dr. Reed:

As per our letter proposal of February 10, 1981, we have completed the methanol production run using the synthesis gas supplied by Rick Kenny of Hazen Research. Before initiating the test run, we checked each of the individual cylinder gas compositions and found a total of two cylinders with out-of-specification N_2 contents, Cylinder #104121X and #104122X. Neither of these cylinders were used in the test.

Nominal reaction conditions for the test were:

Temperature:	250°C
Pressure:	86 ata
Feed Gas Flow:	1200 l/hr (at 1 ata and 60°F)
Catalyst Loading:	0.3 kg catalyst A (as oxide)
Oil Inventory:	1.0 liter Witco 40 mineral oil

A typical feed and product gas analysis is attached as Table 1. The conversion results for this feed gas are quantitatively similar to previous tests we have performed with a simulated Koppers-Totzek gas (35% H_2, 55% CO, 5% CO_2, 5% Ar). A total of 1.65 kg of methanol product was collected. An analysis of the crude product is presented in Table 2. Again, these results are quite comparable to those we have obtained with the similar K-T gas.

CHEM SYSTEMS INC.

Both the product methanol and your high pressure cylinders are being returned as per your directions. Only 1.5 kg of the product has been returned to you. We have retained the balance. The product is cloudy because of difficulty is separating the process oil due to very similar specific gravities. You can achieve a better separation by adding a few percent water to salt out the oil.

Please call me if you have any questions on this material.

Sincerely yours,

CHEM SYSTEMS, INC.

Dr. D. B. Blum
Manager of Process Development

DBB/cd

Enclosure

Table 1

MEOH SYNTHESIS IN A STIRRED AUTOCLAVE

DATE:TIME	? 7-7-81 1750	
RUN ID	? 226-15	
REACTOR LIQUID	? WITCO 40	
CATALYST ID	? CATALYST A POWDER	
INVENTORY	1.	Liters
CAT LOADING	0.3	Kilograms

OPERATING CONDITIONS

TEMPERATURE	250	Degrees Centigrade
PRESSURE	86.03	Atmospheres Absolute
FEED FLOW	4040	Liters/Kilogram-Hour
AGITATOR SPEED	1200	RPM

RESULTS

	FEED		EFFLUENT		DELTA	
					FLOW	
MPONENT	CONC V%	FLOW l/hr	CONC V%	FLOW l/hr	l/hr	gmole/hr
DROGEN	36.85	436.98	21.8	187.02	249.96	11.159
GON	0.	0.	0.	0.	0.	0.
TROGEN	4.35	52.68	6.12	52.54	0.14	0.006
THANE	3.32	40.3	4.7	40.3	-.	-.
MONOX	41.84	507.08	46.05	395.12	111.96	4.998
DIOX	14.38	174.35	21.27	182.49	-8.14	-.363

HYDROGEN CONVERSION	57.2 %	
C MONOX CONVERSION	22.08 %	
SELECTIVITY TO CO-2	7.27 %	
CALC'D MEOH PRODUCT	4.635	gmol/hr

Table 2

Crude Methanol Composition, Wt % (1)	
Methanol	93.33
Ethanol	1.82
Methyl Acetate	0.67
n-Propanol	0.71
i-Butanol	0.22
n-Butanol	0.93
C_5 Alcohols	0.30
C_6 Alcohols	0.22
Other Lights	0.11
Other Heavies	0.11
H_2O	1.58

(1) Components are identified by G.C. retention time comparisons only.

APPENDIX C

ECONOMIC FEASIBILITY OF A SMALL SCALE WOOD GASIFICATION TO METHANOL PLANT

Herbert M. Kosstrin, Ph.D.
Principal Process Engineer
Stone & Webster Engineering Corporation
Boston, Massachusetts 02107

D. Andrew Himmelblau
Process Engineer
Stone & Webster Engineering Corporation
Boston, Massachusetts 02107

ABSTRACT

This paper describes the current economic status of a small scale biomass based methanol plant (BMP) based on the scale-up of the SERI pressurized down-draft oxygen blown reactor. The BMP is designed to be shop fabricated on several skids to take advantage of the economies of one-time engineering and productivity increases associated with shop fabrication. Field installation costs are held to a minimum with this approach, and only minor changes in the standard design are due to site specific criteria.

The economic analysis is based on the Nth plant in a series of BMPs and considers the product to be sold as fuel methanol (octane enhancer/neat methanol) in the local plant area. Thus, the plant is of small scale (~ 8 MM gal/yr) and takes advantage of the federal alcohol fuel tax credit. The analysis concludes that the concept of this type of small scale skid fabricated plant is attractive even in today's market conditions (depressed methanol price), with several sites in the western United States being identified as potential sites for the first commercial unit.

ECONOMIC FEASIBILITY OF A SMALL SCALE WOOD GASIFICATION TO METHANOL PLANT

INTRODUCTION

Methanol is currently produced commercially worldwide via the conversion of synthesis gas derived from natural gas, refinery off-gas, petroleum, or coal. Methanol is currently used as a chemical feedstock (formaldehyde, acetic acid, MTBE - an octane enhancer), a final product (solvents), as an octane enhancer (Oxinol) and as a straight fuel ("neat" methanol). The concept of a small scale wood to methanol facility is based on the potential expansion of the fuel methanol market, (octane enhancer or "neat" methanol). These plants would be potentially competitive in localities where the cost of transportation of conventionally produced methanol is high and where there are sufficient raw materials to supply the plant and local markets to sell the product. The economic potential of the concept is enhanced by the current federal alcohol fuels tax credit which is applicable to methanol produced from biomass and sold in the fuel market.

This paper addresses a particular wood to methanol conversion facility based on the scale-up of the Solar Energy Research Institute's (SERI) pressurized down-draft oxygen-blown biomass gasifier. The investment analysis of this concept using other oxygen blown biomass gasification reactors would probably not change the feasibility of the production of methanol from wood.

SUMMARY

The conversion of wood (biomass) to methanol can be performed in a manner similar to that of coal conversion. A wood to methanol conversion facility would contain unit operations (equipment) that are commercially available except for the wood gasifier.

The design capacity of the Biomass Methanol Plant (BMP) is limited to approximately 8 x 10^6 gal/yr for three reasons:

- To ensure that the potential number of sites is not unduly restricted by the availability of the biomass resource,
- The local market should be able to utilize the methanol product without incurring substantial transportation charges, and
- A sufficient number of similar plants can be built to take advantage of repetitive manufacturing and engineering, and shop fabrication techniques in order to reduce unit capital costs.

The feasibility of the small scale BMP has been evaluated by addressing three areas:

- Site selection

- Technical feasibility, and,
- Profitability

The site was selected based on the availability of raw materials and the cost of transporting conventionally produced methanol to the region. With all other factors being equal the maximum transportation costs of conventional methanol determined the prime site. The area around Spokane, Washington was used to evaluate the concept of a small scale biomass to methanol conversion facility.

The biomass based methanol plant utilizes commercially available equipment to the greatest extent possible. The design is similar to a coal to methanol facility. The SERI gasifier, which has operated at a nominal throughput of 1 ton per day, is the only developmental unit. The scale-up of the SERI reactor is the major detail that needs verification prior to the construction of a BMP, if the concept is economically viable. The design basis of the plant is given in Table 1.

The investment analysis of the BMP is based on the Nth plant in a series of BMP's, and is carried out using a DCFROR type of analysis on a constant dollar basis (1984 dollars), with an equity to debt ratio of 75/25. The return on equity is set at 15 percent after taxes and the "real" interest on the debt is 8 percent. The construction period for the Nth plant including engineering, design, installation and startup, is estimated to take 18 months. The total facilities investment is $22,153,000. The basis for the investment analysis is given in Table 2.

The sensitivity analysis, which varies parameters such as capital costs, wood price, oxygen price and by-product credits (CO_2) defines the potential range of required methanol selling price, with the assumption that the minor technical uncertainties associated with gasifier scale-up are resolved without a major change in plant operation. This price range is 70 to 111¢/gal of methanol.

The potential maximum gross revenue, to the BMP, of selling fuel methanol in the Spokane, Washington area is $1.18. This is based on the following price components:

Component	Value (¢/gal)
U.S. Gulf Coast price (of Methanol)	42
Transportation Costs to Spokane	26
Alcohol Fuel Tax Credit (AFTC)	50
Equivalent Methanol Gross Revenue	118

It is seen that the predicted maximum potential revenue derived from selling methanol at Spokane (including the Federal tax credits) exceeds the range of required selling prices to allow a 15 percent return to investors.

TABLE 1

BIOMASS BASED METHANOL PLANT - BASIS OF DESIGN

ITEM	BASIS
Raw Wood Feed	Whole Tree Chips - 50 percent Moisture Content - 311.4 Tons per Day
Onsite Storage (wood and methanol)	Seven (7) Days
Processed Wood Feed	Pin Chips (3/8 In. Dia. x 1½ In. L) 16 Percent Moisture Content - 173.2 Tons/day
Gasifier	SERI Downdraft, Oxygen Blown, Pressurized
Gasifier Pressure	150 psig
Gasifier Size	8.5 Ft Internal Diameter
Gasifier Heat Loss	2 Percent of Input HHV
Wood Carbon Conversion to Gas	98 Percent
Gasifier Throughput	1.78 MM Btu/Ft^2 - Hr
Acid Gas Removal	Benfield - Hot Potassium Carbonate Followed by Zinc Oxide Guard Catalyst
Methanol Synthesis	Lurgi Low Pressure Process
Methanol Yield	77.1 Tons/day (7.68 MM gal/yr)
Methanol Quality	Fuel Grade (see Table 6)
Energy Integration	1. All Steam Generated Internally; 2. Electricity - Part Internally Generated, Part Purchased
Solid, Liquid, Gaseous Wastes	System Designed to Meet Local/Federal Regulations
Oxygen Supply	Purchased Over The Fence

TABLE 2

BASIS FOR INVESTMENT ANALYSIS[a]

COMPONENT	AMOUNT
Plant Life	20 years
Operating Factor	7,884 hr/yr (90 percent)
Equity/Debt	75 percent/25 percent
Minimum Return on Equity Required	15 percent DCFROR (after tax)
Interest Rate during Construction	8 percent real
Methanol Production Rate	7.68 MM gal/yr
Tax Rate	50 percent
Investment Tax Credit	10 percent
Renewable Energy Tax Credit	10 percent
Alcohol Fuel Tax Credit	50¢/gal
Construction Time	18 months
Wood Cost	$30/BDT
Oxygen Cost	$52.82/ton

(a) The investment analysis is based on a discounted cash flow rate of return (DCFROR) in constant 1984 dollars. The cost of capital (Rate of Return) and interest rates are net of inflation.

exceeds the range of required selling prices to allow a 15 percent return to investors.

FINDINGS

The economic success of a small scale, biomass-based methanol plant (BMP) is based on taking advantage of the high transportation costs for conventionally produced methanol and the Federal alcohol fuels tax credit to enable the product methanol to be sold competitively in the local market for automotive fuel use. The alcohol fuel tax credit is available since the methanol is produced from biomass.

The capital costs for the BMP are detailed in Table 3 and the annual operating costs are shown in Table 4. The primary operating cost components are shown to be wood, oxygen and labor.

The important findings of this study (for the Nth plant) are summarized below:

Component	Parameter
Wood Consumed	311.4 tons per day (at 50% moisture)
Oxygen Consumed	58.2 tons per day
Methanol Produced	77.1 tons per day (7.68 MM gal/yr)
Capital Cost	$22,153,000
Operating Costs	58.94¢/gal
Methanol Selling Price Range	70-111¢/gal
Methanol Selling Price (Base Case)	86¢/gal

In the Spokane area, the minimum return (DCFROR = 15%) can be obtained with a selling price (86¢/gal) that is less (by 32¢/gal) than the potential maximum methanol gross revenue (of 118¢/gal). Although in this analysis the alcohol fuels tax credit is required to attract private investment, any increase in the domestic methanol price directly offsets the need to depend on the tax credit on a one for one basis.

The differential between the potential gross revenue for methanol and the required methanol selling price is significant. This 32¢/gal differential enables regions with lower transportation cost to become potentially viable sites for a BMP (as long as the AFTC is fully realized). Most sites in Tier II (transportation costs 15-25¢/gal) become acceptable as long as raw material prices and labor costs are not substantially different from the Spokane (base case) location. This increase in the number of potential sites substantiates the assumption of a sufficient number of BMPs to

TABLE 3

BIOMASS BASED METHANOL PLANT

CAPITAL COST - BASE CASE

COMPONENT	COST
Material and Equipment	$11,354,900
Field Labor (including Contractor's Fee)	4,610,000
Freight and Tariffs	189,100
Total Base Cost	16,154,000
Land Cost	30,000
Engineering and Construction Management	1,870,000
AFI and Process Development Allowance	1,700,000
Total Installed Cost	19,754,000
Initial Catalysts and Chemicals	207,000
Startup Expenses (2 months)	751,000
Interest During Construction	1,156,000
Working Capital	285,000
Total Facilities Investment	$22,153,000

TABLE 4

BMP ANNUAL OPERATING COSTS SUMMARY[a]

COMPONENT	COST ($)	METHANOL COMPONENT COST ¢/GAL
Wood ($30/ton)	1,534,424	19.98
Oxygen ($52.82/ton)	1,009,443	13.14
Electricity (4.07¢/kWh)	176,894	2.30
Catalysts and Chemicals	236,567	3.08
Miscellaneous	99,798	1.30
Labor	720,000	9.38
Maintenance	507,000	6.60
Insurance and Taxes	242,310	3.16
	4,526,436	58.94

[a]Methanol production rate is 7.68×10^6 gal/yr

justify the economics associated with the skid design and N^{th} plant criteria.

RECOMMENDATIONS

Since the technology to convert synthesis gas to methanol is well established, the main technical questions raised in this study relate to the performance of the SERI gasifier, which converts wood to synthesis gas. Additional pilot plant testing, both at the current scale and at a larger scale, is required to confirm gasifier product yields, unit capacity, and operational integrity.

These data confirmations may result in changes to the design basis which potentially could cause a change in the base case DCFROR and make the facility more or less dependent on the alcohol fuel tax credit.

The analysis of the BMP has indicated (with the assumptions made) that the concept of a small scale biomass-based methanol plant can be an attractive investment, once the few remaining technical issues are resolved.

Therefore, it is recommended that further testing be conducted on the current SERI pilot plant to answer the questions enumerated in this study[1]. With positive results from this small scale testing, a larger unit should be built to answer the questions concerning scale-up and operational integrity.

DESIGN PHILOSOPHY

The design of the biomass-based methanol plant (BMP) is predicated upon the concepts of standardizing construction and maximizing shop fabrication to reduce plant capital cost. A manufacturing facility is envisioned producing the several skids of equipment that would be connected in the field. Only minor changes in skid-mounted components are required for different sites. Several plants could be shop fabricated each year.

The scale of the plant is based on the largest vessel in the plant that can be shipped by truck or rail without special permits. Based on estimated gasifier yields and throughput, the constraining vessel is the gasifier. The base case plant produces 7.68×10^6 gal/yr of fuel grade methanol.

Outside services such as oxygen, water, sewerage, and electricity are available at the site as needed. Otherwise the plant is constructed as a grass roots plant, unassociated with any other chemical plant (except the oxygen plant). Fuel grade methanol is being produced, consequently purification requirements are lower than for industrial grade methanol.

The overall process design is based on three primary requirements:

- Methanol production is maximized.

- Energy integration is used to avoid importing supplementary fuel and electricity.

- Except for the gasifier, all processing equipment selected are commercially available, i.e., no "black box" unit operations are used to resolve design problems.

Site Selection

A primary assumption for this study is that the methanol produced will be used as a motor fuel product. Initially, methanol will be used as an octane enhancer and potentially as a neat motor fuel (90 percent methanol, 10 percent gasoline). This motor fuel assumption, results in a restriction of potential sites to population concentrations of more than 225,000. Other uses could potentially increase the number of sites.

The major factor in selecting a site is to establish the delivered price of conventional methanol to the region. Other factors include the price and availability of the raw materials (wood, oxygen, power, etc.), the potential for by-product sales, and the ability of the local region to utilize the product.

The cost of transporting methanol from the major domestic production sites is shown in Figure 1. SWEC has established three tiers of transportation costs for site selection.

Tier I	Transportation Costs	less than 15¢/gal
Tier II	Transportation Costs	15-25¢/gal
Tier III	Transportation Costs	greater than 25¢/gal

Tier I encompasses almost the entire U.S.A. east of the Mississippi, the major western cities on the inland waterways (Kansas City, Omaha, Tulsa), and the Pacific Coast (San Diego, Los Angeles, San Francisco, Portland, Seattle). Tier II encompasses areas such as Denver, inland California (Fresno), part of inland Washington State and Oregon, the upper midwest (Minnesota, Wisconsin, eastern Dakotas), Hawaii, and coastal Alaska. Tier III includes the major western inland cities: Salt Lake City, Utah; Albuquerque, New Mexico; Spokane, Washington; Boise, Idaho; Las Vegas, Nevada; and Pheonix, Arizona.

The regions in Tier III are the most likely to be able to support a methanol plant if adequate raw materials are available. For the study, a Tier III site, Spokane, Washington, has been selected.

Additional sites outside of Tier III may be economically viable, due to special circumstances such as state incentives and the potential utilization of low cost waste feedstocks.

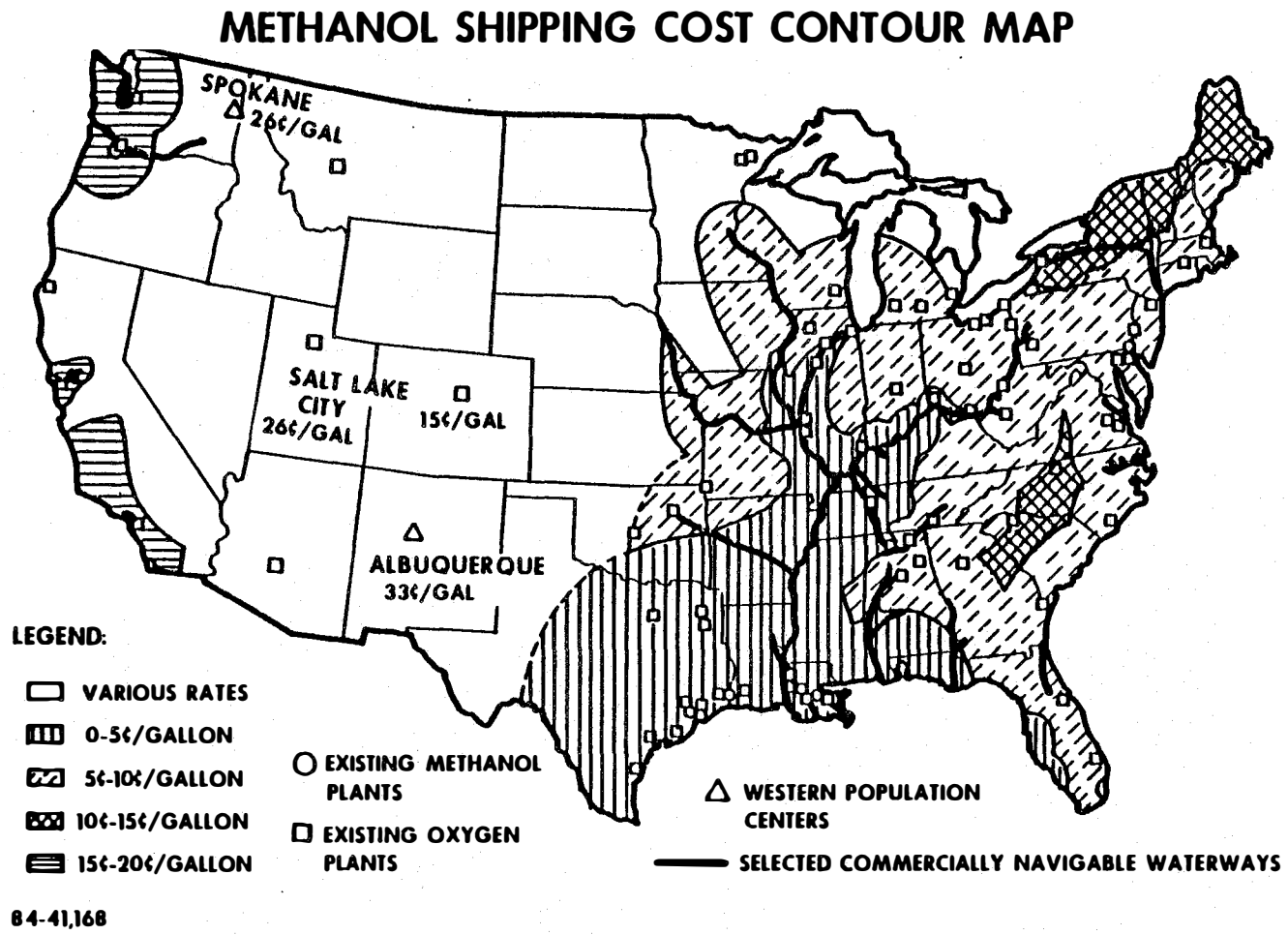

FIGURE 1 METHANOL SHIPPING COSTS

Technical Feasibility

The biomass-based methanol plant utilizes commercially available equipment to the greatest extent possible. The SERI gasifier, which has operated at a nominal throughput of 1 ton per day, is the only developmental unit. The process integration and engineering design for the base case design concentrated on the scale-up of the SERI gasifier, maximizing methanol production, minimizing importation of auxiliary fuel, and the use of a skid-mounted design.

Scale-Up

The analysis of the potential problems in scaling-up the SERI gasifier concentrated on oxygen distribution, uniform wood distribution, and gas flow. Nonuniform gas flow would be the result of bridging of the bed (sticky wood or ash fusion) or plugging of the bed (fines generation). The maximum gasifier size was limited to what easily fit a rail transportable skid with minimization of field installation. The present design of 8.5 ft ID and 10 ft OD, with a throughput of 1.78 MM Btu/hr-ft^2, was chosen as a reasonable scale-up when considering other solid fuel gasifiers, the SERI pilot plant design, and transportation limitations.

Engineering Design

The BMP incorporates several energy and process integration steps to increase product output and reduce energy damand (Figure 2). The more important process design improvements are:

- The use of an indirectly heated wood drier. This allows the drier exhaust steam to be reused, via vapor compression, as the heat source for the acid gas stripper reboiler.

- The use of direct water injection to supply steam for the shift reaction. Water is injected into the raw synthesis gas for cooling and to supply the shift steam.

- The use of a Pressure Swing Adsorption (PSA) unit for increased methanol production. Approximately 75 percent of the hydrogen from the methanol purge gas is recovered and recycled to the methanol synthesis unit, increasing the yield about 7 percent (from 72 to 77 tpd). The remaining purge gas is fed to a diesel engine generator set to produce power and steam.

- The use of a small fluidized bed combustor to burn combustible wastes, i.e., gasifier char and wood fines. This eliminates a majority of the solid waste disposal problem and provides fuel for the generation of the balance of process steam requirements, and startup steam.

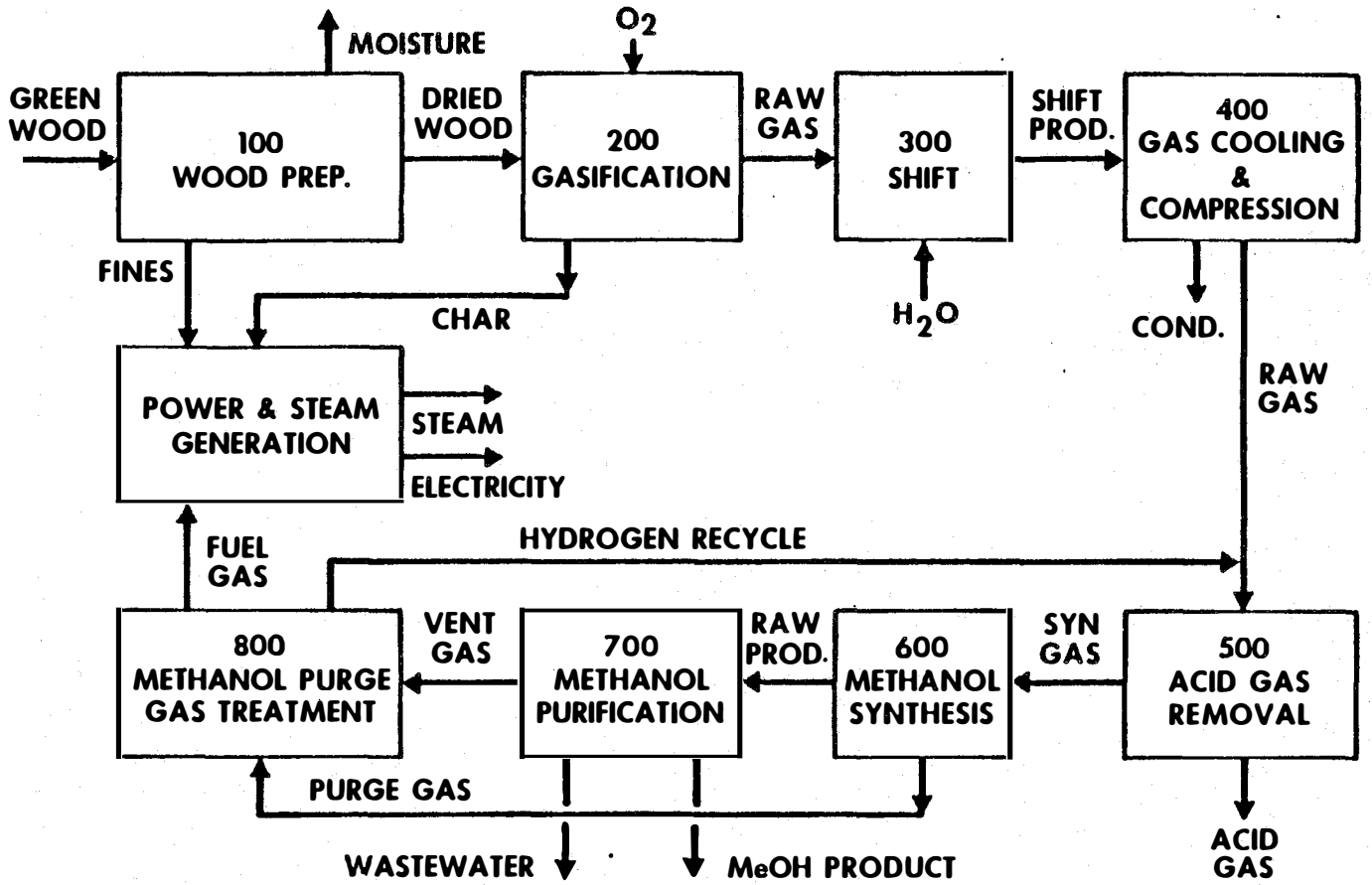

FIGURE 2 BMP PROCESS BLOCK FLOW DIAGRAM

Skid-Mounted Design

The BMP consists of eleven sections (areas) in which maximum utilization of shop fabrication and skid mounting of equipment has been used to reduce field installation. Only Section 100 - "Wood Handling and Preparation" has not been designed for skid mounting. This is due to the size and elevations of the conveyors, screens, and other equipment that make field installation more practical.

In the remaining ten sections, most of the equipment is skid-mounted except for the major towers, which are free standing. There are a total of 46 individual skids of which 13 are vendor-supplied packages and 7 are air-cooled heat exchangers placed on top of several other skids. The total number of skids is large but many skids are of moderate size. The maximum size of the skids was based on standard rail shipment. This allows a basic envelope of 12 ft wide by 12 ft high by 80 ft long.

Conceptual Design

The design basis for the BMP is shown in Table 1, with the gasifier raw gas composition given in Table 5. The plant size has been set by the maximum gasifier size and throughput selected. Maximum gasifier size has been set at 10 ft OD to be rail shippable and still allow good internal distribution of solids. Gasifier inside diameter (ID) is then approximately 8.5 ft, allowing for about 9 in. of refractory and a flow area of about 56.7 ft^2. Assuming a feed rate of 1.78 MM Btu feed (HHV) per hour per square foot, and a dry wood heating value of 8,417 Btu/lb (HHV), the dry wood (ash free) flow into the gasifier is about 12,000 lb/hr. This translates into a methanol production rate of about 77 tons per day. The gasifier is the largest (diameter) vessel used in the process and is the constraining piece of equipment with respect to plant scale.

The BMP is divided into the following eleven plant sections:

Section	Description
100	Wood Handling and Preparation
200	Gasification
300	Shift
400	Gas Cooling and Compression
500	Acid Gas Removal
600	Methanol Synthesis
700	Methanol Purification and Storage
800	Methanol Purge Gas Treatment

TABLE 5

GASIFIER OUTPUT [a]

GAS COMPOSITION COMPONENT	MOLES	MOLE %
H_2	332.2	35.3
CO	287.8	30.6
CO_2	178.0	18.9
CH_4	30.0	3.2
H_2O	108.9	11.6
N_2	3.5	0.4
SO_2	0.1	0.01
NH_2	0.2	0.02
H_2S	---	(b)
COS	---	(b)
		100.03

(a) Wood carbon conversion 98 percent.

(b) $SO_2/COS/H_2S$ molar ratio is 130/20/6 as per T. Reed data point number 15. Reed, T.B., Markson, M., and Graboski, M. - "The SERI High Pressure Oxygen Gasifier" presented at the Biomass-To-Methanol Specialist's Workshop, March 1982, Durango, Colorado

900	Wastewater Treatment
1000	Steam Plant and Process Water Treatment
1100	Utilities and Buildings

The following is a general discussion of processing steps and requirements of the BMP.

The sequence of process steps for methanol production from wood via gasification is straightforward. A simplified block flow diagram is shown in Figure 2. The wood to be gasified must be sized and dried to specification. This requires screening for oversized and undersized material. The prepared wood must be pressurized in a lock hopper in order to be fed to the gasifier. The raw gas must be converted to the proper stoichiometry for methanol synthesis. Because the shift conversion of carbon monoxide to hydrogen (to produce the proper hydrogen-to-carbon oxides ratio) produces additional carbon dioxide, carbon dioxide removal occurs after the shift operation.

The carbon monoxide shift is insensitive to operating pressure and can occur at gasifier pressure, while the removal of carbon dioxide is dependent on carbon dioxide partial pressure. Since complete removal of carbon dioxide is not required (nor desired), the pressure at which carbon dioxide is removed is an economic consideration; removal can occur at any pressure between gasification (150 psig) and methanol synthesis (1000 psig).

The method of carbon dioxide removal depends on capital cost and energy consumption. At intermediate pressures between gasification and methanol synthesis, the most economic process is likely to be Benfield scrubbing. Additionally, the Benfield potassium carbonate solution will pick up any sulfur dioxide generated in the flaming pyrolysis zone of the gasifier and does not need refrigeration. The acid gas scrubbing is located after the first stage of raw gas compression and before the second and last stage of compression. The raw gas is scrubbed to remove particulate and tars before compression.

The next step is to remove any residual sulfur that may remain in the gas to avoid poisoning the methanol synthesis catalyst. Adsorption of reduced sulfur species onto zinc oxide is the only practical method to reduce sulfur to less than 0.1 ppm. Conversion to raw methanol can then proceed. The raw methanol product must then be purified. In this case, the methanol must only be degased and dehydrated. The product specification for the methanol is given in Table 6. Inert gases (nitrogen and methane) must be removed from the methanol reactor system to avoid accumulation.

Energy integration is an important design factor. Because most of the major design steps are straightforward, the plant design options deal largely with matching energy sources and sinks to minimize

TABLE 6

METHANOL PRODUCT SPECIFICATION

CHARACTERISTIC	METHOD	SPECIFICATION[a]
Methanol content		99.40[b]
Water content	ASTM-D-1364	0.025[c]
Residue of Evap (mg/100 mL)	ASTM-D-1353	1.0
Acid (as acetic acid)	ASTM-D-1613	0.002
Alkalinity (as ammonia)		0.00030
Chloride (max)	Spec. ion electrode	0.0001
Lead (g/gal)	ASTM-D-3116	0.01
Phosphorous (g/gal)	ASTM-D-3231	0.005
Sulfur	ASTM-D-2622	0.025
Iron, volatile (mg/L)	Photometry	0.02
Permanganate No. (min)	ASTM-D-1363	60 min
Acetone No. (max)	Chromatography	0.002
9-11 psi RVP Unleaded gasolines (seasonally) added for volatility (volume percent)	ASTM-D-439-89	9.0-11.0

[a]weight percent except as noted

[b]California Energy Commission specification is 99.85.

[c]California Energy Commission specification is 0.05.

equipment costs and energy import. Design options that have been used include indirect drying of wood to recover the wood moisture latent heat as steam, fluidized-bed combustion of wood fines and other combustible wastes to balance the steam load, and utilization of the methanol synthesis purge gas (after hydrogen recovery and recycle) as diesel fuel to generate plant electricity.

Proper treatment of waste streams is also an important design factor for the plant. Low cost capture of the hydrogen sulfide in the acid gas (from the Benfield unit) with iron oxide (sponge iron) and phenol extraction from gasifier condensate are utilized to limit capital expenditures.

The design material balance is shown in Figure 3, with the corresponding energy balance in Figure 4.

The overall conversion of gasified dry wood to methanol is 53 weight percent for the base case (50 percent based on total dry wood). Carbon conversion to methanol is 40 weight percent. Most of the carbon lost is in the form of carbon dioxide (50 weight percent of wood carbon). For comparison, when methane is converted to methanol, carbon conversion is approximately 72 percent. It is estimated that when western subbituminous coal is converted to methanol, carbon conversion to methanol is approximately 47 percent (with purchased oxygen).

The energy efficiency of converting green wood to methanol is approximately 58 percent. Net drying losses are small because of heat recovery from the wood vapor. Fourteen percent of the wood energy (the methanol synthesis purge gas) is used to generate electricity. For comparison, when methane is used to produce methanol, methane enthalpy conversion to methanol is approximately 59 percent on a higher heating value basis. When western coal is converted to methanol, enthalpy conversion is approximately 54 percent, excluding air separation power.

ECONOMIC ANALYSIS

Economic Basis

The economic feasibility of the biomass based methanol plant (BMP) is based on the Nth plant in a series of identical BMP's. The only changes in the BMP's design would be dictated by site specific conditions, such as, climatic conditions, environmental requirements, and geotechnical limitations. A discounted cash flow (DCF) type of analysis is used to determine the rate of return available to investors for such a plant. In order to eliminate the need to estimate future inflation rates, the analysis is performed in constant 1984 dollars. The economic parameters for the BMP are given in Table 2.

The product methanol from the BMP will be competing with methanol that can be supplied from other domestic or international sources for the fuel/octane enhancer market. It has been assumed that

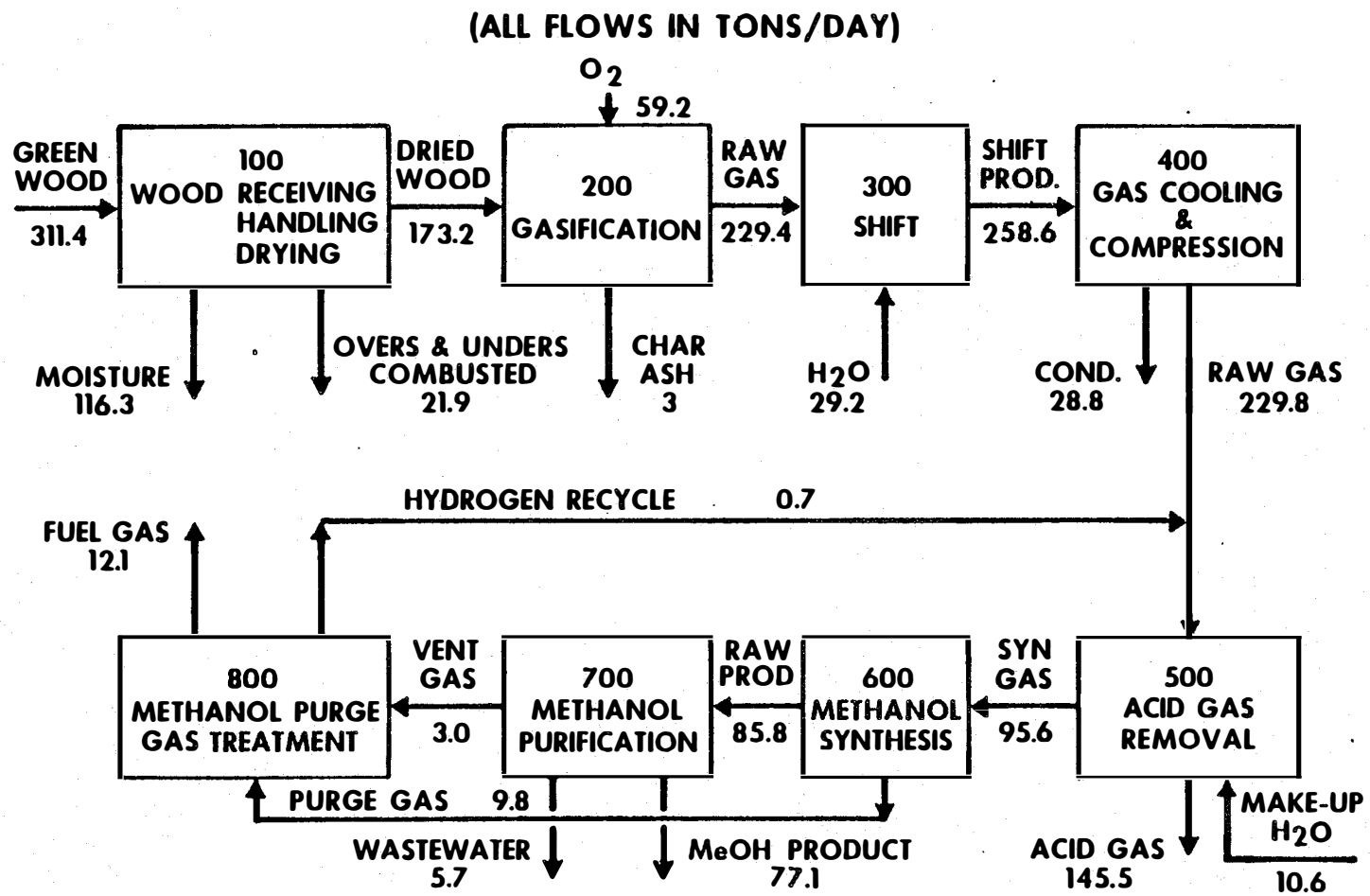

FIGURE 3 BMP MATERIAL BALANCE

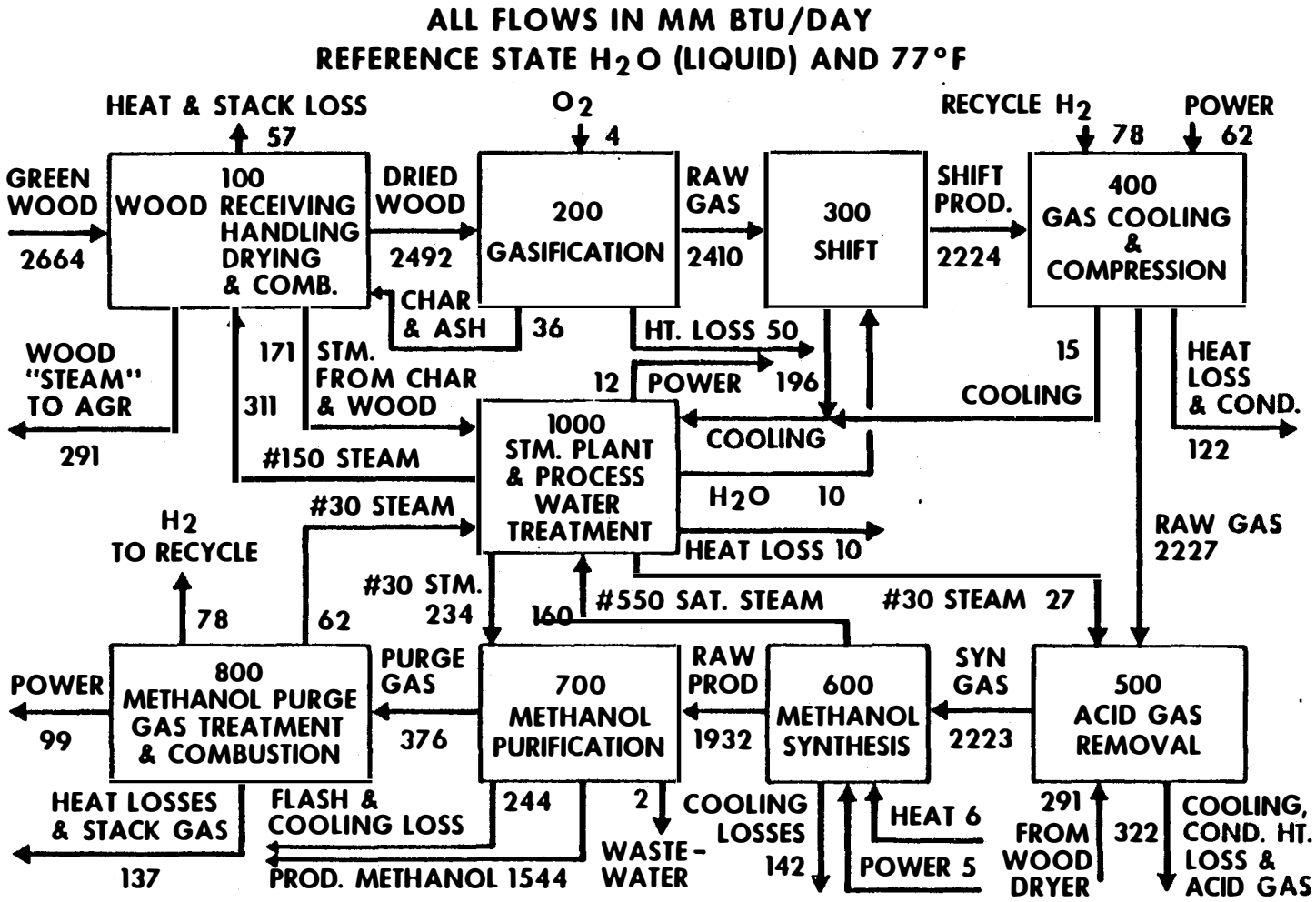

FIGURE 4 BMP ENERGY BALANCE

methanol produced from the BMP can be sold in Spokane at the U.S. Gulf Coast price plus a transportation differential. This analysis gives a current sales price of 68 cents per gallon (42¢/gal plus 26¢/gal transportation). Additional revenue accrues to the facility through the Federal Alcohol Fuel Tax Credit. This credit is currently equivalent to 50 cents per gallon of alcohol produced from sources other than natural gas, coal, or peat, i.e., biomass. Therefore, the maximum gross revenue derived from selling methanol on a cash flow basis is $1.18/gal (Table 7). To keep the economic analysis on a more general basis, no state tax credits have been assumed. There are, however, several states which grant tax credits for fuel methanol.

Summary

The investment analysis of the biomass-based methanol plant (BMP) takes into consideration the off design conditions by performing a sensitivity analysis. The sensitivity analysis considers variation in operational availability (stream factor), raw materials cost (wood, oxygen, electricity), by-product credits, and capital costs.

The sensitivity analysis on the base case design is then extended by considering technical improvements in the design which improve the economics. The base case considers 7,884 hours per year (90 percent stream factor) of plant operation. The plant has been designed to accomoodate this level of operation via increased capacity in the solids handling areas and on-line sparing of critical process pumps.

The analysis is based on a constant dollar basis (1984 dollars), with an equity to debt ratio of 75/25 and current prices for conventional methanol. It is recognized that the current supply/demand situation in the methanol market is resulting in a domestic price structure that is depressed from historical levels. It is unknown as to how long this pricing structure will persist, and the following analysis should be judged to be conversative. The total facilities investment is estimated to be $22,153,000 including contingency (Table 3).

It is assumed that the minimum acceptable after tax discounted cash flow rate of return (DCFROR) on a constant dollar basis is 15 percent and the interest on debt is 8 percent (net of inflation). Taking full advantage of the Alcohol Fuel Tax Credit of 50¢/gal, the maximum gross revenue obtained from selling the methanol product is $1.18/gal in the Spokane area.

This BMP design results in the following range of required methanol selling prices to meet the DCFROR criteria:

	Case	Methanol Selling Price (¢/Gal)
A)	Pessimistic	111
B)	Most likely	86

TABLE 7

MAXIMUM POTENTIAL METHANOL REVENUE

COMPONENT	VALUE (¢/GAL)
U.S. Gulf Coast Price	42
Transportation Costs to Spokane	26
Alcohol Fuel Tax Credit	50
Maximum Potential Methanol Revenue	118

C) Optimistic	70

Figure 5 shows the DCFROR versus methanol selling price for the base case.

The two design alternatives, doubling of the plant size and reforming of the purge gas result in the following reduction in the required methanol selling prices, for Case B.

Design Alternative	Methanol Price Savings (¢/Gal)
Doubling of the plant size	17
Reforming of the purge-gas	6

The analysis shows the need to utilize all or part of the Alcohol Fuel Tax Credit in order to attract investors to finance this type of facility. However, any rise in the price of domestic methanol in combination with debt financing and inclusion of the improvements identified in the alternative design cases would reduce the need to depend on the tax credit to attract investors to this concept.

Although the specific investment analysis is based on a Spokane, Washington site, other sites in the Tier III transportation region (see Figure 1) would be acceptable. Sites in other regions would become attractive as the price of methanol rises or under special circumstances, such as local incentives or inexpensive feedstocks.

Capital Costs

The capital costs of the Biomass-Based Methanol Plant (BMP) are shown in Table 3, wherein the total facilities investment is $22,153,000. The costs have been divided into materials and equipment, field installation labor, freight and tariffs, engineering and construction management, initial charge of catalysts and chemicals, interest during construction, and working capital. The working capital is based upon 7 days' storage of both raw materials and finished product plus 0.9 percent of the total base cost for spare parts and miscellaneous materials. The basis for the cost estimate is the engineering design performed as a part of the study. This cost estimate is based on the installation of the Nth plant in a series of BMPs and the skid-mounted nature of a majority of the equipment. The Nth BMP is assumed to be constructed over an 18-month schedule. During this period, interest during construction is calculated using an S curve (for the expenditure of funds) at a real interest rate (net of inflation) of 8 percent.

An allowance has been added to the capital cost estimate, it is made up of two factors. An Allowance for Indeterminates (AFI) is taken as a percentage of total materials and labor cost (not including subcontractor's fee and overhead) and is based on the known level of detail of the engineering design (e.g., the AFI goes down with a

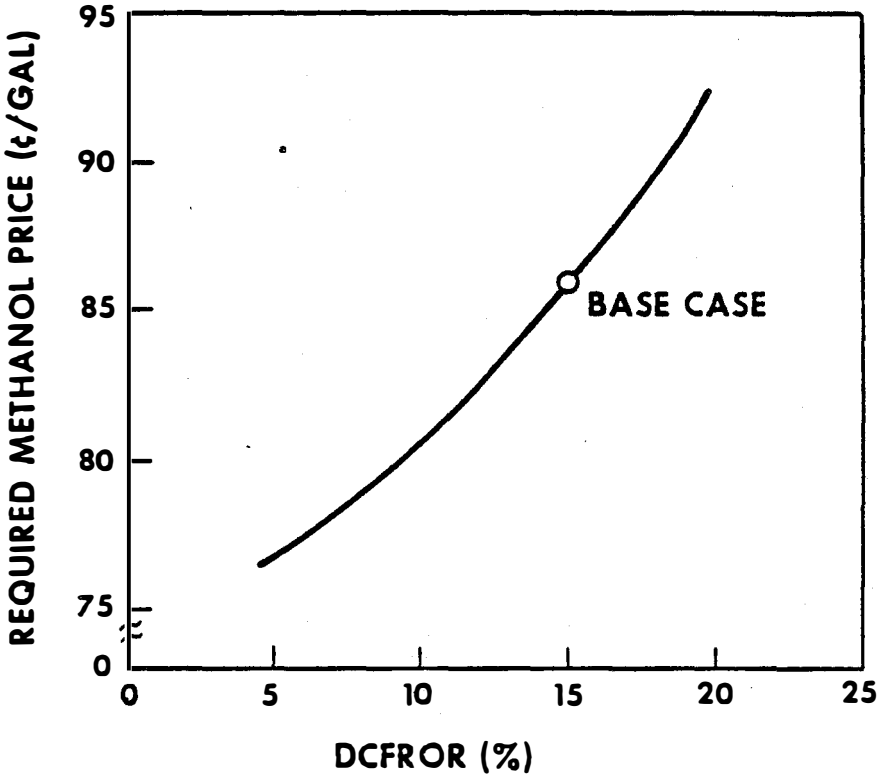

FIGURE 5 METHANOL SELLING PRICE VS DCFROR

greater level of detail). The Process Development Allowance (PDA) is a method of recognizing the higher cost of designing and fabricating a first-of-a-kind piece of equipment and is applied to process units of the plant that are not presently available on a commercial level. In the BMP, only the gasifier is not a commercially proven unit. The other system to which a PDA is applied, because of limited commercial experience or a slightly different application, is the phenol extraction unit. The AFI has been set at 10 percent (1.5 million dollars) while the PDA is determined in accordance with the Gas Research Institute Procedure and is approximately $200,000.

The construction of the first plant of this type would result in an increased capital cost of approximately 2 million dollars. The increases result from the following areas:

- Additional one-time engineering required for the initial modular design and first of a kind project.
- Additional startup time for the first of a kind project.
- Increased financing costs due to a longer project schedule.

The cost of installation is based upon the prevailing union wage rates in the Spokane, Washington vicinity. The Spokane site is located in Tier III, a region with high to methanol transportation costs. Other potential site locations in Tier III included Salt Lake City, Utah and Albuquerque, New Mexico.

Revenues

The potential revenues from the BMP come from two sources, the sale of methanol and the sale of carbon dioxide. In general, raw carbon dioxide can be sold, to a distributor for purification and sale, for approximately $10/ton. Although a CO_2 by-product credit was not taken for the base case because there is not a sufficient market in Spokane to justify the sale of this product from the BMP, the effect of CO_2 revenue on plant economics for other sites is discussed later.

The total potential revenues from the sale of the methanol product is calculated from three independent factors: the current U.S. Gulf Coast selling price, the transportation costs to Spokane, and the Federal Alcohol Fuel Tax Credit (Table 7). For the base case analysis it is assumed that the full effect of the Fuel Alcohol Tax Credit is reflected in the maximum potential revenues from the sale of methanol. The methanol from the BMP is eligible for the tax credit since the feedstock is biomass. At the present time (September 1984), the domestic methanol price is low due to excess methanol production capacity. The potential effect of an increase in the U.S. Gulf Coast price on the economics of the BMP is discussed below.

Operating and Maintenance Costs

The operating costs for the BMP include wood, oxygen, manpower, electricity, chemicals, catalysts, water, fuel, and waste disposal costs. Table 4 summarizes these various costs for the BMP. The manpower costs include 76½ percent of wages for overhead. The overhead costs were specifically calculated for a small plant and include such items as taxes, benefits, security, janitorial services, sales cost, office supplies, payroll, accounting and legal services. Maintenance costs are calculated as a percentage of plant section base cost. Insurance and local taxes are taken as 1.5 percent of the BMP's total base cost.

Investment Analysis

The current (September 1984) selling price of methanol (42¢/gal, U.S. Gulf Coast) are substantially below the price that would be expected using a reasonable rate of return on investment for natural gas based plants. This shows that current market conditions are forcing domestic producers to absorb certain costs of production. This situation, complicates the determination of an acceptable rate of return on which to base an investment analysis for the BMP.

The minimum rate of return that would be acceptable to an investor is dependent upon the level of risk that is perceived. Two components of risk are apparent in this project:

- Inability to sell the methanol product, and
- potential problems in operation.

The inability to sell the methanol product is of prime concern, since the technological problems would be known from the pilot plant and operation of previous plants. The risk of selling the product is concerned with market penetration and the availability of co-solvents. In the context of the constant dollar nature of this analysis and the present level of real rate of return obtainable on secure debt securities (approximately 8 percent), an after tax DCFROR of 15 percent was considered the minimum return that an investor would expect for this project.

Methanol Selling Price

The variation of selling price with DCFROR is shown in Figure 5. The minimum price required to achieve the desired DCFROR of 15 percent is seen to be 86¢/gal. In the Spokane area, with the assumption of full tax credits (50¢/gal) over the life of the project, the maximum potential revenues exceeds the required selling price by 32¢/gal. It should be recognized the elimination of the tax credit or the inability to use at least 36 percent of the credit (18¢/gal) will result in a BMP (in Spokane) with an insufficient return to attract investors (assuming a minimum DCFROR of 15 percent). The portion of the methanol revenues which is assumed to be contributed by the Federal tax credit may be contributed via

price increases in conventional methanol, state subsidies for biomass based methanol, or higher transportation cost for conventional methanol.

The change in required methanol selling price with variations in parameters such as plant capital cost, raw materials prices, plant operation, and by-product credits were evaluated in a sensitivity analysis which also determined the range of potential rates of return. The effect of these parameters on the required methanol selling price to meet the required 15 percent DCFROR for the base case plant is also discussed. This information can also be used to evaluate sites other than Spokane (in conjunction with the transportation costs), if the price of raw materials and the saleability of by-products are known.

Capital Costs

Figure 6 shows the effect of a change in capital cost on the required methanol selling price. Variations in capital cost of approximately 10 percent ($2.2 million), are equivalent to approximately a 2.7¢/gal change in methanol selling price. One area of potential capital cost reduction is in field (installation) labor. If labor productivity is increased by 20 percent (i.e., non-union labor) the capital costs of base case plant could be reduced by approximately $900,000.

The base case economics assume the design and construction of the Nth plant. As stated, the capital cost of the first plant would increase by approximately $2.0 MM. This would increase the required methanol selling price by approximately 2.5¢/gal.

Stream Factor

The sensitivity of the required methanol selling price to the on-line availability of the BMP (stream factor) to produce methanol is shown in Figure 7. The base case assumes that the plant operates 7,884 hours per year or 90 percent of the available time. A reduction in availability to 70 percent would require a selling price of 99.7¢/gal. A 10 percent change in availability results in approximately a 6¢/gal change in the required methanol selling price. This calculation demonstrates the critical nature of the availability of the plant to return on investment.

Raw Material Costs and By-Product Credits

The sensitivities of raw material prices, i.e., wood, oxygen, electricity, and of by-product revenue, e.g., carbon dioxide, can be analyzed as direct changes in the required methanol selling price. Table 8 gives the results of a unit price change in each of these commodities. Any change in revenues of $76,800 is equivalent to 1¢/gal in methanol price.

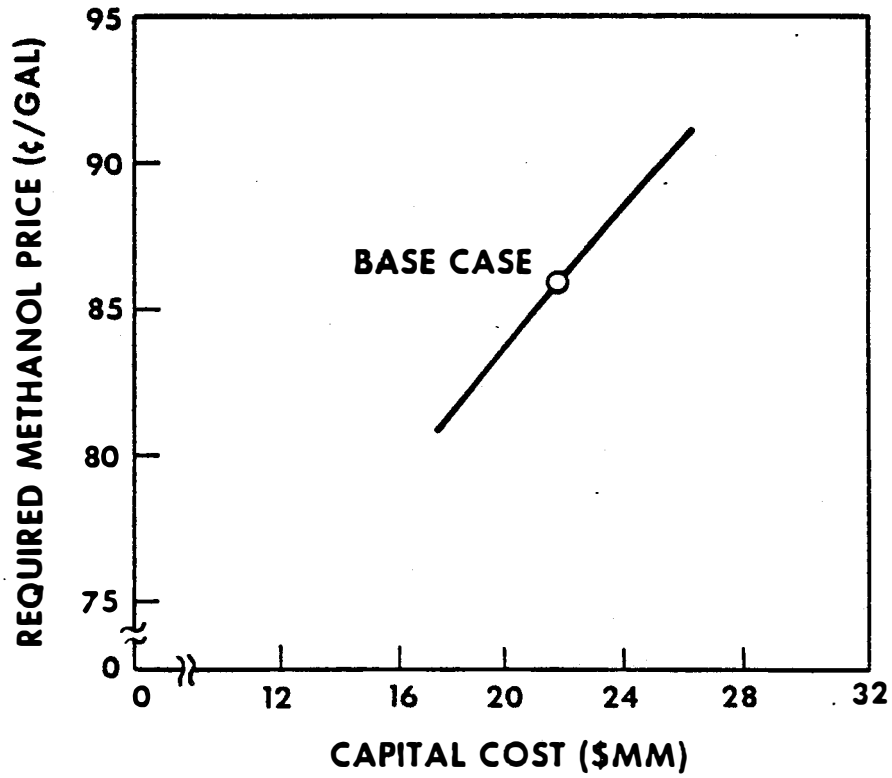

FIGURE 6 METHANOL SELLING PRICE VS CAPITAL COSTS

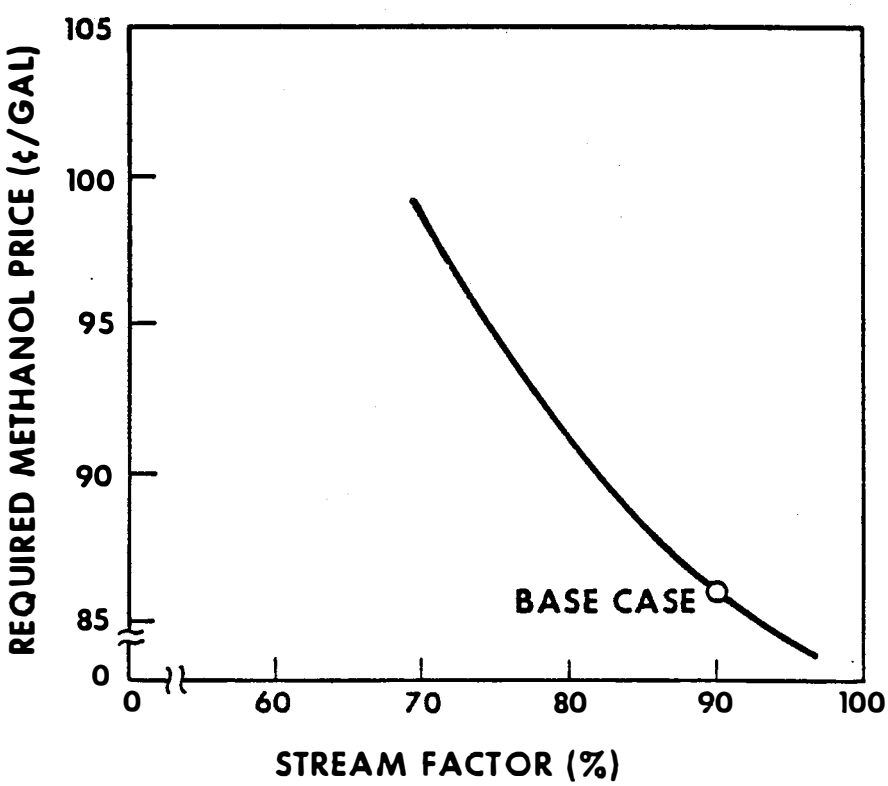

FIGURE 7 METHANOL SELLING PRICE VS STREAM FACTOR

TABLE 8

METHANOL SELLING PRICE CHANGES DUE TO COMMODITY PRICE CHANGES

COMMODITY	UNIT PRICE CHANGE	EQUIVALENT PRICE CHANGE (¢/GAL)
Wood	+$10/dry ton	+6.66
Carbon dioxide	+$10/ton	-4.91
Oxygen	+$10/ton	+2.49
Electricity[a]	+1¢/KWh	+1.56

[a] The change in electricity includes electricity for oxygen production at 0.995 ¢/gal and electricity for the BMP at 0.566 ¢/gal.

Discussion of Results

Alternative Sites

The sensitivity analysis can be used to estimate the appropriateness of an alternative site. For example, the ability to sell carbon dioxide at ($10/ton) can offset an increase in wood costs of approximately $7.40/ton, or can reduce the amount of revenue required from the tax credit by 4.9¢/gal. In conjunction with the transportation cost map (Figure 1), a quick approximation can be made as to what additional sites are viable, or what magnitude of incentives are required to establish a BMP in a specific location. For example, a BMP sited in the State of Hawaii with electricity priced at 7¢/KWh (Δ = +3¢/KWh) and wood costing $37/BDT (Δ = +$7/BDT), would raise the required selling price by 9.35 ¢/gal (to 95¢/gal) to maintain base case DCFROR (15 percent). In addition, in Hawaii, the transportation differential is reduced by 6 ¢/gal (20¢ vs 26¢), this lowers the maximum selling price to $1.12/gal.

The sensitivities can also be used to perform a quick analysis in order to evaluate the potential of a new feedstock. For example, rice hulls can currently be obtained at zero cost (Δ = -$30/ton) in the Gulf Coast region. This area also has oxygen available at approximately $40/ton (Δ = -$12.82/ton), and a ready market for carbon dioxide (Δ = +10/ton). This combination of revenues and material savings of approximately 28¢/gal more than compensates for the fact that there is no transportation differential (e.g., 26¢/gal for Spokane) to include in the potential revenue formula. This quick analysis indicates that rice hulls may make a reasonable alternative feedstock to test in the gasifier, and that a more detailed analysis is justified.

Combination of Parameters

The sensitivity analysis has considered the effect of individual parameters on the economics of the plant. The question then arises as to the effect of a combination of parameters of the site specific case of Spokane, Washington. This combination of parameters results in a range of required selling prices, which when compared to the maximum potential market revenues (including the AFTC) gives and indication of the level of risk in the venture. Two cases are considered, a pessimistic case and an optimistic case. The pessimistic case considers a capital cost of $24,000,000 (+10 percent), a stream factor of 70 percent (-20 percentage points), and a wood price of $40/ton (+10/ton). The optimistic case considers a capital cost of $20,000,000 (-10 percent), a stream factor of 95 percent (+5 percentage points), a wood price of $20/ton (-$10/ton), and the sale of CO_2 at $10/ton (+$10/ton).

The pessimistic case would occur with a tight supply of wood, some plant operational difficulties, and capital cost within the accuracy of the current estimate. This scenario results in a DCFROR of 15 percent at the methanol selling price of $1.11/gal. This price

is still below the maximum potential revenues for ($1.18/gal) methanol in Spokane, taking the full 50¢/gal AFTC.

The optimistic case may occur by obtaining diseased wood, establishing a new market for carbon dioxide, not encountering plant operational problems, and reducing the capital cost within the accuracy of the current estimate. This scenario results in a DCFROR of 15 percent at the methanol selling price of 70¢/gal. The case utilizes only 4 percent (2¢/gal) of the Federal Alcohol Fuel Tax Credit.

Alternative Designs

The design of the BMP has defined a starting point in the economic analysis of the concept of a small-scale methanol production facility. Several technical changes to this design have been investigated in order to gain additional insight into plant operating conditions that can improve the overall economics. Of the three design variations on the base case (higher gasifier operating pressure, higher wood moisture content, and reforming the purge gas methane) only the case of reforming the purge gas showed any significant improvement in the economics.

The alternative design of reforming the purge gas increases the methanol production to 8.77 MM gal/yr from 7.68 MM gal/yr. This design also increases total capital expenditures by approximately $1,000,000, but reduces the required methanol selling price by 6¢/gal to 80¢/gal to achieve the required DCFROR (15 percent). This increase in production (~14 percent) can be sold in the local market without any significant change in the market penetration assumptions. This design alternative should be incorporated in any revision to the base case design.

The potential economic effect of increased capacity, on the BMP, was investigated by doubling the gasifier throughput and thus the methanol output. It is necessary to recognize that at a production rate of 15.36 MM gal/yr of methanol, a portion of the product may have to be shipped a considerable distance to market and thus reduce the revenue received by the BMP.

However, for this particular analysis, the assumption of local sales was retained. The reduction in required methanol selling price to maintain the base DCFROR of 15 percent is approximately 17¢/gal. This is due to economics of scale in both the BMP and the oxygen plant (to be built by the oxygen supplier). This calculation demonstrates the importance of accurately defining both the gasifier throughput and the local market, in order to size the BMP properly.

RESEARCH AND DEVELOPMENT NEEDS

The next milestone in the commercialization of the small scale biomass-to-methanol concept is the scale-up of the SERI gasifier. The SERI gasifier has been tested only at a scale approximately 1/400 of the base case commercial design used in this study. An

intermediate sized pilot plant should be built to evaluate the gasifier at a scale compatible with confirming all operating concepts and assumptions, but still small enough to build and operate without great expense. Some of the required information should first be obtained in the existing pilot facility to ensure that the commercial biomass from methanol plant designs are achievable and to incorporate this information into the design of the larger pilot unit.

The following information can be obtained with the current SERI pilot plant gasifier and is needed to provide process and specification information for an actual large pilot or demonstration plant design:

- Reproducible, tightly closed energy and material balances to accurately verify gas yields and composition. Elemental balances (C, H, O, S, and N) should also be closed. Operating conditions should be at 150 psig with oxygen.

- Determination of the sulfur species present in the gas phase to properly design sulfur removal facilities prior to methanol synthesis, and establish acceptable acid gas disposal methods.

- Analysis of raw gas condensate from scrubbing (especially tar compounds condensed) to design a condensate treatment system.

- Determination of particle size distribution and disposition (grate, cyclone, or scrubber) of the char and ash.

In addition, the following information would be useful in broadening the application of the SERI gasifier.

- Operation with wood feed at higher moisture contents (especially wood with only surface moisture removed) to establish yields and gas composition.

- Operation with waste product feedstocks such as rice hulls to determine the suitability of gasifying low cost materials.

Concurrently, a test of indirect drying of wood should be arranged to determine the heat transfer coefficients and conditions needed for indirect drying of wood chips to 15-17 percent moisture content in commerical equipment. Mechanical designs for oxygen distribution and solids agitation should be made.

Once the above information has been obtained, the gasifier should be scaled up to a size at which the oxygen distribution system and mechanical agitation can be realistically tested for mechanical integrity and suitability. Maximum gasifier throughput should also be studied at this phase. In addition, gasifier feed size should be

re-evaluated and variations (if any) in yield, gas composition, throughput, or gasifier operability with feedstock size should be noted. The larger pilot work should reconfirm the design assumptions and energy and material balances produced from the data to be taken in the existing smaller pilot plant. A continuous 30 day run should be a minimum goal to evaluate reliability, integrity of materials, and the mechanical design.

The size of the larger pilot gasifier should be approximately 3 ft, inside diameter, or 4.5 ft, outside diameter. At the current assumed throughput, approximately 2 tph of green wood would be required. Because downstream processing technology is commercial and does not need to be integrated directly with the gasifier, the raw gasifier product can be burned or flared.

This gasification technology should be scale-up to this larger size pilot plant to answer the questions enumerated in this section.

REFERENCES

1. Kosstrin et. al. Economic Feasibility Study of a Wood Gasification Based Methanol Plant, final report under SERI Subcontract ZX-3-0-3095-1. To be published